VON WILLEBRAND FACTOR GLYCANS – MODIFIERS OF FUNCTION & PROTEOLYSIS

A Thesis Submitted to the University of London for the Degree of Doctor of Philosophy in the Faculty of Medicine

By

Thomas Anthony Jude McKinnon BSc(Hons)

Department of Haematology
Imperial College London
Hammersmith Hospital Campus
Commonwealth Building
Du Cane Road
W12 0NN

BIBL LONDON UNIV

January 2007

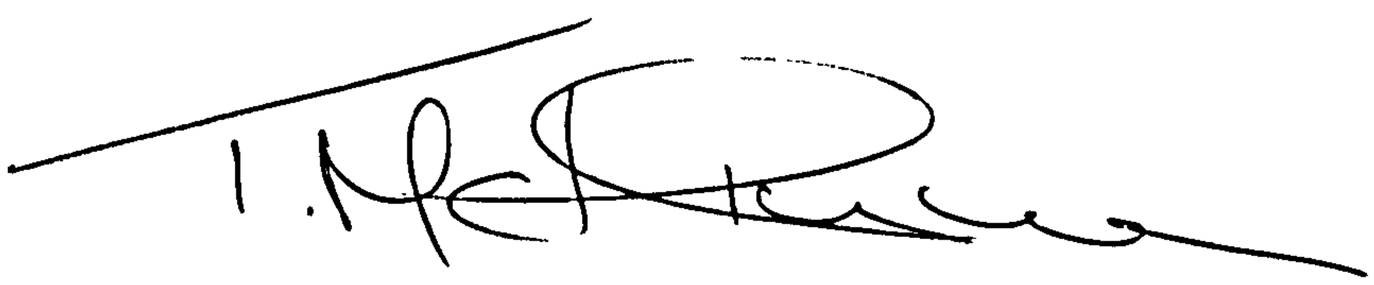
ABSTRACT

Von Willebrand factor (VWF) is a large multimeric plasma glycoprotein essential to normal haemostasis. A major determinant of plasma VWF levels is ABO blood group with levels in group O individuals 25-30% less than non-group O individuals. Previous reports have suggested that ABO(H) blood group sugars, presented on the *N*-linked glycan chains of VWF, modulate susceptibility to proteolysis by ADAMTS13. To extend this hypothesis, plasma samples were collected from individuals with the rare Bombay blood group that do not present H-antigen structures. Absence of H-antigen from Bombay VWF was demonstrated by H on VWF ELISA and western blot analysis. VWF:Ag measurement demonstrated that VWF:Ag levels in Bombay individuals were significantly lower (median = 0.69 IU/ml) than in control groups A, B and AB. ($p<0.05$). Susceptibility of purified HMW-VWF fractions to cleavage by plasma derived and recombinant ADAMTS13 was assessed using VWF:CB and VWF multimer gels and demonstrated that Bombay VWF was cleaved significantly faster than O or AB VWF. Increasing urea concentration (0.5 to 2M) increased the cleavage rate for each blood group, but eliminated the differences between groups, implying that reduction in the number of terminal sugars on VWF *N*-linked glycans increases susceptibility of globular VWF to ADAMTS13 proteolysis. Interestingly two *N*-linked glycan sites are present within the A2 domain (N1515 and N1574) close to the ADAMTS13 cleavage site (Y1605M1606). A ~55kDa tryptic fragment of VWF was isolated by ion-exchange chromatography. N-terminal and mass spectroscopy analysis demonstrated that the fragment comprised VWF residues 1493-1877, incorporating the ADAMTS13 cleavage site and sites N1515 and N1574. PNGase F digestion showed that both predicted *N*-linked sites were occupied and western blotting with anti-H lectin demonstrated that both are likely to present complex sugar structures capped with blood group sugars. Sequence analysis of the VWF A2 domain from 59 species showed that both sites are highly conserved, indicating their importance. The techniques developed to analyse ABO and Bombay VWF were then applied to artificially modified VWF. Neuraminidase and PNGase F digestion of purified VWF was performed to produce glycan modified VWF. Removal of VWF sialic acid did not affect multimeric structure or collagen binding but decreased susceptibility to ADAMTS13 proteolysis. Digestion with PNGase F (PNG-VWF) resulted in the removal of >90% VWF *N*-linked glycans

and increased susceptibility to ADAMTS13 proteolysis and also allowed proteolysis in the absence of urea. PNG-VWF also bound ADAMTS13 with ~4-fold increased affinity and was able to bind ADAMTS13 when in a globular conformation. To examine the effect of specific glycan chains, the two A2 domain glycans, N1515 and N1574 were mutated to glutamic acid residues and expressed in HEK293T cells. Mutation of the sites did not affect secretion of the molecule or formation of Weibel-Palade bodies and the multimeric structure and affinity for collagen was not altered. N1515Q was proteolysed by ADAMTS13 at a similar rate to wtVWF, but N1574Q was cleaved significantly faster and was also cleaved in the absence of urea. Furthermore, N1574Q bound ADAMTS13 with ~2-fold increased affinity compared to wild type VWF. Together these results demonstrate that the glycan moiety of VWF plays an important role in modulating the interaction of VWF with ADAMTS13. Specifically, glycosylation at N1574Q protects the molecule from ADAMTS13 proteolysis. The effect of glycan modification and mutation on susceptibility to ADAMTS13 cleavage and ADAMTS13 binding can be used to construct a model in which glycans limit ADAMTS13 cleavage of VWF by a combination of steric effects and local and long range conformational effects.

DECLARATION OF ORIGINALITY

I hereby declare that this thesis is the result of my own work that has been carried out between November 2003 and December 2006 in the Department of Haematology, Imperial college school of Medicine, Hammersmith Campus, London. All work and data analysis of the results were performed by myself, unless otherwise specified in the text.



Thomas McKinnon

ACKNOWLEDGEMENTS

Ok, I'm writing the acknowledgements so that means that this has finally come to an end!!! Woo Hoo!!!!! So many people to thank so here it goes!

First and foremost, my supervisor Dr Mike Laffan. Mike has been a totally brilliant supervisor and has provided countless amounts of support and enthusiasm, especially when things were tough at the beginning of this project. His door has always been open for a chat, to offer help and advice and he has always encouraged me to pursue my own ideas and allowed me to develop as a scientist. Secondly, I would like to thank my other supervisor, Dr James O'Donnell, for giving me the chance to do this project and for supporting me when things were not working at all! Like Mike, James has been highly supportive and has allowed me to develop my own ideas. I've been very lucky to have two such excellent supervisors.

A big thank you to Dr Alain Chion, (aka Master Yoda!). Without Alain's excellent technical help and advice, large amounts of this thesis would not have happened! Cheers Alain! I would also like to thank Dr Anna Randi for all her support and advice during the latter half of this project. And a big thank you to Prof Lane and Jim Crawley for all their help during my time in the lab.

Also, a special thank you to the trustees of the James Capel Foundation for all their support.

Big thank yous to the other guys in the lab for making the past 3 years so much fun! Jonathon you have to be the nicest guy ever! I will miss hearing you talk to yourself and the crafty "Friday after work beer"! Michelle, thanks for keeping me topped up with coffee! Gina, I know you have left, but I miss you lots, thanks for all our little chats we used to have!

Thank you also to my family who have been so supportive over the past three years. All the words of encouragement have kept me going when times have been tough! Thanks to Den and Matt for proof reading part of this thesis (I now know what an Oxford comma is!) Thanks to Chris and Mick, and Amy, Luke and Gareth for all their love and support that made me stick with this at the beginning and getting this thesis printed! (And for doing the contents page for me!!!) And thanks to John and Emma and Theresa and Mick for all their love and encouragement.

Thank you also to Maureen and Sandy for your love and support, and some seriously excellent cooking!!

And I have to motion the boys! Gordy, Pete, Steve Harry, Steve (aka DJ Stacks), Ben, Alex, Mike and Lucy! Thanks for your support over the past three years and for being wonderful friends. Liam, I would like to take this opportunity to say you are a total……..great guy! Cheers for all your help mate and for being a truly great friend! "I'm learning!"

Finally, two very big thank yous. Firstly to my darling fiancée Melanie. Thank you honey for putting up with all the stress and me being grumpy sometimes! The thought of you has kept me going, and I dedicate this to you. I love so you very very much. xxx

And last, but certainly not least, thank you Dad. Thank you for your love and support and for encouraging me to go to university and then on to do a PhD. None of my achievements would have been possible without you.

I love you very much Dad. Thank you.

CONTENTS

TITLE.....1

ABSTRACT.....2

DECLARATION OF ORIGINALITY.....4

ACKNOWLEDGEMENTS.....5

CONTENTS.....7

LIST OF FIGURES.....15

LIST OF TABLES.....18

LIST OF ABBREVIATIONS.....19

CHAPTER 1: INTRODUCTION.....22

1.1 VON WILLEBRAND FACTOR.....22

1.2.1 VWF Tissue Distribution and Sites of Synthesises.....22

1.2.2 VWF Gene Structure.....22

1.2.3 Transcriptional Regulation of the VWF Gene.....23

1.3 VWF SYNTHESIS AND PROCESSING.....23

1.3.1 *N*-linked Glycosylation.....24

1.3.2 Dimerisation.....24

1.3.3 *N*-linked Glycan Processing.....24

1.3.4 O-linked Glycosylation.....24

1.3.5 Sulphation.....25

1.3.6 Multimerisation.....25

1.3.7 Propeptide Cleavage.....26

1.4 VWF STORAGE AND SECRETION.....27

1.4.1 Weibel-Palade Bodies.....27

1.4.2 Regulated Secretion.....28

1.5 VWF STRUCTURE AND FUNCTION.....30

1.6 THE D DOMAINS.....32

1.6.1 Factor VIII Binding.....33

1.6.2 P-Selectin Binding.....34

1.7 A1A2A3 DOMAINS.....34

1.7.1 Platelet GPIbα.....36

1.7.2 Heparin.....37

1.7.3 Collagen Binding.....37
1.7.4 A2 Domain.....39
1.8 D4 AND B DOMAINS.....39
1.9 THE C DOMAINS AND THE CYSTEINE KNOT.....39
1.10 VWF FUNCTION IN COAGULATION.....40
1.10.1 Blood Vessel and Blood Flow Dynamics.....40
1.11 VWF AND PRIMARY PLATELET PLUG FORMATION.....41
1.11.1 Platelet Adhesion.....41
1.11.2 Platelet Aggregation.....43
1.11.3 VWF Self-Association.....43
1.12 VON WILLEBRAND DISEASE.....44
1.13 REGULATION OF VWF FUNCTION.....48
1.13.1 ADAMTS13.....48
1.13.2 ADAMTS13 Interaction with VWF.....50
1.13.3 VWF Cleavage by Thrombospondin-1.....51
1.14 GLYCOSYLATION.....52
1.14.1 *N*-linked Glycosylation.....52
1.14.1.1 *N*-linked glycan synthesis.....52
1.14.1.2 Effect of *N*-linked glycans on protein folding.....54
1.14.2 O-linked Glycosylation.....56
1.14.2.1 Synthesis of O-linked glycans.....56
1.15 GLYCAN STRUCTURE OF VWF.....57
1.15.1 O-linked Glycosylation of VWF.....58
1.15.2 *N*-linked Glycosylation of VWF.....59
1.16 FUNCTION OF VWF GLYCANS.....62
1.16.1 Multimeric Structure.....62
1.16.2 Platelet Aggregation.....63
1.16.3 Protection from Proteolytic Cleavage.....64
1.16.4 Collagen Binding.....64
1.16.5 VWF Clearance.....64
1.16.6 VWF Clearance – Role of Carbohydrate.....65
1.17 VWF LEVELS IN HUMAN PLASMA.....67
1.17.1 Regulatory Defects of VWF Expression.....67
1.17.2 Environmental Influences.....67

1.17.3 Ethnic Group.....68
1.17.4 Defects of the VWF Gene.....68
1.17.5 Other Quantitative Trait Loci.....68
1.18 THE ABO BLOOD GROUP SYSTEM.....68
1.18.1 ABO Genotype.....71
1.18.2 Bombay and Para-Bombay Phenotype.....71
1.19 RELATIONSHIP BETWEEN ABO BLOOD GROUP AND PLASMA VWF LEVELS.....71
1.20 AIMS OF THESIS.....73

CHAPTER 2: MATERIALS AND METHODS.....74
2.1 PURIFICATION OF BLOOD GROUP SPECIFIC VWF FROM PLASMA....74
2.1.1 Cryoprecipitation.....74
2.1.2 Gel Filtration.....74
2.2 PURIFICATION OF VWF FROM HAEMATE P.....75
2.2.1 Gel Filtration.....75
2.2.2 Heparin-Sepharose Affinity Chromatography.....75
2.3 ANALYSIS OF PURIFIED VWF.....76
2.3.1 VWF:Ag ELISA.....76
2.3.2 Collagen Binding Assay.....77
2.3.3 VWF Multimer Analysis.....78
2.3.4 H-antigen on VWF ELISA.....79
2.4 SDS POLYACRYILAMIDE GEL ELECTROPHORESIS (SDS-PAGE).....79
2.4.1 Coomassie Staining.....80
2.4.2 Silver Staining.....80
2.4.3 Western Blot.....80
2.5 EXPRESSION AND PURIFICATION OF ADAMTS13.....81
2.5.1 Expression of ADAMTS13.....81
2.5.2 Purification of rADAMTS13.....82
2.5.2.1 Desalting.....82
2.5.2.2 Nickel Affinity Chromatography.....82
2.6 ANALYSIS OF ADAMTS13 CONCENTRATION.....82
2.6.1 BCA Assay.....82
2.6.2 ADAMTS13 ELISA.....83

2.7 CLEAVAGE OF FULL-LENGTH VWF BY ADAMTS13 – OVERVIEW.....84
2.7.1 Cleavage by Cryo-Depleted Plasma.....84
2.7.2 Cleavage by Recombinant ADAMTS13.....84
2.8 GENERATION OF VWF PROTEOLYTIC FRAGMENTS BY TRYPSIN DIGESTION.....85
2.8.1 Ion-Exchange Chromatography.....85
2.8.2 H-antigen Blot.....85
2.8.3 N-terminal Sequencing.....86
2.9 GLYCOSIDASE DIGESTIONS.....86
2.10 LECTIN ELISA.....86
2.11 VWF:ADAMTS13 BINDING ASSAYS.....88
2.11.1 Modified VWF:ADAMTS13 Binding Assays.....89
2.12 GENERAL MOLECULAR BIOLOGY TECHNIQUES.....90
2.12.1 Agar Plates and Luria-Bertani (LB) Media ± Ampicillin.....90
2.12.2 Restriction Enzyme Digests.....90
2.12.3 Agarose Gel Electrophoresis.....90
2.12.4 Gel Extraction.....91
2.12.5 Ligations.....91
2.12.6 Transformations.....91
2.12.7 Isolation of Plasmid DNA.....92
2.12.8 Site-Directed Mutagenesis.....92
2.13 CLONING AND EXPRESSION VECTORS.....93
2.13.1 pBlueScript®.....93
2.13.2 pGEM-7Zf(+).....94
2.13.3 pcDNA3.1/*Myc*-His A(+).....95
2.14 GENERATION OF FULL LENGTH VWF EXPRESSION VECTOR AND VWF MUTANTS.....96
2.14.1 Overview.....96
2.14.2 Amplification of the 3' Terminal End of VWF.....97
2.14.2 Generation of VWF Restriction Digest Fragments.....97
2.14.3 Generation of VWF Glycan Mutants.....97
2.14.4 Completion of Wild Type and Mutant VWF Constructs.....98
2.14.5 Sequencing.....98

2.14.6 Glycerol Stock.....98
2.15 CELL CULTURE.....100
2.15.1 General Tissue Culture.....100
2.15.2 Revival of Human Embryonic (HEK) 293T cells from Liquid Nitrogen... 100
2.15.3 Cell Passage.....100
2.15.4 Transient Transfection of HEK293T cells.....100
2.16 FIXATION AND STAINING OF HEK293T CELLS FOR IMMUNOFLUORESCENCE MICROSCOPY.....101
2.17 STATISTICAL ANALYSIS.....101

CHAPTER 3: EFFECT OF ABO AND BOMBAY BLOOD GROUP ON PLASMA VWF LEVELS AND SUSCEPTIBILITY TO CLEAVAGE BY ADAMTS13.....103
3.1 INTRODUCTION.....103
3.2 COLLAGEN BINDING ASSAY (CBA).....104
3.3 ABO(H) ANTIGEN ON BOMBAY/PARA-BOMBAY VWF.....109
3.4 VWF:Ag LEVELS IN BOMBAY PLASMA.....111
3.5 PURIFICATION OF BLOOD GROUP SPECIFIC VWF.....113
3.6 PURIFICATION OF RECOMBINANT ADAMTS13.....115
3.7 CLEAVAGE OF BLOOD GROUP SPECIFIC VWF BY ADAMTS13.....117
3.8 ANALYSIS OF BOMBAY VWF MULTIMERIC STRUCTURE AND COLLAGEN BINDING ACTIVITY.....120
3.9 VWF GLYCANS, CONFIRMATION AND ADAMST13 PROTEOLYSIS....122
3.10 DISCUSSION.....124
3.10.1 Optimisation of Collagen Binding Assay and Multimer Gels.....124
3.10.2 Multimer Analysis.....125
3.10.3 Plasma VWF levels and the Bombay Phenotype.....126
3.10.4 ADAMTS13 Proteolysis of Blood Group Specific VWF.....128

CHAPTER 4: ANALYSIS OF VWF GLYCAN STRUCTURE.....131
4.1 INTRODUCTION.....131
4.2 *IN SILICO* ANALYSIS OF VWF GLYCAN STRUCTURE.....132
4.2.1 Prediction of O and *N*-linked Glycosylation Sites in VWF.....132
4.2.2 Alignment of VWF A2 Domain Sequences.....136

4.3 EXPERIMENTAL ANALYSIS OF VWF GLYCAN STRUCTURE.....139
4.3.1 Purification of VWF from Haemate P – Gel Filtration.....139
4.3.2 Purification of VWF from Haemate P –
Heparin-Sepharose Chromatography.....141
4.3.3 Preliminary Glycan Profile of VWF *N*-linked Glycans.....144
4.3.4 Presence of H-antigen on the ADAMTS13 Cleavage Products of VWF.....146
4.3.5 Trypsin Digestion of VWF and Ion-Exchange Chromatography.....148
4.3.6 Analysis of VWF Tryptic Fragment.....150
4.3.7 Analysis of Glycosylation and Presence of H-antigen on
VWF 55kDa Tryptic Fragment.....151
4.4 DISCUSSION.....153
4.4.1 *In Silico* Analysis of VWF Glycan Structure.....153
4.4.2 Experimental Analysis of VWF *N*-linked Glycans.....157

CHAPTER 5: EFFECT OF VWF GLYCAN MODIFICATION ON THE INTERACTION WITH ADAMTS13.....159
5.1 INTRODUCTION.....159
5.2 GLYCOSIDASE DIGESTION AND LECTIN ANALYSIS.....160
5.3 CONFIRMATION OF VWF *N*-LINKED GLYCAN REMOVAL.....163
5.4 MULTIMERIC STRUCTURE AND COLLAGEN BINDING OF GLYCAN MODIFIED VWF.....165
5.5 EFFECT OF VWF GLYCAN MODIFICATION ON SUSCEPTIBILITY TO CLEAVAGE BY ADAMTS13.....167
5.5.1 Effect of VWF Sialic Acid on Susceptibility to Cleavage by ADAMTS13..167
5.5.1.2 Effect of sialic acid removal from blood group specific VWF on Susceptibility to Cleavage by ADAMTS13.....170
5.5.2 Effect of VWF *N*-linked Glycans on Susceptibility to Cleavage by ADAMTS13.....172
5.5.3 Cleavage of PNG-VWF in the Absence of Urea.....175
5.6 Effect of VWF Glycan Modification on Binding of ADAMTS13 to VWF.....177
5.6.1 Optimisation of VWF:ADAMTS13 Plate Binding Assay.....177
5.6.2 Binding of ADAMTS13 to Neu and PNG-VWF.....181
5.6.3 Binding of ADAMTS13 to Globular VWF.....182
5.7 DISCUSSION.....185

5.7.1 Modification of VWF Glycan Structure.....185
5.7.2 Functional Analysis of Glycan Modified VWF.....187
5.7.3 Effect of Sialic Acid Removal on the Interaction with ADAMTS13.....187
5.7.4 Effect of *N*-linked Glycan Removal on the Interaction with ADAMTS13...189

CHAPTER 6: EXPRESSION AND CHARACTERISATION OF VWF A2 DOMAIN GLYCOSYLATION MUTANTS.....192
6.1 INTRODUCTION.....192
6.2 Construction of a Full Length VWF Expression Vector and Mutagenesis of N1515 and N1574.....193
6.2.1 Mutagenesis of pBlueScript to remove the KpnI restriction site.....195
6.2.2 PCR of VWF 3' end.....195
6.2.3 Further generation of VWF construct.....198
6.2.4 Generation of VWF glycan mutants.....200
6.2.5 Completion of FL-VWF construct and cloning into pcDNA3.1.....200
6.3 EXPRESSION OF RECOMBINANT VWF.....202
6.4 ANALYSIS OF NTERCELLULAR STORAGE OF VWF.....204
6.5 CHARACTERISATION OF VWF GLYCAN MUTANTS.....206
6.6 ANALYSIS OF rVWF GLYCAN STRUCTURE.....209
6.7 CLEAVAGE OF VWF GLYCAN MUTANTS BY ADAMTS13.....210
6.8 CLEAVAGE OF VWF GLYCAN MUTANTS IN THE ABSENCE OF UREA.....213
6.9 BINDING OF ADAMTS13 TO VWF N1574Q.....215
6.10 DISCUSSION.....216
6.10.1 Expression of Recombinant VWF.....216
6.10.2 Analysis of Recombinant VWF Glycan Structure.....218
6.10.3 ADAMTS13 Cleavage of VWF Glycan Mutants.....219

CHAPTER 7: DISCUSSION, CONCLUSIONS & FUTURE DIRECTIONS...221
7.1 DISCUSSION AND CONCLUSIONS.....221
7.2 FUTURE DIRECTIONS.....233
7.2.1 Role of VWF *N*-linked Glycosylation in Determining VWF Structure and Function.....233
7.2.2 Producing a Comprehensive Glycan Map of VWF.....234

7.2.3 Role of VWF O-linked Glycosylation.....235
7.2.4 Relationship between VWF Proteolysis and Clearance.....235

REFERENCES.....236

APPENDICES.....261
Appendix I – Restriction enzymes and buffers.....261
Appendix II – Oligonucleotide primers.....262
Appendix III – Buffers and solutions.....263

PUBLICATIONS ARISING FROM THIS WORK.....264
PAPERS PUBLISHED.....264
ABSTRACTS LEADING TO ORAL OR POSTER PRESENTATION.....264

LIST OF FIGURES

Figure 1.1 Dimerisation and multimerisation of VWF.....26

Figure 1.2 Post translational modification of VWF.....29

Figure 1.3 Domain structure of VWF.....31

Figure 1.4 VWF A domains.....35

Figure 1.5 Distribution of VWF multimers in VWD.....47

Figure 1.6 Domain structure of ADAMTS13.....49

Figure1.7 *N*-linked glycan processing.....55

Figure 1.8 Major structure of the O-linked glycans of VWF.....58

Figure 1.9 Primary glycan structure of a major *N*-linked glycan isolated from VWF.....59

Figure 1.10 Primary structure of a tetraantennary glycan isolated from VWF..... 60

Figure 1.11 VWF glycosylation sites.....61

Figure 1.12 Construction of ABO antigens.....70

Figure 2.1 pBlueScript cloning vector.....93

Figure 2.2 pGEM cloning vector..... 94

Figure 2.3 pcDNA3.1/*myc*-His A(+) mammalian expression vector.....95

Figure 2.4 VWF restriction sites and digestion fragments.....96

Figure 2.5 Outline of cloning steps used to generate FL-VWF constructs.....99

Figure 3.1 Optimal coating collagen concentration.....106

Figure 3.2 Collagen binding assay optimisation.....107

Figure 3.3 CBA standard curve.....108

Figure 3.4 H antigen on VWF ELISA..... 110

Figure 3.5 H on VWF western blot.....110

Figure 3.6 VWF levels in Bombay plasma..... 112

Figure 3.7 Purification of blood group specific VWF from plasma.....114

Figure 3.8 Purification of recombinant ADAMTS13..... 116

Figure 3.9 CBA analysis ADAMTS13 cleavage of blood group specific VWF..... 118

Figure 3.10 Multimer gel analysis of ADAMTS13 cleavage of blood group specific VWF.....119

Figure 3.11 Analysis of Bombay VWF collagen binding and multimeric distribution.....121
Figure 3.12 Effect of increasing urea concentration on susceptibility of blood group specific VWF to ADAMTS13 proteolysis..... 123

Figure 4.1. NetOGlyc prediction of O-linked glycosylation of VWF..... 134
Figure 4.2. NetNGlyc prediction of *N*-linked glycosylation of VWF.....135
Figure 4.3. Protein sequence alignment of the VWF A2 domain from 59 species...137
Figure 4.4 Gel filtration of Haemate P.....140
Figure 4.5 Effect of sample loading flow rate on VWF recovery from a Heparin-Sepharose column..... 142
Figure 4.6 Heparin-Sepharose purification of gel filtered Haemate P.....143
Figure 4.7 Preliminary glycan profile of VWF *N*-linked glycans.....145
Figure 4.8 H-antigen on ADAMTS13 cleavage products..... 147
Figure 4.9 Ion-exchange chromatography of trypsin digested VWF..... 149
Figure 4.10 Analysis of VWF tryptic fragment.....150
Figure 4.11 Analysis of glycosylation and presence of H-antigen on VWF 55kDa tryptic fragment.....152
Figure 4.12 Predicted model of the VWF A2 domain.....156

Figure 5.1 Lectin analysis of α-2(3,6,8,9) neuraminidase and β-galactosidase digested VWF.....161
Figure 5.2 Lectin analysis of PNGase F and α-2(3,6,8,9) neuraminidase digested VWF.....162
Figure 5.3 Conformation of VWF *N*-linked glycan removal.....164
Figure 5.4 Multimer analysis of glycan modified VWF.....165
Figure 5.5 Binding of glycan modified VWF to collagen.....166
Figure 5.6 Collagen binding assay of ADAMTS13 cleavage of Ctrl and Neu-VWF.....168
Figure 5.7 Multimer gel analysis of ADAMTS13 cleavage of Ctrl and Neu-VWF.....169
Figure 5.8 The effect of sialic acid removal from blood group specific VWF on susceptibility to cleavage by ADAMTS13..... 171

Figure 5.10 Collagen binding assay of ADAMTS13 cleavage of control and PNG-VWF.....173
Figure 5.11 Cleavage of Neu/PNG-VWF.....174
Figure 5.12 Cleavage of PNG-VWF in the absence of urea.....176
Figure 5.13 Optimal VWF plate coating concentration.....179
Figure 5.14 Binding of ADAMTS13 to VWF +/- EDTA.....179
Figure 5.15 Binding of ADAMTS13 active site mutant to VWF.....180
Figure 5.16 Binding of ADAMTS13 to immobilised VWF.....181
Figure 5.17 Binding of ADAMTS13 to globular VWF.....183
Figure 5.18 Binding of ADAMTS13 to collagen bound VWF.....184

Figure 6.1 VWF restriction sites and digestion fragments.....194
Figure 6.2 Restriction enzyme analysis of mutagenesis of pBS.....196
Figure 6.3 PCR and generation of VWF 3' end.....197
Figure 6.4 VWF restriction fragments and analysis of pBS^{-KpnI}VWF(BamHI-AgeI).....199
Figure 6.5 Analysis of pBS^{-KpnI}FL-VWF.....201
Figure 6.6 Expression of rVWF in HEK293T cells.....203
Figure 6.7 Analysis of intercellular storage of VWF.....205
Figure 6.8 Characterisation of VWF glycan mutants.....207
Figure 6.9 Collagen binding analysis of rVWF.....208
Figure 6.10 Lectin analysis of rVWF glycan structure.....209
Figure 6.11 Collagen binding assay of ADAMST13 cleavage of VWF glycan mutants.....211
Figure 6.12 Multimer gel analysis of ADAMST13 cleavage of VWF glycan mutants.....212
Figure 6.13 Collagen binding assay of ADAMTS13 cleavage of VWF glycan mutants in the absence of urea.....214
Figure 6.14 Binding of ADAMTS13 to recombinant VWF.....215

Figure 7.1 Distances between N1574 and A2 domain surface residues important forADAMTS13 binding.....229

LIST OF TABLES

Table 1.1 Carbohydrate composition of VWF.....57

Table 2.1 Primary and secondary antibodies and their concentrations used for western blotting.....81

Table 2.2 Lectins, their targets and dilutions used for western blot and lectin ELISA.....87

ABBREVIATIONS

Å	Angstrom
Abs	Absorbance
ADAMTS13	A Disintegrin and Metalloprotease with ThromboSpondin motif
ADP	Adenosine diphosphate
AFM	Atomic force microscopy
As	Asialo
Ag	Agalacto
As/Ag	Asialo/Agalacto
BCA	Bicinchoninic acid
B_{max}	Maximal binding
bp	Base pair
CBA	Collagen binding assay
cDNA	Complementary deoxyribonucleic acid
CHO	Chinese hamster Ovary
CIAP	Calf intestinal alkaline phosphatase
CK	Cysteine knot
CMV	Cytomegalovirus
ConA	Concanavalin A
CUB	Complement components C1r/C1s, Uegf and Bone morphogenic protein 1
DDAVP	1-deamino-8-D-arginine vasopressin
ddH_2O	double distilled water
DMSO	Dymethyl sulfoxide
DNA	Deoxyribonucleic acid
dNTP	deoxynucleoside triphosphate
EBL	Elderberry bark lectin
EC	Endothelial cells
E.coli	*Escherichia coli*
EDTA	Ethylenediaminetetraacetic acid
ELISA	Enzyme-linked immunosorbent assay
Endo F	endo-β-*N*-acetylglucosaminidase F
ER	Endoplasmic reticulum
FBS	Fetal bovine serum
FL-VWF	Full length VWF
FPLC	Fast protein liquid chromatography
FVIII	Factor VIII
GP	Glycoprotein
HEK	Human embryonic kidney fibroblast
HMW	High molecular weight
HRP	Horseradish peroxidase
HUVEC	Human Umbilical Vein Endothelial Cells
kb	Kilobase
k_{cat}/k_m	Catalytic efficiency or specificity constant
K_D	Equilibrium dissociation constant
kDa	Kilodaltons
LAD	Ladder
LB	Luria-Bertani medium
LMW	Low molecular weight
Log	Logarithm

M	Molar
mA	Milliamps
MCS	Multiple cloning site
mg	Milligram
Mins	Minutes
ml	Millilitre
mM	Micromolar
MMW	Medium molecular weight
mRNA	Messenger ribonucleic acid
MW	Molecular weight
n	Number
ng	Nanogram
N-linked	Asparagine linked
nM	Nanomolar
nm	Nanometre
NP	Normal plasma
O-linked	Serine/Threonine linked
OPD	O-phenylenediamine dihydrochloride
Pa	Pascal
pBS	pBlueScript
PBS	Phosphate buffered saline
PBS-T	Phosphate buffered saline and Tween 20
PCR	Polymerase chain reaction
PDI	Protein disulphide isomerise
PEI	Polyethylenimine
pM	Picomolar
PNGase F	Peptide: *N*-Glycosidase F
r	Recombinant
RCA-I	Ricinus Communis Agglutinin I
RER	Rough endoplasmic reticulum
rpm	Revolutions per minute
RT-PCR	Reverse transcription-polymerase chain reaction
Sec	Seconds
SDS	Sodium dodecyl sulphate
SDS-PAGE	Sodium dodecyl sulphate polyacryilamide gel electrophoresis
SPR	Surface plasmon resonance
t½	Half-life
TBS	Tris buffered saline
TC	Tris-citrate
TGN	Trans Golgi network
TSP-1	Thrombospondin-1
TSR	Thrombospondin repeat
U	Unit
UL-VWF	Ultra large Von Willebrand Factor
UV	Ultraviolet
µg	Microgram
µl	Microlitre
µM	Micromolar
V	Volts
v/v	volume per unit volume

VWD	Von Willebrand Disease
VWF	Von Willebrand Factor
VWF:Ag	Von Willebrand Factor antigen
VWF:CB	Von Willebrand Factor collagen binding
VWFpp	Von Willebrand Factor propeptide
wtVWF	wild type VWF
WP	Weibel-Palade bodies

SUGAR ABBREVIATIONS AND SYMBOLS

Fuc	Fucose
Gal	Galactose
GalNAc	*N*-acetylgalactosamine
Glc	Glucose
GlcNAc	*N*-acetylglucosamine
Man	Mannose
NeuAc	Sialic acid

CHAPTER 1

1. INTRODUCTION

1.1 VON WILLEBRAND FACTOR

Von Willebrand Factor (VWF) is a large multimeric plasma glycoprotein essential to normal haemostasis. Firstly; VWF acts as the carrier molecule for pro-coagulant Factor VIII (FVIII), extending its half life within the circulation by protecting it from proteolytic degradation by proteases such as activated protein C.[1] Secondly, VWF supports platelet adhesion to thrombogenic surfaces at sites of vascular injury.[2]

1.2.1 VWF Tissue Distribution and Sites of Synthesises

VWF is found in plasma, endothelial cells (EC), megakaryocytes and the subendothelial matrix. *In-vivo* biosynthesis of VWF is limited to EC and megakaryocytes.[3] In EC, VWF is either constitutively secreted or stored in Weibel-Palade bodies and megakaryocyte VWF is stored in the α-granules of its platelet progeny.[4] The majority of circulating VWF is derived from the endothelium. In a porcine model with hereditary VWF deficiency, total body irradiation and subsequent transplantation of normal bone marrow restores a normal platelet count, but does not re-establish the plasma VWF pool.[5] Evidence also suggests that expression of VWF may vary between vascular beds. Immunohistochemistry performed on porcine blood vessels showed that VWF was consistently present in venous EC, with the exception of the pulmonary vein, but was absent from the majority of arterial EC, except the distal abdominal aorta, the vasa vasorum of the thoracic aorta and the pulmonary artey.[6] Analysis of VWF expression in mice using quantitative RT-PCR and in-situ hybridisation analysis, demonstrated that VWF mRNA levels were highest in EC derived from the spleen, aorta, lung and spleen, with the lowest levels in the liver, gut and kidney. It was also again demonstrated that VWF expression was higher in venous EC than arterial EC.[7]

1.2.2 VWF Gene Structure

The VWF gene is located distally on the short arm of chromosome 12 (12p13.2) and spans ~180kb of genomic DNA. After transcription the mRNA product is spliced to 52 exons.[8] Exon 1 represents a 5' untranslated sequence,[9] exons 2-18 encode a signal and

propeptide sequence and exons 19-52 encode for the mature VWF subunit.[8] A non-processed VWF pseudogene is located on chromosome 22 (22q11) which is ~29kb in length, spanning exons 23-34 of the functional VWF gene and has 97% sequence homology.[10,11] The VWF pseudogene contains multiple stop codons, indicating that it is not a functional human gene.[10]

1.2.3 Transcriptional Regulation of the VWF Gene

Regulation of VWF gene expression has been investigated using the promoter sequence linked to a reporter gene.[12] The promoter sequence comprised of base pairs -487 to +247 (numbered relative to the transcription start site) was sufficient to mediate endothelial specific expression of the reporter gene. Deletion analysis demonstrated that a 112bp fragment: -90 to +22, contained core promoter activity.[12,13] As well as the transcription start site, this region also contains a TATA box at position 30 and a CCAAT box located 8bp downstream of the TATA box. Deletion analysis also demonstrated a strong silencer sequence upstream of the core promoter at base pairs -487 to -312 that is activated by an *NF-1* protein that was shown by DNase footprint analysis to interact with nucleotides -440 to -470.[14]

The effect of the silencer sequence is counteracted by transcription factors of the GATA family, that bind to a positive regulatory sequence in exon one, at base pairs +150 to +247. This positive regulatory element is therefore responsible for overcoming the effect of the silencer region and also confers EC specificity on the core promoter.[12] DNA sequence analysis of the positive regulatory sequence predicted a GATA binding site at +222 and also an *SP1* binding site at +180. Mutation of the *SP1* site had no effect on transcriptional activity, but mutation of the GATA site resulted in significant reduction of reporter gene expression, demonstrating the positive regulatory sequence with an intact GATA binding site is required to active VWF gene expression in EC.[12] Finally another negatively regulatory element has been located in the region -89 to +244, that is able to bind the *Oct-1* transcriptional repressor.[13]

1.3 VWF SYNTHESIS AND PROCESSING

Following translation of the VWF mRNA, pre-pro-VWF is synthesised, comprised of a 21 amino acid N-terminal signal peptide, a 741 amino acid pro-peptide and a 2050 amino acid mature protein. Pre-pro-VWF undergoes extensive post-translational modifications as it passes through the endoplasmic reticulum (ER) to either be stored or

secreted.[15] VWF is also unique in that it undergoes two distinct polymerisation steps in separate organelles; dimers of VWF are formed in the ER and multimerisation occurs in the Golgi or post-Golgi network.

1.3.1 *N*-linked Glycosylation

The signal peptide of the primary VWF translation product directs the protein to the rough endoplasmic reticulum (RER) where the signal peptide is cleaved and initial *N*-linked glycosylation occurs, resulting in the addition of high-mannose sugar structures to a predicted 16 asparagine residues; twelve in the mature subunit and four in the pro-peptide.[16] *N*-linked glycosylation is essential for dimerisation of VWF, since treatment of endothelial cells with Tunicamycin, an antibiotic that prevents N-linked glycosylation[17], results in the accumulation of pro-VWF monomers in the ER.[18] The *N*-linked glycans of VWF are discussed in further detail in section 1.15.2.

1.3.2 Dimerisation

Dimerisation of VWF monomers also occurs in the ER through the formation of intersubunit disulphide bonds between cysteine residues located in the C-terminal region of each mature VWF monomer.[19,20] Studies have demonstrated that monomeric VWF is retained in the ER by binding to ER regulatory proteins, such as BiP, and is subsequently degraded.[18,21]

1.3.3 *N*-linked Glycan Processing

Following dimerisation, VWF is transported to the Golgi apparatus for modification of the *N*-linked glycan chains. Mannose residues are trimmed and there is addition of galactose and terminal sialic acid residues, producing complex glycan structures.[22] Interestingly, further carbohydrate processing of VWF may occur in the trans-Golgi network (TGN) where the A, B and H blood group glycosyltransferases are present. It has been demonstrated that the *N*-linked glycans of VWF present the ABO(H) blood group antigens.[23]

1.3.4 O-linked Glycosylation

There is further addition of carbohydrate structures in the Golgi with the attachment of a predicted ten O-linked glycan chains to serine and threonine residues.[16] At present there

is no experimental evidence to suggest that the O-linked glycans present the ABO(H) blood group sugars.

1.3.5 Sulphation

Sulphation of VWF takes place in the TGN. A study by Carew demonstrated that one of the N-terminal *N*-linked glycans is sulphated as are *N*-linked glycans present in the propeptide.[24] Furthermore, inhibition of sulphation does not affect VWF multimerisation, storage or stability.[24]

1.3.6 Multimerisation

Multimerisation of pro-VWF dimers occurs in the TGN by the formation of intermolecular disulphide bonds between cysteine residues located at the N-terminal ends of adjacent molecules.[20,25] Multimerisation of VWF is dependent on the presence of calcium and an acidic pH (~6.0), conditions typical of the TGN. Treatment of HUVEC's with ammonium chloride causes increased pH within acidic organelles and results in the secretion of un-multimerised VWF dimers and treatment with chelating agents such as EDTA also inhibit multimerisation.[18,26] Furthermore the presence of the propeptide is essential for multimerisation.[21] Recombinant expression of VWF with the propeptide sequence deleted results in the secretion of VWF dimers.[27] Co-transfection of cells with sequences encoding for the VWF propeptide, and VWF with the propeptide sequence deleted, result in the secretion of fully multimerised VWF, demonstrating that the propeptide does not need to be a continuous part of the VWF structure.[21] The propeptide contains vicinal cysteine motifs similar to motifs found at the active site of protein disulphide isomerise (PDIs), suggesting that the propeptide may have intermolecular PDI-like enzyme activity involved in the formation of disulphide bonds required for multimerisation.[28]

1.3.7 Propeptide Cleavage

Cleavage of the propeptide takes place in the TGN and is mediated by the enzyme furin,[29] with cleavage occurring at the C-terminal end of the RSKR sequence. Pro-VWF is cleaved *in-vitro* when it is co-transfected with furin, but not with other endoproteases.[30] After furin cleavage, the propeptide remains non-covalently associated with VWF.[29] The propeptide remains associated to VWF until it is secreted with mature VWF in equimolar amounts, but is found in the circulation at an ~10 fold lower concentration due to its shorter half-life.[31-33]

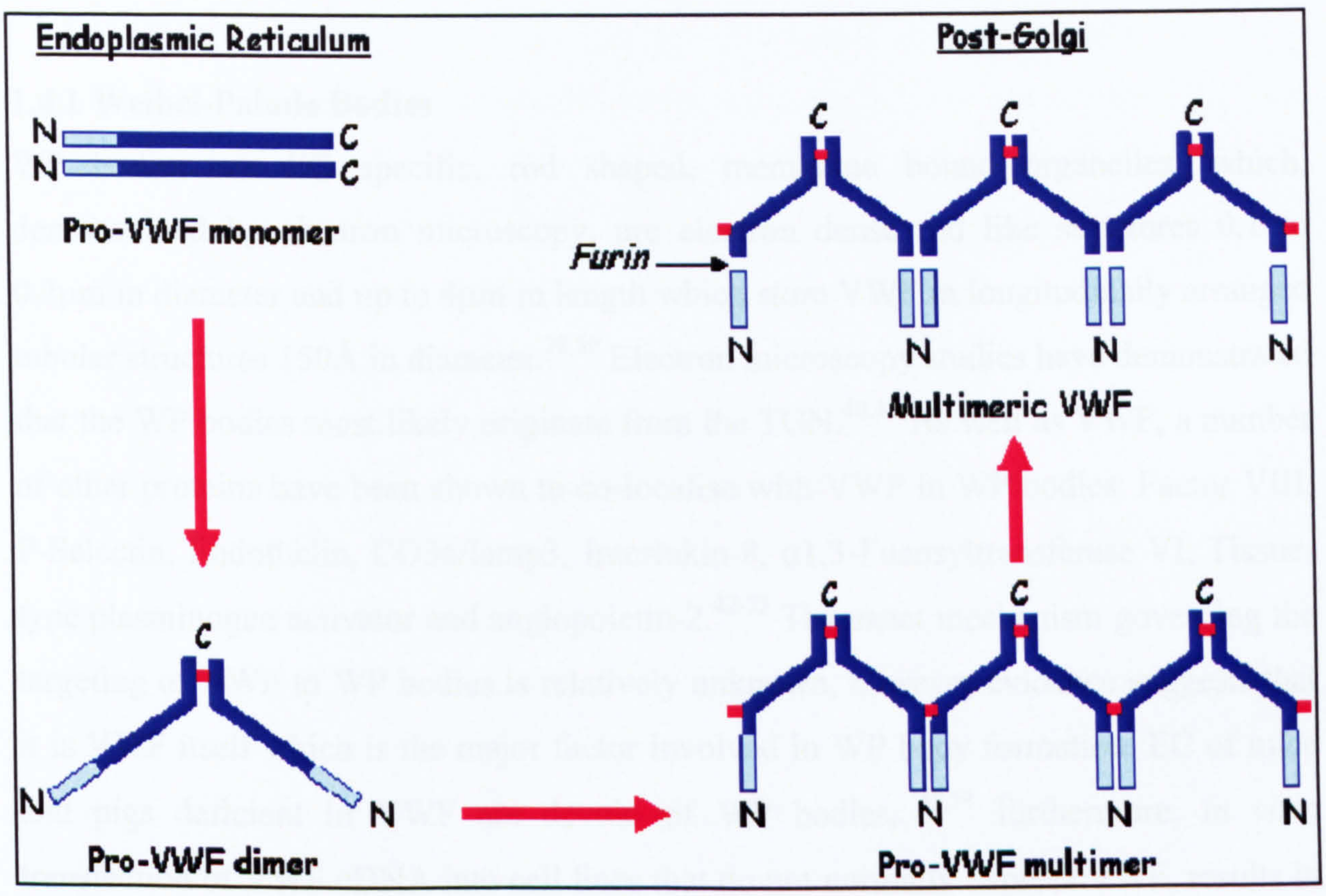


Figure 1.1 Dimerisation and multimerisation of VWF

Within the ER, VWF dimers are formed by intersubunit disulphide bonds between cysteine residues located in the C-terminal region of each mature VWF monomer. Multimerisation of pro-VWF dimers occurs in the post-Golgi by the formation of intermolecular disulphide bonds between cysteine residues located at the N-terminal ends of adjacent molecules. Following multimerisation, the propeptide is cleaved by furin, and remains non-covalently associated with VWF.

1.4 VWF STORAGE AND SECRETION

The mature VWF product maybe either constitutively secreted or stored in Weibel-Palade bodies in EC. Megakaryocyte VWF is stored in the α-granules of the platelet progeny and is released upon platelet activation.[34] The majority of VWF synthesised by EC is constitutively secreted (~95%) and is comprised of low to medium molecular weight VWF multimers.[35] The remaining VWF stored in Weibel-Palade (WP) bodies is comprised of the highest molecular weight and most biologically active multimers.[36] VWF circulates in plasma at a concentration of ~10μg/ml with a half-life of ~12 hours.[31,37]

1.4.1 Weibel-Palade Bodies

WP bodies are EC specific, rod shaped, membrane bound organelles, which, demonstrated by electron microscopy, are electron dense rod like structures 0.1 to 0.2μm in diameter and up to 4μm in length which store VWF in longitudinally arranged tubular structures 150Å in diameter.[38,39] Electron microscopy studies have demonstrated that the WP bodies most likely originate from the TGN.[40,41] As well as VWF, a number of other proteins have been shown to co-localise with VWF in WP bodies: Factor VIII, P-Selectin, Endothelin, CD36/lamp3, Interlukin-8, α1,3-Fucosyltransferase VI, Tissue-type plasminogen activator and angiopoietin-2.[42-52] The exact mechanism governing the targeting of VWF to WP bodies is relatively unknown, however evidence suggests that it is VWF itself which is the major factor involved in WP body formation. EC of mice and pigs deficient in VWF are devoid of WP bodies, [53,54] furthermore, *in vitro* transfection of VWF cDNA into cell lines that do not normally express VWF, results in the formation of VWF containing storage granules that share morphology very similar to WP bodies.[41,55-57] The exact structural aspects of VWF that lead to the genesis of WP bodies are unknown. One hypothesis suggests that multimerisation of VWF in the TGN is a prerequisite for WP body formation, since only cells that can synthesise multimeric VWF form WP-like storage granules. In addition, cells transfected with VWF cDNA containing mutations that result in defective multimerisation are devoid of WP-like structures.[41,55,58] However, contrary to this a number of studies have shown that multimerisation is not required for WP formation and VWF storage.[28,57] VWF expressed with the C domains deleted so that dimerisation could not occur, still formed storage granules.[57] Also, in a recent study, three mutations, Cys1225Gly, Cys788Arg and Arg273Trp, that cause multimerisation defects, were all shown to form WP-like

structures when transfected into HEK293T cells,[56] although changes were observed in the length of time required to form the storage structures and in the length and number of WP-like bodies formed.[56]

There is also some conflicting evidence as to whether cleavage of the propeptide is required for WP body formation. In AtT-20 or RIN 5F cells, an intact furin cleavage site was required for storage of VWF.[59] However, in monkey kidney CV-1 cells expression of a VWF mutant that lacks the propeptide cleavage site but is able to form covalently linked polymers, resulted in the formation of Weibel-Palade body-like vesicles[41] and this has also been observed in other subsequent studies.[60]

There is strong evidence however, that the propeptide is essential for WP body formation. VWF expressed lacking the propeptide was shown not to form WP-like structures,[61] however, expression of the propeptide alone was sufficient for the formation of storage granules.[61] If the propeptide was co-expressed with propeptide deleted VWF, then storage granules were observed. The propeptide is also able to direct non-related VWF proteins to storage granules. Expression of a chimeric construct, with the VWF propeptide and C3α protein demonstrated that the presence of the propeptide re-routed a normally constitutively secreted protein to the regulated storage pathway.[62]

1.4.2 Regulated Secretion

VWF and associated WP body proteins are released in response to a number of agonists. In all cases the secretion of the WP body contents involves the translocation of the WP bodies from the cytoplasm towards the plasma membrane and the fusion of these vesicles with the plasma membrane.

Thrombin, histamine, fibrin, complement components C5a and C5b-9, oxidative stress and leukotrienes have been shown to induce VWF release by mediating a rise in the concentration of cytosolic free Ca^{2+} ($[Ca^{2+}]$).[63-70] Regulated secretion of VWF can also be induced by secretagogues, such as epinephrine, adenosine or the vasopressin analogue DDAVP (1-deamino-8-D-arginine vasopressin).[71-73] DDAVP is used in the clinical treatment of VWD and several other bleeding disorders.[72] Physical activity and other acute stresses raise plasma VWF levels; evidence suggests that this is mediated by epinephrine induced EC secretion.[74] Finally other factors such as shear stress or hypoxia have also been shown to induce EC to secrete the store of VWF.[75,76]

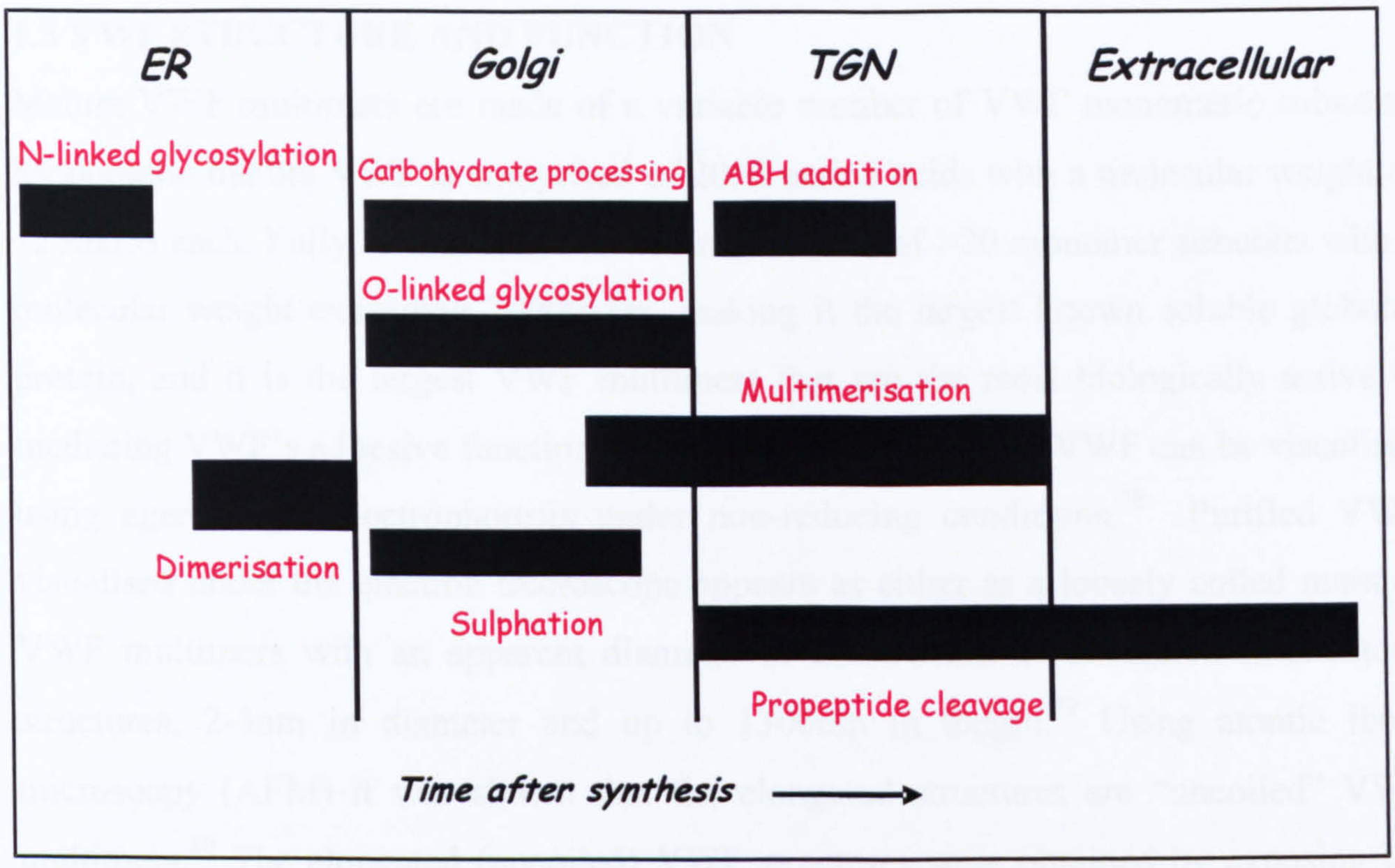


Figure 1.2 Post translational modification of VWF

Following translation the signal peptide directs VWF to the ER where the signal peptide is cleaved and initial *N*-linked glycosylation occurs and C-terminal dimers are formed. The molecule passes to the Golgi where there is further carbohydrate processing, the addition of O-linked carbohydrates and sulphation of N-terminal *N*-linked glycans. Further carbohydrate processing may take place in the TGN with the addition of ABO blood group sugars to *N*-linked glycan chains. Also in the TGN, VWF multimers are formed by intermolecular disulphide bonds between N-terminal cysteines of adjacent molecules. Cleavage of the propeptide occurs, and the VWF molecule is either constitutively secreted into the circulation or stored within the cell.

1.5 VWF STRUCTURE AND FUNCTION

Mature VWF multimers are made of a variable number of VWF monomeric subunits. Monomeric mature VWF is comprised of 2050 amino acids with a molecular weight of ~250kDa each. Fully multimerised VWF may consist of >20 monomer subunits with a molecular weight exceeding 20000kDa, making it the largest known soluble globular protein, and it is the largest VWF multimers that are the most biologically active in mediating VWF's adhesive function.[77] The multimeric nature of VWF can be visualised using agarose gel electrophoresis under non-reducing conditions.[78] Purified VWF visualised under the electron microscope appears as either as a loosely coiled mass of VWF multimers with an apparent diameter of 200-300nm or elongated filamentous structures, 2-3nm in diameter and up to 1300nm in length.[79] Using atomic force microscopy (AFM) it was shown that the elongated structures are "uncoiled" VWF multimers.[80] The elongated (uncoiled) VWF structures were obtained by exposing the molecule to shear stress; with 35dyn/cm^2 being the critical shear stress needed to cause VWF to change confirmation to an extended structure exposing intra-molecular domains.[80] This level of shear stress is within physiological levels found in the arterial circulation.[81] As will be discussed later, this conformational change in VWF is essential for various functional aspects of the molecule; for example the interaction with GPIbα and exposure of the cleavage site for the VWF cleaving protease. To mimic the unravelling effect of shear stress on VWF *in vitro,* denaturants such as urea and guanidine HCl or modulators such as the antibiotic, ristocetin or the snake venom, botrocetin may used.

Each pro-VWF monomer is comprised of four types of homologous repeating domains. There are four D domains, a truncated D domain, three A domains, three B domains and two C domains and a CK domain arranged in the order:

NH_2-D1-D2-D'-D3-A1-A2-A3-D4-B1-B2-B3-C1-C2-CK-COOH

The D1 and D2 domains represent the propeptide and are removed from the mature molecule as previously discussed. Each mature subunit contains a large number of cysteine residues (169 out of 2050 (~8%)) and in the secreted protein there are no free sulphydryl groups, suggesting that all cysteine residues not forming intermolecular disulphide bridges are paired in intramolecular disulphide bonds.[16,19,20]

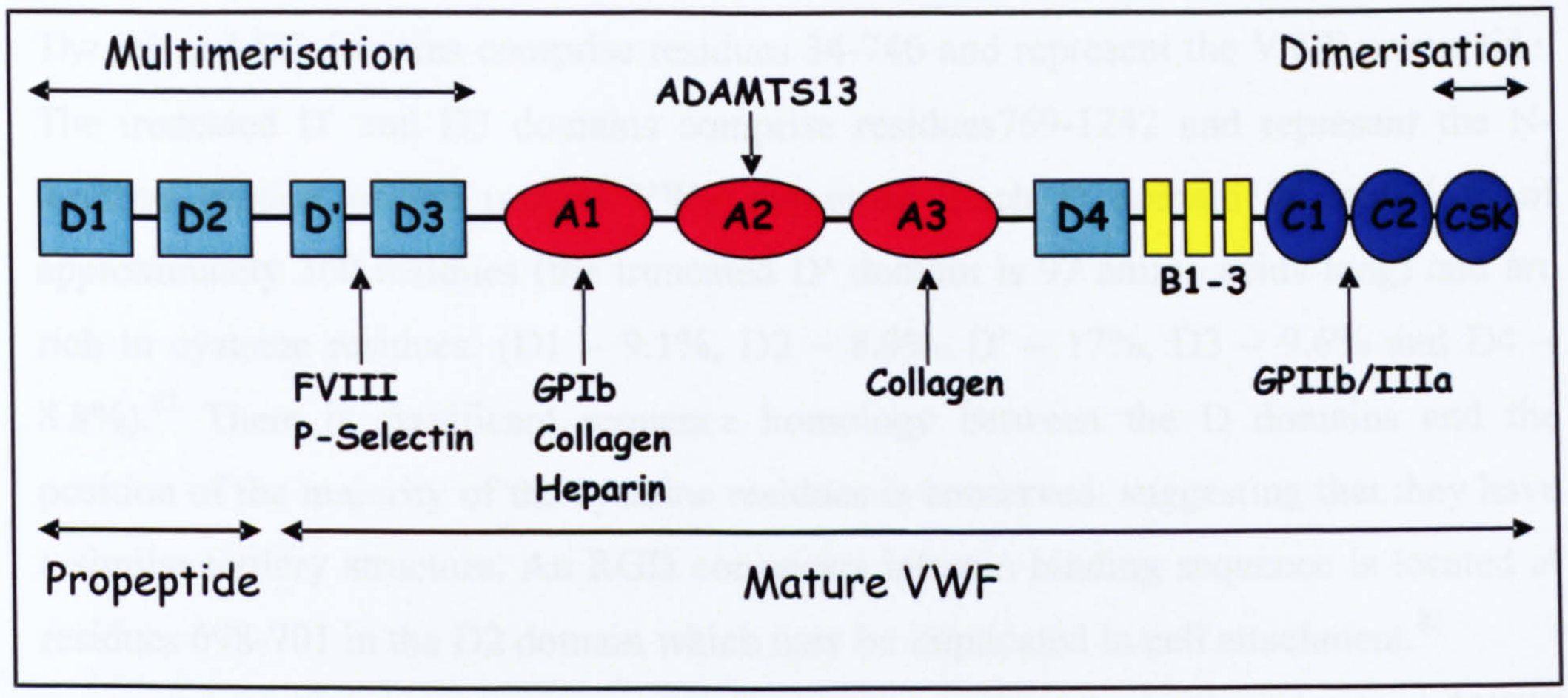


Figure 1.3 Domain structure of VWF

VWF is comprised of four homologous repeating domains: four D domains, a truncated D' domain, three A domains, three B domains, two C domains and a cysteine knot domain (CSK). VWF dimers are formed by intramolecular disulphide bonds at the C-terminus and multimers form by intramolecular disulphide bonds at the N-terminus. Shown on the figure are the binding site for various ligands and the ADAMTS13 cleavage site within the A2 domain.

1.6 THE D DOMAINS

The D1 and D2 domains comprise residues 34-746 and represent the VWF propeptide. The truncated D' and D3 domains comprise residues769-1242 and represent the N-terminal portion of the mature VWF monomer. Each D domain is comprised of approximately 360 residues (the truncated D' domain is 97 amino acids long) and are rich in cysteine residues. (D1 – 9.1%, D2 – 8.9%, D' – 17%, D3 – 9.6% and D4 – 8.8%).[82] There is significant sequence homology between the D domains and the position of the majority of the cysteine residues is conserved, suggesting that they have a similar tertiary structure. An RGD consensus integrin binding sequence is located at residues 698-701 in the D2 domain which may be implicated in cell attachment.[82]

As previously discussed the propeptide (D1-D2) is required for multimerisation of VWF and direction to VWF storage granules.[61] The propeptides of several hormones and enzymes have been demonstrated to aid the correct folding of the mature protein acting as molecular chaperones.[83,84] Studies have shown that the propeptides of the hormones: subtilisin, preprosomatostatin, lactase-phlorizin hydrolase and prouroguanylin assist in protein folding and stabilisation prior to protein maturation.[85-89] Analogous to this, the VWF propeptide functions as an intramolecular chaperone folding VWF into the correct orientation necessary for proper intermolecular disulphide bond formation.[90] Furthermore, evidence suggests that the VWF propeptide needs to be intact for multimerisation to occur. Deletion of either the D1 or D2 domain results in the production of un-multimerised VWF dimers.[91] Moreover, studies on a number of naturally occurring mutations in the VWF propeptide, (Tyr87Ser,[90] Arg273Trp,[92] Asn528Ser,[93] Gly550Arg,[94] Cys623Trp[95] and 625insGly[95]) show that although the mutations do not occur in close proximity to any functional areas, they all result in aberrant multimerisation.[90]

The D' and D3 domains comprise the N-terminal portion of the mature VWF subunit and contain the sites for multimerisation, and the FVIII and P-Selectin binding sites. Both the D' and D3 domains are required for multimerisation to occur. A study by Voorberg *et al* demonstrated that recombinant VWF produced with deletion of either the D' or D3 or both domains, did not form multimers.[25] In addition this study showed that a VWF construct composed of only the D1-D2-D'-D3 domains was able to form intermolecular disulphide bonds, further highlighting that multimerisation is independent from dimerisation.[25]

Digestion of plasma VWF with V8-protease and trypsin generates a dimeric fragment spanning residues 1036-1491 with the flanking regions being monomeric.[96] This demonstrated that all the intersubunit disulphide bonds must occur within these residues. Thus the D3 domain contains the cysteine residues necessary for multimer formation. In a study by Azuma *et al* a smaller VWF fragment was isolated spanning residues 1212-1491. Individual mutation of cysteine residues 1222, 1225 and 1227 to alanine prevented polymerisation of a recombinant VWF fragment spanning residues 1204-1493.[97] However, a study by Dong *et al* showed that mutation of these residues in full length VWF (FL-VWF) did not affect processing, multimerisation or secretion of VWF, suggesting that intersubunit disulphide bonding differs between FL-VWF and truncated VWF.[98] Furthermore this study showed that Cys1142 was essential for multimerisation. Mutation to alanine resulted in the secretion of VWF dimers only.[98] Other studies have implicated Cys1130, Cys1149, Cys1157 and Cys1234 as important cysteine residues required for multimerisation.[99,100]

Although the D' domain does not contain cysteine residues involved in intersubunit disulphide bond formation, mutations occurring in the D' domain have an adverse effect on VWF multimerisation. For example the naturally occurring C788R mutation causes the formation of only low molecular weight multimers,[101] as does the C804F mutation.[102] This suggests that although the D' domain does not directly participate in intersubunit disulphide bonding, correct folding of the D' domain is essential for multimerisation to occur, thus it may have a molecular chaperone type role comparable to that of the propeptide.

1.6.1 Factor VIII Binding

As mentioned previously, VWF acts as the carrier molecule for FVIII. This is essential to the survival of FVIII in the circulation,[103] prolonging its half-life from 2 to 12 hours,[103] stabilising the FVIII molecule and protecting it from inactivation by protein C[104,105] and preventing activation and inactivation by Factor Xa.[106,107] Furthermore, VWF also acts a cofactor for thrombin catalyzed cleavage of the FVIII light chain.[108]

FVIII circulates with VWF in a non-covalently associated complex, (99% VWF:1% FVIII.) FVIII binds to VWF with a K_D of 200-400pM[109], but the affinity of FVIII for VWF is decreased when VWF is bound to collagen (K_D 5nM).[110] All sizes of VWF multimers bind FVIII with the same affinity.[111] The formation of the VWF:FVIII complex has a rapid association rate ($K_{on} = 5.9 \times 10^6\ M^{-1}s^{-1}$), this rapid formation of the

complex prevents the interaction of FVIII with other ligands.[112] The binding site for FVIII is located in the D' and D3 domains, (residues 769-1242)[113,114] with a possible critical role for resides 841-859.[115-117]

1.6.2 P-Selectin Binding

The D'D3 domains of VWF have also been shown to participate in binding to P-Selectin. A study by Padilla *et al* demonstrated that newly secreted ultralarge VWF multimers are anchored to EC by P-Selectin. CHO cells expressing P-Selectin were able to anchor VWF molecules to their surface under flow conditions, visualised by the appearance of string like structures able to support platelet adhesion.[118] Using a cellular based system, it was confirmed that P-Selectin is dependent on VWF for recruitment to WP bodies, and was shown that P-Selectin interacts with VWF via the VWF D'D3 domains.[119]

1.7 A1A2A3 DOMAINS

VWF contains 3 homologous A domains that span residues 1260-1874, (A1 domain 1260-1453, A2 domain 1498-1668, A3 domain 1691-1874.)[120] The three domains share approximately 30% homology. The A1 and A3 domains both contain an intramolecular disulphide bond that forms loops of approximately 187 residues (Figure 1.3). The A2 domain lacks this conserved cysteine loop. The crystal structures for both the A1 and A3 domains have been resolved.[121,122] A domains are also found in other proteins, including immune system leukocyte integrins LFA-1 and Mac-1, components of the complement system, Factor 2B and component C and cell adhesion molecules, in all these molecules, A domains play a role in mediating interactions with specific ligands.[123]

The A1 domain of VWF contains binding sites for the platelet receptor GPIbα,[96] heparin,[124] sulphatides,[125,126] minor binding sites for collagen types I and III and a binding site for collagen type VI. The A2 domain contains the cleavage site for the VWF cleaving protease ADAMTS13, the linker region between A1 and A2 is involved in leukocyte binding[127] and the A3 domain contains the major collagen binding site.

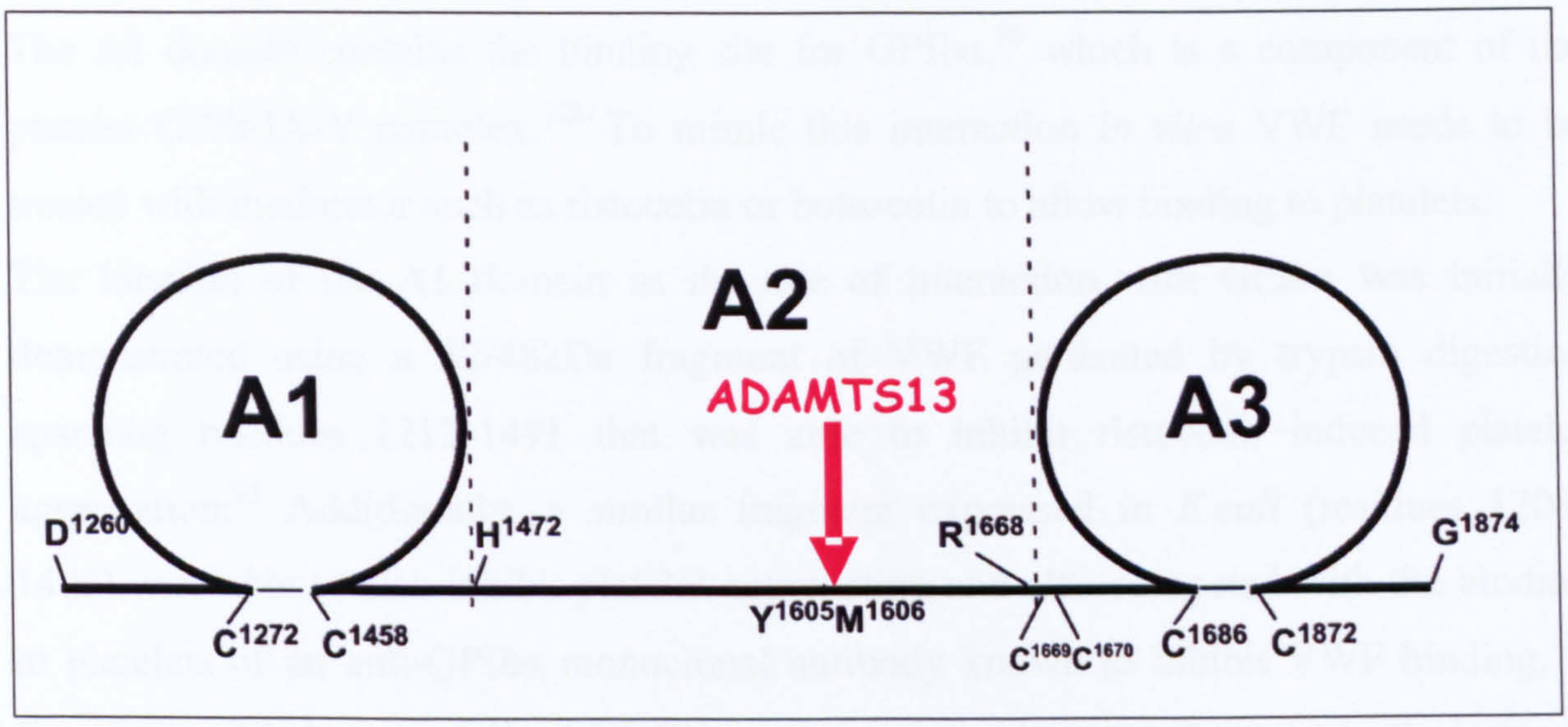


Figure 1.4 VWF A domains

Both the A1 and A3 domain contain an intramolecular disulphide bond between cysteine residues, leading to the formation of a loop of 187 amino acids. The ADAMTS13 cleavage site (Y1605-M1606) is located in the middle of A2 domain.

1.7.1 Platelet GPIbα

The A1 domain contains the binding site for GPIbα,[96] which is a component of the platelet GPIb-IX-V complex.[128] To mimic this interaction *in vitro* VWF needs to be treated with modulator such as ristocetin or botrocetin to allow binding to platelets.

The location of the A1 domain as the site of interaction with GPIbα was initially demonstrated using a 52/48kDa fragment of VWF generated by trypsin digestion spanning residues 1212-1491 that was able to inhibit ristocetin induced platelet aggregation.[96] Additionally, a similar fragment expressed in *E.coli* (residues 1208-1496), was able to also inhibit platelet aggregation and also competed with the binding to platelets of an anti-GPIbα monoclonal antibody known to inhibit VWF binding.[129] Finally, an A1 domain deleted VWF mutant was unable to mediate ristocetin induced platelet aggregation.[130] Although the specific residues involved in the interaction with GPIbα are unknown, a study using *E.coli* expressed A1 domain demonstrated that the VWF GPIbα binding domain contained multiple interaction sites and the residues between the A1 domain intramolecular bond, (Cys1272-Cys1458) were important in the interaction.[131] Furthermore a study using synthetic VWF peptides showed that residues Asp1277-Glu1305 represented a major site of adherence to GPIb.[132] Specific mutations; R1287S, G1324S, H1326T, T1357S/E1359A, Q1367R and S1370R[133] and also Glu1260Ala and Arg1274Ala,[134] all reduced recombinant VWF A1 domain-ristocetin/botrocetin induced binding to platelets. To assess binding kinetics of the VWF:GPIbα interaction, a recombinant fragment of GPIbα has been expressed spanning the first 289 residues of GPIbα. Recombinant VWF A1 domain binds to this fragment with a K_D of 3.3μM.[135] Using Surface Plasmon Resonance, full length VWF has been shown to bind to rGPIbα with a K_D of 30nM.[136] Finally, a recent study has suggested that the D'D3 domains shield the A1 domain, modulating its interaction with GPIb-IX-V. Recombinant VWF lacking the D'D3 domains was more effective at binding platelets and isolated D'D3 region could inhibit the interaction of D'D3 deleted VWF with GPIbα.[137] Furthermore, it was demonstrated that the D'D3 region was in close proximity to the A1 domain in soluble VWF but not when VWF was immobilized.[137]

1.7.2 Heparin

The VWF A1 domain has also been shown to contain a heparin binding site, indicating that VWF may interact with matrix heparin-like glycosaminoglycan.[138] An initial study demonstrated that the 52/48kDa tryptic fragment of VWF was able to inhibit the binding of FL-VWF to heparin and was also able to bind heparin itself.[124,139] Binding to heparin was dramatically decreased if A1 domain deleted VWF.[130] A recent study has demonstrated that residues Lys1362 and Arg1395 and clusters 1332-1336 and 1405-1408 are essential residues for heparin binding with in the A1 domain.[140]

1.7.3 Collagen Binding

Collagen is the main component of the extracellular matrix capable of binding VWF. The major types of collagen involved in this interaction are types I and III. Collagen type III is present in the sub-endothelium and is exposed after limited injury insult to the endothelium, whereas collagen type I is located deeper in the vessel wall so is only exposed after extensive injury. Both the A1 and A3 domains contain collagen binding sites. Initial studies with the tryptic 48/52kDa A1 domain VWF fragment demonstrated that this portion of the VWF molecule could inhibit binding of FL-VWF to collagen, suggesting this fragment contained a collagen binding site.[141] Similar studies using trypsin and V8 protease generated fragments demonstrated that two distinct domains of VWF could interact with collagen types I and III,[142] and the region 1674-2128 contained a binding site for type III collagen.[143] It has also been established that the propeptide contains a collagen binding site, however since the propeptide is removed during multimer assembly this is unlikely to be significant.[144] Further studies using purified recombinant A1 domain failed to demonstrate any binding to collagen,[129,145,146] and deletion of the A1 domain failed to prevent VWF interacting with collagen types I and III.[130] These results indicated that whilst a collagen binding site may be present within the A1 domain, it is only a minor binding site and the results obtained with the tryptic fragments of VWF may be explained by contamination by full length VWF material after purification of the fragments. Evidence that the major collagen binding site was located in the A3 was obtained by a study showing that recombinant A3 domain could inhibit binding of multimeric VWF to collagen and could bind collagen with a K_D of ~2-3μM,[147] and a further study using an A3 domain deleted VWF mutant showed abolished binding to type III collagen.[148]

Mutagenic studies of the VWF A3 domain demonstrated that residues Asp1742, Ser1783 and His1786 are essential for collagen binding and mutation of residues Ile1738, Thr1740, Val1760, Glu1764, Arg1726 and Arg1779 decreases collagen binding at least 10 fold, suggesting that these residues are important.[149,150] These residues define a flat hydrophobic region at the front face of the A3 domain that represent the collagen binding site.[150,151] Recently, the VWF binding sequence in type III collagen has been shown to be RGQOGVMGF (where O is hydroxproline).[152]

A recent study however has proposed a model in which both domains support adhesion to collagen in a synergistic fashion. Using both SPR and a plate based collagen binding assay, Morales *et al* showed that recombinant A1 (rA1) domain bound to both types I and III collagen with higher affinity than recombinant A3 domain and furthermore collagen bound rA1 was able to support platelet adhesion under flow conditions. Examination of the binding kinetics obtained by SPR showed that the A1 protein has lower association and dissociation rates and A1 domain was also less effective at inhibiting the binding of multimeric VWF to collagen. The authors results proposed that the major binding site for collagen is located in the A3 domain, and this mediates a fast association to decelerate the rapid flowing VWF. Binding to collagen via the A3 domain causes a conformational change that exposes a cryptic collagen binding site in the A1 domain that adds to the overall affinity of VWF for collagen.[153] This conclusion is supported by evidence that mutations in the A1 domain, G1324S[153] and R1308L[154] cause impaired collagen binding by affecting the conformation of the A1 domain.[153,154]

The multimeric nature of VWF is important in determining the affinity for collagen,[155] with the highest molecular weight multimers have more collagen binding sites and therefore bind to collagen with the highest affinity, K_D 1-7nM.[156] Based on the crystal structure of the A3 domain the interaction of the A3 domain collagen is achieved through interactions between negatively charged residues on the A3 domain and positively charged residues on collagen. The absence of a pronounced binding groove precludes a large van der Waals surface interaction between the A3 domain and collagen and is consistent with the low affinity for collagen of a single A3 domain and the requirement for multimeric VWF for tight association with collagen.[122]

Finally, the A1 domain has been shown to contain the binding site for collagen type VI which is abundant in the arterial subendothelium.[157,158]

1.7.4 A2 Domain

The VWF A2 domain harbours the cleavage site for the VWF cleaving protease, ADAMTS13.[159] Recombinant VWF with the A2 domain deleted is not cleaved by ADAMTS13.[160] As will be further discussed, ADAMTS13 cleaves the Tyr1605-Met1606 bond in the A2 domain, regulating VWF multimeric size, and thus VWF functional activity. Although the crystal structure of the VWF A2 domain has not yet been resolved a homology model has been proposed where the Tyr1605-Met1606 bond is buried within the domain.[161] For ADAMTS13 cleavage of VWF to occur the VWF molecule must adopt an unfolded conformation to expose the cleavage site. This occurs *in vivo* under shear stress conditions[162] and may be replicated *in vitro* by the use of denaturants.[161] Without the use of *in vitro* denaturants cleavage does not occur.[161]

1.8 D4 AND B DOMAINS

The D4 and B 1-3 domains form the region of the VWF monomer in-between the A3 domain and the C1 domain. Little investigation has focused on this portion of the VWF molecule, as such, no functional role has been determined for either the D4 or B domains. Expression of rVWF with the D4 domain deleted had no effect on VWF multimeric structure and did not alter binding of VWF to type III collagen,[156] and recombinant D4 domain was also unable to inhibit VWF binding to type VI collagen.[157] Further investigation is needed to ascertain the role of these domains.

1.9 THE C DOMAINS AND THE CYSTEINE KNOT

The C domains and the cysteine knot (CK) domain are located at the C terminal end of the VWF monomer. The C1 and C2 domains span residues 2255-2645 and have sequence homology to cysteine rich domains found in thrombospondin and alpha-procollagen types I and III.[163] The C1 domain contains the RGDS (Arg-Gly-Asp-Ser) sequence required for binding to the platelet GPIIbIIIa receptor and also to the HUVEC vitronectin receptor.[164]

The CK domain spans the final 90 C-terminal residues of VWF from 2724-2813 and contains the cysteine residues involved in the formation of VWF dimers. The CK domain is homologous with the cysteine knot family of proteins and the VWF CK domain is particularly similar to the CK domains found in several epithelial mucins and Norrie disease protein (norrin) that form oligomers through C-terminal CK domains.[165-167] The CK domains are characterised by 6 conserved cysteine residues, with disulfide

bonding occurring between cysteines 2 and 5 and between cysteines 3 and 6 and this defines a ring that is penetrated by a disulfide bond between cysteines 1 and 4, with additional un-conserved cysteine residues that differ between CK domains, mediating dimerisation.[168] Analysis of the VWF CK domain demonstrated that it contains the 6 conserved cysteine residues; Cys2724-Cys2774 (bond 1-4), Cys2750-2804 (bond 2-5) and Cys2754-Cys2806 (bond 3-6). Mutation of two of the un-conserved cysteine residues in the VWF CK domain, C2771 and C2773, prevented dimerisation, indicating these cysteine residues are necessary for dimerisation of VWF.[19,169] Furthermore molecular modelling based on transforming growth factor β, suggested that these two residues were pivotal in forming inter-molecular disulphide bonds to form VWF dimers.[19]

1.10 VWF FUNCTION IN COAGULATION

Haemostasis is a regulated response to maintaining blood flow within the vascular system; preventing blood loss at sites of vessel injury but at the same time maintaining blood fluidity.

At sites of vascular injury three events occur to prevent blood loss:

1) Vasoconstriction to reduce blood flow, 2) Formation of the primary platelet plug – this is a rapid process that limits blood loss but is unstable and 3) Stabilisation of the platelet plug – this occurs via the coagulation cascade which culminates in the generation of thrombin; this in turn converts soluble fibrinogen to fibrin, which enmeshes the initial platelet aggregation and converts the primary platelet plug to a firm stable haemostatic plug. Platelets themselves are disc shaped, anucleated blood cells, derived from megakaryocytes. Upon insult to the endothelium platelets adhere either directly to the endothelium, under low shear stress conditions or via the interaction with VWF, under high shear stress conditions.

1.10.1 Blood Vessel and Blood Flow Dynamics[170]

In a blood vessel, red blood cells represent the majority of the circulating mass and as such they occupy most of the lumen, forcing white blood cells and platelets to the sides of the vessel.[171] Assuming blood follows the properties of a Newtonian fluid, the velocity profile of blood will be parabolic. Therefore, the velocity of the blood flow through the vessel will be maximal in the centre and will decrease towards the vessel wall. The fluid in the blood vessel can be thought of as being in different layers called

planes or laminae, moving at different velocities. The difference in velocity between the layers creates the shearing flow, i.e. the sliding motion between two adjacent laminae. Shear stress is the tangential force per unit area of contact between the laminae and is expressed in Pascal (Pa) using the International System of Units or dyn/cm^2 in the CGS system. ($1Pa = 10\ dyn/cm^2$)

Shear rate is the rate of change in velocity between laminae with respect to the distance from the axis of the vessel. It is expressed in velocity divided by distance, in units of s^{-1}.

In Newtonian fluids there is a linear relationship between shear stress and shear rate. Maximal shear rate occurs at the sides of the vessel, while minimal shear rate occurs at the centre of the vessel.

Platelets and the vessel wall can be viewed as two juxtaposed surfaces. The platelets are in the fluid phase while the vessel wall is stationary. In order for bonds to form between platelets and vessel wall, the two need to be 10nm or less apart from each other. When a platelet is in close enough proximity for a bond to occur, it must do so before the distance between itself and the vessel wall is increased. Thus, the initial interaction requires a fast on-rate. The interaction between platelet and vessel wall also needs to withstand the force (drag) applied to it by the moving fluid. The higher the shear forces, the higher the drag. The shear forces have an effect on the platelet bonds formed with the vessel wall; the interaction is subjected to torque, where the fluid flow and the spherical nature of the platelets produce a rotating motion; where bonds at the front of the platelet/vessel interaction are compressed and bonds at the rear are subjected to tensile stress.

At sites of vascular injury VWF is essential to the initiation of platelet adhesion and therefore subsequent haemostatic plug formation, since it is able to resist the haemodynamic forces and provide a rapid link between the extracellular matrix and platelets.

1.11 VWF AND PRIMARY PLATELET PLUG FORMATION

1.11.1 Platelet Adhesion

Upon vascular insult, VWF acts to mediate platelet adhesion to the subendothelium and platelet-platelet aggregation.[172] VWF is especially important for these processes under conditions of high shear stress and rapid blood flow; such conditions are found in arterioles and stenosed arteries.[173] After exposure of the subendothelium, VWF is able to interact with the exposed subendothelial matrix proteins, principally collagen via the

A3 domain, anchoring it to the subendothelium and as discussed this may induce a conformational change allowing interaction of the A1 domain with collagen as well. Furthermore, HMW-VWF multimers (that are the most biologically active) are released from the WP bodies in EC, in the basolateral direction, and are bound to the subendothelium before reaching the circulation.[174] Depending on the vascular segment involved in the process, the subendothelial matrix may contain sufficient endogenous VWF to support platelet adhesion alone.[175,176] Indeed analysis of different collagen preparations showed that fibrillar collagen contained a substantial quantity of VWF that could enhance platelet aggregatory responses.[177] However, when no endogenous VWF is present the process of platelet adhesion is not affected. Vascular beds that do not contain endogenous VWF can support platelet adhesion[6] and this is also demonstrated by experiments on pigs with VWD that do not secrete VWF into the blood stream or the subendothelial matrix. Infusion of VWF concentrate into the pigs corrected the plasma defect and returned haemostasis to normal, even though there was an absence of endogenous VWF.[178] Thus plasma VWF is able support platelet aggregation regardless of the presence of endogenous VWF.

The shear forces that are encountered cause VWF to undergo a conformation change resulting, as discussed, in the un-coiling of the molecule into its elongated confirmation.[80] This exposes the binding site for GPIbα and provides the initial point of interaction between VWF and platelets.[173] The binding of platelet GPIbα to VWF has an extremely fast association rate so that platelets may be tethered even at very high flow rates.[173] Above a threshold value of wall shear stress rate of ~1000 per second, the interaction of VWF with GPIbα is the only interaction that can initiate adhesion.[170] The interaction also has a fast dissociation rate and as such cannot provide irreversible platelet adhesion. However, the interaction serves to arrest the movement of the platelet and using video microscopy, platelets are observed to move slowly along the immobilised VWF in the direction of the flow.[173] This movement along VWF after the interaction with GPIbα is associated with platelet activation.[179] Intracellular signals are generated that in turn activate protein kinases that cause platelet activation. Upon activation the shape of the platelet changes to become more spherical and extrude long pseudopods that enhance interaction with adjacent platelets. A release reaction occurs resulting in the secretion of ADP, serotonin, fibrinogen, lysosomal enzymes, β-thromboglobulin, heparin neutralising factor and also platelet VWF. The platelet membrane also exposes more negatively charged phospholipids to provide an optimal

surface for binding of other coagulation factors. The activation of platelets also leads to activation of platelet receptor GPIIbIIIa (integrin $\alpha_{IIb}\beta_3$) and P-Selectin on the platelet surface. GPIIbIIIa interacts with the RGDS sequence in the VWF C1 domain, forming an irreversible bond that arrests the platelet's movement and stabilises the GPIbα interaction and thus mediates platelet adhesion.[180,181]

Under conditions of low shear stress platelets are able to interact directly with the exposed subendothelial matrix. Recently the dimeric form of platelet receptor GPVI has been shown to bind directly to fibrous collagen present in the subendothelium,[182,183] stimulating platelet adhesion and activation.[184] The platelet collagen receptor, GPIaIIa (integrin $\alpha_2\beta_1$) is also able to directly interact with collagen[185] and there is evidence that platelet glycoprotein V (part of the GPIb-V-IX receptor) also plays a role in adhesion to collagen.[186]

1.11.2 Platelet Aggregation

Once platelets have adhered to the site of vascular injury further platelets are recruited to the site to form the primary platelet plug. This is mediated by VWF interacting with GPIbα and GPIIbIIIa in the same way as described above and fibrinogen interacting with GPIIbIIIa. Platelets can also bind, via GPIbα, to P-Selectin on activated platelets.[187] At low wall shear stress rate of ~100 per second, as commonly found in the venous circulation,[171] fibrinogen interacting with GPIIbIIIa forms the predominant link between aggregated platelets,[188] although VWF competes with fibrinogen for GPIIbIIIa.[189] At high shear rates however, fibrinogen alone is unable to support platelet aggregation and VWF is required to further the formation of the platelet aggregate.[190-192] Platelet VWF can also be involved in the formation of the platelet plug. However, since it is released from the α-granules of activated platelets it is unlikely to be involved in the initial adhesion of platelets to the site of vascular injury. Platelet VWF has been shown to mediate platelet aggregation at high shear stress and therefore is involved in the extension of the platelet aggregate after the initial adhesion of platelets to the exposed subendothelium.[192]

1.11.3 VWF Self-Association

Evidence from recent studies has suggested that VWF is also able to self-associate under flow conditions during platelet adhesion. In a study by Savage *et al* (2001)[193]

platelets perfused over immobilised recombinant VWF lacking the A1 domain, failed to tether to the surface. However they adhered if they were perfused over the A1 domain deleted VWF with soluble VWF. Likewise, perfused platelets failed to interact with collagen bound recombinant A3 domain, but adhered if they were perfused with soluble VWF.[193] These observations suggest that self-assembly of VWF multimers occurs at sites of vascular injury and this may aid the formation of the platelet plug.[193] A further study also demonstrated that VWF in suspension was able to self-associate in the presence of high shear stress.[194] Finally, the self assembly of VWF was investigated using a static plate binding assay that demonstrated the interaction between immobilised and soluble VWF involved multiple domains.[195]

1.12 VON WILLEBRAND DISEASE

Von Willebrand Disease (VWD) is the most common human congenital bleeding disorder, affecting 1% of the population. The disease was first identified by Dr Eric Von Willebrand in 1924 in families from the Aland islands who had a bleeding tendency distinct from haemophilia and other forms of bleeding diathesis.

VWD results from either a qualitative or quantitative deficiency in VWF, caused by mutations at the *VWF* locus. Symptoms vary according to severity of the disease and include epistaxis, gingival bleeding, menorrhagia, prolonged bleeding from trivial wounds, skin bruises and haematomas and gastrointestinal bleeding in more severe cases. Severe deficiency of VWF or abnormalities in its interaction with FVIII, causes a secondary moderate deficiency of FVIII, with typical haemophilia symptoms such as haemarthrosis and deep tissue bleeding.

VWD is a heterogeneous disorder, classified into three major categories. Type I VWD refers to a partial quantitative deficiency. Type 2 VWD refers to qualitative deficiency and type 3 VWD results from a total VWF deficiency.

Type 1 VWD is the most common VWD deficiency (70% of all VWD patients). By definition its is a quantitative deficiency, caused by mutations that impair VWF synthesis and/or secretion, but normal VWF function and multimer distribution are retained. However an increasing body of evidence suggests that more detailed analysis of VWF from patients with type 1 VWD shows subtle abnormalities in multimer composition and distribution. This is more consistent with the dominant-negative effect of many type 1 VWD associated mutations. Type I VWD can be inherited as a dominant or recessive trait, depending on the specific mutation and on the variable penetrance.

Type 3 VWD is characterised by total absence or minimal detectable VWF protein in plasma. It is a recessive disorder resulting from mutation of both copies of the VWF gene. Heterozygotes for these mutations are normally unaffected and do not present with a type 1 or type 3 VWD phenotype. The distinction between the two forms is made from a clinical point of view, since type 3 VWD have more severe symptoms.

Type 2 VWD is characterised by normal or reduced plasma VWF antigen, with disproportionate loss of certain functions. It includes a series of subtypes (2A, 2B, 2M, 2N). Inheritance is dominant, with the exception of type 2N and a rare variant of type 2A.

Type 2A VWD is the most common qualitative deficiency. It is associated with the absence of large and intermediate molecular weight VWF multimers (Fig 1.6), which are the most effective in haemostatic activity. Type 2A VWD is usually transmitted as a dominant disorder caused by single amino acid substitution usually within the A1 and A2 domains. Two distinct molecular mechanisms are involved in causing the type 2A VWD phenotype and the corresponding causative mutations are designated group I and group II. Group I mutations are associated with impaired assembly and secretion of normal VWF multimers. It is assumed that only the larger multimers carrying these mutations are retained in the endoplasmic reticulum, since they have incorporated a large number of mutant subunits interfering with processing and secretion process. Group II mutations are associated with normal processing and secretion of VWF multimers. Loss of large and intermediate molecular weight multimers then occurs in plasma, due to increased susceptibility to proteolysis by ADAMTS13. Molecular

modelling of the A2 domain suggests that these mutations may change the conformation of the molecule, and thereby leading to an unfolded domain more susceptible to proteolytic cleavage. A distinct set of mutations within the propeptide also cause a recessive form of type 2A VWD by impairing multimer assembly in the Golgi. The basis for the recessive clinical phenotype is not completely understood.

Type 2B VWD is characterised by increased affinity of VWF for platelet GPIbα. Different point mutations have been identified all clustered in the region of the A1 domain, which contains the GPIbα binding site. Paradoxically, this abnormality does not lead to thrombosis but to a bleeding phenotype. This can be explained by the presence of increased clearance of both VWF and platelets, leading to absence of haemostatically effective high molecular weight multimers in plasma and intermittent thrombocytopenia.

Type 2M VWD is characterised by normal VWF multimers distribution but decreased platelet adhesion. Mutations associated with this particular phenotype have been identified in GPIbα binding site in A1 domain and they cause a disruption of this interaction

Type 2N VWD shows preserved platelet-dependent functions and normal VWF multimeric pattern, but decreased FVIII binding and subsequently low FVIII levels due to enhanced clearance. All the mutations described are located in the region of VWF containing FVIII binding site (i.e. D'D3). The phenotype is autosomal recessive, since FVIII binding to VWF is not dependent on VWF multimeric size. Furthermore, VWF is physiologically in excess compared to FVIII and thus the amount of VWF synthesized by a single allele is sufficient to bind all the circulating FVIII.

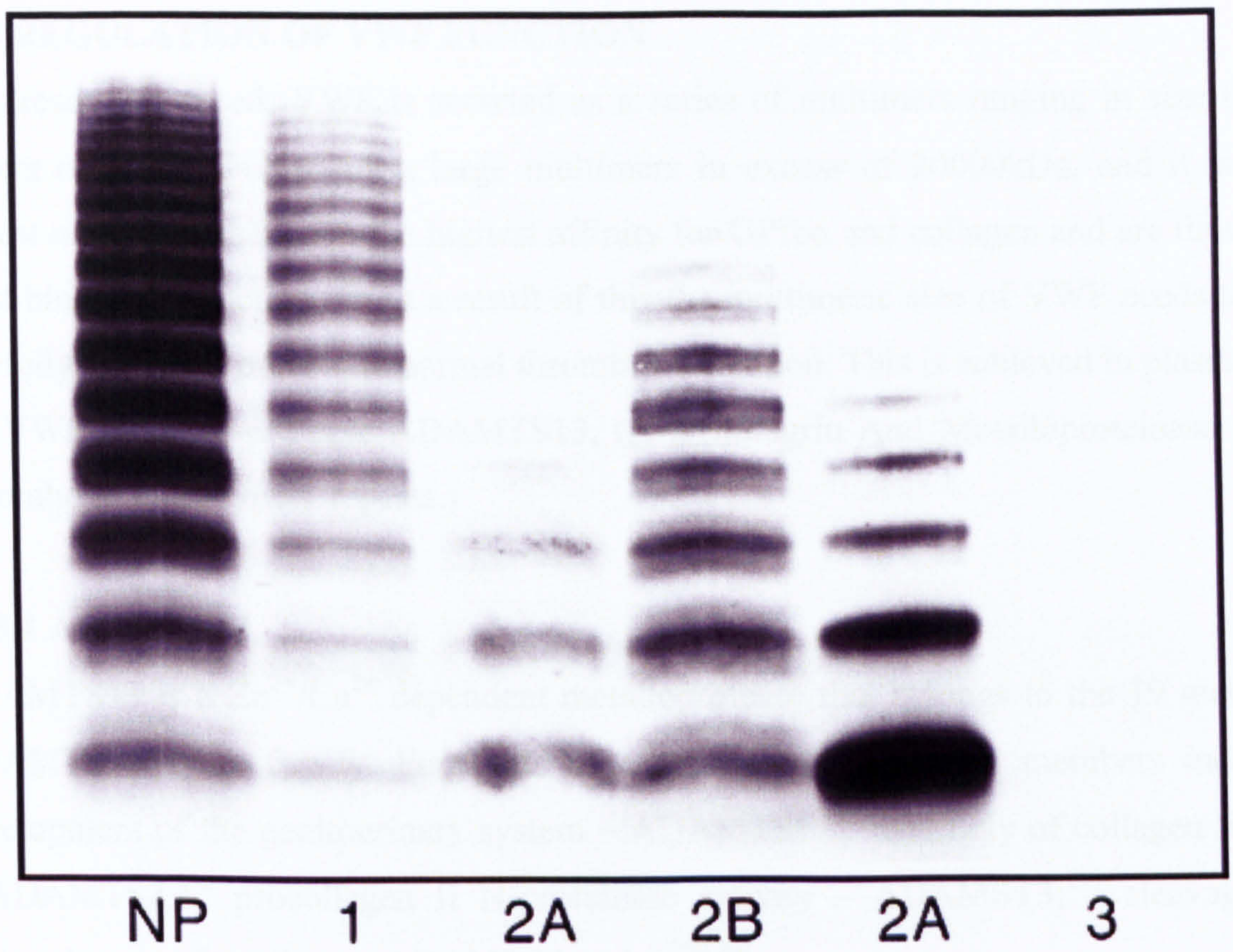


Figure 1.5 Distribution of VWF multimers in VWD

Multimer analysis of a patient with type 1 VWD shows a normal multimer distribution compared to normal plasma (NP). Patients with type 2A VWD and type 2B VWD present an abnormal multimer profile with the absence of high and medium molecular weight multimers.(Figure reproduced from Sadler 1988)[2]

1.13 REGULATION OF VWF FUNCTION

As already discussed, VWF is secreted as a series of multimers ranging in size from dimers of 500kDa up to ultra large multimers in excess of 20000kDa, and it is the largest multimers that have the highest affinity for GPIbα and collagen and are thus the most biologically active.[196] As a result of this the multimeric size of VWF needs to be carefully regulated prevent abnormal thrombus formation. This is achieved in plasma by the VWF cleaving protease ADAMTS13, (A Disintegrin And Metalloproteinase with ThromboSpondin type-1 repeats.)

1.13.1 ADAMTS13

ADAMTS13 is a Zn^{2+}/Ca^{2+} dependent metalloprotease that belongs to the 19 member ADAMTS enzyme family. Functions of other ADAMTS family members include; development of the genitourinary system – ADAMTS1,[197] assembly of collagen fibrils – ADAMTS2,[198] procollagen II N-proteinase activity – ADAMST3,[199] cleavage of proteoglycans of cartilage – ADAMTS4 and 5.[200,201]

The human ADAMTS13 gene is located on chromosome 9 (9q34), spanning 37kb of genomic DNA and encodes for 29 exons. The transcription mRNA product is ~5kb and encodes for a 1472 amino acid protein.[202] The apparent mass of ADAMTS13 is ~190kDa compared with a calculated molecular weight of 145kDa; this difference is most likely due to glycosylation, with ADAMTS13 containing 10 potential N-linked glycosylation sites.[203] The primary site of synthesis is in the liver, with a number of studies reporting most active expression in hepatic stellate cells.[202-207] However a recent study detected ADAMTS13 in both arterial and venous endothelial cells by immunofluorescence staining, and RT-PCR analysis confirmed that ADAMTS13 was synthesised in these cells.[208] ADAMTS13 is secreted constitutively in to the blood as an active protease and has a plasma concentration of ~1-2μg/ml (5-10nM) with a half-life of 2-3 days.[209,210]

ADAMTS13 is a multi domain protein consisting of a signal peptide, a propeptide, a metalloprotease domain, a disintegrin domain a thrombospondin type-1 motif (TSR), a cysteine-rich domain, a spacer domain, seven additional TSRs and two CUB domains.[203]

The metalloprotease domain contains the active enzymatic site and its activity is dependent on the presence of Zn^{2+} and Ca^{2+} ions and therefore is inhibited by divalent chelating agents such as EDTA.[159]A molecular model based on homology with

adamalysin II suggests that three histidine residues; His244, 228 and 234, coordinate the catalytic Zn^{2+} ion at the active site.[211] A potential calcium binding site, conserved in most ADAMTS13 family members, is predicted to lie on the opposite side to the catalytic domain and may involve residues Glu83, Asp173, Cys281 and Asp284.[203]

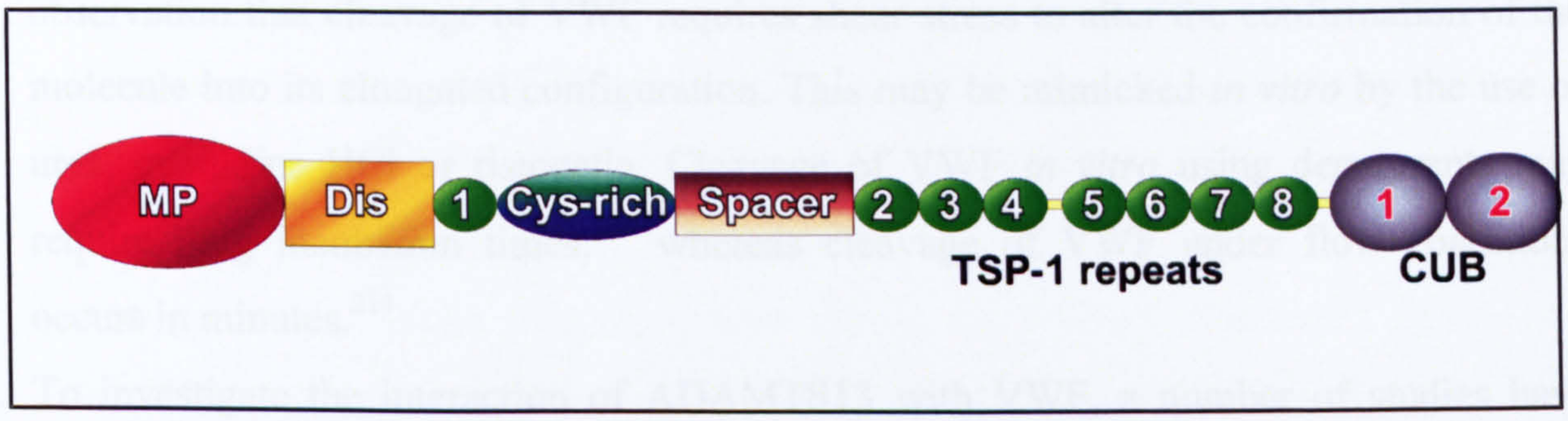


Figure 1.6 Domain structure of ADAMTS13

ADAMTS13 is a multi domain protein containing a metalloprotease domain (MP), a disintegrin domain (Dis) a thrombospondin type-1 motif (TSR), a cysteine-rich domain, a spacer domain, seven additional TSR's. Interestingly ADAMTS13 is the only ADAMTS family member to posses two CUB domains, located at the C-terminal end of the protein,

BIBL. LONDON UNIV.

1.13.2 ADAMTS13 Interaction with VWF

As previously discussed, ADAMTS13 is responsible for the cleavage of VWF at the Y1605-M1606 bond in the VWF A2 domain, generating 176kDa and 140kDa fragments found in the circulation[212] and thus regulates VWF multimeric size. Cleavage of VWF by ADAMTS13 is responsible for the characteristic triplet structure observed in multimeric analysis of VWF. Molecular models of the A2 domain suggest that the Y1605-M1606 bond is buried within the domain[161,213] and this is supported by the observation that cleavage of VWF requires shear stress to alter the confirmation of the molecule into its elongated configuration. This may be mimicked *in vitro* by the use of urea, guanidine HCl or ristocetin. Cleavage of VWF *in vitro* using denaturants may require long incubation times,[196] whereas cleavage of VWF under flow conditions occurs in minutes.[214]

To investigate the interaction of ADAMTS13 with VWF, a number of studies have employed the use of short recombinant substrates to avoid the use of denaturants or the need for shear stress. Kokame *et al* demonstrated that the shortest VWF fragment that could be cleaved by ADAMTS13 was a 73 amino acid fragment (VWF73) spanning residues 1596-1668 of the A2 domain.[215] Other studies have used VWF115 substrate, spanning residues 1554-1668 of the A2 domain.[216] Both these short substrates do not require urea for cleavage, indicating the structure is permissive to ADAMTS13 cleavage.

Whilst the A2 domain contains the ADAMTS13 cleavage site, evidence suggests that the primary binding site for ADAMTS13 lies in the A3 domain. A study by Dong *et al* showed that under flow conditions and by the use of SPR that ADAMTS13 bound with the greatest affinity to recombinant A3 domain, compared to A1 or A2 domains.[217] However in a subsequent study, the presence of the A3 domain had no effect on the rate of proteolysis[218] and this was further supported by a study using a VWF fragment spanning residues 1554-1874, (designated VWF115-A3), for which the rate of proteolysis was shown to be similar to the VWF115 substrate spanning residues 1554-1668, indicating that the presence of the A3 domain had no effect on the rate of proteolysis by ADAMTS13.[216] The latter study also determined a specificity constant (K_{cat}/K_m) of ~8×10^4 M^{-1} s^{-1} which was close to the apparent K_{cat}/K_m value obtained for full length multimeric VWF of ~3.4×10^4 M^{-1} s^{-1}.[219]

It has also been demonstrated that binding of VWF to GPIbα enhances ADAMTS13 cleavage of VWF. Recombinant VWF A2A3 was cleaved ~10 fold faster than

recombinant A1A2A3, indicating that A1 domain inhibited cleavage, but this inhibition can be relieved by binding of the A1 domain to GPIbα or heparin.[218]

The domains of ADAMTS13 are also important in the interaction with VWF. The spacer domain is essential for activity. Truncations of ADAMTS13 up to the metalloprotease domain, the disintegrin domain and the cysteine rich domain were unable to bind (or bound with low affinity) or cleave FL-VWF or VWF73.[220-222] However addition of the spacer domain restored protease activity, indicating that it is essential for ADAMTS13 activity.[220-222] Using a plate binding assay, it was demonstrated that ADAMTS13 truncated up to the first thrombospondin repeat bound VWF with a Kd 206nM; addition of the spacer domain increased the affinity to Kd 26nM which was comparable to the affinity of wild type ADAMTS13 for VWF, (Kd 14nM.)[222] Similar results were also obtained with the VWF73 substrate.[220] It was also shown that individual domains of ADAMTS13 could bind to VWF73; Disintegrin domain – K_D = 489nM, first TSR – K_D = 136nM, Cysteine rich domain – K_D = 121nM and Spacer domain – K_D = 108nM.[223] This suggests that all the proximal C-terminal domains act in cooperation to confer an efficient recognition of the substrate.

Conflicting data exists as to the function of the CUB domains (Complement components C1r/C1s, Uegf (sea urchin fibropellins) and Bone morphogenic protein1.) These domains are not present in other ADAMTS family members, but they are present in other proteins involved in developmental processes (embryogenesis, organogenesis, innervation), suggesting they can have a role in protein-protein interactions.[224]

1.13.3 VWF Cleavage by Thrombospondin-1

As well as cleavage by ADAMTS13, VWF multimer size is also regulated to some degree by a protein disulphide bond reductase, identified as thrombospondin-1 (TSP-1.)[225] A study by Xie *et al* showed that incubation of VWF with purified TSP-1 resulted in the formation of thiol dependent complexes of VWF and TSP-1, and the generation of free thiols in VWF, furthermore the multimeric size of VWF was reduced. Also, an inverse relationship was demonstrated between the plasma molar ratio of VWF/TSP-1 and VWF multimeric size.[225] Moreover, the administration of TSP-1 to mice resulted in a reduction of VWF multimeric size.[225] A subsequent study demonstrated, that surprisingly, the average VWF multimer size was reduced in TSP-1 null mice.[226] TSP-1 has been shown to interact with the VWF A3 domain,[225,226] and as previously discussed the A3 domain may harbour the primary binding site for ADAMST13.[217] This suggests

that TSP-1 may compete with ADAMTS13 for binding to VWF and inhibit to some degree ADAMST13 proteolysis. This study also showed that TSP-1 is stored in the α-granules of platelets and is able to reduce platelet VWF multimer size upon platelet lysis or activation. This was unable to occur in the TSP-1 null mice, and resulted in increased collagen and platelet binding. This implies that TSP-1 controls plasma derived and platelet derived VWF in different ways and the action of TSP-1 maybe more relevant to platelet derived VWF.[226]

1.14 GLYCOSYLATION

The process of glycosylation involves the attachment of mono, oligo or polysaccharides to proteins or lipids and occurs as a post-translational modification. Glycosylation is known to affect protein folding, localization and trafficking, protein solubility, antigenicity, biological activity and half-life, as well as cell-to-cell interactions.[227-229] The majority of glycan structures fall into three groups: those attached to lipids and those attached to proteins via a nitrogen atom (*N*-linked) or an oxygen atom (O-linked).

1.14.1 *N*-linked Glycosylation

N-linked glycosylation is the best understood glycosylation pathway and results from the attachment of glycan chains to the amide nitrogens of asparagine side chains. For *N*-linked glycosylation to occur the asparagine residue has to be part of the sequence; Asn-Xaa-Ser/Thr, where Xaa can be any amino acid except proline,[230] and there is some limited evidence that Thr at position 3 is increases the chance that the site will be occupied.[231] There are also exceptional cases where *N*-linked glycosylation can occur at the sequence Asn-Xaa-Cys.[232] There are three types of *N*-linked glycan; high-mannose, hybrid and complex, that all contain a common core, but differ in the terminal elaborations extending from the basic structure.

1.14.1.1 *N*-linked glycan synthesis

The synthesis of *N*-linked glycan may be divided into three stages: 1) formation of a lipid-linked precursor oligosaccharide, 2) *en bloc* transfer of the precursor to the protein of peptide and 3) processing of the oligosaccharide.[22]

Generation of the glycan begins with the synthesis of a $Glc_3Man_9GlcNAc_2$ structure attached via a pyrophosphate linkage to a lipid dolichol. This initially occurs on the cytoplasmic side of the ER with the enzyme, UDP-GlcNAc – dolichol phosphate *N*-

acetylglucosamine-1-phosphate transferase, attaching a GlcNAc residue from a UDP-GlcNAc nucleotide donor to the lipid linked dolichol. Further dolichylpyrophosphate enzymes catalyse the attachment of a second GlcNAc residue and five mannose residues from GDP-Man donors, forming a $Man_5GlcNAc_2$ structure.[233,234] The structure is translocated across the ER membrane and becomes inaccessible to cytoplasmic enzymes. Once translocated, four subsequent mannose residues are attached followed by three glucose residues, with the sugars donated from dolichol linked monosaccharides on the ER membrane.[22] The next stage in *N*-glycan synthesis involves the transfer of the $Glc_3Man_9GlcNAc_2$ structure to the nascent polypeptide chain. This occurs in the lumen of the ER and is catalysed by the enzyme, oligosaccharyltransferase, that transfers the glycan to the asparagine residue, with the energy for the reaction being derived from the cleavage of the phosphate-glycan bond.[235,236]

After transfer to the nascent peptide chain, synthesis of the glycan is completed by a series of processing steps that involves the removal and addition of sugar residues. Initially the three glucose residues are removed within the ER by Glucosidase I, which removes the terminal α1-2 linked glucose residue, then Glucosidase II which removes the two inner α1-3 linked glucose residues.[237] As will be discussed, removal of the glucose residues allows the newly formed glycoprotein to enter the calnexin-calreticulin cycle which ensures that the protein is folded correctly and is then transported to the Golgi body for further carbohydrate processing. As the glycoprotein leaves the ER, ER Mannosidase I removes a mannose residue, then following transportation to the Golgi, Golgi Mannosidases IA, IB and IC remove some or all of the four α1-2 linked mannose residues from the glycan chain. Glycans that undergo no further processing are termed high-mannose structures.[22] Further construction of hybrid and complex structures occurs by the addition of a GlcNAc residue by GlcNAc transferase I, in the medial region of the Golgi body, then removal of two mannose residues by Mannosidase II and the addition of a further GlcNAc residue by GlcNAc transferase II. At this stage, the glycan is of the most abundant bi-antennary type, however other distinct GlcNAc transferases can initiate further branching to form less common tri and tetra-antennary structures. The glycan structure can then be further elaborated in the trans-Golgi network by the addition of galactose residues by galactosyltransferases and terminal sialic acid residues by sialyltransferases.[22]

1.14.1.2 Effect of *N*-linked glycans on protein folding

As mentioned, removal of glucose residues from the *N*-linked glycan allows the glycoprotein to enter the calnexin-calreticulin cycle. Calnexin (membrane-bound) and calreticulin (soluble) are homologous ER lectins that bind transiently to virtually all newly synthesized monoglucosylated glycoproteins.[238,239] Once two of the glucose residues have been removed by Glucosidase I and II, the newly synthesised glycoprotein can bind to either calnexin or calreticulin.[240,241] Calnexin and calreticulin are then able to complex with the thiol oxidoreductase, ERp57.[242] Transient disulphide bonds are formed between the glycoprotein and ERp57 and these serve as intermediates in oxidation and isomerization reactions and lead to the formation of correctly paired disulfide bonds within the glycoprotein.[243] Once the protein is correctly folded Glucosidase II removes the remaining glucose residue and the glycoprotein dissociates from calnexin or calreticulin. The high mannose glycan structure may then bind to mannose specific lectins such as ERGIC-53 and VIP36 for transport to the Golgi.[244] If the protein is misfolded, the glycan chains are re-glucosylated by an ER glucosyltransferase, (Uridine diphosphate (UDP)–glucose:glycoprotein glucosyltransferase), and re-binds to either calnexin or calreticulin; the process is repeated until the protein is correctly folded or degraded.

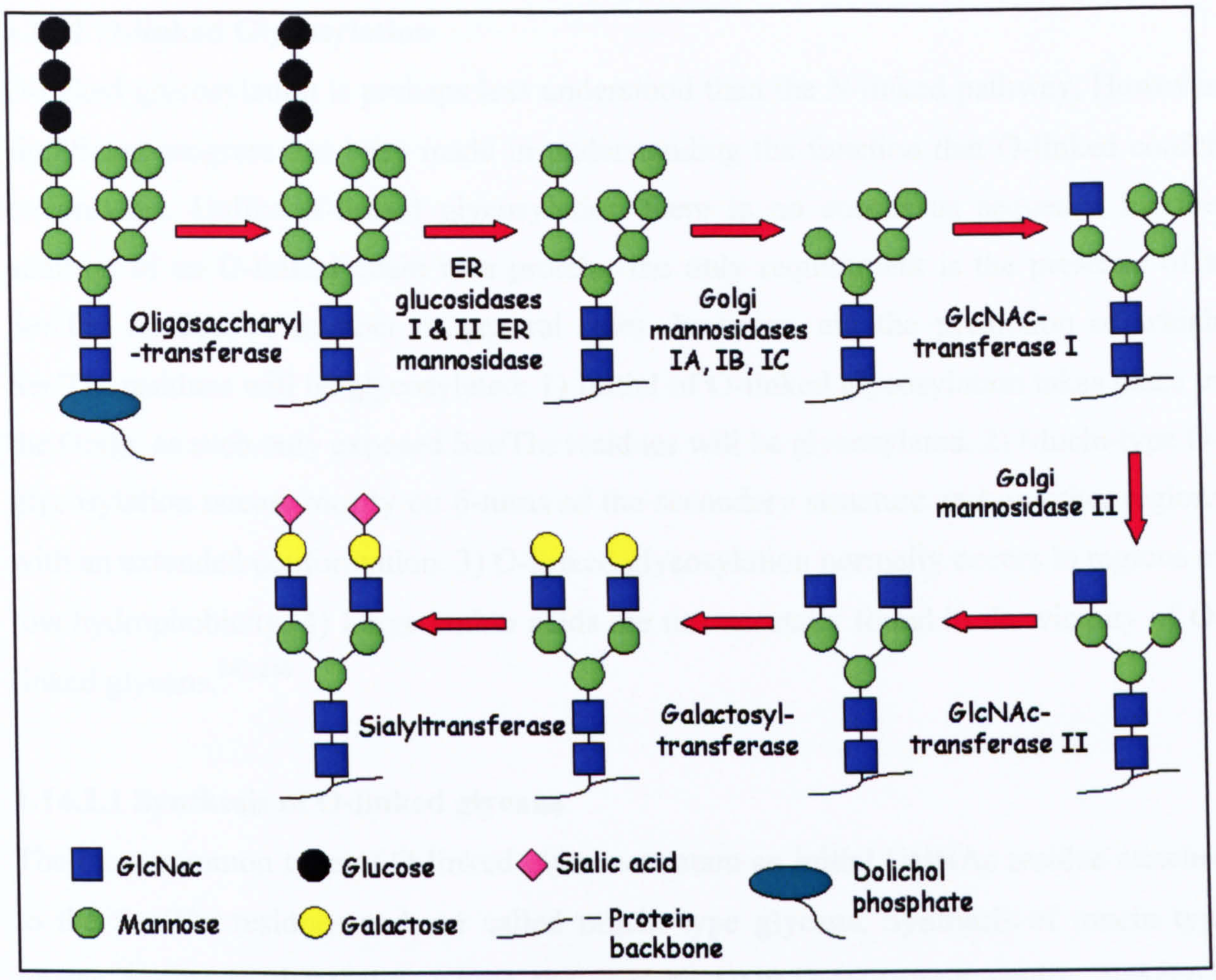


Figure1.7 *N*-linked glycan processing

Following synthesis of the lipid-linked precursor oligosaccharide within the ER, the enzyme oligosaccharyltransferase transfers the Dolichol linked $Glc_3Man_9GlcNAc_2$ structure to the nascent polypeptide chain and further carbohydrate processing occurs through a series of steps that add and remove sugar residues. Within the ER, glucosidases I & II and ER mannosidase removes terminal glucose and mannose residues. Within the *cis*-Golgi and medial Golgi further mannose residues are removed and GlcNAc residues added to the glycan chain. The glycan is completed by addition of galactose and sialic acid residues within the *trans*-Golgi network. The example shown in this figure represents the synthesis of a complex *N*-linked glycan. Alternative pathways of digestion and sugar addition result in the formation of other glycan structures such as high mannose or hybrid structures.

1.14.2 O-linked Glycosylation

O-linked glycosylation is perhaps less understood than the *N*-linked pathway. However significant progress has been made in understanding the function that O-linked confer on proteins. Unlike *N*-linked glycosylation there is no consensus sequence for the addition of an O-linked chain to a protein, the only requirement is the presence of a Ser/Thr residue. A number of general rules, however, aid the prediction of which Ser/Thr residues will be glycosylated: 1) Initial of O-linked glycosylation takes place in the Golgi, as such only exposed Ser/Thr residues will be glycosylated. 2) Mucin-type O-glycosylation occurs mostly on β-turns of the secondary structure and on other regions with an extended conformation. 3) O-linked glycosylation normally occurs in regions of low hydrophobicity. 4) Large amino acids are not normally found in the vicinity of O-linked glycans.[245,246]

1.14.2.1 Synthesis of O-linked glycans

The most common type of O-linked glycans contain an initial GalNAc residue attached to the Ser/Thr residues and are called mucin type glycans. Synthesis of mucin type glycan begins in the Golgi, where the enzyme UDP-GalNAc:polypeptide *N*-Acetyl-galactosaminyltransferase (GalNAc-T) facilitates the addition of a GalNAc residue to the Ser/Thr residue.[247] In total nine mammalian GalNAc-T have been identified, although some specificity has been demonstrated, most cell types express multiple GalNAc-T.[248,249] Galactosyltransferse enzymes can then attach a Gal residue to the GalNAc forming the core 1 structure. The core 1 structure can then be modified by the addition of further sugar residues to form other core structures, with eight core structures identified so far.[250] Most commonly, the core 1 structure may be either terminated by the addition of two sialic residues, or the enzyme UDP-GlcNAc:Galβ1-3GalNAcα1-R-β1-6GlcNAc transferase (core 2 GlcNAc-T) attaches a GlcNAc residue to core 1 to form the core 2 structure.[251] After the synthesis of a core 2 structure, a β1-4Gal-T acts to produce a β1-6 linked lactosamine that can be extended into polylactosamine by β1-3GlcNAc-T and β1-4Gal-T, or the structure can be terminated by the addition of sialic acid residues.[250]

1.15 GLYCAN STRUCTURE OF VWF

As discussed, VWF undergoes extensive post translational modifications resulting in the addition of a potential 16 *N*-linked glycan chains and 10 O-linked glycans chains, so that the total carbohydrate component of VWF accounts for ~15% of its total molecular weight.[16] Analysis of the carbohydrate component of VWF demonstrated both the presence of mannose and GalNAc residues in VWF, indicating that both O and N-linked glycan chains were incorporated in to the molecule,[252,253] with *N*-linked glycan accounting for 70% of the carbohydrate component and O-linked glycans accounting for 30%.[254] The carbohydrate composition of VWF can be seen in table 1 below.

Sugar Residue	% total protein weight
Sialic acid	3.7
Galactose	2.4
N-Acetylglucosamine	4.0
Mannose	3.2
Fucose	1.0
N-Acetylgalactosamine	0.7

Table 1.1 Carbohydrate composition of VWF

Carbohydrate accounts for 15% of the total molecular weight of VWF and the presence of both mannose and GalNAc residues confirms that VWF undergoes both N- and O-linked glycosylation. (Reproduced from Sodetz *et al*)[253]

1.15.1 O-linked Glycosylation of VWF

VWF contains 10 predicted sites of O-linked glycosylation; 1248, 1255, 1256, 1263, 1468, 1477, 1486, 1487, 1679 and 2298. Eight of these are clustered in two groups of four between the A1 and A2 domains. Many soluble glycoproteins contains clusters of O-linked glycans at hinge or linker regions between folded domains.[255] The specific function of this is unknown, but evidence suggests it gives rigidity to flexible regions of the protein.[256] The structure of a major VWF O-linked glycan has been determined to be a tetrasaccharide containing two sialic acid residues, a Gal residue and a GalNac residue (Figure 1.8). As described above this represents a disialyted core 1 structure and represents >70% of VWF O-linked glycans.[257]

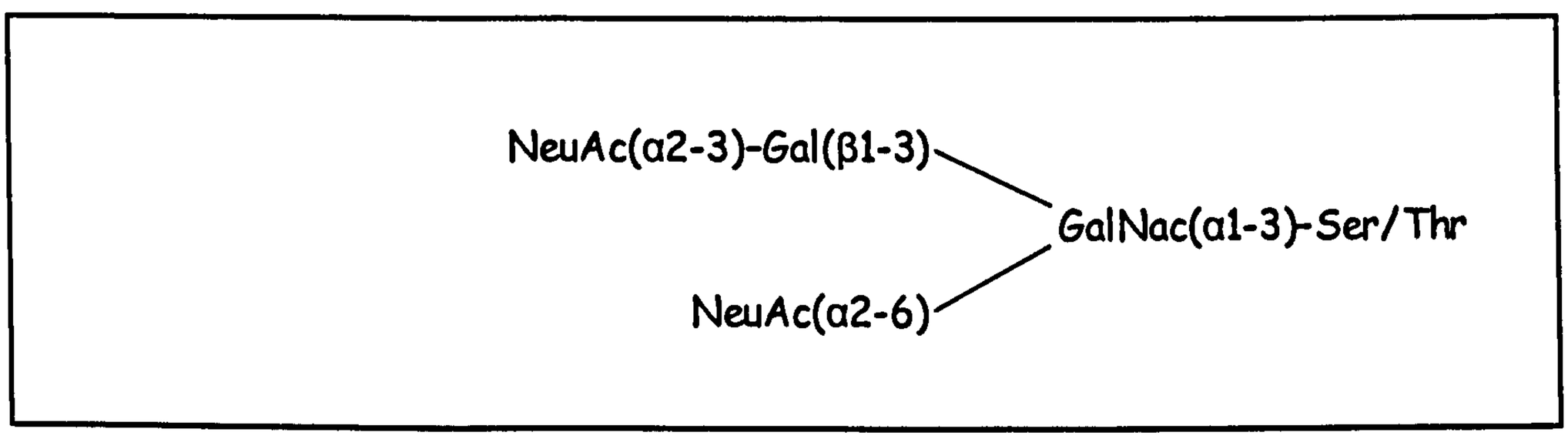


Figure 1.8 Major structure of the O-linked glycans of VWF

VWF is predicted to contain 10 O-linked glycan sites, with the major O-linked glycan shown to be a disialyted core 1 structure. This structure is also known as the t-antigen.

1.15.2 *N*-linked Glycosylation of VWF

VWF is predicted to be *N*-linked glycosylated at 4 sites within the propeptide: N99, N156, N211 and N666 and at 12 sites within the mature subunit: N857, N1147, N1231, N1515, N1574, N2223, N2290, N2357, N2400, N2546, N2585, N2790.[16]

In a number of initial studies glycan structures were isolated and sequenced. Samor *et al* (1982) characterised a major *N*-linked glycan and proposed a bi-antennary, monosialylated glycan of the *N*-acetyllactosaminic type. Further work by Debeire *et al* (1983) confirmed the observation of this glycan structure and showed that the primary structure contained single polylactosamine extensions and also contained an α1-6 linked Fucose residue. Furthermore this glycan structure accounted for 60% of the total *N*-linked structures released from VWF.[258]

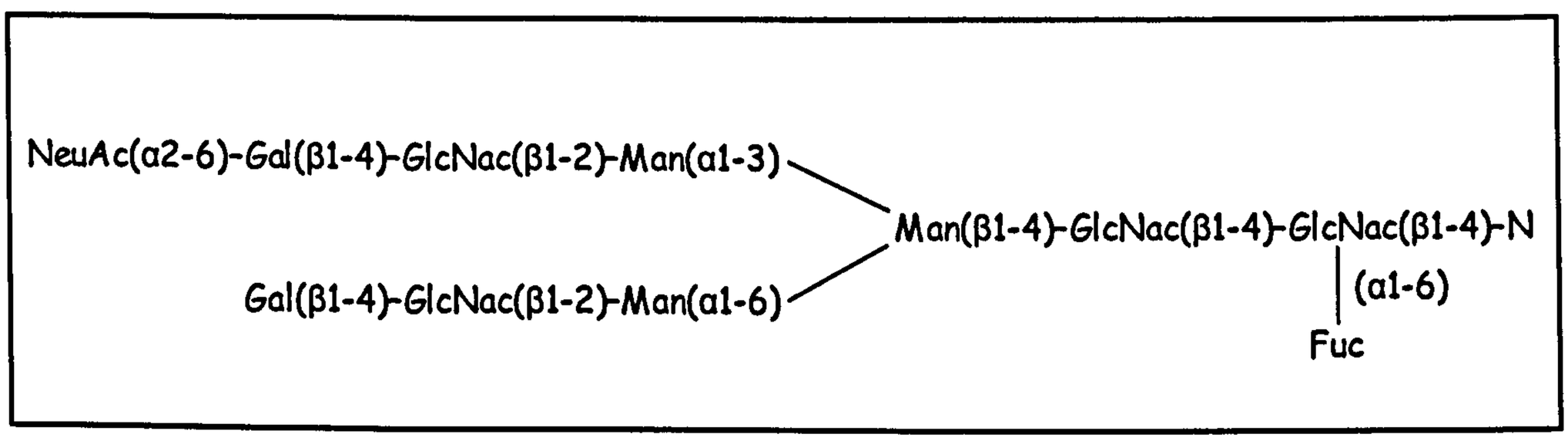


Figure 1.9 Primary glycan structure of a major *N*-linked glycan isolated from VWF

The major *N*-linked glycan presented on VWF is a bi-antennary, monosialylated glycan with a single polylactosamine extensions and an α1-6 linked fucose. This glycan structure was predicted to account for 60% of the *N*-linked glycan. (reproduced from Debeire *et al*)[258]

A later study by Samor *et al* also reported a monosialyated, monofucosylated, tetra-antennary structured glycan with single polylactosamine extensions.[259]

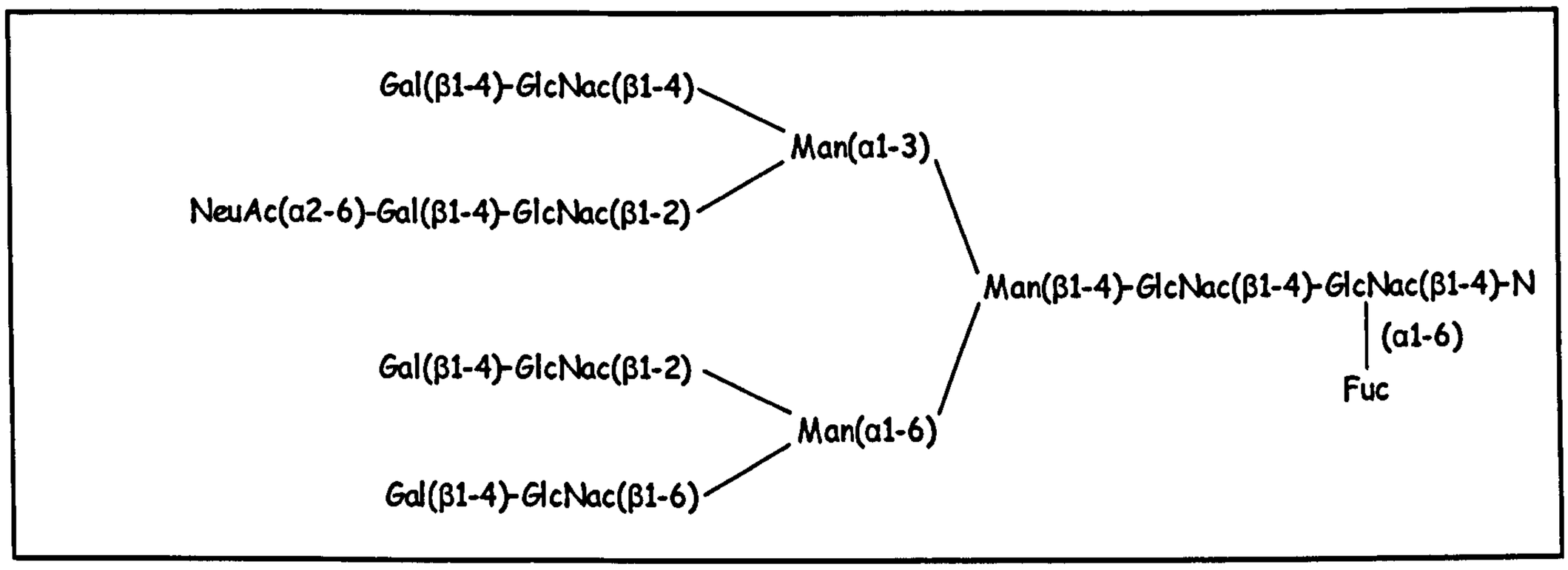


Figure 1.10 Primary structure of a tetraantennary glycan isolated from VWF

(reproduced from Samor *et al*)[259]

A detailed study of VWF *N*-linked glycans was performed by Matsui, Titani and Mizuochi. (1992).[23] *N*-linked glycans were released from VWF by hydrazionolysis and purified by lectin affinity chromatography and the glycans sequenced by sequential exoglycosidase digestion in conjunction with methylation analysis. They confirmed that the major type of *N*-linked glycan presented by VWF was the bi-antennary type (78.2%). Of these bi-antennary glycans, 70% did not have a bisecting GlcNAc residue. Mono-antennary structure comprised 0.4% of the total *N*-linked structures, tri-antennary 12.3% and tetra-antennary 2.3%. Furthermore a small number (0.8%) high mannose structures were observed.[23] An interesting and significant finding was that a number of the *N*-linked chains presented the ABO(H) blood group sugars.[23] This had also been reported in 1979 by Sodetz,[253] but the observation had not been supported by later studies.[254,258] Further study using blood group sugar specific antibodies and lectins confirmed that the VWF does indeed present ABO blood group sugars. Interestingly in the same study, α-2-macroglobulin and FVIII were also shown to present the blood group sugars.[260]

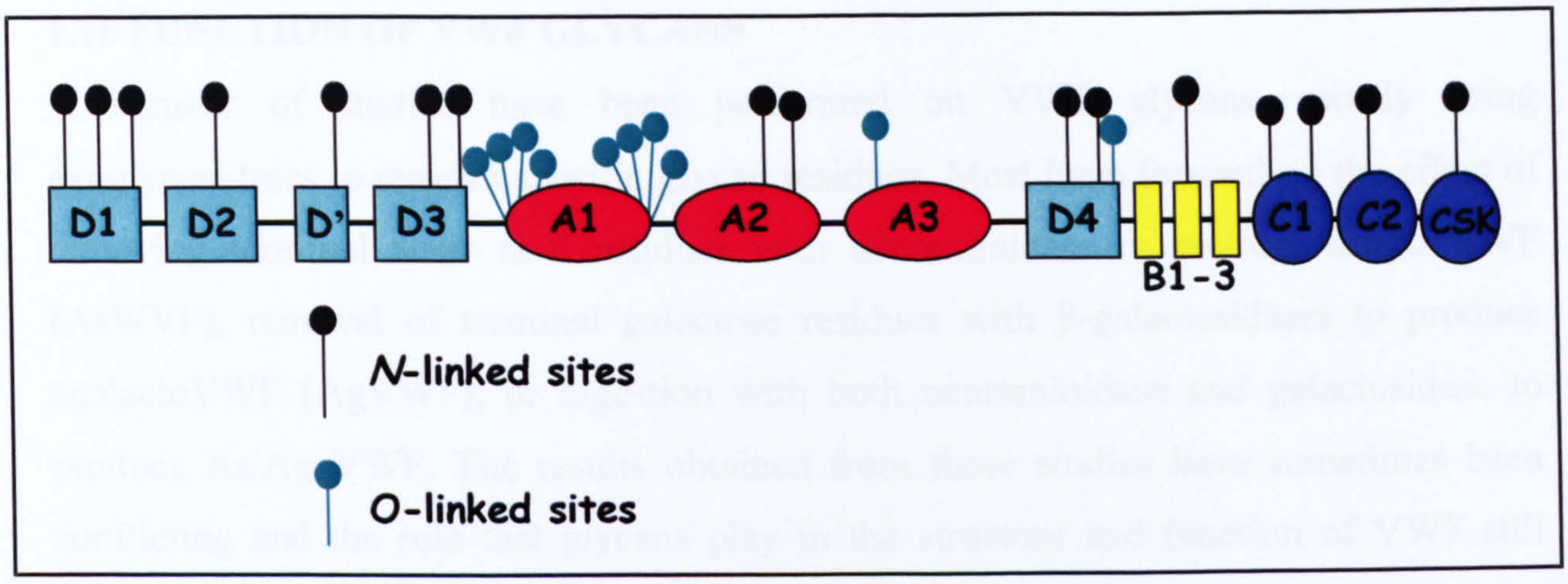


Figure 1.11 VWF glycosylation sites

From the primary amino acid sequence and early work by Titani *et al*, VWF is predicted to contain 10 O-linked glycosylation sites and 16 *N*-linked sites. Of the N-linked sites, four occur in the propeptide (D1-D2) and the remaining twelve are spread throughout the molecule. Eight of the O-linked sites are predicted to be clustered around the A1 domain flanking regions.

1.16 FUNCTION OF VWF GLYCANS

A number of studies have been performed on VWF glycans, mostly using exoglycosidases to remove specific glycan residues. Most have focused on the effect of removing terminal sialic acid residues with neuraminidase to produce asialo VWF (AsWVF), removal of terminal galactose residues with β-galactosidases to produce agalactoVWF (AgVWF), or digestion with both neuraminidase and galactosidase to produce As/Ag VWF. The results obtained from these studies have sometimes been conflicting and the role that glycans play in the structure and function of VWF still remains, in part, inconclusive.

1.16.1 Multimeric Structure

As mentioned previously, *N*-linked glycosylation is essential for dimerisation of VWF, since treatment of endothelial cells with Tunicamycin results in the accumulation of VWF monomers within the cell. It is not known if all the *N*-linked sites need to be occupied for dimerisation/multimerisation to occur or if an individual site(s) are required. However, VWF expressed with the A2 domain deleted, thus lacking *N*-linked sites N1515 and N1574, formed normal VWF multimers, suggesting in part that it is specific glycan site(s) that are essential to proper multimer formation. Studies using exoglycosidases to alter VWF glycan structure have demonstrated removal of sialic acid does not affect VWF multimeric structure. [261-264] However, conflicting results have been obtained with regard to the removal of terminal galactose residues. Removal of galactose residues from AsVWF was demonstrated to affect multimeric structure, causing a loss of high molecular weight multimers and an increase in low molecular weight sepecies.[263-265] One of these studies also reported loss of HMW multimers when just the terminal galactose residues were removed.[263] However this finding has not been confirmed. In contrast to this, a study by Federici *et al* showed that removal of sialic acid and galactose residues did not alter VWF multimeric structure and furthermore treatment with neuraminidase, β-galactosidase and endo F, removed 83% of VWF carbohydrate and did not affect multimeric structure.[262]

1.16.2 Platelet Aggregation

A number of studies have investigated the effect of VWF glycan structure on VWF platelet aggregation function with conflicting results. Several studies have suggested that AsVWF is able to induce spontaneous platelet aggregation in the absence of ristocetin and increases ristocetin mediated aggregation.[266-268] However, other studies have obtained results where AsVWF causes a decrease in ristocetin mediated platelet aggregation,[269-271] and further studies have observed no effect of AsVWF on ristocetin independent or mediated aggregation.[263,272-275] In a study by Lawrence and Gralnick wild type and AsVWF preparations were perfused over human umbilical artery segments. Compared to wtVWF, AsVWF caused a 69% reduction in platelet binding,[276] demonstrating that under flow conditions (at least in this study) AsVWF had a negative effect on VWF platelet binding function. However, a later study by Bastida *et al* did show that AsVWF increased platelet aggregation under flow conditions.[277] The reason for the disagreement between these two studies is not clear. More recently, the platelet binding function of VWF was assessed using recombinant A1 domain produced in *E.coli*, (thus lacking glycosylation) and was compared to A1 domain expressed in CHO cells that follow glycosylation pathways. The non-glycosylated A1 domain bound to platelets in a platelet binding assay with slightly higher affinity compared to the glycosylated form, apparent K_D = 1.4μM compared to 4.5μM.[146] The binding site for GPIb is located in the A1 domain[96] and is flanked by a potential 8 O-linked glycan sites, clustered in two groups of four, either side of the A1 domain. It is therefore feasible that any effect of VWF glycosylation on the interaction with GPIb will be mediated by these glycans. In a study by Carew *et al* (1992), VWF was expressed in Chinese Hamster Ovary Cells (CHO) with a reversible defect of O-linked carbohydrate metabolism. Both wtVWF and VWF lacking O-linked glycans bound to type I collagen and heparin with similar affinity, but O-less VWF was less able to bind to formalin fixed platelets and induce ristocetin mediated platelet agglutination.[278] In a study by Schulte *et al* (2004) recombinant A1 domain was expressed in COS-7 cells with point mutations to alanine of the predicted O-linked glycosylation sites: T1248, S1253, T1255, T1256 and T1468. Recombinant A1 was also expressed in the presence of an inhibitor of O-linked glycan synthesis, α-N-acetyl-α-galactosaminide.[279] O-less A1 domain increased platelet aggregation, as did S1253A, T1255A and T1468A.[280] One potential difference for the observations in these two mentioned studies is the latter used recombinant A1 domain and thus has no need to use ristocetin to modulate the interaction with GPIb.[280]

However, the role that VWF glycans play in its platelet adherence function still remains unresolved.

1.16.3 Protection from Proteolytic Cleavage

A number of studies have shown that the glycan component of VWF protects against proteolytic cleavage. Federici *et al* demonstrated that As and As/Ag VWF were more susceptible to cleavage by plasmin.[262] After incubation with plasmin (32μg/ml) for 4 hours, wild type VWF had no major loss of HMW multimers, where as AsVWF was reduced to medium to LMW multimers and As/Ag VWF was cleaved to dimers and monomers.[262] Furthermore a study by Berkowitz *et al* presented a similar finding where As and As/Ag VWF were more susceptible to cleavage by plasmin and also trypsin and chymotrypsin.[261] This increased susceptibility to proteolysis may explain why, in the studies mentioned above, removal of glycan resides affected multimeric structure, since contaminating proteases may have been present in the VWF preparations used. Other studies have also demonstrated that the glycan moiety of glycoproteins can protect against proteolytic cleavage. Nonglycosylated fibronectin was shown to be more susceptible to proteolytic degradation that the glycosylated form.[281]

1.16.4 Collagen Binding

Little work has been performed on the effects of VWF glycan structure on collagen binding. A study by Kessler *et al* showed that AsVWF bound to type I collagen similarly to wild type VWF, and As/AgVWF bound to type I collagen with reduced affinity.[265] However, this study also demonstrated a loss of HMW multimers on removal of galactose residues. Therefore the reduction in collagen binding function may represent a loss of HMW VWF multimers rather than a direct effect of removing galactose residues.

1.16.5 VWF Clearance

Although significant progress has been made in defining the biosynthesis and the structure and function of VWF, comparatively little is known about the removal of VWF from the circulation. Sodetz *et al* studied the clearance of ^{125}I labelled human VWF (hVWF) in healthy New Zealand white rabbits and showed that VWF was cleared in a biphasic pattern, with an initial distribution rate phase of $t_{1/2}$ = 3hours and an elimination phase of $t_{1/2}$ = 19hours.[269] The biphasic clearance pattern has also been

demonstrated in Female Sprague Dawley rats;[282] distribution phase $t_{1/2}$ = 35mins, elimination phase $t_{1/2}$ = 245mins and also in VWF deficient mice; distribution phase $t_{1/2}$ = 13mins, elimination phase $t_{1/2}$ =180mins.[283] In the latter study, Lenting *et al* showed that a similar pattern of clearance was observed for both high and low molecular weight hVWF preparations, indicating that in the VWF-knockout murine model clearance is independent of multimer size.[283] However in a study using Dutch Kookier dogs with hereditary VWF deficiency that had undetectable VWF levels, the half life for HMW weight VWF was ~21hours, but for LMW VWF the half life was only 9hours,[284] and moreover in the study using Sprague Dawley rats it was the highest molecular weight multimers that were cleared the fastest.[282] These results suggest that further work is needed to determine the relationship between VWF multimeric size and rate of clearance. As yet, the relationship between ADAMTS13 cleavage of VWF and clearance has not been determined.

In the Lenting *et al* study using the murine model, the clearance of a number of truncated recombinant VWF variants were investigated. The results suggested that a major receptor site for clearance was located in the A1A2A3 domains; since clearance rates of recombinant A1A2A3 were comparable to FL-VWF.[283] The D4-CSK domains appeared to have a regulatory role by enhancing VWF clearance with deletion of the D4-CSK domains reducing the rate of clearance. The D'D3 domains were observed to have a negative regulatory role by decreasing the rate clearance, with their deletion resulting in ~2 fold increased clearance, suggesting that the D'D3 region of VWF has a preventive role in VWF clearance.[283] Furthermore this study also demonstrated that mutation of Arg1205 in the D3 domain markedly increased clearance, suggesting that mutation of Arg1205 abrogated the protective effect of the D'D3 domains. Finally, using the same model, Van Schooten *et al* demonstrated that mutations of cysteine residues C1130, C1149 and C2671 resulted in increased clearance.[285]

1.16.6 VWF Clearance – Role of Carbohydrate

The carbohydrate moiety of many plasma glycoproteins has been shown to influence hepatic clearance rates.[286] Removal of terminal sialic residues and subsequent exposure of galactose residues has been shown to increase the rate of clearance for a number of proteins, such as prothrombin and thyroxine-binding globulin.[287-290] Removal of sialic acid from carbohydrate chains increases clearance via binding to the asialoglycoprotein receptor; that recognises newly exposed galactose and GalNac residues. A number of

other carbohydrate receptors are also expressed in the liver that recognise, mannose/N-acetylglucosamine, fucose and phosphomannosyl.[286]

Studies using the rabbit model to investigate clearance showed that asialo VWF labelled with ^{125}I was cleared more rapidly from the circulation, having a half life of 5mins compared to 240mins for wild type VWF.[269] This was also accompanied by appearance of the ^{125}I VWF in the liver, and hepatic clearance was inhibited by simultaneous infusion of asialo-α-1-acid glycoprotein that binds the asialoglycoprotein.[269] *In vitro* analysis of VWF binding to the asialoglycoprotein receptor showed that wild type exhibited negligible binding, whereas binding of AsVWF was comparable to binding of asialo-α-1-acid glycoprotein. When the terminal galactose residues were removed from AsVWF, binding was abolished, demonstrating that terminal Galβ1-4GlcNAc is the VWF glycan sequenced recognised by the asialoglycoprotein receptor.[270] However, other terminal sugars may play a role in VWF clearance, since other asialo glycoproteins with terminal sugars other than galactose have been shown to be cleared faster than the corresponding wild type protein.[291,292] Furthermore the hepatic asialoglycoprotein receptor has been shown to have 60-fold greater affinity for GalNAc over galactose.[293] A murine model has also been made where expression of the ST3Gal-IV sialyltransferase has been inactivated. This results in decreased sialic acid content on VWF , and thus increased terminal galactose presentation. In the ST3Gal-IV sialyltransferase mice, VWF is cleared faster compared to normal mice.[294] This demonstrates that sialic acid prevents clearance of VWF. In addition, a subpopulation of humans with abnormally low VWF levels were identified that had increased galactose exposure on VWF, providing further evidence that exposure of galactose residues result in increased VWF clearance.

A natural murine model has also provided evidence that VWF glycans can play a critical role in VWF clearance. The RIIIS/J mouse is an inbred strain that has reduced plasma VWF levels of up to 20-fold compared to wild type.[295] The gene responsible for this, Mvwf, is an allele of a N-acetylgalactosaminyltransferase, Galgt2. Mvwf is located on chromosome 11,[296] distant from the murine VWF gene located on chromosome 6.[297] In normal humans and animals expression of Galgt2 is limited to the kidney and intestines. In the RIIIS/J mouse gene expression of Galgt2 is switched from the intestinal epithelial cells to vascular endothelial cells causing aberrant glycan modification of VWF which results in increased GalNAc presentation on VWF glycans.[298] This aberrantly glycosylated VWF was shown to be cleared faster from the

circulation by the asialoglycoprotein receptor, with a half-life of 25mins compared to 300mins for wild type murine VWF.[298] Finally, the O-linked glycans of VWF may also play a role in clearance. Using the Female Sprague Dawley rats, VWF deficient of O-linked glycans was shown to be cleared faster than wild type VWF.[282]

1.17 VWF LEVELS IN HUMAN PLASMA

The average plasma VWF concentration is ~10μg/ml (35nM based on a monomer molecular weight of 270kDa). The normal distribution of plasma VWF concentration across the population shows a wide range with a skewed distribution towards higher levels.[299] The normal laboratory range for VWF is 5-15μg/ml. Low levels or deficiency of VWF has long been established as a cause of a bleeding tendency known as Von Willebrand Disease.[2] Conversely, an accumulating body of evidence suggests that elevated VWF levels may represent a risk factor for myocardial infarction and venous thromboembolic disease.[300-304] Furthermore a recent study by Bongers *et al* (2006) showed evidence that high levels of VWF increase the risk of first ischemic stroke.[305] Various genetic and non-genetic factors contribute to the large variation seen in VWF levels across the population with a major contributing factor to the variation being ABO blood group status.

1.17.1 Regulatory Defects of VWF Expression

Three single nucleotide polymorphisms in the 5' promoter region of the VWF gene (C/T at -1234; A/G at -1185 and G/A at -1051) have been shown to exert a major influence on plasma VWF levels.[306] Individuals with genotype CCAAGG had mean VWF levels of 0.96U/ml, compared to mean levels of 0.78U/ml individuals with genotype TTGGAA.

1.17.2 Environmental Influences

A number of environmental factors can also increase plasma VWF levels. These include increasing age, gender (women higher than men), exercise and any cause of the acute phase response, e.g. malignancy, infection or inflammation.[300] Chronically elevated VWF levels have also been described in a number of vascular disorders including severe atherosclerosis and diabetes.[307]

1.17.3 Ethnic Group

VWF levels also vary across ethnic groups, with Caucasians having significantly lower levels than African-Americans.[300,308-310] Differences in VWF are also observed between African-Americans and Indians, with levels significantly higher in Africans.[310] No difference in levels is observed between Caucasians and Indians.[310]

1.17.4 Defects of the VWF Gene

As previously mentioned, individuals with type 1 VWD have reduced VWF levels and individuals with type 3 VWD have virtually complete VWF deficiency as a result of mutations at the *VWF* locus. The most common type 3 mutation is a single cytosine deletion at nucleotide 2435 that results in a frame shift in exon 18.[311] A full list of all the known VWD causing mutations can be found on the ISTH SSC VWF information home page at: http://www.vwf.group.shef.ac.uk/

1.17.5 Other Quantitative Trait Loci

As well as the VWF gene, other gene loci can exert major quantitative effects on plasma VWF levels. The most common of these is the ABO blood group locus on chromosome 9q34. Individuals of blood O have generally 20-30% lower levels of VWF compared to non-O blood groups.[312] Evidence from twin studies has shown that 66% of the total variation in plasma VWF levels is genetically determined, and 30% of the total variation is explained the ABO blood group effect on VWF levels.[312]

1.18 THE ABO BLOOD GROUP SYSTEM

The ABO blood group system was first described by Karl Landsteiner in the early 1900's, and it's molecular basis was reported in 1990 by Yamamoto.[313] The antigens of the ABO system (A, B, and H) consist of a series of complex glycan chains that differ only with respect to their terminal sugar residues, with the terminal sugars representing the antigenic structure.[314]

The H (Fuc α1→2 Gal β1→4 GlcNAc β1→) antigen is formed by the addition of a fucose residue to the terminal galactose residue of a specific precursor glycan chain (Figure 1.12). This reaction is catalysed by α(1,2)-fucosyltransferase (H-transferase), encoded by the *FUT 1* locus located on chromosome 19. Addition of this fucose moiety to the precursor chain is essential before further addition of the A (GalNAc α1→3 [Fuc

α1→2] Galβ 1→4 GlcNAc β1→) or B (Gal α1→3 [Fuc α1→2] Galβ 1→4 GlcNAc β1→) determinants can occur. In blood group A and B individuals, different alleles at the ABO blood group locus (9q34) encode for either α-1,3-N-acetylgalactosaminyltransferase (A transferase) transferase or α-1,3-galactosyltransferase (B transferase), respectively. Consequently A and B glycans differ only in respect to the terminal carbohydrate moiety expressed (Figure 1.12). AB individuals express both the A and B transferases. In group O individuals, the *O* allele does not encode any functional transferase enzyme so that they continue to express terminal H structures only.

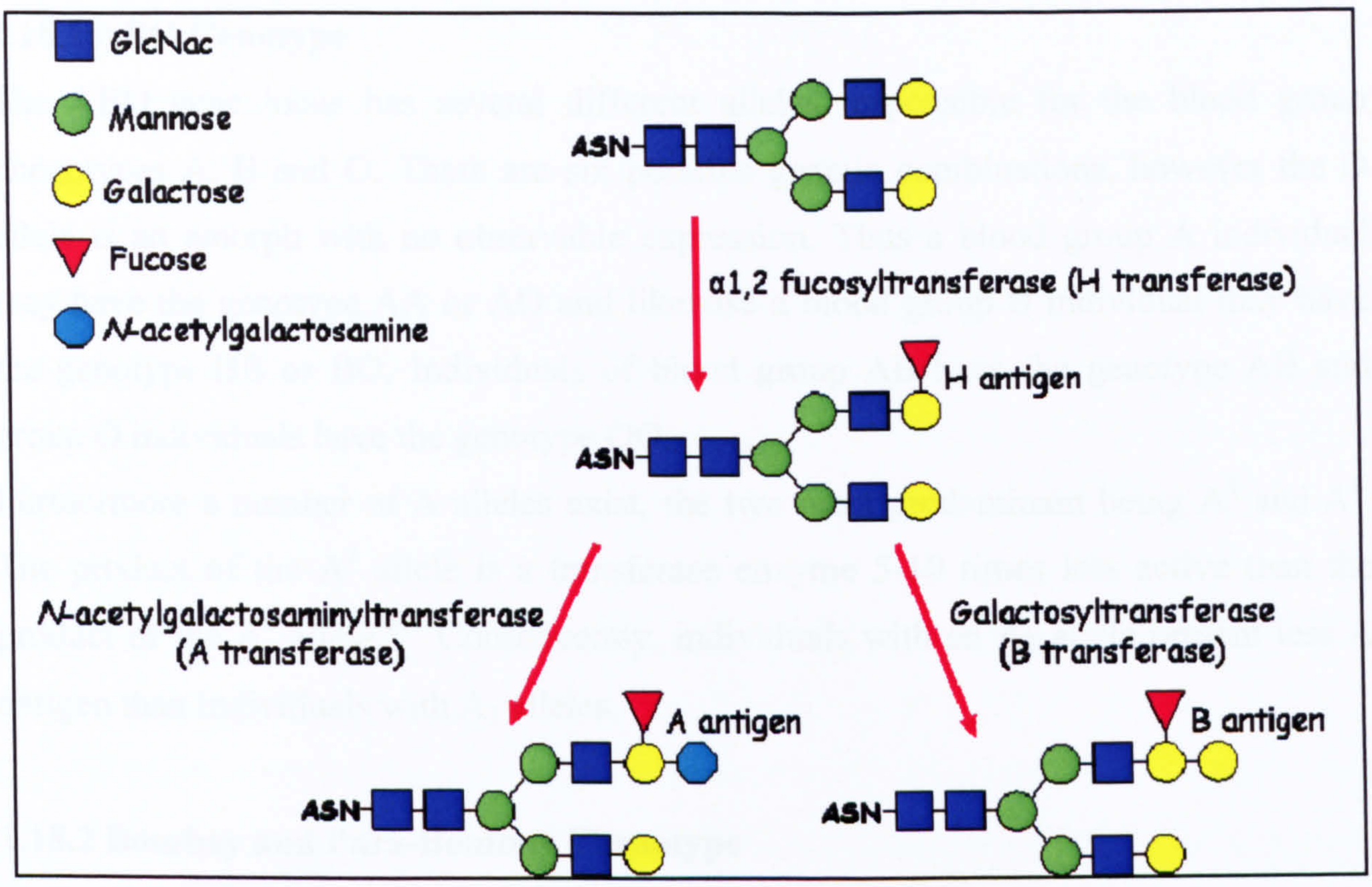


Figure 1.12 Construction of ABO antigens

The blood group antigens are formed by the addition of specific sugar residues to a precursor glycan chain. α1,2 fucosyltransferase (H transferase) adds a fucose residue in an α1-2 linkage to the terminal region of the pre-cursor glycan chain forming the H antigen. Formation of the H antigen is necessary for further formation of the A and B antigens. Individuals of blood A, express a *N*-acetylgalactosaminyltransferase (A transferase) that adds a *N*-acetylgalactosamine residue to the H structure. Individuals of blood group B express a galactosyltransferase (B transferase) that adds a galactose residue to the H structure. Individuals of blood group AB express both A and B transferases and convert H structure to both A and B antigens. Individuals with blood group O only express the H structure.

1.18.1 ABO Genotype

The ABO gene locus has several different alleles responsible for the blood group phenotypes A, B and O. There are six possible genetic combinations, however the O allele is an amorph with no observable expression. Thus a blood group A individual may have the genotype AA or AO and likewise a blood group B individual may have the genotype BB or BO. Individuals of blood group AB have the genotype AB and group O individuals have the genotype OO.

Furthermore a number of A alleles exist, the two most predominant being A^1 and A^2. The product of the A^2 allele is a transferase enzyme 5-10 times less active than the product of the A^1 allele.[315] Consequently, individuals with an A_2 allele present less A antigen than individuals with A_1 alleles.

1.18.2 Bombay and Para-Bombay Phenotype

In human tissues, H antigen can be synthesised by two distinct α-1,2-fucosyltransferases. One is the *H* gene *(FUT1)*-encoded H enzyme that regulates expression of ABH antigens in red blood cells. The other is the *Secretor* gene *(FUT2)*-encoded Se enzyme that regulates expression of ABH antigens in the gastrointestinal tract and secretions. Very rare individuals with the Bombay phenotype are non-secretors who also fail to express H transferase (*FUT 1*). Such people cannot synthesise A or B antigenic structures regardless of their ABO blood group genotype, and ABH antigens are absent from both their erythrocytes and secretions. Para-Bombay individuals also fail to express H transferase, but do express the *FUT2* (Secretor) encoded α-1,2-fucosyltransferase, so that ABH antigens are present in their secretions but not on their erythrocytes.

1.19 RELATIONSHIP BETWEEN ABO BLOOD GROUP AND PLASMA VWF LEVELS

An effect of ABO blood group on VWF was first demonstrated by Preston *et al* in 1964 with the lowest levels observed in individuals of blood group O,[299] and has subsequently been confirmed in larger studies[309,312,316-321] with blood group O individuals having generally ~30% lower VWF levels than non-group O individuals. Moreover the largest of these studies, Gill *et al* (1987), with 1100 normal individuals, demonstrated significant difference in VWF levels between non-O blood groups.[316] Levels were highest in AB individuals, followed by group B, group A and lowest levels

were observed in group O individuals. Shima *et al* also showed that the ABO effect was the same if the measure of VWF was functional rather than antigenic. Furthermore, multimer analysis showed that VWF multimer structure did not between blood groups.[319]

As well as ABO phenotype having an effect on VWF levels, ABO genotype has also been shown to effect VWF levels. As expected lowest VWF levels were observed in genotype 00, (Blood group O) and it was shown that individuals heterozygous for the O allele – genotypes AO and BO, had significantly lower levels of VWF than individuals not carrying an O allele.[319,320,322]

The mechanism by which ABO blood group has an effect on VWF levels is unknown. However linkage analysis suggests that the effect is due to a direct functional effect of the ABO locus rather than a linkage disequilibrium.[320] O'Donnell *et al* suggested that H-antigen expression on VWF mediates the ABO effect on plasma VWF levels, with an inverse correlation between H antigen on VWF expression and plasma VWF levels.[322] How H-antigen expression can influence VWF levels is not clear, however as demonstrated with the RIIIS/J mouse, the presence of a single glycan moiety can influence plasma VWF levels. It is also interesting that levels of platelet VWF, that has been shown not to present the ABO antigens, are not affected by ABO blood group.[323] Furthermore, a study by *Bowen* showed that ABO blood group altered susceptibility to proteolysis by ADAMTS13. Multimer analysis and CBA showed that purified blood group O with was cleaved faster than non-O blood group VWF.[324] As discussed the carbohydrate component of VWF protects against proteolytic cleavage and the glycan structure of other proteins has been shown to protect against proteolysis. It is also interesting that the ADAMTS13 cleavage site is in the vicinity of two *N*-linked glycan sites; N1515 and N1574. How these may affect cleavage is undetermined.

1.20 AIMS OF THESIS

The overall aim of this thesis is to investigate the effect of VWF glycans on the function of the VWF molecule with specific attention to the effect the glycans have on the interaction with ADAMTS13. Initially this will involve the purification of VWF from plasma and FVIII/VWF concentrates and require the development of collagen binding and multimer gel assays to assess functional aspects of VWF and to analysis proteolysis by ADAMTS13. The first part of the investigation will focus on the role of the blood group sugars presented on VWF, in mediating plasma VWF levels and susceptibility to ADAMTS13 proteolysis. Specifically, I will examine VWF from individuals with the rare Bombay Phenotype and determine the effect this phenotype has on VWF function.

I plan to then analyse VWF both *in silico* and experimentally to investigate further the glycan structure of the molecule and the occupancy of specific glycan sites and presentation of blood group sugars.

To further the investigation, I will examine the effect of altering other glycan structures present on VWF, by enzymatic digestion to removal specific sugar residues or structures and develop lectin analysis assays to assess the extent of sugar alteration. Furthermore, I will use site directed mutagenesis to mutate specific *N*-linked glycosylation sites and the glycan modified VWF preparations will be analysed for their functional activity, with specific attention paid to the effect on the interaction with ADAMTS13.

CHAPTER 2

2. MATERIALS AND METHODS

2.1 PURIFICATION OF BLOOD GROUP SPECIFIC VWF FROM PLASMA

2.1.1 Cryoprecipitation

Cryoprecipitation was used to extract VWF from plasma, exploiting the phenomenon that various circulating proteins precipitate out of solution at temperatures of 4°C or less. Plasma surplus to requirements was obtained from the National Blood Transfusion Service. Two units of blood group specific fresh frozen plasma (~300ml per unit) were thawed overnight at 4°C. Thawed plasma was pooled in a pre-chilled glass beaker and slowly stirred and 50% ethanol pre-chilled to 4°C was added drop wise to a final concentration of 8%v/v. The plasma/ethanol was stirred for 30mins then decanted into pre-chilled 250ml centrifuge tubes in an ice bucket. The resulting precipitate was then harvested by centrifugation; 3500rpm for 30mins at 4°C. The cryo-supernatant was decanted off, aliquoted and stored at -80°C for later use as a source of ADAMTS13. The VWF rich pellet was resuspended in 10ml of Tris-Citrate (TC) buffer (20mM Tris, 10mM sodium citrate, pH 7.4). and centrifuged at 11500rpm for 30mins at 22°C. The supernatant was removed and was further purified by size exclusion chromatography.

2.1.2 Gel Filtration

Gel filtration or size exclusion chromatography separates proteins on the basis of size. Smaller proteins enter the gel filtration matrix more readily and have a retarded passage through the column, where as larger proteins do not enter the gel filtration matrix and pass more readily through the column.

To isolate high molecular weight VWF, a Sepharose 2B-CL gel filtration column (Amersham Pharmacia, UK) (600mm × 26mm, 318.5ml volume) was pre-equilibrated overnight with 2 column volumes of Tris-citrate (TC) buffer. The cryoprecipitated VWF (~10ml) was applied to the column at a flow rate of 0.7ml/min, then eluted with TC buffer at flow rate 1ml/min. Fifty two, 5ml fractions were collected (A1-E4). VWF concentration was determined by VWF antigen ELISA, multimeric composition was

analysed by VWF multimer gels and collagen binding assay and purity assessed by silver staining.

2.2 PURIFICATION OF VWF FROM HAEMATE P

2.2.1 Gel Filtration

A commercial VWF/FVIII concentrate, Haemate P® (ZLB Behring, Germany) was used to obtain large quantities of VWF. Haemate P® was resuspended in 10ml of H_2O and centrifuged at 4000g for 5mins. This was loaded on to a Sephacryl-400 gel filtration column (Amersham Pharmacia, UK) (600mm × 26mm, 320ml volume) that had been pre-equilibrated with 2 column volumes of Buffer A, (100mM NaCl, 20mM Tris-HCl, pH7.4). The column was eluted at a flow rate of 1ml/min and fifty-two 5ml fractions were collected (A1-E4). Fractions B7-D12 were pooled for further purification by Heparin-Sepharose affinity chromatography.

2.2.2 Heparin-Sepharose Affinity Chromatography

A SK-16 chromatography column (Amersham Pharmacia, UK) was packed with 30ml of Heparin-Sepharose 6 fast flow (Amersham Pharmacia, UK) according to manufacture's instructions. Briefly, the empty SK-16 column was washed with ddH_2O and the bottom outlet tube connected to an AKTA FPLC machine. The column was flushed with 20mM Tris-HCl pH 7.4, and then 35ml of Heparin-Sepharose 6 fast flow was poured into the column chamber with a smooth continuous motion. The remaining column space was filled with 20mM Tris-HCl pH 7.4 and the plunger inserted into the top of the column. The Heparin-Sepharose was allowed to settle for 1min, before a flow rate of 5ml/min was applied to the column for 20mins to ensure the resin was fully packed. The plunger was then pushed ~5mm into the top of the resin. The final column had a volume of 30ml and a maximum flow rate of 3.5ml/min.

To purify VWF, the column was equilibrated with 2 column volumes of Buffer A, then gel filtered fractions B7-D12 were passed over the column at a flow rate of 0.4ml/min. After sample loading was complete, the column was washed with Buffer A until the baseline had returned to zero. VWF was eluted from the column with elution buffer (300mM NaCl, 20mM Tris-HCl, pH 7.4). Three 10ml fractions were collected and dialysed into 20mM Tris-HCl, pH 7.4 overnight at 4°C. VWF concentration was determined by VWF antigen ELISA, multimeric composition was analysed by VWF

multimer gels and collagen binding assay and purity assessed by Coomassie and silver staining.

2.3 ANALYSIS OF PURIFIED VWF

2.3.1 VWF:Ag ELISA

VWF antigen (VWF:Ag) was measured by sandwich enzyme-linked immunosorbent assay. MaxiSorp plates (Nunc) were coated with polyclonal anti-VWF antibodies (Dako) diluted 1/500 in 50mM carbonate buffer, pH9.6, overnight at room temperature. Wells were then washed 3 times with PBS-T [PBS, Tween 20 (0.1% v/v)] and 100µl of test samples applied to the wells at dilutions 1:10-1:60. Reference plasma (Technolcone, UK) diluted 1:10-1:320 was used as a standard. After 1 hour incubation at room temperature wells were washed, and 100µl anti-VWF-HRP (Dako) diluted 1/1000 in PBS-T was added to the wells and allowed to incubate for 1 hour at room temperature. After a final 3 washes, 180µl substrate (Sigma colour fast OPD tablets) was added to the wells and the reaction stopped with 100µl 1M H_2SO_4 after ~2-3mins. Absorbance was recorded at 492nm (UV-1601 spectrophotometer, Shimadzu). A standard curve was generated plotting VWF concentration on the x-axis against absorbance on the y-axis. VWF concentration was expressed a percentage, with reference plasma diluted 1:10 representing 100% VWF. Graphs were plotted in Microsoft Excel and the equation-of-the-line and R^2 values were calculated using the "add trendline" function. The equation-of-the-line was given in the format:

$$y = mx + c$$

Where: y is the absorbance value, m is the gradient of the slope, x is %VWF and c is the y intercept.

To calculate the %VWF of unknown samples the equation was rearranged to:

$$x = (y - c) / m$$

Absorbance values (y) of the unknown samples were substituted into the equation and returned a %VWF value. 100% was taken to equal 1U/ml which is ~10µg/ml. Unless stated all VWF concentration were expressed in µg/ml.

2.3.2 Collagen Binding Assay

Collagen binding activity (VWF:CB) is recognised as a sensitive measure of high-molecular weight VWF (HMW-VWF). The highest molecular weight VWF multimers bind collagen with the greatest affinity. VWF:CB of plasma and purified VWF was determined using an ELISA based collagen binding assay. Initially VWF:CB was assessed using a commercial ELISA (Technoclone, UK) according to the manufacturer's recommendations. However an in-house VWF:CB was developed as part of this project. Human type III collagen prepared from the placenta by trypsin digestion (Sigma, UK C-4407) was dissolved for 16 hours at 4°C in 200mM acetic acid (final concentration of 0.1mg/ml). Dissolved collagen was aliquoted and stored at -20°C until use. Aliquots were only used once and never refrozen. To determine optimal coating concentrations and coating times, collagen was diluted to 1-15µg/ml in 50mM carbonate buffer, pH 9.6 and 100µl per well, applied to MaxiSorp plates (Nunc) and incubated from 24 hours up to 49 days at room temperature. After coating, wells were washed 3 times with phosphate buffered saline with 0.1% Tween (PBS-T) and blocked with 2%BSA-PBS-T for 1 hour at room temperature. After blocking, wells were washed 3 times as before and samples diluted 1:10 to 1:240. Reference plasma (Technolcone, UK) diluted in the same way was used as standard. 100µl of sample or standard was applied to each well. After incubation for 2 hours at room temperature, wells were washed 3 times with PBS-T and anti-VWF-HRP antibody was applied to the wells, (1/1000 in PBS-T) for 1 hour. After a final wash step, 180µl substrate solution (Sigma colour fast OPD tablets) was added to the wells, the reaction stopped with 100µl 1M H_2SO_4 after ~5mins, and the absorbance measured at 492nm. Inter and intra experimental coefficients of variation were <5%.

A standard curve was prepared as described for VWF:Ag ELISA plotting %CBA along the x-axis (reference plasma diluted 1:10 = 100% CBA) and absorbance along the y-axis. Since the curve began to slightly plateaux at the 1:10 dilution the curve was linearised by taking the Log_{10} values of the %CBA standards. The equation-of-the-line was given in the format:

$$y = mx - c$$

Where: y is the absorbance value, m is the gradient of the slope, x is the %CBA and c is the y intercept.

To calculate the %CBA of unknown samples the equation was rearranged to:

$$x = (y + c) / m$$

Absorbance values (y) of the unknown samples were substituted into the equation and a Log_{10} value was obtained and converted to %CBA by use of the inverse Log function.

To demonstrate that the assay was sensitive to VWF multimeric size, plates were incubated with purified, high molecular, medium molecular and low molecular weight VWF fractions that had been standardised for VWF:Ag. Bound VWF was detected as described above. Finally, to ensure that the interaction between VWF and collagen was specific, MaxiSorp plates were coated with equivalent amounts of type III collagen, type IV collagen and BSA and then incubated with pooled normal plasma diluted as described.

2.3.3 VWF Multimer Analysis

The multimeric pattern of VWF may be visualised by analysis in agarose gels under non-reducing conditions. VWF multimer analysis was performed using a modification of previous methods. Low resolution (0.8-1.3%) and high resolution (1.5-2.5%) agarose gels (1.5mm diameter) were prepared by dissolving 0.8-2.5g high gelling temperature agarose (Seakem) in 100ml of gel buffer [200mM Tris, 100mM glycine, 0.1% sodium dodecyl sulphate (SDS), pH 9.0] and cast using a Bio-Rad mini gel casting system and stored at 4°C for a minimum of 2 hours and a maximum of 7 days. Samples were diluted 1:10 with sample buffer (10mM Tris, 1mM EDTA, 2% SDS, 8M urea, 0.01% bromophenol blue, pH 8.0) and incubated for 30mins at 60°C. Gels were assembled in a Bio-Rad mini-gel electrophoresis tank and running buffer (100mM Tris, 150mM glycine, 0.1% SDS, pH 8.4) applied to the tank and cooled at 4°C for 30mins. 10µl of sample was applied to each well and electrophorised at 60V for 20mins then 35V until the tracking dye had reached the end of the gel. After electrophoresis, transfer of protein to Hybond nitrocellulose membranes (Amersham Pharmacia, UK) was carried out for 2 hours at 400mA at 4°C. The membranes were then rinsed in PBS-T, and blocked for 1 hour with 5% membrane blocking reagent/PBS-T (Amersham Pharmacia, UK). Finally, the membranes were incubated with anti-VWF-HRP antibody (DAKO) diluted 1/1000 for 1 hour. After washing, bound antibody was detected with ECL chemiluminescent kit (Amersham Pharmacia, UK) and exposure to Amersham Hyper-Film.

2.3.4 H-antigen on VWF ELISA

Presence and quantification of H antigen on VWF was preformed using a modified sandwich ELISA. 96 well plates (Nunc) were coated with rabbit anti-human VWF antibody diluted 1/500 in 50mM carbonate buffer and incubated overnight. After washing 3 times with PBS-T, wells were blocked with 2% BSA for 1 hour. After a further 3 washes plasma or purified VWF samples were added at dilutions 1:10-1:240 and incubated for 2 hours. Pooled group O plasma was used as reference. Plates were washed then incubated for 1 hour with biotin conjugated *Ulex Europaeus Agglutinin I* (UEA) (Vector labs, UK) diluted 1/1000 in PBS-T. Plates were washed 3 times then incubated with streptavidin conjugated HRP (Vector Labs, UK) for 45mins diluted 1/1000. After a final 3 washes, 180µl substrate (Sigma colour fast OPD tablets) was added to the wells and the reaction stopped with 100µl 1M H_2SO_4. Absorbance was recorded at 492nm (UV-1601 spectrophotometer, Shimadzu). Concentrations of unknown samples were read from the standard curve, the same samples analysed for H-antigen were also analysed for VWF:Ag as described, and the amount of H-antigen was expressed per unit of VWF.

2.4 SDS POLYACRYILAMIDE GEL ELECTROPHORESIS (SDS-PAGE)

SDS-PAGE is used to separate proteins on the basis of their molecular weight. Treatment with the anionic detergent, sodium dodecyl sulphate (SDS) denatures proteins to their primary structure and confers on them a negative charge. Different concentrations of NuPAGE Bis-Tris precast polyacryilamide gels (Invitrogen) were used to resolve proteins of different molecular weights using this technique.

Samples to be analysed under non-reducing conditions were diluted with 2 X SDS loading buffer, (200mM Tris, 8%SDS, 0.4% Bromophenol blue, 50% glycerol). Samples to be analysed under reducing conditions were diluted with the same buffer containing 4% w/v β-mercaptoethanol. A pre-stained molecular weight protein marker (Invitrogen) was run in parallel with all samples. Samples were heated for 15mins at 95°C, then electrophoresis was carried out in NuPAGE gels (Invitrogen) at 200V constant, until the gel dye had reached the end of the gel (~40mins). Detection of proteins was performed by Coomassie staining, silver staining and western blotting.

2.4.1 Coomassie Staining

Non-specific detection of proteins was achieved using SimplyBlue™ SafeStain (Invitrogen, UK), that has a detection limit of 7ng total protein. After SDS-PAGE, gels were washed 3 times with ddH_2O for 5mins, then incubated with 25ml SimplyBlue™ SafeStain for 1 hour at room temperature on a shaker. Gels were then washed with double distilled H_2O (ddH_2O) until the gel was distained. Gels were dried using gel Dryer 583 (Bio-Rad, UK) for two hours.

2.4.2 Silver Staining

Non-specific detection of proteins was also performed using silver staining which is more sensitive than Coomassie staining, with a detection limit of 0.2-0.6ng of protein. Silver staining was performed using the PlusOne™ silver stain kit, (Amersham Pharmacia, UK) as per manufactures instructions. Briefly, gels were fixed in 40% ethanol, then sensitised, before being stained with silver nitrate, and visualisation of proteins bands.

2.4.3 Western Blot

Detection of specific proteins in an electrophoresed sample was achieved by western blot analysis. After electrophoresis, gels were equilibrated in transfer buffer for 15mins. Proteins were transferred to nitrocellulose membranes (Amersham Pharmacia, UK) using a Trans-Blot Electrophoretic Transfer Cell (Bio-Rad), in the presence of ice to prevent overheating, and under stirring conditions to ensures equal ionic distribution. Transfer was carried out for 60mins at 100V constant. After transfer, non-specific sites were blocked with 2.5% membrane blocking reagent (Amersham Pharmacia, UK) in PBS-T, for either 1 hour on a shaker at room temperature or overnight at 4°C. After rinsing in PBS-T, membranes were incubated for 1 hour with the relevant primary antibody diluted in PBS-T on a shaker at room temperature. Membranes were then washed with PBS-T for 1×15mins and 4×5mins, then incubated with secondary antibody linked to HRP, diluted in PBS-T for 1 hour at room temperature on a shaker. After washing as before, protein was detected with an ECL chemiluminescent kit (Amersham Pharmacia, UK). Briefly, equal amounts of solutions A and B are applied to the membrane for 1min then the membrane is exposed to Hyper-Film (Amersham Pharmacia, UK) and developed.

Primary Antibody	Concentration	Secondary Antibody	Concentration
Rabbit polyclonal Anti-VWF-HRP (Dako)	1/1000	N/A	N/A
Mouse Anti-myc (Invitrogen)	1/5000	Goat Anti-mouse-HRP (Dako)	1/2000
Mouse polyclonal Anti-ADAMTS13 protease domain	1/4000	Goat Anti-mouse-HRP (Dako)	1/2000

Table 2.1 Primary and secondary antibodies and their concentrations used for western blotting

2.5 EXPRESSION AND PURIFICATION OF ADAMTS13

2.5.1 Expression of ADAMTS13

Recombinant ADAMTS13 (rADAMTS13) was prepared from HEK293 cells that had been previously stably transfected with the full length ADAMTS13 cDNA, cloned by Dr James Rance into the mammalian expression vector pcDNA3.1 in frame with a C-terminal myc/His tag. Culture of HEK293 cells stably expressing ADAMTS13 was performed as described in section 2.15. Cells were cultured in growth media in T175 flasks (Nunc) and cultures were expanded until ~20 T175 flasks were obtained. Growth media was removed from the flasks and after washing each flask twice with sterile PBS, 25ml Optimem conditioned media was added to each flask and incubated for 3 days at 37°C, 5% CO_2. Conditioned media was collected and filtered through a 0.5mm Nalgene filter to remove cell debris. The conditioned medium was then concentrated to 50ml using the Labscale™ TFF system (Millipore, UK) with the Pellicon XL 10kDa filter (Millipore, UK).

2.5.2 Purification of rADAMTS13

2.5.2.1 Desalting

Concentrated and filtered serum-free conditioned medium was desalted using a Hi Prep™ 26/10 desalting column (Amersham Pharmacia, UK). The desalting column allows the separation of high molecular weight species (>5kDa) from low molecular species (<1kDa) using the principle of size exclusion chromatography. The column was washed with 300ml ddH_2O, then equilibrated with 100ml of 20mM Tris-HCl, 500mM NaCl, 20mM imidazole, pH 7.8. Concentrated and filtered serum-free conditioned medium was applied to the column and the early eluted fraction were collected to be further purified.

2.5.2.2 Nickel Affinity Chromatography

The desalted media was subjected to nickel affinity chromatography using Nickel charged columns that bind His-tagged proteins allowing contaminants to be removed. Desalted media was passed over a 5ml Ni^{2+} His trap chealting column (Amersham Pharmacia, UK) in 20mM Tris-HCl, 500mM NaCl, 20mM imidazole, pH 7.8. Once the baseline had returned to zero, the column was washed with 20mM Tris-HCl, 30mM NaCl, 20mM imidazole, pH 7.8, then eluted with 20mM Tris-HCl, 500mM NaCl, 500mM imidazole, pH 7.8. Eluted fractions were dialysed into 20mM Tris-HCl (pH 7.8) using 10kDa molecular weight cut-off dialysis membranes (Pierce, UK). Concentration of ADAMTS13 was assessed using the BCA assay and an ADAMTS13 ELISA (see below), purity was assessed using SDS-PAGE in 4-15% gels as earlier described

2.6 ANALYSIS OF ADAMTS13 CONCENTRATION

2.6.1 BCA Assay

The total protein concentration was determined using a BCA total protein assay kit (Pierce, UK). This method is based on the ability of proteins to reduce Cu^{+2} to Cu^{+1} (cuprous ion) in an alkaline medium. The purple-coloured reaction product is formed by the chelation of two molecules of bicinchoninic acid (BCA) with one cuprous ion. The colorimetric intensity correlates with the protein concentration. Bovine serum albumin (BSA) was used as a standard and a series of dilutions of known concentrations (range 15-2000µg/ml) were prepared. Different dilutions (neat, 1:5, 1:10) of the unknown sample were prepared simultaneously. 25µl of each standard or unknown sample were

applied in duplicate to the wells of a microtitre plate. 200µl of the working reagent were added to each well and incubated at 37°C for 30 minutes on a plate shaker. The absorbance was measured at 540 nm using a plate reader (iEMS Reader MF, Labsystems). The protein concentration of the unknown sample was determined by reading from the BSA standard curve.

2.6.2 ADAMTS13 ELISA

To more accurately determine the concentration of ADAMTS13 an Enzyme-Linked ImmunoSorbent Assay (ELISA) was optimised in our laboratory by Dr James Crawley. MaxiSorp plates (Nunc) were coated overnight at 4°C with Rabbit polyclonal anti-ADAMTS13 antibody, (depleted of antibodies against the ADAMTS13 TSP2-4 domains) diluted to 10µg/ml in 50mM carbonate buffer (pH 9.6). After coating, wells were washed 3 times with PBS-T and blocked with PBS-T-2.5%BSA for 1 hour at room temperature. After blocking, wells were washed 3 times as before and 100µl of test samples or Reference plasma (Technolcone) at dilutions 1:10, 1:20, 1:40, 1:60, 1:120 and 1:240 were added to the wells and incubated for 2 hours at room temperature. The plate was then washed 3 times with PBS-T and 100µl of rabbit biotinylated anti-ADAMTS13 TSP2-4 diluted to 0.5µg/ml in PBS-T-1%BSA was applied to the wells and incubated for two hours at room temperature. After washing, the wells were incubated for 1 hour with streptavidin-HRP diluted 1/1000 in PBS-T-1%BSA. After a final wash step, 180µl substrate (Sigma colour fast OPD tablets) was added to the wells, the reaction stopped with 100µl 1M H_2SO_4, and the absorbance measured at 492nm. A standard curve was plotted as described for the VWF:Ag ELISA. Reference plasma diluted 1:10 was taken to be 100% ADAMTS13 with an approximate value of 100% = 1µg/ml.

2.7 CLEAVAGE OF FULL-LENGTH VWF BY ADAMTS13 – OVERVIEW

Cleavage of FL-VWF by ADAMTS13 *in vitro* requires the presence of urea to presumably unfold or uncoil VWF into a confirmation suitable for cleavage, by exposing the ADAMTS13 cleavage site in the A2 domain, and also requires the presence of Ca^{2+} or Ba^{2+} ions to activate ADAMTS13. The source of ADAMTS13 used in the assays was either recombinant material (prepared as described in section 2.5) or cryo-depleted plasma (prepared from cryoprecipitation of VWF, section 2.1.1). Analysis of ADAMTS13 proteolysis of VWF was performed by CBA or VWF multimer gel analysis.

2.7.1 Cleavage by Cryo-Depleted Plasma

Cryodepleted plasma obtained after the cryoprecipitation of VWF was used as a source of ADAMTS13. The concentration of VWF and multimeric composition was determined using VWF multimer gels and VWF ELISA as described. ADAMTS13 concentration was determined by ADAMTS13 ELISA.

50µl of cryodepleted plasma (typical ADAMTS13 concentration of 0.8µg/ml = ~4nM) was added to 50µl reaction buffer (50mM Tris-HCl, 375mM NaCl, 25mM $BaCl_2$) and activated for 20mins at 37°C. 100µl high molecular weight-VWF (HMW-VWF) was then added to a final concentration of 5µg/ml. Aliquots were taken for the zero time point, then 150µl of the reaction mixture was carefully applied to the surface of circular dialysis membranes (Millipore VSWP, 25mm) floating on the surface of 50ml dialysis buffer (0.5-4M urea in 5mM Tris-HCl, pH 8.0) contained in a 50ml plastic tube and incubated at 37°C. Aliquots were removed at specific time points and rate of proteolysis assessed as described by CBA (section 2.3.2).

2.7.2 Cleavage by Recombinant ADAMTS13

Recombinant ADAMTS13 (final reaction concentration of 15nM) was pre-incubated with 10mM $BaCl_2$ for 15mins at 37°C to activate ADAMTS13. Activated ADAMTS13 was then added to the reaction mixture containing 5mM $BaCl_2$, 1.5M urea and 20mM Tris-HCl, pH 7.8. VWF was added to a final concentration of 5µg/ml to start the reaction. Aliquots were taken for time point zero, and the reaction incubated at 37°C and aliquots removed at specific time points for analysis of cleavage by CBA and VWF multimer gel analysis (sections 2.3.2 and 2.3.3 respectively).

2.8 GENERATION OF VWF PROTEOLYTIC FRAGMENTS BY TRYPSIN DIGESTION

Trypsin – Bovine pancreatic type I (Sigma, UK), was dissolved in 200mM sodium acetate, 0.02% sodium azide, pH 7.0 to a final concentration of 40800U/ml, aliquoted and stored at -20°C until use. To generate tryptic fragments, VWF was digested with trypsin at a final concentration of 2500U/mg VWF. In initial experiments 1mg of VWF was digested for 0-90mins at 37°C. In subsequent experiments, to generate significant amounts of VWF tryptic fragments, 10mg of VWF was digested for 30mins at 37°C. Reactions were terminated by the addition of 100mM Aprotinin and 100mM Soya bean trypsin inhibitor (Sigma, UK) and were immediately subjected to initial purification by ion-exchange chromatography.

2.8.1 Ion-Exchange Chromatography

To separate the tryptic fragments of VWF, the trypsin digest was subjected to ion exchange chromatography (IEC), that separates proteins/peptides on the basis of charge. The trypsin digestion reactions were passed through a 5ml Hi Trap Q anion exchanger column. (Amersham Pharmacia), that had been pre-equilibrated with 10 column volumes 20mM Tris-HCl, pH 7.4, at a flow rate of 1ml/min. Once baseline had returned to zero, a gradient of 0-500mM NaCl in 20mM Tris-HCl, pH 7.4 over 60mins, flow rate 1ml/min was applied to elute the column. Eluted fractions were collected then dialysed overnight into 20mM Tris-HCl, pH 7.4. Collected, dialysed fractions were analysed by SDS-PAGE in 4-12% and 12% gels as previously described (section 2.4). Protein bands were detected by Coomassie staining or western blotting followed by probing with anti-VWF-HRP (section 2.4.3) or *Ulex europaeus* as described below.

2.8.2 H-antigen Blot

Western blotting followed by probing with the H-antigen specific lectin, *Ulex europaeus* was performed essentially as just described (section 2.4.3) but with some essential modifications. Following transfer of proteins to nitrocellulose membranes, non-specific sites were blocked with 3% membrane blocking buffer (Amersham Pharmacia, UK) overnight at 4°C. Biotinylated *Ulex europaeus* was diluted 1/500 in Tris buffered saline (TBS) supplemented with divalent ions (50mM Tris, 150mM NaCl, 1mM $MgCl_2$, 1mM $CaCl_2$, 1mM $MnCl_2$) and 2% membrane blocking buffer and incubated at room temperature for 2 hours on a shaker. Membranes were washed with

PBS-0.5% Tween for 2×10mins, then 7×5mins. Membranes were then incubated with streptavidin-HRP (Amersham Pharmacia) diluted 1/1000 in PBS-0.1% Tween and 2% membrane blocking buffer. After washing for 1×15mins and 4×5mins with PBS-T, membranes were developed as described (Section 2.4.3).

2.8.3 N-terminal Sequencing

N-terminal sequencing of VWF tryptic fragments was performed by Alta Biosciences, Birmingham.

2.9 GLYCOSIDASE DIGESTIONS

Modification of VWF glycan structure was performed using specific glycosidase enzymes to remove specific glycan structures or residues from VWF. In all experiments VWF was diluted to a final concentration of 100μg/ml in 20mM Tris-HCl, pH 7.4. Neuraminidase (NEB, UK) at a final concentration of 0.5U was used to remove terminal α2-3,6,8,9 linked sialic acid residues. β-galactosidase (Calbiochem, UK) at a final concentration of 0.5-5U was used to remove terminal galactose residues and PNGase F (NEB, UK) at a final concentration of 2U was used to remove whole *N*-linked glycan chains. All digestions were performed overnight at 37°C. As a control to compare the removal of VWF glycans under non denaturing and denaturing conditions 100μg/ml VWF was denatured with 1% β-mercaptoethanol for 20mins at 90°C. NP-40 (NEB) was added to a final concentration of 10% v/v and the reaction incubated with the appropriate glycosidase overnight at 37°C. Removal of glycans was assessed using SDS-PAGE in 5% gels followed by staining with anti-VWF-HRP to detect the expected shift in mobility and by lectin ELISA's to quantify removal of sugars.

2.10 LECTIN ELISA

The glycan component of VWF was assessed by sandwich enzyme-linked immunosorbent assay using lectins that recognise specific sugars structures. MaxiSorp plates (Nunc) were coated with polyclonal anti-VWF antibodies (Dako) diluted 1/500 in 0.05M carbonate buffer, overnight at room temperature. After washing 3 times with PBS-T, 100μl samples or standards were added to the wells and allowed to incubate for 1 hour at room temperature. After washing, 100μl of the appropriate biotinylated-lectin (Dako) diluted in TBS supplemented with divalent ions (Tris buffered saline, 1mM

$MgCl_2$, 1mM $CaCl_2$, 1mM $MnCl_2$) at dilutions shown in Table 2.2, was added to each well and incubated for 2 hours at room temperature. After washing, 100µl streptavidin-HRP (Amersham Pharmacia, UK) diluted 1/1000 in PBS-T was added to the wells and incubated for 45mins at room temperature. After a final 3 washes, 180µl substrate (Sigma colour fast OPD tablets) was added to the wells and the reaction stopped with 100µl 1M H_2SO_4. Absorbance was recorded at 492nm (UV-1601 spectrophotometer, Shimadzu). Concentrations of unknown samples were read from the standard curve prepared using dilutions of pooled normal plasma. In some experiments glycan modified was bound directly to the MaxiSorp plate then detected with the appropriate lectin. (For binding of VWF directly to the plate refer to section 2.11)

Lectin	**Dilution for western blot**	**Dilution for ELISA**	**Glycan target**
Elderberry Bark Lectin (EBL)	1/5000	1/5000	Terminal sialic acid residues
Ricinus Communis Agglutinin I (RCA-1)	1/1000	1/2000	Terminal galactose residues
Concanavalin A (ConA)	1/1000	1/5000	Complex *N*-linked glycans
Ulex Europaeus Agglutinin I	1/2000	1/1000	H-antigen

Table 2.2 Lectins, their targets and dilutions used for western blot and lectin ELISA

2.11 VWF:ADAMTS13 BINDING ASSAYS

The binding of ADAMTS13 to VWF was assessed using a plate binding assay. To optimise coating conditions, MaxiSorp plates (Nunc), were coated with VWF 0.5-15ng/µl diluted in PBS or 50mM carbonate buffer, pH 9.8 and incubated overnight at either room temperature or 4°C.

In subsequent experiments, plates were coated with 100µl per well of Control VWF (Ctrl-VWF) or glycan altered VWF at a final concentration of 5ng/µl and incubated overnight at 4°C. Unbound VWF was removed and after washing 3 times with PBS-T, wells were blocked with PBS-T-2%BSA for 1 hour at room temperature. After washing, the wells were incubated with 100µl of 1-125nM ADAMTS13 diluted in PBS-2%BSA, for 2 hours at room temperature with gentle shaking. Wells were then washed and incubated for 1 hour at room temperature with either, anti-ADAMTS13 TSP2-4 depleted antibody diluted 1/5000 in PBS-2%BSA or biotinylated anti-TSP2-4 diluted 1/5000 in PBS-2%BSA. Wells were then washed again and incubated with either goat anti-rabbit Ig-HRP (1/2000 in PBS-2%BSA) for 1 hour or Streptavidin-HRP (1/1000 in PBS-T) for 45mins at room temperature. After a final wash step, 180µl substrate (Sigma colour fast OPD tablets) was added to the wells, the reaction stopped with 100µl 1M H_2SO_4, and the absorbance measured at 492nm.

The absorbance values were plotted against the ADAMTS13 concentration, using Graph Pad Prism 4 software. The data was fitted to the equation:

$$B = \frac{B_{max} \times [X]}{K_D + [X]}$$

where B is the binding expressed in absorbance unit, B_{max} is the maximal binding when saturation is reached, [X] is the ligand (ADAMTS13) concentration and K_D is the equilibrium dissociation constant.

2.11.1 Modified VWF:ADAMTS13 Binding Assays

To further investigate the binding of ADAMTS13 to VWF the method used to capture VWF was modified to examine ADAMTS13 binding to different conformations. In the first modification MaxiSorp plates were coated with a monoclonal anti-VWF antibody, ESVWF8 (American diagnostica) that is directed against the C-terminus of VWF. The antibody was diluted 1/500 in carbonate buffer, pH9.6 and plates were coated overnight at 4°C. Following removal of unbound antibody and washing with PBS-T, plates were incubated with 100µl per well VWF diluted to a final concentration of 5µg/ml in PBS-T for 2 hours at room temperature. After washing with PBS-T, ADAMTS13 was applied and detected as described in 2.11.

The second modification examined ADAMTS13 binding to collagen bound VWF. Collagen plates were prepared as described 2.3.2 and following blocking were incubated with 100µl per well VWF diluted to a final concentration of 5µg/ml for 2 hours at room temperature. After washing with PBS-T, ADAMTS13 was applied and detected as described in 2.11.

2.12 GENERAL MOLECULAR BIOLOGY TECHNIQUES

2.12.1 Agar Plates and Luria-Bertani (LB) Media ± Ampicillin

LB media and LB agar were dissolved in ddH_2O and autoclaved according to manufacture's instructions. Ampicillin was added to a final concentration of 100µg/ml once the temperature of the media was below 55°C. For agar plates 20ml of molten LB agar was poured into a 10cm^2 petri dish and allowed to set. LB media and LB agar was stored for a maximum of 2 weeks at 4°C. In some instances, blue/white screening was used to select positive recombinant clones. For this, 40µl of a 2% X-gal solution and 7µl of IPTG were spread on agar plates and allow to dry at least 2 hours before the plate was used.

2.12.2 Restriction Enzyme Digests

Restriction digests were performed using New England Biolabs restriction enzymes and buffers as stated in Appendix I. All digests were performed using ~5ng DNA and 20U of the appropriate enzymes, diluted in the appropriate NEB buffer, for 2 hours at 37°C. For restriction digests generating vector fragments to be used in subsequent downstream cloning applications, 5' and 3' phosphates were removed by to prevent re-ligation. For this, 5U of calf intestinal alkaline phosphatase (CIAP) (Invitrogen, UK) were added to the restriction digest reaction for the last 5mins.

2.12.3 Agarose Gel Electrophoresis

Agarose gel electrophoresis was used to visualise DNA fragments and separate them according to size. Agarose gels, 0.8-1.5%(w/v), were prepared using multi-purpose agarose (Bioline) in TBE buffer containing 5µg/ml SYBR™ safe DNA gel stain (Invitrogen, UK). The concentration of agarose depended on the size of DNA being separated. After dissolving the agarose, gels were poured and allowed to polymerise for 20mins at 4°C. Samples were diluted with loading buffer containing 40% sucrose to allow samples to deposit in the wells and Bromophenol blue as a tracking dye to monitor progressing of the samples. A 1kb DNA ladder (NEB, UK) was also run alongside all samples. Electrophoresis was carried out at 75V constant, for 20-80mins.

2.12.4 Gel Extraction

DNA bands containing desired fragments of desired material were purified from agarose gels using the QIAquick gel extraction kit (QIAgen, UK) as per manufactures instructions. Briefly, bands of interest were excised from the gel using a clean razor blade, weighed and solubilised with 3 volumes buffer QG for 10mins at 50°C. Once dissolved, 1 x volume of isopropanol was added and the sample applied to the silica-gel column and centrifuged for 1min at 13000rpm to bind DNA. 0.5ml Buffer QG was applied to the column and centrifuged for 1min to remove traces of agarose, then the 0.75ml Buffer PE was applied to the column and centrifuged to wash the DNA. A further 1min spin was performed to remove all traces of wash buffer. DNA was eluted by the addition of 30µl Buffer EB and centrifugation for 1min at 13000rpm.

2.12.5 Ligations

Vector and insert fragments to be ligated were visualised after gel extraction on agarose gels (as described) to roughly quantify the amount of DNA present and ligation was carried out with a vector:insert ratio of 1:3. Vector and insert were mixed together with 2µl 5x ligase buffer (50mM Tris-HCl, pH7.5, 10mM dithiothreitol, 1mM adenosine triphosphate and 25µg/ml BSA), 1µl T4 DNA ligase (Invitrogen) in a final reaction volume of 10µl, and incubated overnight at 4°C.

2.12.6 Transformations

0.5-2µl of a ligation reaction or Plasmid were incubated with 20µl of Subcloning Efficiency DH5α Pre-Competent cells™ on ice for 30mins. Cells were then heat shocked for 20seconds at 37°C and returned to ice for 2mins. 200µl of pre-warmed SOC media (Invitrogen) was added to the cells and incubated for 1 hour at 37°C in a shaker at 250rpm. The cell suspension was then plated onto pre-warmed agar plates containing ampicillin and incubated overnight at 37°C.

For mutagenesis reactions transformation were performed essentially the same way, but with the following changes: DH5α cells were replaced by XL10-Gold ultra competent *E.coli* cells (Stratagene) and following 30mins incubation on ice the cells were heat-shocked at 42°C for 30 seconds. All subsequent steps remained the same.

2.12.7 Isolation of Plasmid DNA

Isolation of plasmid DNA was performed using; plasmid Miniprep kits (Qiagen) for small scale plasmid isolation (up to 20µg DNA) and plasmid endo free Maxiprep kits (Qiagen, UK) for large scale plasmid isolation (up to 500µg DNA), both according to manufactures instructions. Both kits operate on a principle of bacterial cell lysis, followed by precipitation of denatured proteins, chromosomal DNA, cellular debris, then clean up of plasmid DNA.

2.12.8 Site-Directed Mutagenesis

Mutations were introduced in to VWF cDNA using the QuikChange® XL site-directed mutagenesis kit (Stratagene) in accordance with manufactures instructions. PCR reactions were performed using 2.5U high fidelity *Pfu* ultra DNA polymerase, 125ng of complementary primers containing the mutation of interest, 10ng of DNA template, 1X reaction buffer, 10mM dNTP's and 3µl of QuikSolution in a final volume of 50µl. The primers used in each amplification reaction are shown in Appendix II, with the introduced mutation underlined and in bold. The PCR amplification consisted of an initial denaturation (95°C, 1min); 18 cycles of denaturation (95°C, 50 sec), annealing (60°C, 50 sec) and extension (68°C, 1min per kb); and a final extension at 68°C for 7 minutes. Subsequently, PCR products were digested with 10U of DpnI for 2 hours at 37°C, in order to remove the methylated parental DNA template that did not contain the desired mutation. The mutation reactions were transformed into XL-10 gold cells as described in section 2.12.6.

2.13 CLONING AND EXPRESSION VECTORS

2.13.1 pBlueScript®

The pBlueScript® II SK Phagemid vector (Stratagene), is a high-copy number, 3kb cloning vector. It contains a 21 member multiple cloning site (MCS) and contains a portion of the *lacZ* gene encoding for 131 amino acids of β-galactosidase. As such blue/white screening maybe used to select recombinant clones. The presence of a recombinant insert in the MCS disrupts the *lacZ* gene, and no gene product is expressed. When cultured on agar plates containing X-gal the bacteria appear as white colonies. If the insert is not successfully inserted, the *lacZ* remains intact and is expressed, thus bacterial colonies will appear blue. The vector also contains the pUC origin that enables high-copy number replication in *E.coli* and an ampicillin resistance gene to allow for selection.

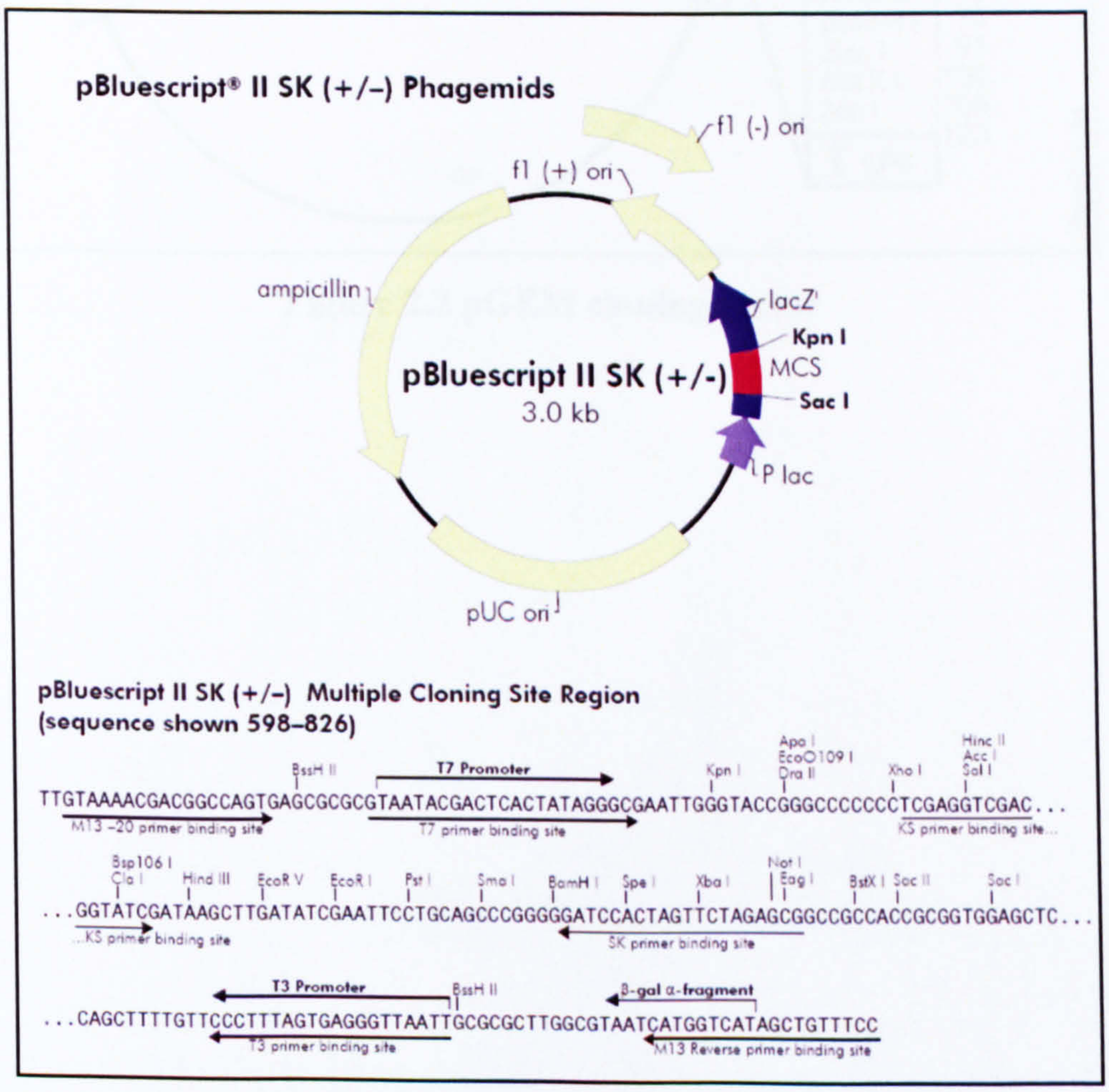


Figure 2.1 pBlueScript cloning vector

2.13.2 pGEM-7Zf(+)

pGEM-7zf(+) (Promega) is a 3kb cloning vector that shares the same features as the pBS vector. Although a *lacZ* gene is present in pGEM, blue/white selection was not used with this vector.

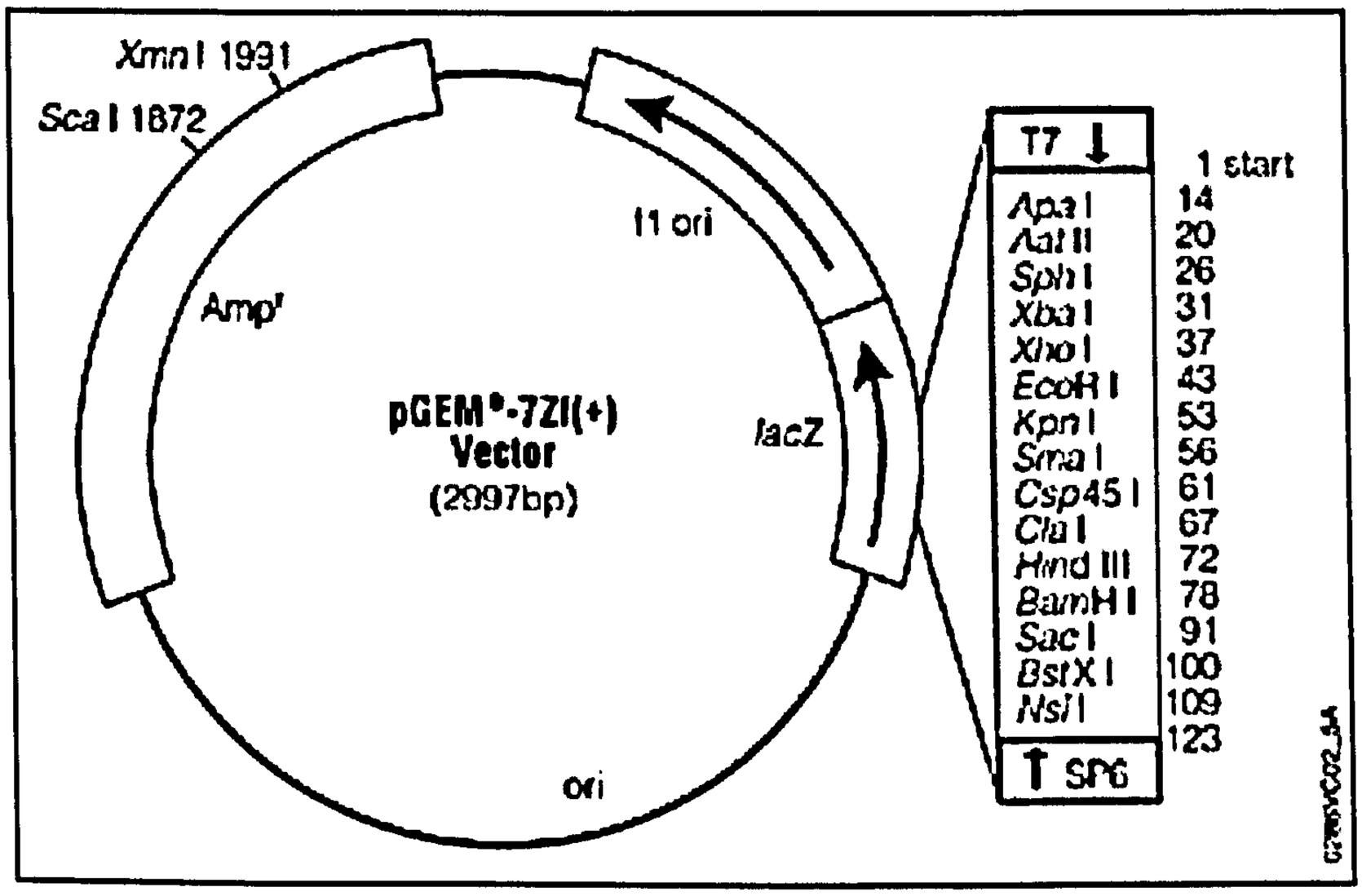


Figure 2.2 pGEM cloning vector

2.13.3 pcDNA3.1/*Myc*-His A(+)

The pcDNA3.1 vector is 5.5Kb in length and it includes a cytomegalovirus (CMV) immediate-early promoter to drive high-level gene expression in mammalian cells, multiple cloning site (MCS), an ampicillin resistance gene to perform the selection of the vector in bacteria cells and a neomycin resistance gene to allow the selection in mammalian cells, a PUC origin which allows high-copy number replication and growth in *E.coli* and a SV40 origin which allows episomal replication in cells expressing the SV40 large T antigen. The pcDNA vector used also contained a myc epitope to facilitate immunodetection, and a 6xHis C-terminal tag to allow purification. However these were not needed for expression of VWF, which was cloned into the AgeI site, removing the sequence for the myc epitope and contained a stop codon, as such the C-terminal His tag was not expressed.

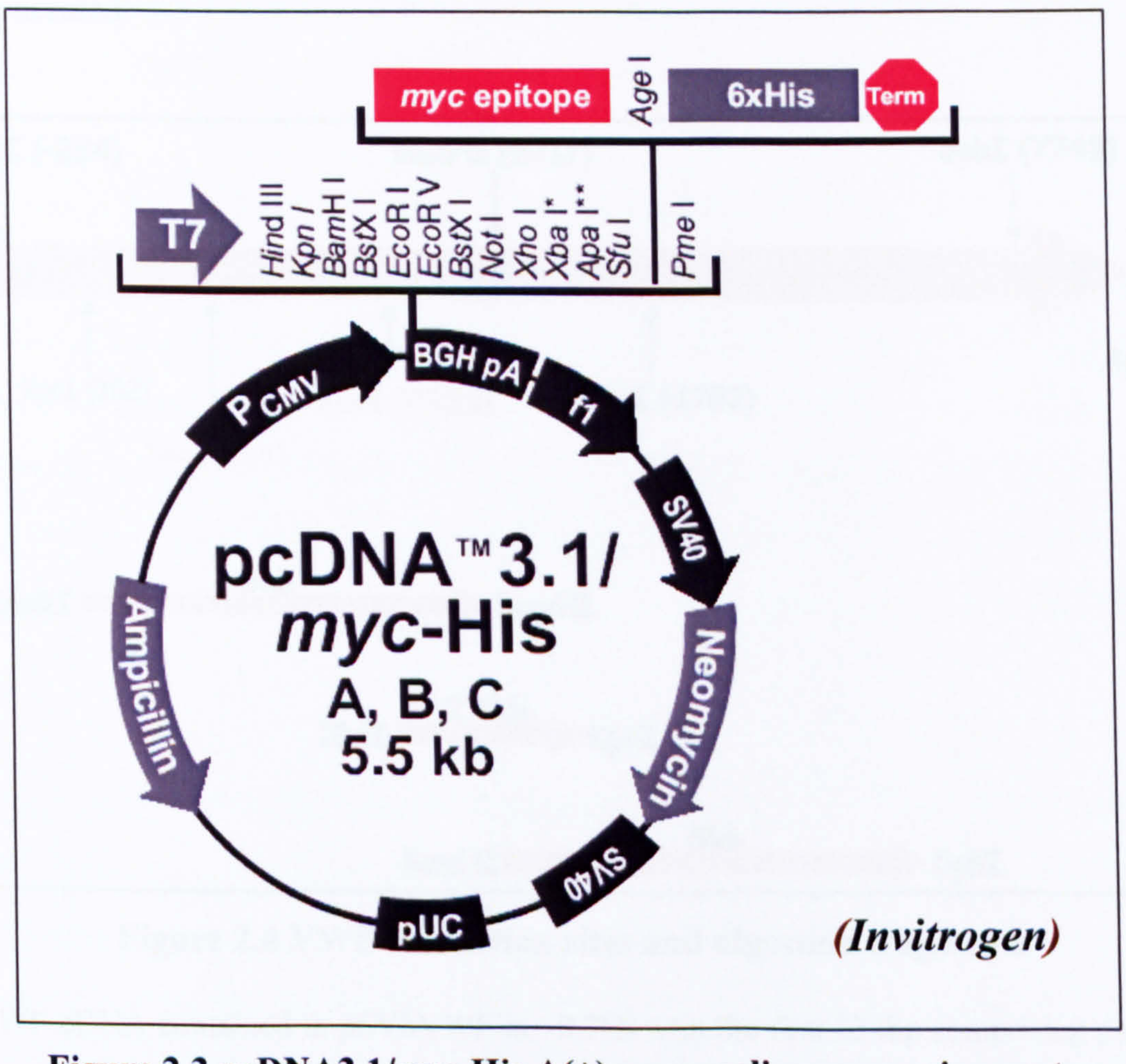


Figure 2.3 pcDNA3.1/*myc*-His A(+) mammalian expression vector

2.14 GENERATION OF FULL LENGTH VWF EXPRESSION VECTOR AND VWF MUTANTS

2.14.1 Overview

Plasmid pSVhVWF containing the full length VWF cDNA and some 5'untranslated sequence was a kind gift from Dr Said Enayat, (Birmingham Children's Hospital.) To facilitate efficient expression of VWF and generation of VWF mutants, the full length cDNA was cloned into the mammalian expression vector pcDNA3.1

Initially, the cloning vector pBlueScript (pBS) was mutated, using the mutagenesis primers in listed in Appendix II, to remove the KpnI restriction site from the multiple cloning site and this vector was designated pBS^{-kpnI}. Figure 2.1 shows the restriction sites present in VWF that were used to generate different fragments of VWF cDNA for the purpose of mutagenesis and cloning and the various VWF cDNA fragments that were generated.

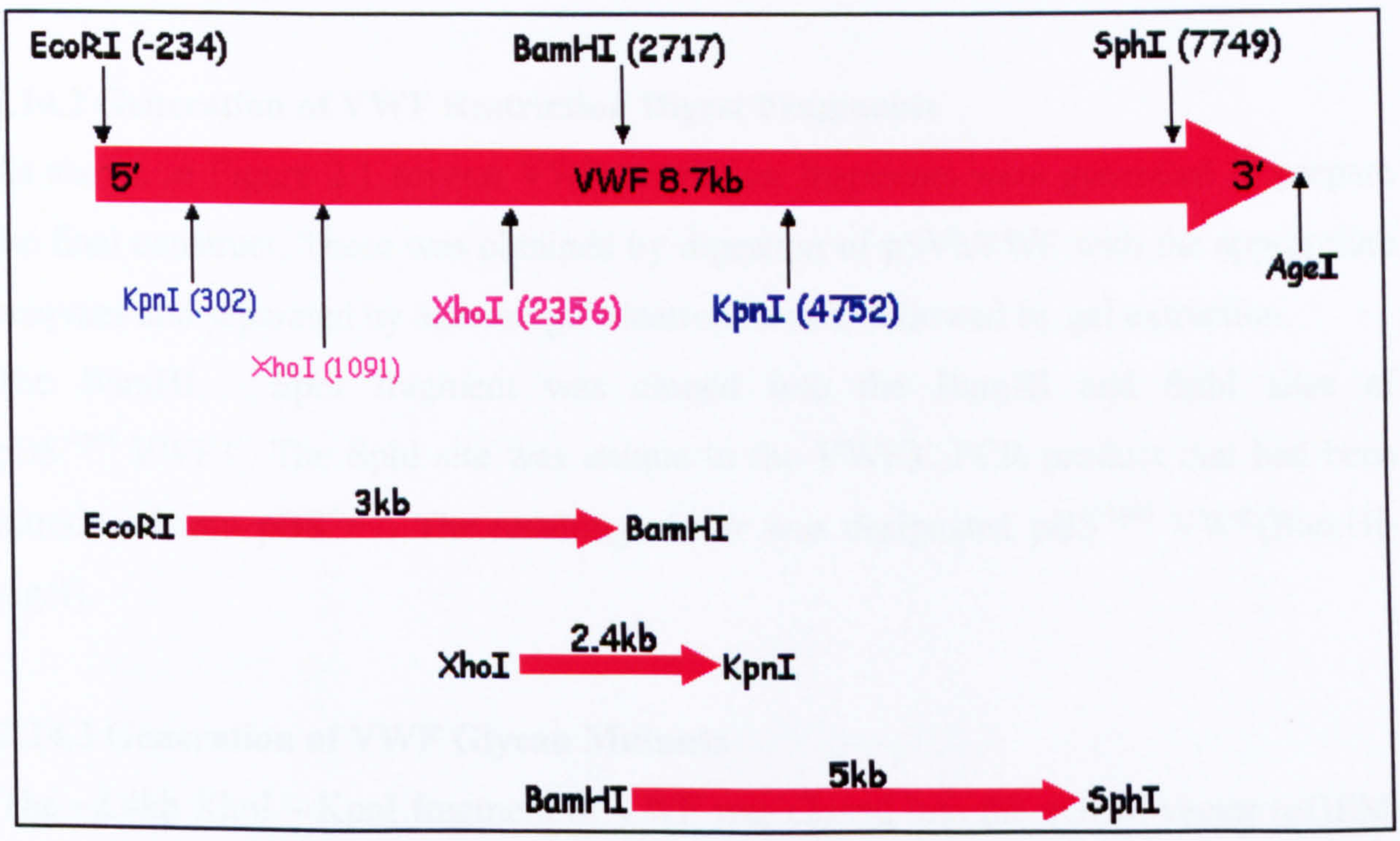


Figure 2.4 VWF restriction sites and digestion fragments

The VWF cDNA contained in pSVhVWF is ~8.7kb with the first 234bp comprising part of the 5'UTR. Base number 1 is taken from the start codon. Shown on the figure are the restriction fragments used to prepare the final VWF construct. The 3' AgeI site was introduced by PCR of the 3' end of the sequence described in the following section. The XhoI – KpnI fragment contains the sequence for residues 786-1584, encompassing the predicted A2 domain *N*-linked glycan sites at N1515 and N1574. This fragment was used to introduce mutations to prevent glycosylation at these sites.

2.14.2 Amplification of the 3' Terminal End of VWF

A PCR product of the terminal 955bp of VWF was generated using primers VWF3' fwd and VWF3' rev (Appendix II). The forward primer was designed to amplify VWF from base number 7487 and introduced 7 random bases followed by an XbaI restriction site before the start of the VWF sequence to be amplified. The reverse primer introduced an AgeI site, followed by a SacI site then 7 random bases immediately after the VWF stop codon. PCR was performed using Platinum *Pfx* high-fidelity DNA polymerase (Invitrogen, UK) in a reaction mixture containing 1X *pfx* reaction buffer, 10mM dNTP's, 50mM $MgSO_4$, 125ng of complementary primers and 10ng template pSVhVWF DNA. The PCR amplification consisted of an initial denaturation (95°C, 2min); 27 cycles of denaturation (95°C, 30sec), annealing (53°C, 30sec) and extension (72°C, 15sec); and a final extension at 72°C for 7 minutes. The resulting VWF3' PCR product was digested with XbaI and SacI then cloned into pBS^{-KpnI} that had been pre-digested and treated with CIAP, to form the vector pBS^{-kpnI} VWF3'.

2.14.2 Generation of VWF Restriction Digest Fragments

As shown in Figure 2.1 several VWF restriction fragments were generated to prepare the final construct. These was obtained by digestion of pSVhVWF with the appropriate enzymes and separated by agarose gel electrophoresis, followed by gel extraction.

The BamHI – SphI fragment was cloned into the BamHI and SphI sites of pBS^{-kpnI} VWF3'. The SphI site was unique to the VWF3' PCR product that had been introduced into pBS^{-KpnI}. The resulting vector was designated pBS^{-kpnI} VWF(BamHI-AgeI).

2.14.3 Generation of VWF Glycan Mutants

The ~2.4kb XhoI – KpnI fragment of VWF was cloned into the pGEM vector (pGEM-VWF(XhoI-KpnI) and used to create mutations of VWF. The XhoI – KpnI fragment contained the sequence for residues 786-1584, encompassing the predicted A2 domain *N*-linked glycan sites at N1515 and N1574. Mutagenesis primers were designed to mutate the asparagine residues to glutamic acid residues. Three mutations were prepared; two single mutations, N1515Q and N1574Q and a double mutation (DM) of both sites. Mutations were generated using the QuikChange® XL site-directed mutagenesis kit (Stratagene) as described (section 2.12.8). The double mutant was produced by successive mutagenesis reactions.

2.14.4 Completion of Wild Type and Mutant VWF Constructs

The constructs, pGEM-VWF(XhoI-KpnI) that contained either wild type (wt) sequence or mutated sequences was digested with BamHI and KpnI and the resulting fragment was cloned into pBS^{-kpnI} VWF(BamHI-AgeI) that had been digested with BamHI and KpnI. Mutation of the KpnI site in the pBS vector was necessary to allow this step to occur. The resulting vectors contained the VWF DNA sequence from base pair 2951 to the stop codon and contained either wild type sequence or mutated sequence.

To complete the full length VWF (FL-VWF) construct, the above vectors were digested with EcoRI and BamHI and the EcoRI – BamHI (Figure 2.1) comprising the 5' end of VWF with some of the 5' UTR region, was cloned into the digested sites. The resulting vectors were designated pBS^{-KpnI} FL-VWF (wt, N1515, N1574 or DM)

The final expression construct was generated by removing the FL-VWF cDNA from the above vectors by digestion with EcoRI and AgeI and the resulting fragments were cloned into the EcoRI and AgeI sites of pcDNA3.1/*myc*-His A(+). The steps used to generate the FL-VWF constructs are outlined diagrammatically in figure 2.2

2.14.5 Sequencing

All the vectors and mutations generated were verified by sequencing to ensure the absence of any unwanted PCR-introduced errors and to check the presence of mutations introduced by site-directed mutagenesis. DNA sequencing was performed at the Imperial College-MRC Genetics Core Facility using an ABI 3700 DNA analyser (Perkin-Elmer).

2.14.6 Glycerol Stock

To store bacteria transformed with the vector constructs, 900µl of the liquid culture was placed into 100µl glycerol (Sigma) to prevent ice crystals forming, vortexed and stored at –70°C.

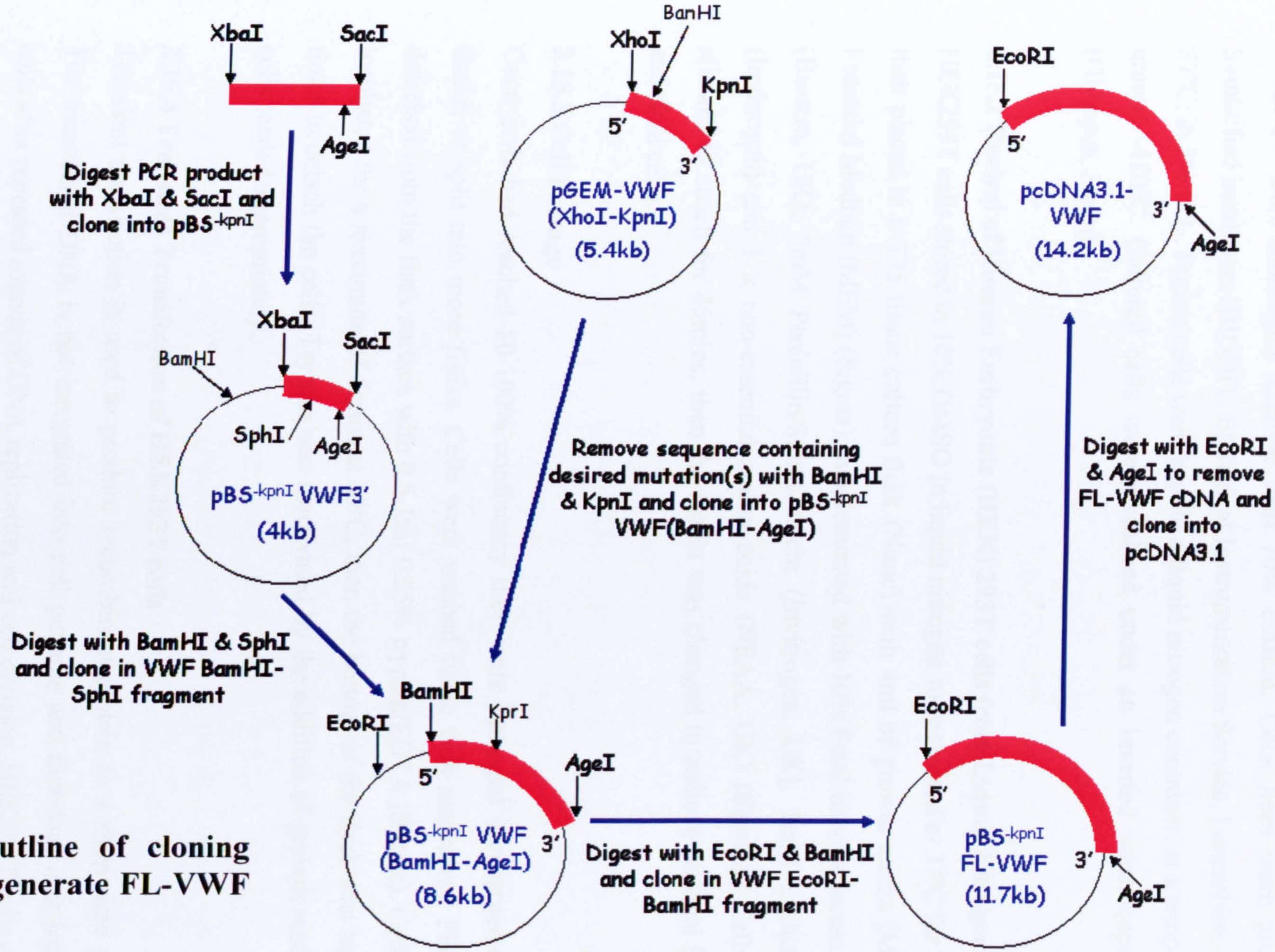


Figure 2.5 Outline of cloning steps used to generate FL-VWF constructs

2.15 CELL CULTURE

2.15.1 General Tissue Culture

All tissue culture was performed in a class II flow cabinet (FASTER BHG 2004, JENCONS-PLS) in a separate laboratory designated specifically for tissue culture. Aseptic technique was used at all times, and all surfaces of the flow cabinet and tubes, flasks etc were thoroughly cleaned with 70% ethanol. Cells lines were grown in humidified incubators (BIOHIT, Biological Instrumentation Service, Lancashire, UK) at 37°C, in 5% CO_2. Frozen cells were kept in a liquid nitrogen container, at a temperature around -180°C. Cultured cells were visualised under an inverted microscope CK2 (Olympus, Japan).

2.15.2 Revival of Human Embryonic (HEK) 293T cells from Liquid Nitrogen

HEK293T cells stored in 10% DMSO in liquid nitrogen were thawed at 37°C for 5mins, then placed in a T75 tissue culture flask (Nunc) with 4ml of growth media [Minimal Essential Medium (MEM) (Sigma), supplemented with 10% Fetal Bovine Serum (FBS) (Biosera, UK), 5mM Penicillin/Streptomycin (Invitrogen, UK), 5mM L-Glutamine (Invitrogen) and 1 x non-essential amino acids (NEAA, UK) (Sigma).] Cells were allowed to attach for 45mins, then the media was changed to remove residual DMSO and dead cells.

2.15.3 Cell Passage

Once cells had reached 80-100% confluency they were passaged into larger culture flasks, or split into more flasks. Cells were washed twice with autoclaved PBS then detached from the flask surface with 0.5-1ml 0.25% trypsin/EDTA (Sigma). Cells were incubated for a maximum of 5mins at 37°C, then the bottom of the flask was tapped 3 times to detach the cells. Trypsin was inactivated by the addition of growth media and cells seeded appropriately.

2.15.4 Transient Transfection of HEK293T cells

Transient transfection is used to produce recombinant protein in a short time period. The transfected DNA is not integrated into cell genome and therefore it is lost from cells after repeated rounds of DNA replication and cell division. HEK293T cells express high levels of SV40 large tumour (T) antigen, which allows episomal replication of SV-40 origin-containing plasmids (i.e. pcDNA 3.1).

Transfection of HEK293T cells with wt-VWF and VWF mutants was performed using 10mM polyethylenimine (PEI). A control transfection was also performed using empty pcDNA3.1/*myc*-His vector. HEK293T cells at ~70% confluency were trypsinised and seeded onto 10cm^2 dishes at ~ 2×10^6 cells/dish in growth media till they reached 70% confluency. DNA solution was prepared by mixing 33µg of plasmid DNA per 10cm^2 dish with 0.625ml of sterile 150mM NaCl. The PEI solution was prepared by mixing 75µl PEI with 0.625ml sterile 150mM NaCl per dish. The PEI solution was then added drop wise to the DNA solution and allowed to incubate for 20mins at room temperature. During the incubation, growth media was removed from the cells and they were washed once with sterile PBS and once with Optimem conditioned medium (Invitrogen). 9mls of Optimem was then added to the cells and the DNA:PEI mixture was applied to the cells. Plates were carefully rocked to spread the transfection complex and were incubated for 2 days at 37°C, 5% CO_2. The conditioned medium was collected and concentrated 10-fold using 100kDa cut off spin filters (Amicon). VWF concentration and multimer composition was determined by VWF ELISA and multimer gel analysis as described.

2.16 FIXATION AND STAINING OF HEK293T CELLS FOR IMMUNOFLUORESCENCE MICROSCOPY

For detection of VWF storage granules in HEK293T cells following transfection with VWF cDNA, transfections were performed as described in the previous section but with the following modification. Before the HEK293T cells were applied to the 10cm^2 dish for transfection, sterile glass cover slips were applied to the plates and the HEK293T cells allowed to grow over them.

Following transfection and 2 days incubation at 37°C, 5% CO_2 as described, the coverslips were removed and placed in 4 well plates (Nunc, UK) and washed 10 times with warm PBS. After washing the cells were fixed with 250µl per coverslip methanol that had been stored at -20°C. Coverslips were placed in a -20°C freezer for 5mins, then the methanol was removed with a pipette and the cells allowed to air dry for 20mins at room temperature. Polyclonal rabbit anti-VWF (Dako, UK) diluted 1/1000 in PBS-3%BSA was applied to the coverslips for 60mins, then the cells were washed 5 times with warm PBS. Following washing, Alexafluor 488 α-rabbit secondary antibody, and topro3 nuclear stain, both diluted 1/1000 in PBS-3%BSA were applied to the coverslips for 20mins in the dark. The coverslips were then washed 10 times with warm PBS and

mounted onto glass slides. Cells were visualised using a Zeiss LSM510 META fluorescence microscope, excitation at 488nm, emission 540nm.

2.17 STATISTICAL ANALYSIS

All quoted p values were obtained using the nonparametric Mann-Whitney U test and were calculated using Analyse-it for Microsoft EXCEL.

CHAPTER 3

3. Effect of ABO and Bombay blood group on Plasma VWF Levels and Susceptibility to Cleavage by ADAMTS13

3.1 INTRODUCTION

As discussed, ABO blood group has a major effect on plasma VWF levels, with individuals of blood group O having levels 20-30% lower than non-O blood groups. This is likely to be related to the fact that the *N*-linked glycans of VWF present the ABO(H) blood group sugars. How ABO blood group affects VWF levels is unknown, however evidence suggests that rate of VWF synthesis and/or secretion is not influenced by ABO blood group.

Within the circulation the multimeric size of VWF is controlled by the VWF cleaving protease; ADAMTS13. Interestingly, an effect of ABO blood group on susceptibility to ADAMTS13 has been demonstrated, with blood group O VWF exhibiting the greatest susceptibility to ADAMTS13 proteolysis.

To further these observations, I have analysed VWF from individuals with the rare Bombay blood group. From Bowen's study it is apparent that loss of A/B sugars results in increased proteolysis by ADAMTS13. I therefore hypothesised that further removal of terminal sugars may increase the rate of proteolysis further. The rare Bombay phenotype provides an ideal reagent to investigate this since naturally altered glycan chains are presented due to the failure to synthesise H-antigen.

The glycan structure of Bombay VWF was analysed with lectin ELISA and western blotting and plasma VWF levels were analysed by VWF:Ag ELISA and compared to a control group of healthy donors. Blood group specific VWF was then purified and subjected to ADAMTS13 cleavage to determine the effect of ABO/Bombay blood group on proteolysis.

In order to assess VWF multimeric structure and analyse ADAMST13 cleavage, a VWF:collagen binding assay (CBA) and VWF multimer gel methods were established.

3.2 COLLAGEN BINDING ASSAY (CBA)

In initial experiments a commercial CBA kit (Technoclone) was used to determine collagen binding activity of plasma and purified VWF. However, this proved to be non-cost effective and therefore an *in-house* CBA ELISA was developed.

Human type III collagen prepared from placenta by trypsin digestion (Sigma C-4407) was selected as the source of collagen since previous reports determined this was one of the most efficient types of collagen, in terms of VWF binding, commercially available. To determine optimal collagen concentration for coating, MaxiSorp plates were coated with increasing collagen concentrations from 1µg/ml to 15µg/ml, diluted in 50mM carbonate buffer, pH 9.2, for 24 hours at room temperature. After washing to remove unbound collagen, plates were blocked with 2%BSA-PBS-Tween, then incubated with normal pooled plasma diluted 1:10-1:320 and bound VWF was detected with anti-VWF-HRP. Optimal binding of plasma VWF to collagen, as reflected by the highest absorbance values and a dose response relationship between absorbance at 492nm and plasma dilution, was demonstrated when a collagen concentration of 5µg/ml was used. (Figure 3.1) At concentrations higher than 5µg/ml the binding of VWF to collagen was decreased (Figure 3.1). In all subsequent experiments a final collagen coating concentration of 5µg/ml was used to prepare CBA plates

Optimal coating time and stability of collagen coated plates was determined by coating plates with type III collagen for 0, 2 hours, 24 hours, 48 hours, 7 days, 14 days, 21 days and 49 days at room temperature, then incubating with normal pooled plasma diluted 1:20. A small amount of binding was observed on plates coated for 2hours, however maximal binding was achieved when plates were coated overnight and no reduction or increase in binding was seen when plates were coated for up to 3 weeks, demonstrating that the plates were stable for at least three weeks (Figure 3.2A). After 7 weeks incubation, binding was greatly decreased (Figure 3.2A) Coated plates were therefore used within a maximum of three weeks. To determine the optimal amount of VWF to load on to each well, CBA plates were incubated with a total amount of VWF from 0-100ng. Binding was linear up to an amount of 50ng, after which binding plateaued, indicating the wells were saturated (Figure 3.2B). To ensure the assay was sensitive to HMW-VWF multimers; HMW, medium MW (MMW) and LMW multimer preparations were standardised to the same VWF:Ag concentration and collagen binding analysed. The highest binding response was observed with HMW-VWF, (taken as 100% CBA), this response decreased for MMW-VWF (~47% CBA) and LMW-VWF

displayed minimal binding, (~9%) (Figure 3.2C). Finally, to confirm that the VWF interaction with collagen was specific, MaxiSorp plates were coated with 5µg/ml of; type III collagen, type IV collagen, (that does not bind VWF), and BSA. Plates were incubated with plasma diluted 1:10-1:320 and detected as described. Normal binding was seen between plasma VWF and type III collagen, however no binding could be detected between plasma VWF and either type IV collagen or BSA coated plates (Figure 3.2D).

To calculate a value for collagen binding activity, a standard curve was prepared using normal pooled plasma and the % collagen binding activity (%CBA) of samples was deduced from the equation-of-the-line of the standard curve. To prepare the standard curve, Log_{10} values were taken of the % normal pooled plasma, (i.e. 1:10 dilution represented 100%; 1:20 represented 50%) and were plotted along the x-axis. Absorbance of the standards was plotted along the y-axis and the equation-of-the-line and the R^2 calculated using the "Add trendline" function in Microsoft Excel. The equation-of-the-line was given in the format:

$$y = mx - c$$

Where: y is the absorbance value, m is the gradient of the slope, x is the %CBA and c is the x/y intercept.

To calculate the %CBA of unknown samples the equation was rearranged to:

$$x = (y + c) / m$$

Absorbance values (y) of the unknown samples were substituted into the equation and a Log_{10} value was obtained and converted to %CBA by use of the invLog function.
A representative standard curve is presented in Figure 3.3.

The coefficient of variation for both the inter and intra assay error was determined to be <5%, demonstrating that the assay was highly reproducible. The assay was also highly cost effective; costing 5 pence per sample compared to £2 per sample using commercially available CBA kits.

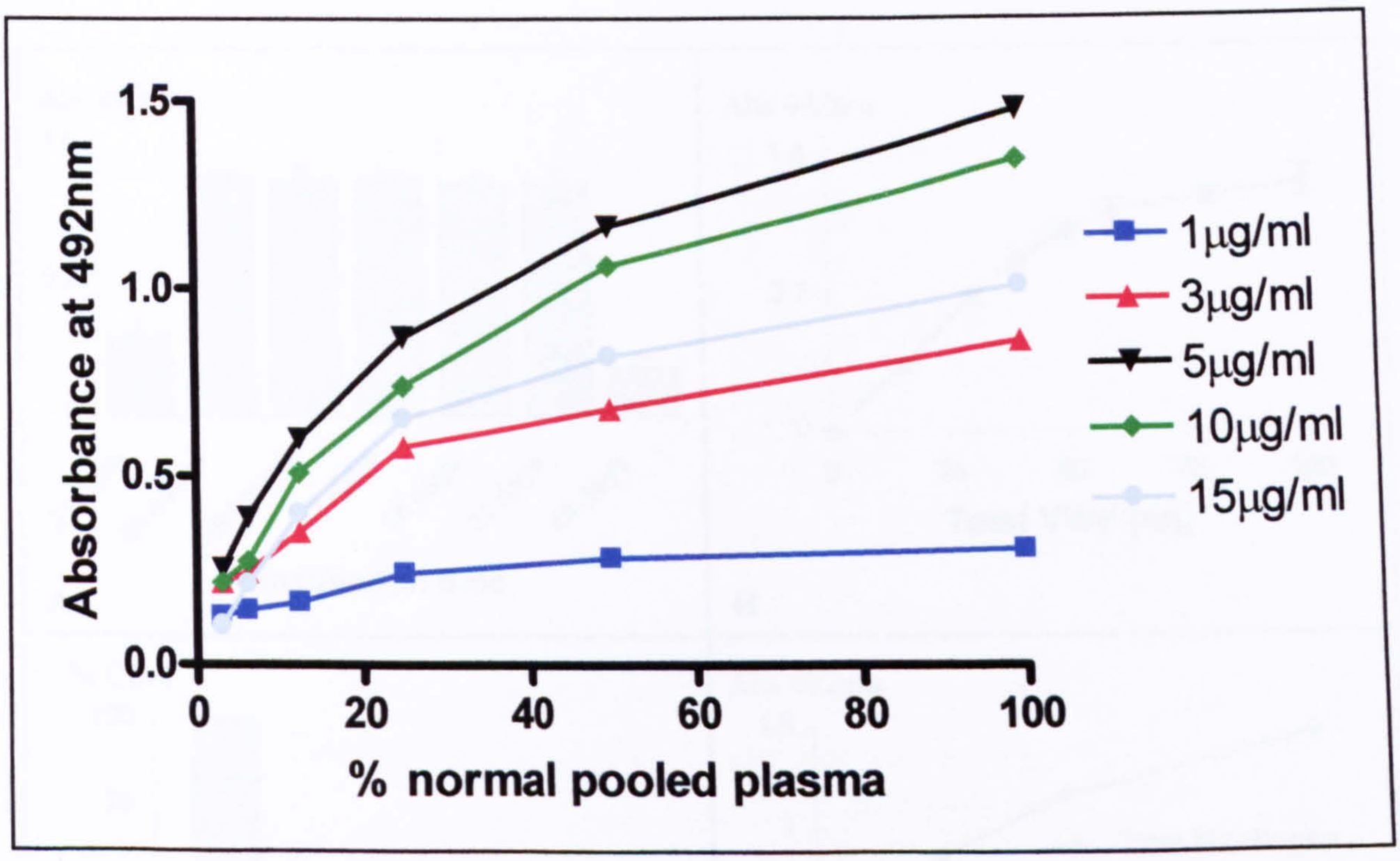


Figure 3.1 Optimal coating collagen concentration

MaxiSorp plates were coated with placenta-derived human type III collagen, diluted from 1-15μg/ml in 50mM carbonate buffer, pH9.6 and incubated at room temperature for 24hours. After washing unbound collagen and blocking, wells were incubated with normal pooled human plasma diluted 1:10-1:320 and bound VWF was detected with anti-VWF-HRP. Maximal binding of VWF to collagen was observed with a coating concentration of 5μg/ml. At concentration higher than 5μg/ml, binding was decreased. In all subsequent assays plates were coated with 5μg/ml collagen.

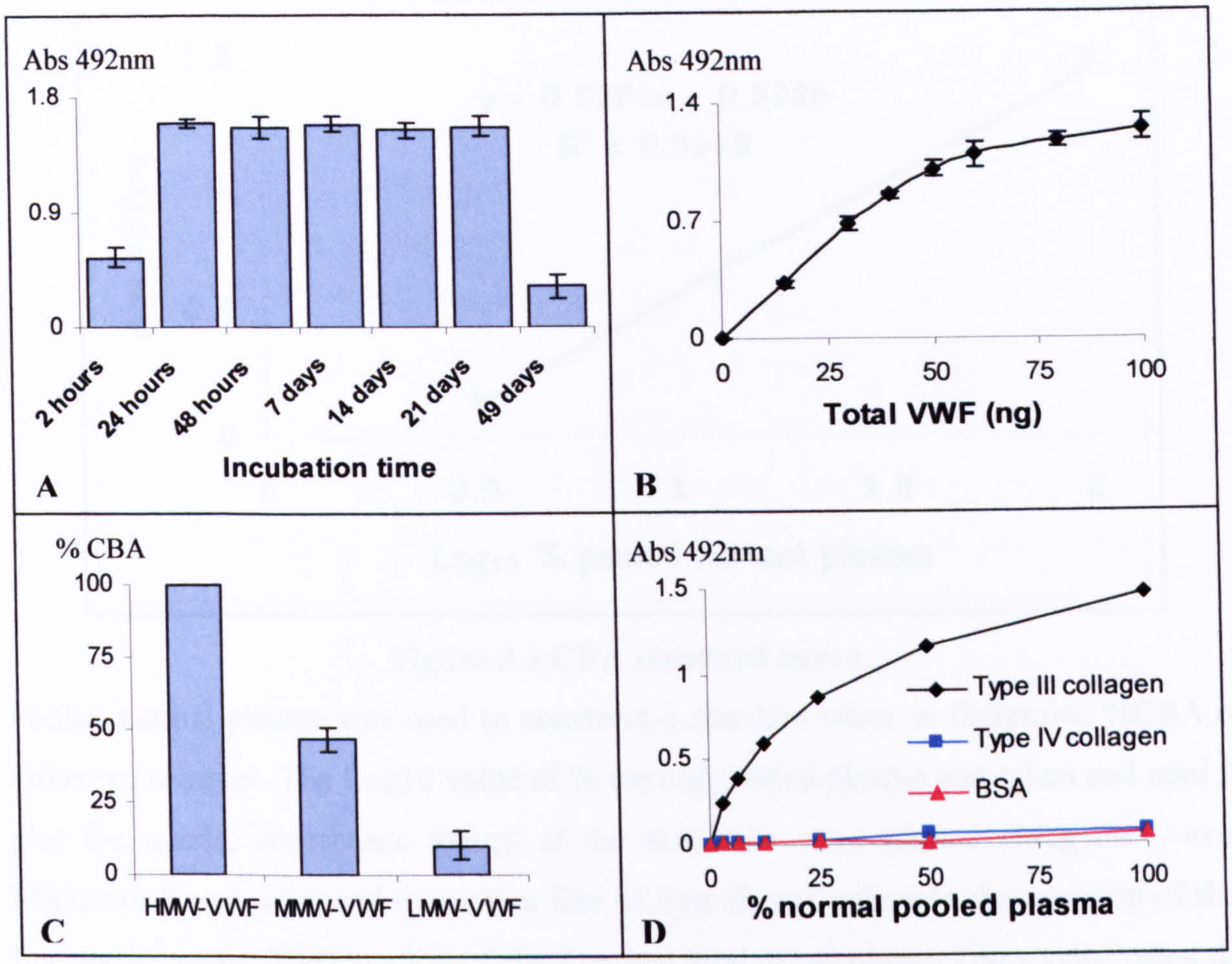


Figure 3.2 Collagen binding assay optimisation

(A) *Effect of coating time*. MaxiSorp plates were coated with collagen for 2 hours up to 49 days, then incubated with plasma diluted 1:20. A small binding response was seen with 2 hours coating time and maximal binding was reached after 24 coating time and remained stable for up to 21 days. After 49 days the binding response greatly decreased. Collagen coated plates were kept for a maximum of 21 days before use.

(B) *Optimal total VWF load*. CBA plates were incubated with total VWF ranging from 0-100ng and bound VWF detected as described. The binding response was linear up to a total load of 50ng after which the wells were saturated and the binding response plateaued.

(C) *Type III collagen preferentially binds HMW-VWF*. CBA plates were incubated with HMW, MMW and LMW-VWF standardised to the same VWF:Ag concentration. Maximal binding (defined as 100% CBA) was observed with HMW-VWF, decreased binding (47%) was observed with MMW-VWF, and minimal binding (9%) was observed with LMW-VWF.

(D) *Specific interaction of VWF with type III collagen*. MaxiSorp plates were coated with 5μg/ml of either; type III collagen, type IV collagen or BSA diluted in 50mM carbonate buffer, pH9.6 and incubated for 24hours. After washing and blocking, plates were incubated with plasma diluted 1:10-1:320 and bound VWF detected as described. VWF bound to type III collagen, but no binding was observed to either type IV collagen or BSA.

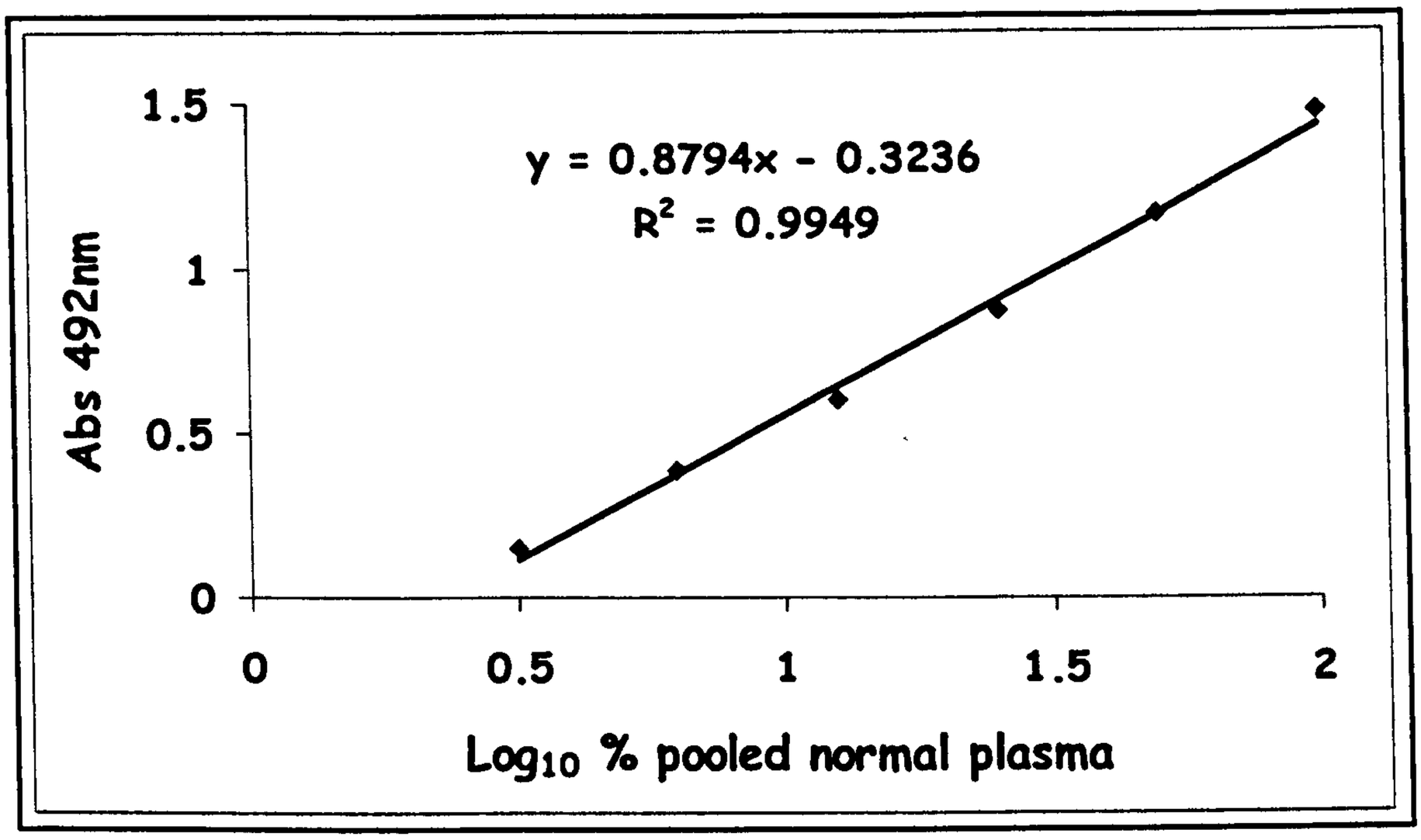


Figure 3.3 CBA standard curve

Pooled normal plasma was used to construct a standard curve to determine %CBA of unknown samples. The Log10 value of % normal pooled plasma was taken and used to plot the x-axis, absorbance values of the standards were plotted along the y-axis. Microsoft Excel was used to apply a line of best fit and calculate the equation-of-the-line and R^2 value. The equation-of-the-line was used to calculate a Log_{10} value using the absorbance values of the samples and %CBA determined by taking the invLog.

3.3 ABO(H) ANTIGEN ON BOMBAY/PARA-BOMBAY VWF

Plasma samples from 47 individuals with the rare Bombay phenotype were collected (Bombay phenotype n=30, para-Bombay phenotype n=17) and the presence of H-antigen on VWF glycans was investigated by a semi-quantitative "H on VWF ELISA" and compared to the H-antigen expression on normal ABO blood group controls. Pooled group O plasma was used to generate a standard curve, with 1U/ml group O plasma set as 1U H-antigen. Concentration of H-antigen was expressed as units of H per unit of VWF. The highest levels of H antigen were detected in blood group O samples; this was decreased in blood group A samples and only a small amount of H was detected in blood group AB samples. In Bombay individuals no evidence of H antigen presentation on VWF glycans was observed, confirming the Bombay phenotype of each sample, (Figure 3.4). Despite the fact that soluble ABH structures are found in the circulation of para-Bombay individuals, there was no evidence of H antigen presentation on VWF in this group. This observation suggests that ABH are added to the N-linked glycans of VWF within EC, rather than acquired in the peripheral circulation following secretion. Clearly both Bombay and para-Bombay phenotypes are thus associated with an alteration in the glycans structure of circulating VWF which is distinct from that observed in normal plasma VWF.

Absence of H antigen presentation was also demonstrated by western blotting analysis of Bombay plasma samples. Duplicate samples of blood group O plasma and Bombay blood group plasma were run through 5% gels under reducing conditions and transferred to nitrocellulose membranes. Membranes were probed with anti-VWF-HRP to detect VWF and *Ulex europaeus* to detect H-antigen. Both O and Bombay plasma samples gave positive signals with anti-VWF-HRP which detected an ~250kDa band, but only O plasma samples stained positive for the H-antigen with *Ulex europaeus* detecting the same sized protein band. No bands were observed in the Bombay samples with *Ulex europaeus* (Figure 3.5), confirming that the H-antigen is not present on Bombay VWF.

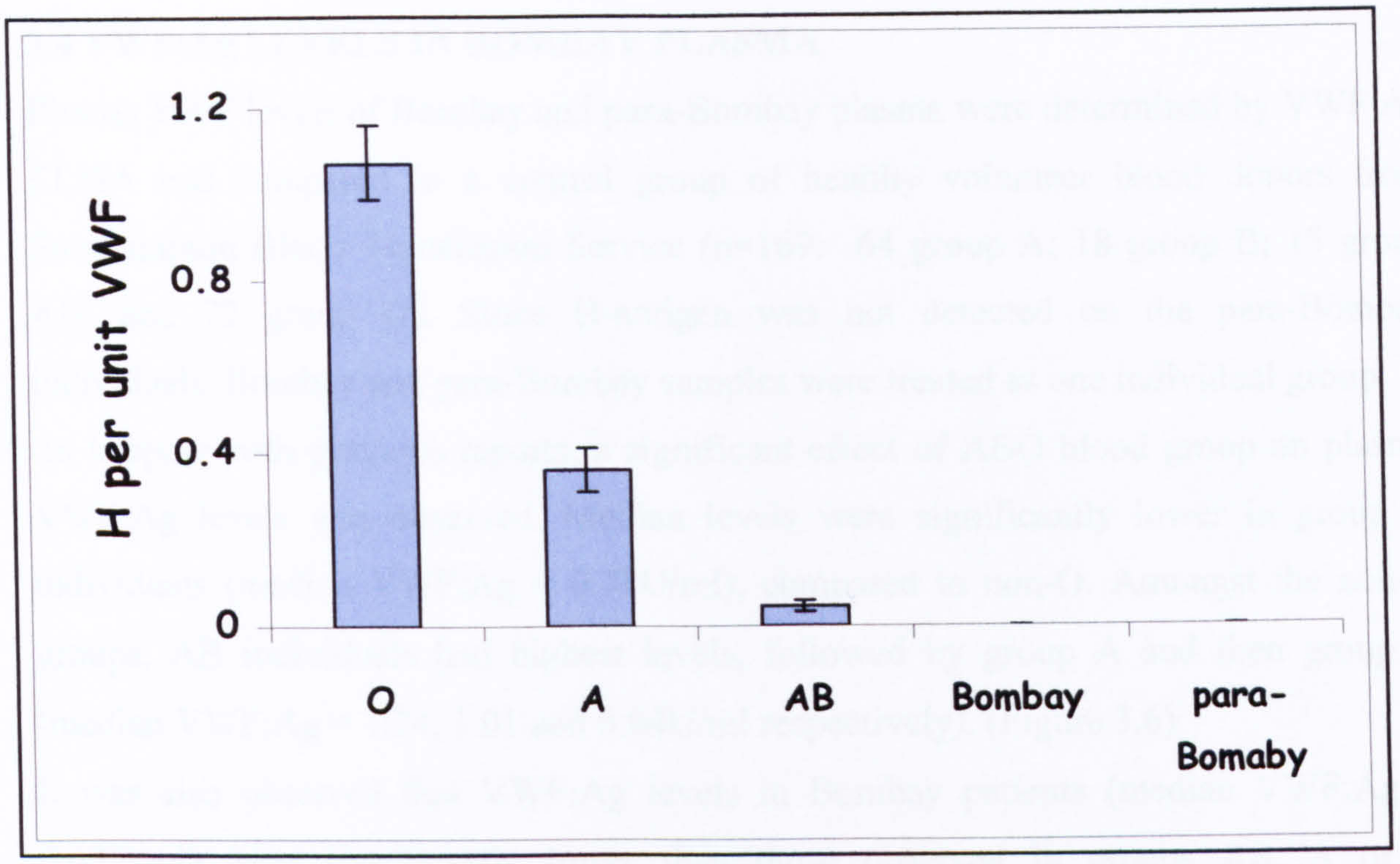


Figure 3.4 H antigen on VWF ELISA

The amount of H antigen on VWF was determined by ELISA and expressed as units of H per unit of VWF. Highest levels of H-presentation were observed on blood group O VWF. No H-antigen presentation was detected on Bombay or para-Bombay VWF.

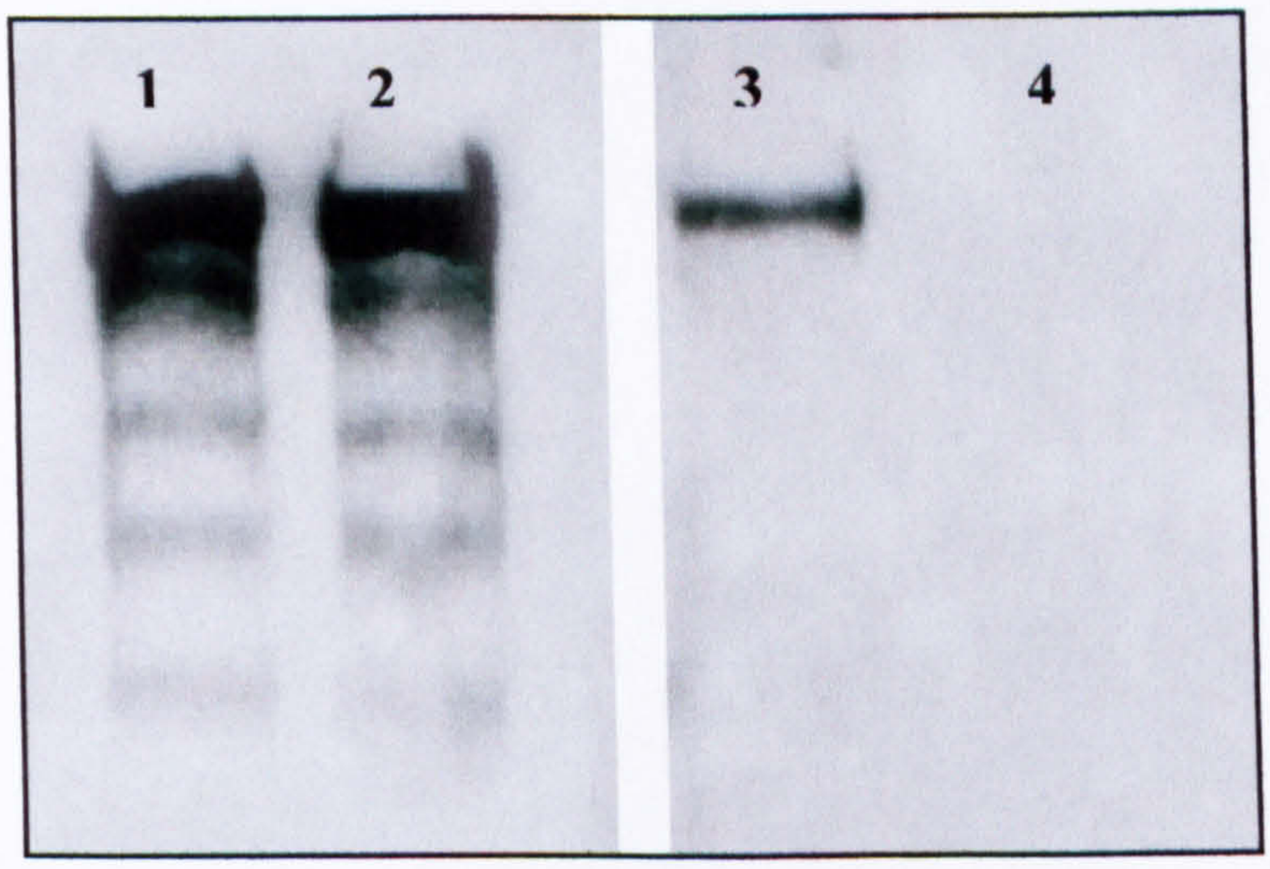


Figure 3.5 H on VWF western blot

O VWF (lane 1) and Bombay VWF (lane 2) were detected in plasma by western blotting and probing with anti-VWF-HRP. Both samples are positive for VWF. H-antigen was detected by probing with the H specific lectin *Ulex europaeus.* O VWF gives a positive signal, demonstrating the presence of the H-antigen (lane 3), no band is detected in Bombay VWF (lane 4), thus Bombay VWF does not present the H-antigen.

3.4 VWF:Ag LEVELS IN BOMBAY PLASMA

Plasma VWF levels of Bombay and para-Bombay plasma were determined by VWF:Ag ELISA and compared to a control group of healthy volunteer blood donors from Southampton Blood Transfusion Service (n=169: 64 group A; 18 group B; 15 group AB; and 72 group O). Since H-antigen was not detected on the para-Bombay individuals, Bombay and para-Bombay samples were treated as one individual group.

In keeping with previous reports, a significant effect of ABO blood group on plasma VWF:Ag levels was observed. Median levels were significantly lower in group O individuals (median VWF:Ag = 0.78U/ml), compared to non-O. Amongst the non-O groups, AB individuals had highest levels, followed by group A and then group B (median VWF:Ag = 1.24, 1.01 and 0.94U/ml respectively). (Figure 3.6)

It was also observed that VWF:Ag levels in Bombay patients (median VWF:Ag = 0.69U/ml) were significantly lower than those observed in groups AB, A or B respectively ($p = <0.05$) Moreover, Bombay VWF:Ag levels were also lower than those in group O individuals, although this difference failed to achieve statistical significance $p = 0.133$ (Figure 3.6).

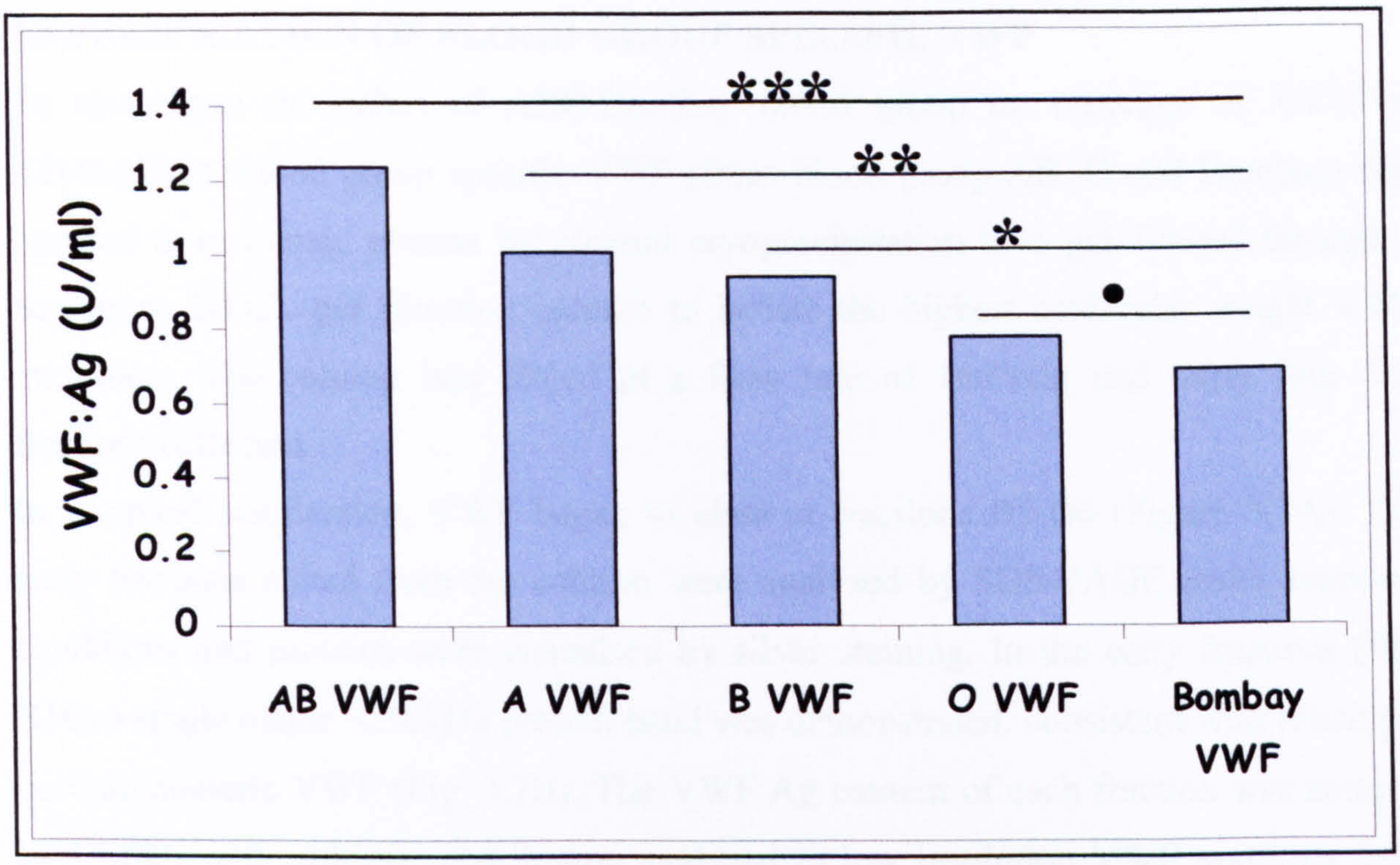


Figure 3.6 VWF levels in Bombay plasma

VWF levels in Bombay plasma were determined by VWF:Ag ELISA and compared to normal controls. Significantly lower levels were observed in blood group O individuals compared to non-O blood groups. Plasma levels of VWF were also significantly lower in Bombay patients compared to non-O blood groups. Although Bombay VWF levels were lower than group O levels, this failed to reach statistical significance. Mean VWF:Ag levels are shown for each blood group.(*** $p<0.001$; ** $p<0.01$; * $p<0.05$, • $p= 0.133$).

3.5 PURIFICATION OF BLOOD GROUP SPECIFIC VWF

To investigate the effect of ABO/Bombay blood group on cleavage of VWF by ADAMTS13, blood group specific VWF (from blood group AB, O and Bombay) was purified from human plasma by ethanol cryoprecipitation then gel filtered through a Sepharose 2B-CL gel filtration column to isolate the highest molecular weight VWF multimers. The column was eluted at a flow rate of 1ml/min and thirty four 5ml fractions collected.

In a typical purification, VWF began to elute at fractions B5-B6 (Figure 3.7A). The early fractions eluted from the column were analysed by SDS-PAGE under reducing conditions and proteins were visualised by silver staining. In the early fractions (B6-B10) a single major ~250kDa protein band was demonstrated, consistent with relatively pure monomeric VWF (Fig. 3.7B). The VWF:Ag content of each fraction was assayed by ELISA, and multimer distribution analysed in low resolution VWF multimer gels. Early eluted fractions (B6-B10) consisted predominantly of HMW-VWF, while later fractions were composed of intermediate and low molecular weight multimers respectively. This is illustrated by a loss of material at the top portion of the gel and the appearance of intermediate and low molecular weight bands (Figure 3.7C). The typical VWF yield for the early eluted fractions was ~10µg/ml.

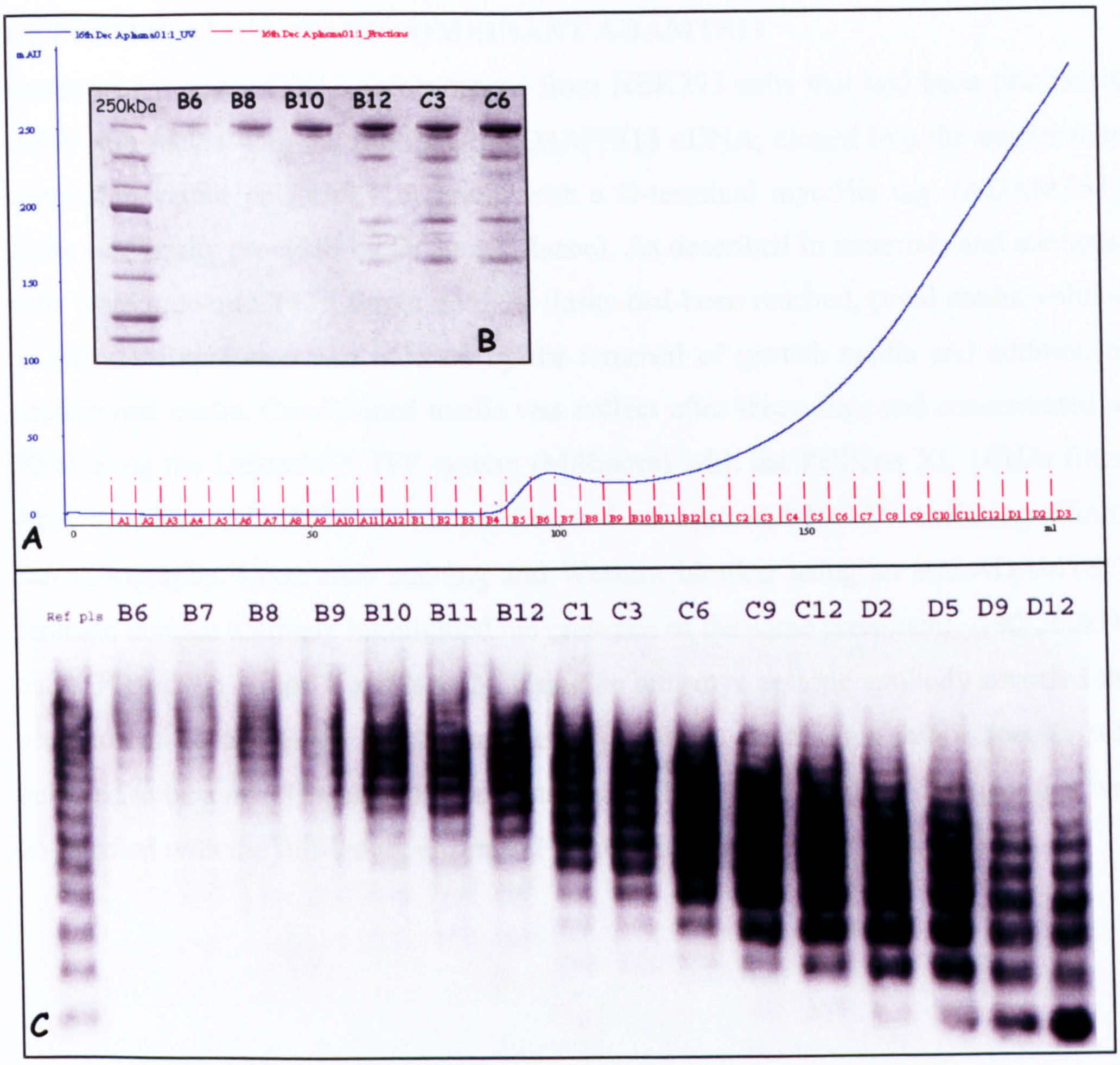


Figure 3.7 Purification of blood group specific VWF from plasma

A) *Gel filtration of cryoprecipitate*. Cryoprecipitate was gel filtered through a Sepharose 2B-CL gel filtration column to purify VWF and separate out the highest molecular weight VWF multimers. The column was eluted at 1ml/min and 5ml fractions were collected. VWF began to elute from the column at fractions B5-B6 and early fractions were analysed for purity by reducing gel electrophoresis followed by silver staining. B) *Silver stain*. Early eluted fractions (B6-B10) demonstrated a single band at ~250kDa consistent with pure monomeric VWF. The presence of other molecular species is detected in later fractions. C) *Multimer analysis of eluted fractions*. Early eluted fractions and representative later eluted fractions were analysed in non-reducing low resolution VWF multimer gels as described. Early fractions (B6-B10) contain the highest molecular weight multimers. Later fractions eluted from the gel filtration contain medium to low molecular multimers.

3.6 PURIFICATION OF RECOMBINANT ADAMTS13

Recombinant ADAMTS13 was prepared from HEK293 cells that had been previously stably transfected with the full length ADAMTS13 cDNA, cloned into the mammalian expression vector pcDNA3.1 in frame with a C-terminal myc/His tag. (ADAMTS13 clone was kindly provided by Dr James Rance). As described in materials and methods, cells were grown in T175 flasks until 20 flasks had been reached, (total media volume of 500ml). Expression was induced by the removal of growth media and addition of conditioned media. Conditioned media was collect after three days and concentrated to 50ml using the Labscale™ TFF system (Millipore) with the Pellicon XL 10kDa filter. After desalting, ADAMTS13 was purified and concentrated by Ni^{2+} chelating affinity chromatography. Coomassie staining and Western blotting using an anti-ADAMTS13 protease domain antibody highlighted the presence of the same prominent ~190-200kDa band (Figure 3.8 – lane 1 and lane 2). Using an anti-myc epitope antibody revealed the presence of an additional but lower intensity ~40kDa band. This minor species was believed to be a *myc*/His tagged C-terminal ADAMTS13 degradation fragment that was co-purified with the full-length enzyme (Figure 3.8 – lane 3).

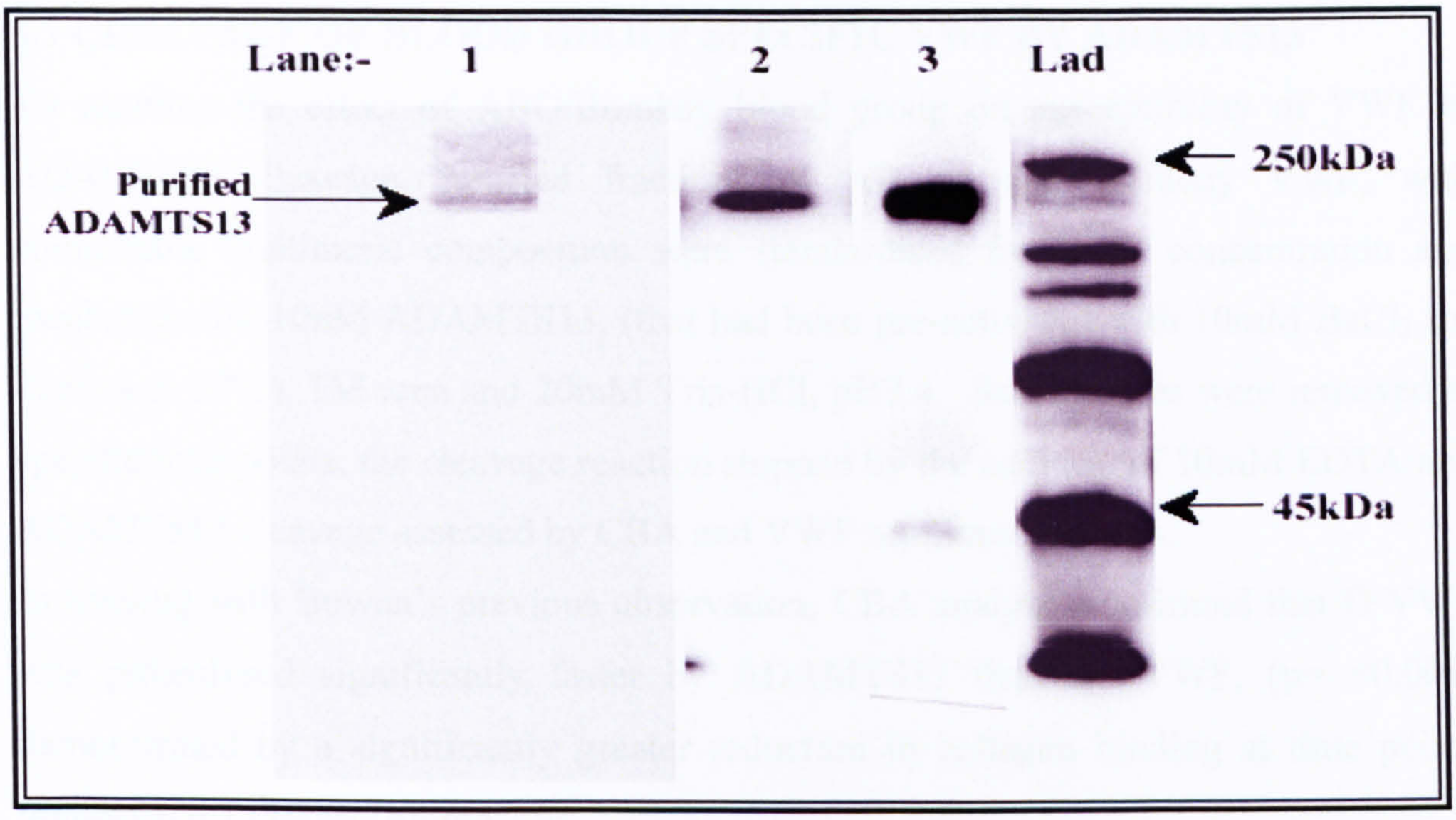


Figure 3.8 Purification of recombinant ADAMTS13

ADAMTS13 was expressed by HEK293 cells stably transfected with the pcDNA3.1+ADAMTS13/*myc*-His expression vector. ADAMTS13 was purified from concentrated and desalted conditioned media using a Ni^{2+}-HiTrap column and electrophorised in 7.5% polyacrylamide gels. Lane 1 - Coomassie stain under non-reducing conditions, demonstrating a single ~190kDa band. Lane 2 & 3 – western blot analysis under reducing conditions with the anti-ADAMTS13 protease domain antibody and anti-*myc* epitope antibody, respectively. The same ~190kDa band is seen in both lanes 2 & 3, confirming the presence of ADAMTS13. A smaller ~40kDa species can be seen in lane 3 and represents an ADAMTS13 degradation product. (Figure kindly supplied by Mr Jonathon Lam)

3.7 CLEAVAGE OF BLOOD GROUP SPECIFIC VWF BY ADAMTS13

To examine the effect of ABO/Bombay blood group on susceptibility of VWF to ADAMTS13 cleavage, purified fractions of AB, O and Bombay VWF, with comparable multimeric composition were standardised for VWF concentration and incubated with 10nM ADAMTS13, (that had been pre-activated with 10mM $BaCl_2$ for 20mins at 37°C), 1M urea and 20mM Tris-HCl, pH7.4. Sub samples were removed at specific time points, the cleavage reaction stopped by the addition of 10mM EDTA and ADAMTS13 cleavage assessed by CBA and VWF multimer analysis.

In keeping with Bowen's previous observation, CBA analysis confirmed that O-VWF was proteolysed significantly faster by ADAMTS13 than AB-VWF, ($p = <0.001$) demonstrated by a significantly greater reduction in collagen binding at time points 90mins and 135mins (Figure 3.9).

Furthermore, it was observed that Bombay VWF was proteolysed significantly faster than both blood group AB- and O-VWF, ($p = <0.001$) with no residual collagen binding activity remaining after 90mins incubation with ADAMTS13. (Figure 3.9)

This observation was corroborated by VWF multimer analysis (Figure 3.10). At time point zero the three VWF samples have similar multimeric composition, consisting of HMW multimers. After 45mins incubation with ADAMTS13, the HMW multimers are lost and medium to low molecular weight multimers appear, however the extent of the loss of HMW multimers is slightly more apparent for O and Bombay VWF compared to AB VWF. After 90mins incubation with ADAMTS13 it is apparent that there is greater loss of Bombay VWF compared to O VWF; and greater loss of OVWF compared to AB VWF.

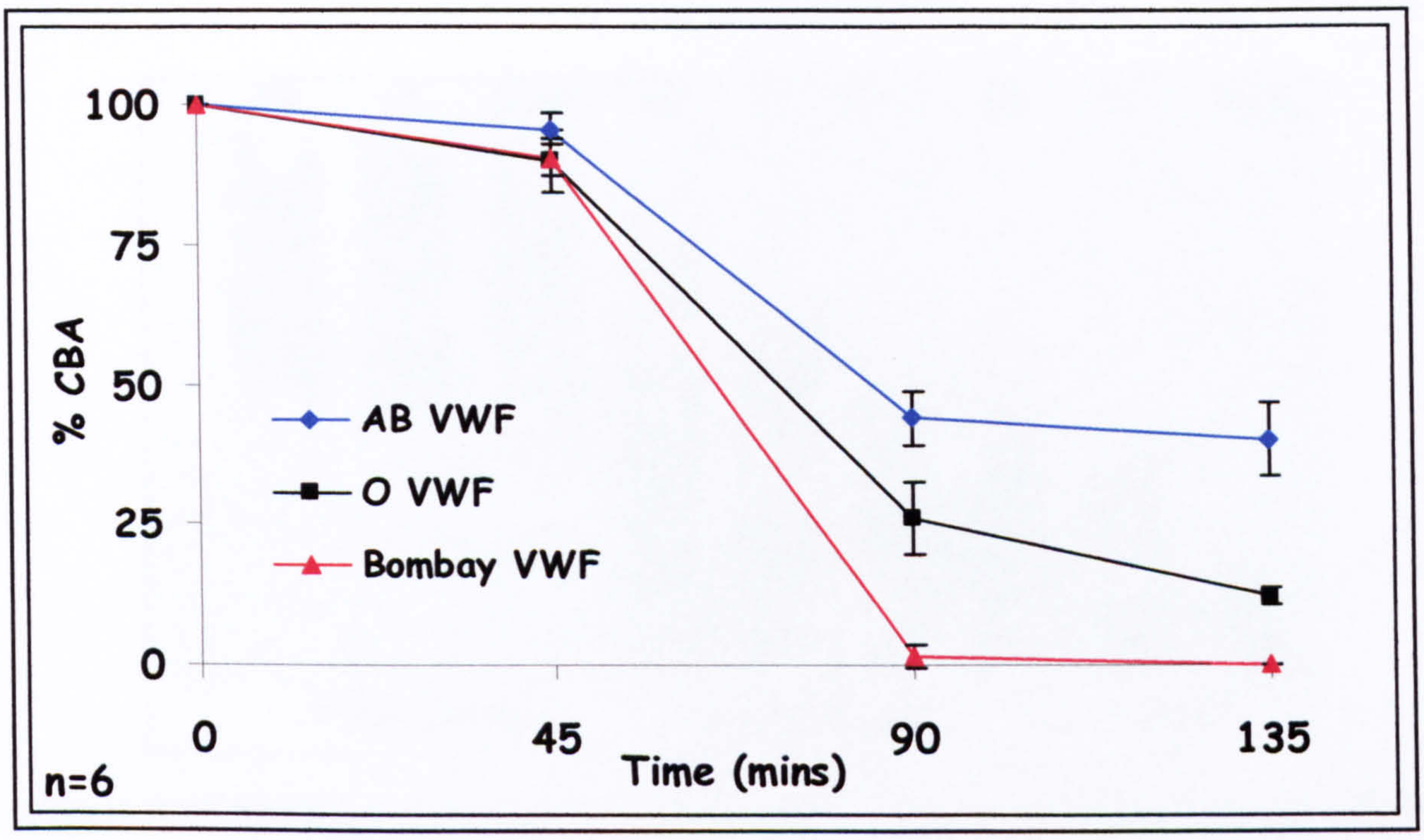


Figure 3.9 CBA analysis ADAMTS13 cleavage of blood group specific VWF

AB, O and Bombay VWF was subjected to cleavage by ADAMTS13 and extent of proteolysis was analysed by CBA. After 90mins incubation with ADAMT13, O VWF has been cleaved faster than AB; demonstrated by the greater reduction in collagen binding activity. Furthermore, Bombay VWF has been cleaved faster than O VWF, with no collagen binding activity remaining. After 135mins incubation the difference in collagen binding activity remains between the O and AB samples. (Values shown are the mean and standard deviation of 6 separate experiments performed in duplicate.)

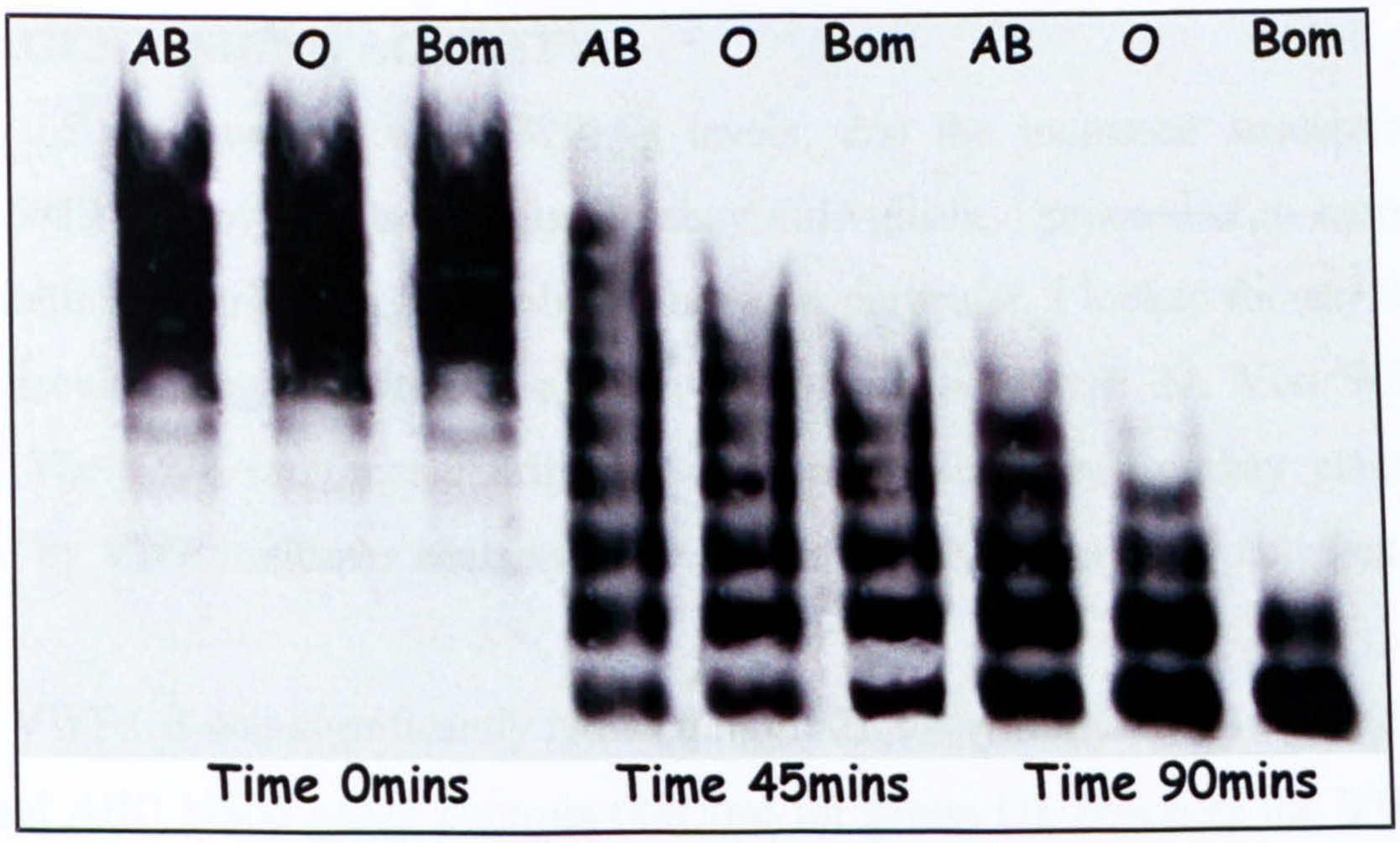


Figure 3.10 Multimer gel analysis of ADAMTS13 cleavage of blood group specific VWF

At time point zero, the three VWF samples have comparable multimeric structure. After incubation with ADAMTS13 for 45mins it is apparent the Bombay VWF (Bom) is being proteolysed faster, illustrated by the greater loss of HMW material and the greater intensity of monomeric VWF compared to O and AB VWF. Likewise O VWF is being proteolysed faster than AB VWF. At time point 90mins, the difference between the loss of multimers is more apparent between the samples, with cleavage occurring in the order Bom>O>AB.

3.8 ANALYSIS OF BOMBAY VWF MULTIMERIC STRUCTURE AND COLLAGEN BINDING ACTIVITY

In view of the lower plasma VWF:Ag levels, and the increased susceptibility to ADAMTS13 proteolysis observed in Bombay individuals, I proceeded to examine the VWF multimer distribution in Bombay plasma. In particular, I looked for any deficit in high-molecular weight multimers as seen in patients with type 2A Von Willebrand disease. The VWF multimer distribution of Bombay and para-Bombay plasmas was assessed by VWF multimer analysis in 1% agarose-SDS gels and by collagen binding assay.

Plasma VWF:CB was significantly reduced in the Bombay samples (71U/ml) compared to normal ABO blood group controls (88U/ml for group O), however the VWF:Ag to CBA ratio remained 1:1 and was not different to other ABO blood groups (Figure 3.11A). Thus the reduced plasma VWF:CB observed is solely due to the lower VWF levels in Bombay plasma. Furthermore, analysis of the multimeric structure of Bombay VWF demonstrated no loss of high molecular weight multimers; with multimer patterns similar to the normal control plasma. Therefore the increased cleavage of Bombay VWF does not alter its multimer distribution with in the circulation.

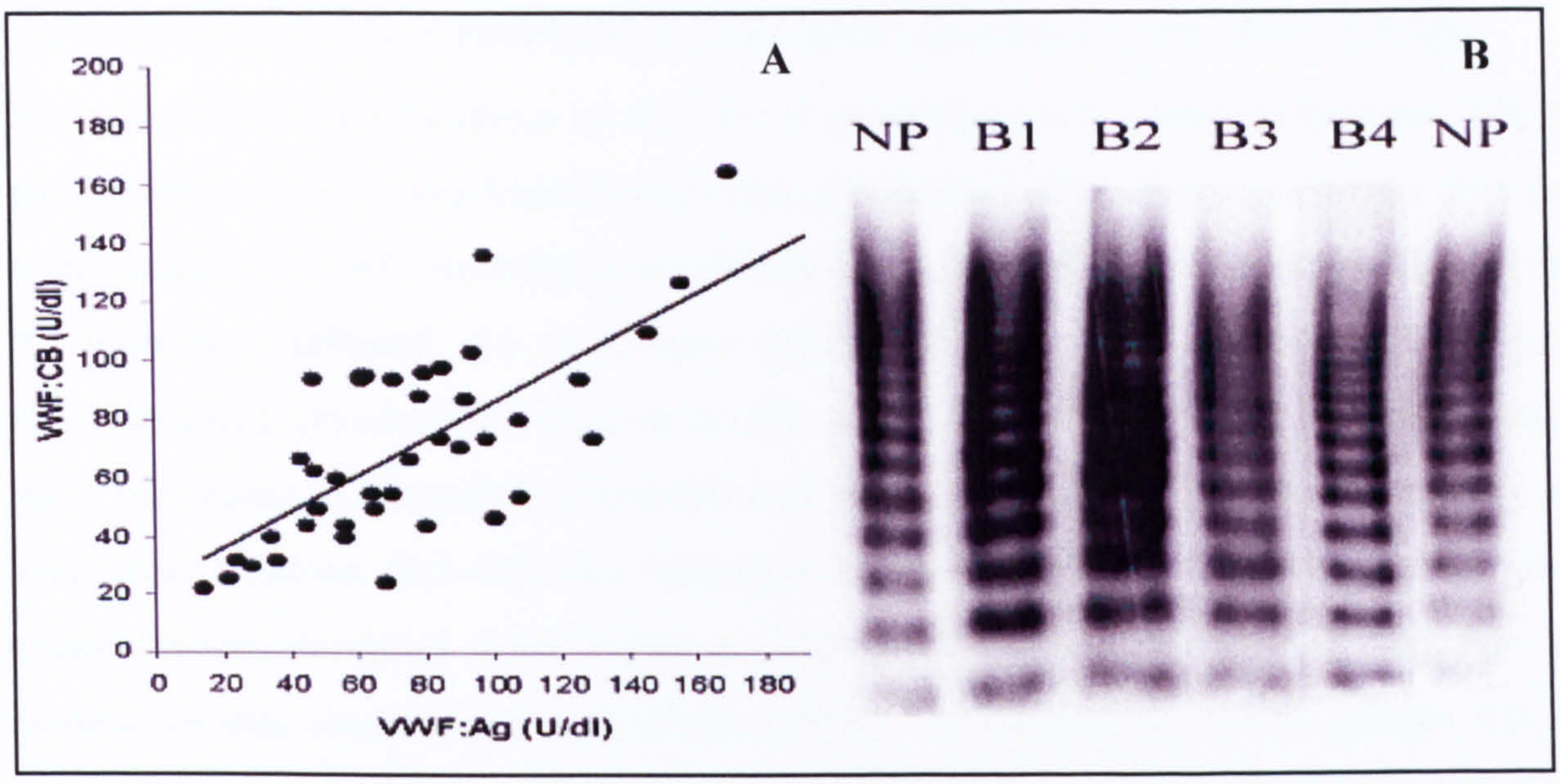


Figure 3.11 Analysis of Bombay VWF collagen binding and multimeric distribution

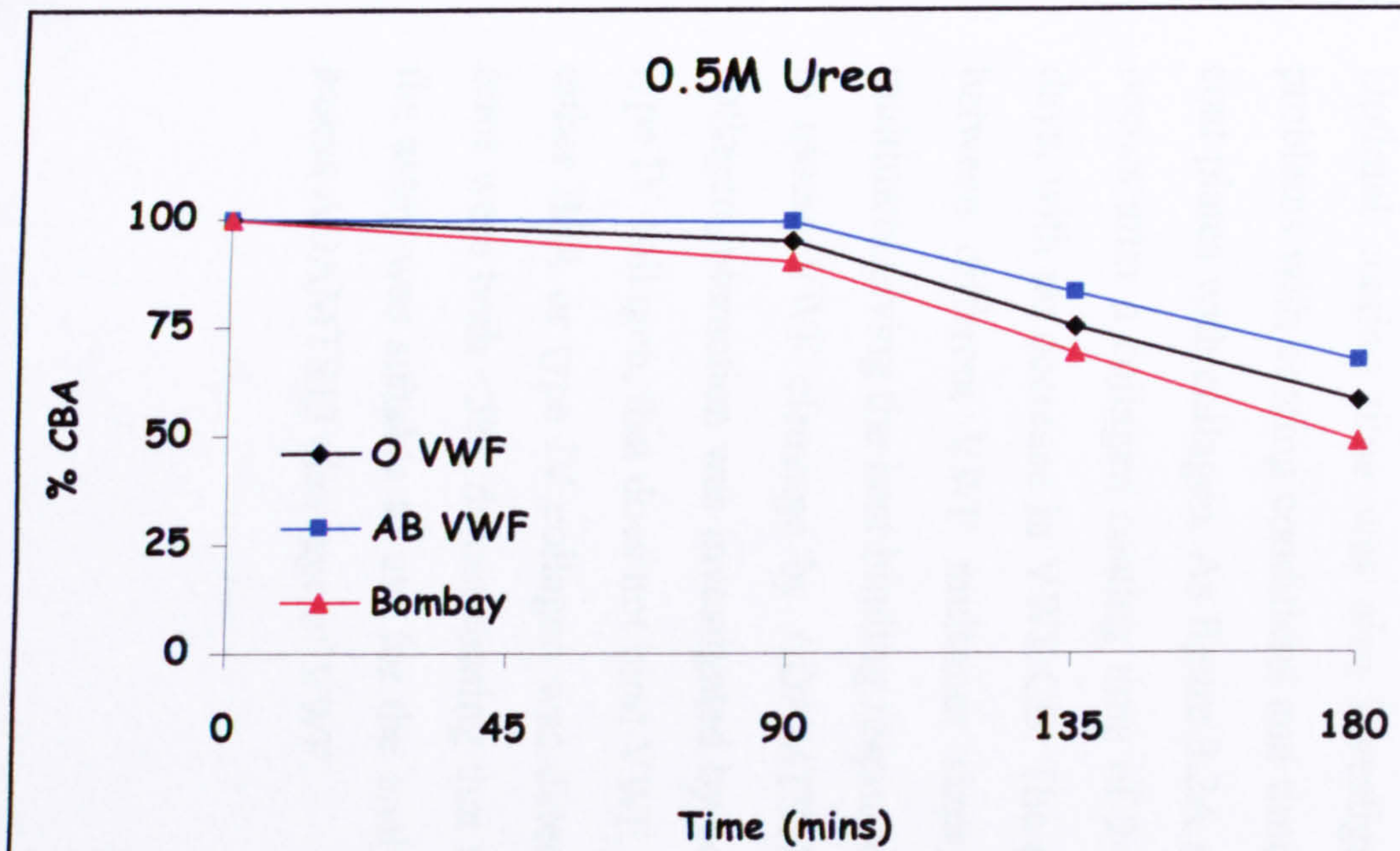
A) *Collagen binding of Bombay VWF.* VWF:CB was significantly reduced for Bombay VWF compared to normal control samples, however the VWF:Ag to VWF:CB ratio remained 1:1, indicating the reduced CBA is due solely to the reduced VWF levels observed in Bombay individuals. B) *Multimeric distribution.* The multimer pattern of four representative Bombay samples as analysed in 1% agarose multimer gels are shown. No loss of high molecular weight multimers is apparent in the Bombay samples compared to the two normal controls.

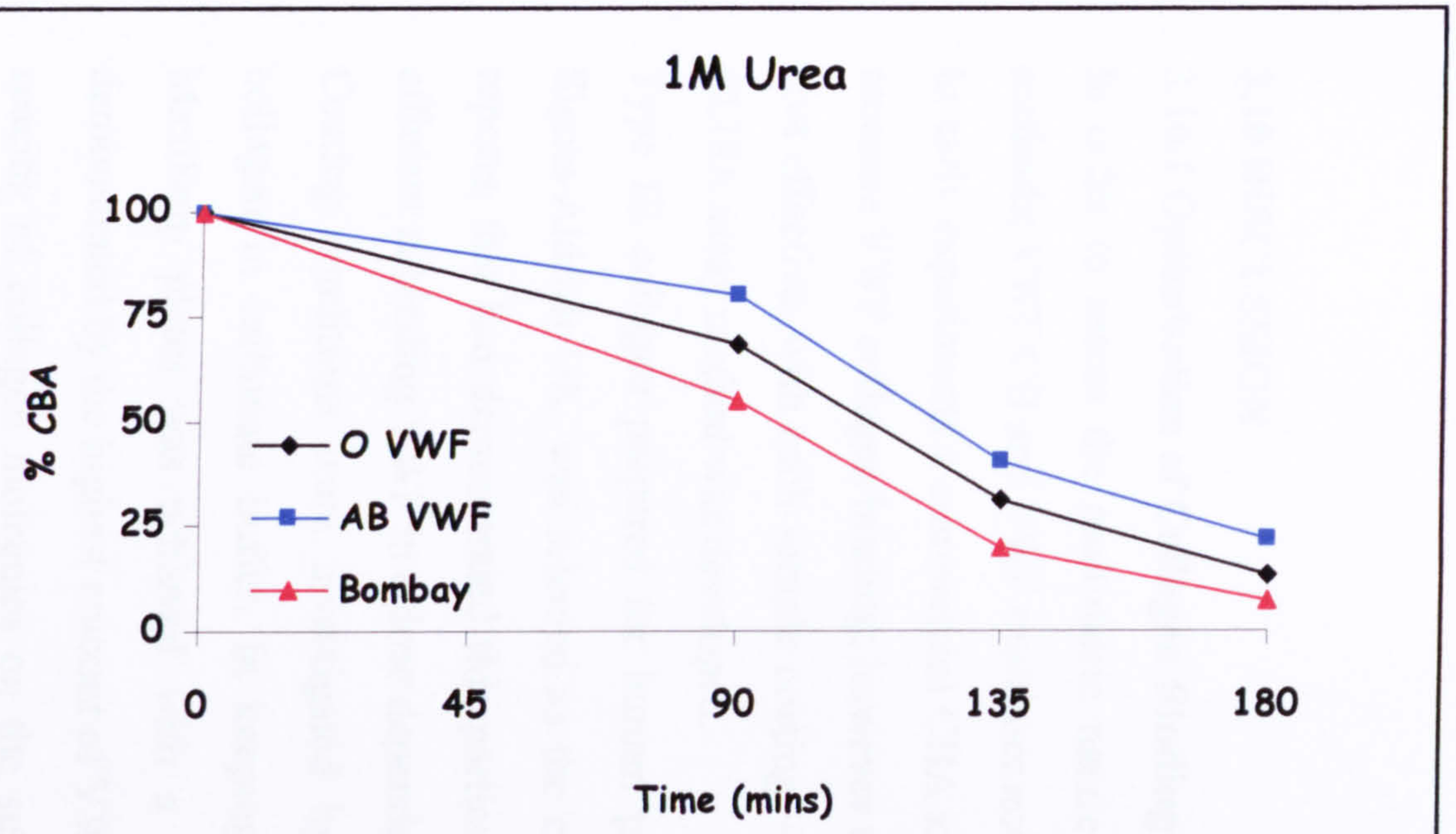
3.9 VWF GLYCANS, CONFIRMATION AND ADAMST13 PROTEOLYSIS

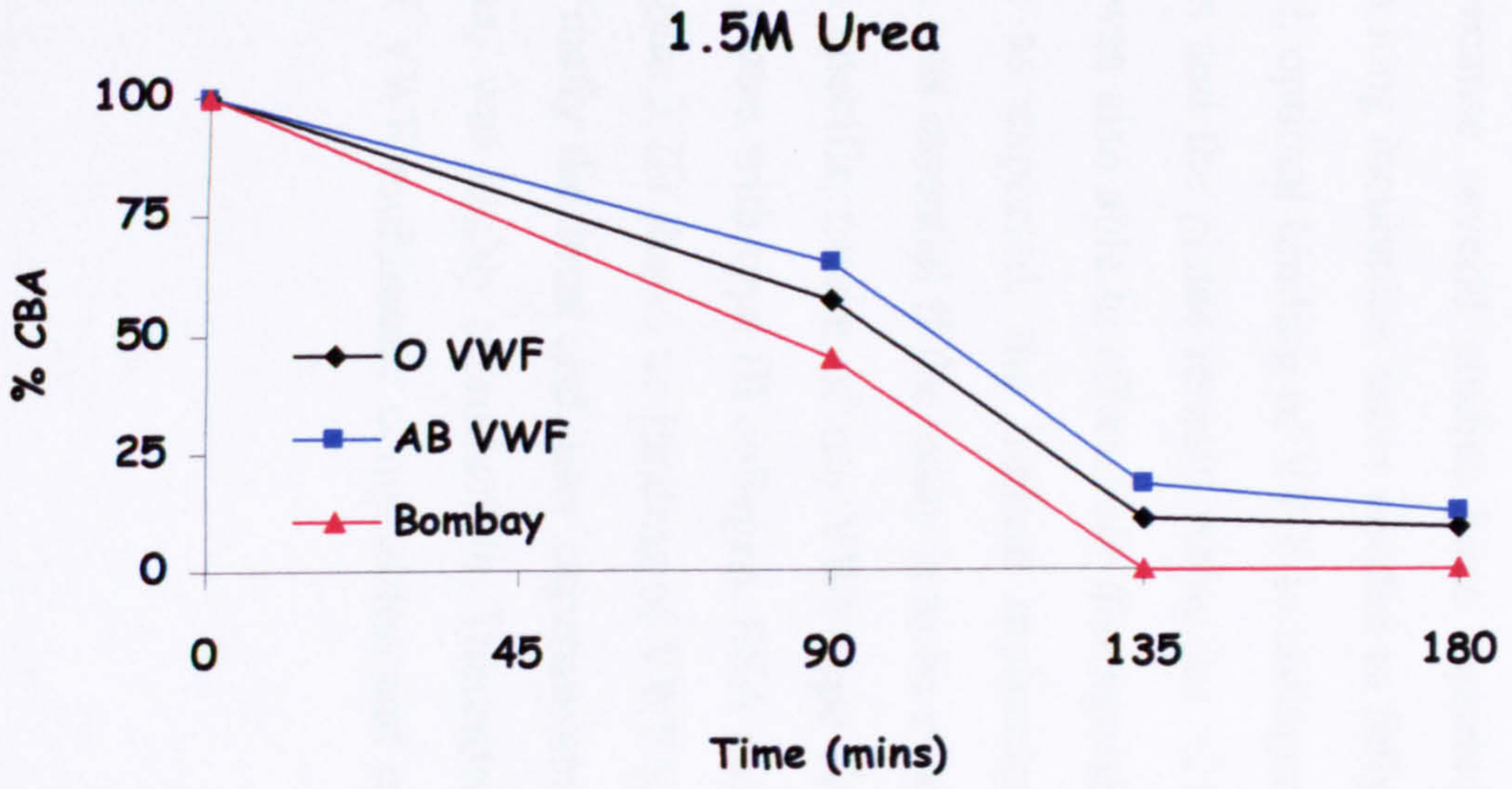
Since an effect of blood group on the rate of proteolysis was observed between AB, O and Bombay VWF, it was hypothesised that changes in VWF glycans structure alter the conformation of VWF, such that accessibility to the ADAMTS13 cleavage site with the A2 domain is affected. To investigate this hypothesis VWF cleavage assays were repeated using cryodepleted plasma as the source of ADAMTS13. Cleavage assays were performed as described (Materials and Methods, section 2.7.1) using a range of urea concentrations (0.5-4M) and cleavage of VWF analysed by CBA. As the urea concentration increased from 0.5M to 2M, a significant increase in the rate of proteolysis was observed for each of the different blood groups studied (groups AB, O and Bombay respectively). In the presence of 4M urea, proteolysis of HMW-VWF by ADAMTS13 was inhibited. At all concentrations of urea studied (<4M), Bombay VWF was proteolysed faster than either groups O or AB respectively. However this difference in susceptibility to ADAMTS13 proteolysis was most marked at 1M urea. As the concentration of urea progressively increased, the difference between AB, O and Bombay became less apparent suggesting that with increased unfolding of VWF the ABO effect is diminished. This suggests that the ABO antigens may alter accessibility of ADAMTS13 to the cleavage site by altering the conformation of the VWF molecule.

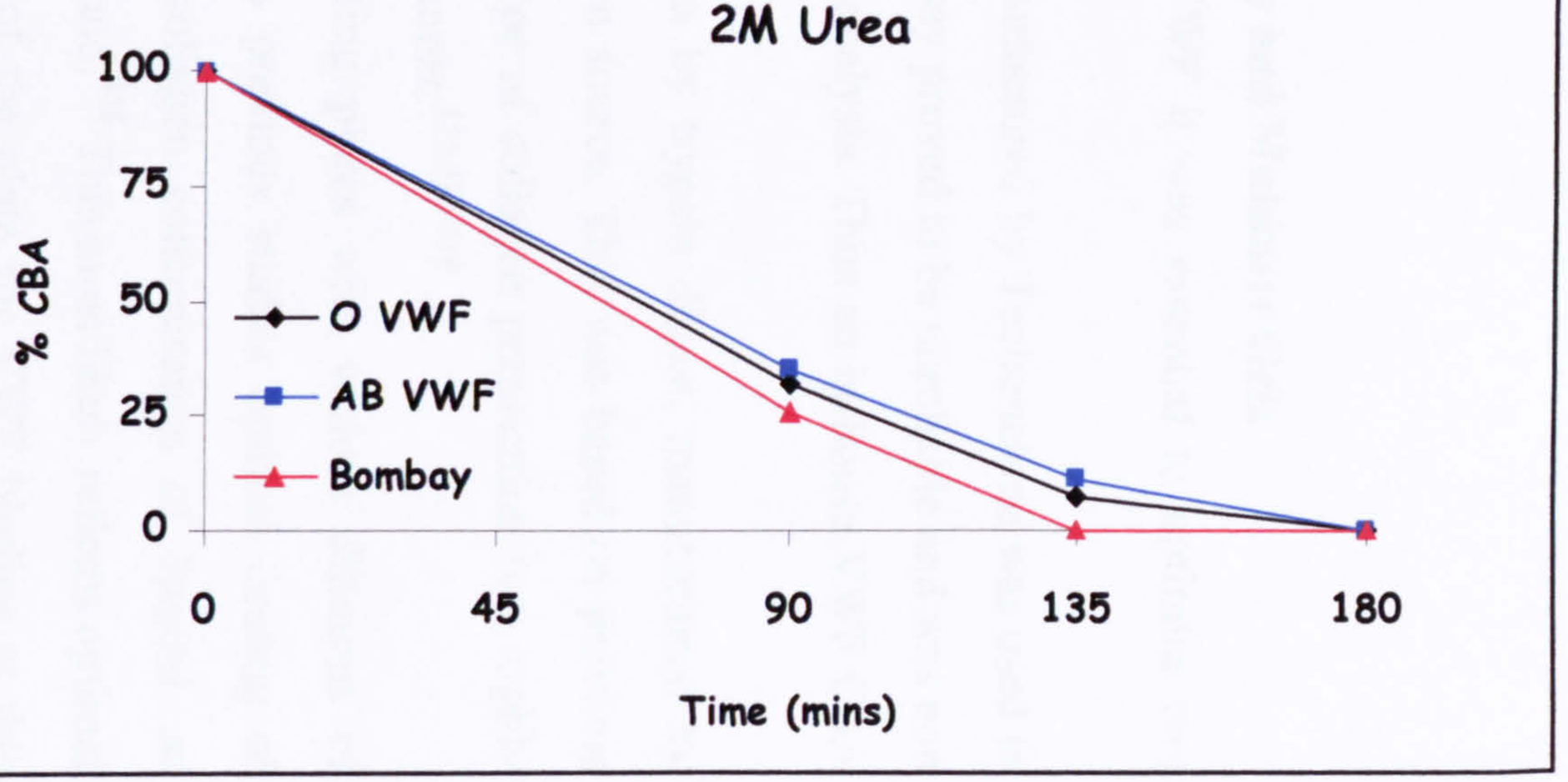
Next page - **Figure 3.12 Effect of increasing urea concentration on susceptibility of blood group specific VWF to ADAMTS13 proteolysis**

Blood group specific VWF was subjected to ADAMTS13 proteolysis using cryodepleted plasma as the source of ADAMTS13. As the urea concentration increased from 0.5-2M the overall rate of proteolysis increased, demonstrated by the greater loss of CBA at time 90mins with increasing urea concentration. At all urea concentrations Bombay VWF is proteolysed faster than O VWF, that is proteolysed faster than AB VWF. The effect is most obvious using 1M urea. However with increasing urea concentration the difference in the rate of cleavage observed between blood groups is diminished.


0.5M Urea
100
75
50
25
0
% CBA
O VWF
AB VWF
Bombay
0
45
90
135
180
Time (mins)


1M Urea
100
75
50
25
0
% CBA
O VWF
AB VWF
Bombay
0
45
90
135
180
Time (mins)


1.5M Urea
100
75
50
25
0
% CBA
O VWF
AB VWF
Bombay
0
45
90
135
180
Time (mins)


2M Urea
100
75
50
25
0
% CBA
O VWF
AB VWF
Bombay
0
45
90
135
180
Time (mins)

3.10 DISCUSSION

3.10.1 Optimisation of Collagen Binding Assay and Multimer Gels

In order to assess the multimeric nature of VWF it was essential to optimise two methods; VWF:CB and VWF multimer analysis.

In early experiments a commercial CBA kit manufactured by Techonclone was used to measure VWF collagen binding; however the assay proved to be unreliable and was non cost effective, with each sample costing ~£2 to analysis. Thus an in-house VWF CBA ELISA assay method was developed.

Type III collagen prepared for human placenta by trypsin digest, manufactured by Sigma-Aldrich UK, was selected as the collagen source. This was based on previous reports, that had demonstrated this particular type of collagen preparation was highly efficient at binding VWF in a dose dependent manner.[155,325-328]

Coating conditions were investigated by coating plates with various dilutions of collagen in carbonate buffer. In keeping with previous studies optimal coating of MaxiSorp plates was achieved with a low collagen concentration of 5µg/ml, as demonstrated by the highest amount of VWF bound.[328] This most likely reflects optimal spacing of collagen molecules on the surface of the plate for VWF binding at this concentration, at higher concentrations, optimal spacing of collagen cannot occur and therefore VWF binding is decreased.[328]

Optimal coating time was also investigated because several studies have reported problems with coating conditions and times with long incubation times needed to fully coat plates with collagen. As figure 3.2A showed, optimal binding of VWF to collagen occurs after a collagen coating time of 24 hours and the plates remain stable for >21 days, with no decrease in VWF:CB. The assay was also able to effectively distinguish between different VWF multimer sizes, with as expected, the highest molecular multimers giving the best binding response. This was essential if the assay is to be used to assess VWF cleavage by ADAMTS13. The specific nature of the VWF-type III collagen interaction was investigated by coating plates with type III collagen, BSA and type IV collagen, that does not bind VWF. As figure 3.2D shows no binding of VWF to either BSA or type IV collagen was detected. Finally the intra and inter experimental error were both <5%, demonstrating that the assay was highly reproducible. Therefore the assay was suitable to use for the analysis of VWF multimeric composition and to assess ADAMTS13 cleavage of VWF.

3.10.2 Multimer Analysis

VWF multimer analysis is used to visualise the multimeric nature of VWF. Although less sensitive than the CBA and one can not easily extrapolate a numerical result for statistical analysis, they do provide a good corroboration of any observations made with collagen binding methods.

VWF multimer analysis is a technically demanding method, with no standardised protocol. The gold standard of VWF multimer analysis is often considered to be the method of Enayat and Hill, using a horizontal electrophoresis system and visualisation of VWF multimers with radioactive iodine (I^{125}), however this is only performed in a few specialised centres.[78] Typically, the method will vary from lab-to-lab, but normally samples are electrophoresed in a non-reduced state through agarose gels in horizontal electrophoresis systems, with gels cast using *in house* apparatus and separate stacking and running gels. VWF multimer bands maybe visualised by autoradiography,[78,329] peroxidise mediated staining,[330-333] or luminography.[334,335] The method can be time consuming, with the whole process from casting the gel to final visualisation of VWF multimer bands, taking up to 5 days. A number of disadvantages exist with horizontal electrophoresis systems; horizontal systems are prone to perturbation by temperature fluctuations, nonuniformity in the field strength of the current, evaporation and condensation and electroendoosmotic effects causing compression of the gel that effectively alters the agarose concentration. Furthermore, the use of separate stacking and running gels requires the formation of a binary gel in which the junction between stacking and running gel is often poorly formed due to the formation of a film at the site where the running gel is sliced before application of the stacking gel.

In initial attempts at VWF multimer analysis, a horizontal gel system was used, however this proved to be unsuccessful, with the quality of gels being poorly reproducible and the method highly time consuming for the number of samples it was possible to analyse. To overcome this a multimer gel was optimised combining two published methods that used vertical gel electrophoresis systems.[336,337] Based on these studies a method was developed where vertical mini-gels were cast without the need for separate stacking and running gels using a Tris-glycine-SDS buffer. Electrophoresis of the samples normally took ~3 hours with the buffer temperature kept between 10-16°C. Following electrophoresis, western blotting was performed has as been described previously for high molecular weight proteins[338] and following blocking of non-specific sites, membranes were probed with anti-VWF-HRP and visualised with ECL

chemiluminescent kit (Amersham). The method was highly reproducible and could be completed in less than a day, furthermore up to 20 samples could be analysed under the same experimental conditions, making the method highly time efficient. Although this method would require further optimisation for the use in a diagnostic environment, for the purpose of analysing basic VWF multimer structure and cleavage of VWF by ADAMTS13, it was highly effective.

3.10.3 Plasma VWF levels and the Bombay Phenotype

A well established association has been recognised between ABO blood group and plasmas VWF levels, with individuals of blood group O having plasma VWF levels 25-30% lower than those of non-O blood groups (A, B and AB). The physiological mechanism by which ABO blood group affects VWF levels is unknown, however the ABH antigenic determinants have been identified on the *N*-linked glycans of plasma VWF according to the blood group of the individual. Despite the fact that these different blood group antigens are expressed on a minority of the N-linked chains of plasma VWF, and that they differ only with respect in regards to a single sugar moiety, they significantly influence plasma VWF:Ag levels. To further explore this observation, samples were collected from 47 individuals with the rare Bombay / para-Bombay blood group.

The Bombay blood group was first identified by Bhende *et al* in three unrelated individuals in Mumbai, (formerly Bombay) in 1952, who failed to present H-antigen on the surface of their red blood cells and had plasma antibodies that could react with the O(H), A and B antigens.[339] The failure to present H antigen is due to mutations of the *H* gene (FUT1) and of the *Se* gene (FUT2) that encode distinct α1-2 fucosyltransferases.[340] The H gene regulates the expression of H antigen on red blood cells,[341,342] and the Se gene regulates the expression of H antigen in the gastrointestinal tract and in secretions.[343] Individuals with the true Bombay phenotype are homozygous for null alleles at both the *H* and *SE* gene loci and therefore do not present H antigen on the surface of red blood cells and do not secrete H antigen.[339,343] Individuals with the para-Bombay phenotype are homozygous for null alleles at the *H* locus but have at least one functional *SE* allele;[343,344] such that H-antigen is found in their secretions.

The frequency of the Bombay and para-Bombay phenotypes is low; ~1 per million individuals in Europe is affected[345] although higher frequencies are observed in Japan, (1 in 300,000) India, (1 in 10,000) and Taiwan (1 in 8000, para-Bombay).[346,347] Neither

phenotype appears to confer any deleterious effects, except in circumstances requiring blood transfusion, where Bombay and para-Bombay individuals are incompatible with all donors except other H-deficient individuals.[343]

Analysis of plasma VWF of individuals with the Bombay and para-Bombay phenotype confirmed the failure to express the H-antigen, with both lectin ELISA and western blotting confirming the H-antigen was not presented on VWF. This was compared to normal ABO blood type samples that did present the H antigen and also demonstrated by lectin ELISA and western blotting. The observation that no H on VWF expression was found in para-Bombay individuals in spite of the fact that soluble ABH structures are secreted into their circulation,[343] indicates that ABH sugars are added to the N-linked glycan chains during the extensive post-translational modifications that VWF undergoes in EC prior to secretion. (Since no H antigen was detected on VWF from either Bombay of para-Bombay individuals, it was decided to treat them as one single group, referred to as Bombay.)

Quantification of plasma VWF levels in the Bombay samples compared to normal ABO controls, confirmed the observation that plasma VWF levels are generally lower in blood group O individuals, and furthermore it was observed that VWF levels in the Bombay individuals were significantly lower than levels in the non-O blood groups. Although VWF:Ag levels were also lower in Bombay individuals compared to individuals of group O, this result failed to achieve significance.

It is still unclear how the ABO(H) sugars influence plasma VWF levels. However, since the FUT1 and FUT2 loci responsible for the Bombay/para-Bombay phenotypes are located on chromosome 19, distinct from the ABO locus on chromosome 9, the effect is likely be due to a functional effect of the ABH antigen presentation, rather than rather than linkage-disequilibrium between the *ABO* locus and another unidentified VWF regulatory locus.[320] Current data also suggests that the effect is not due to an influence on the rate of VWF synthesis and /or secretion, although this has been difficult to investigate since VWF synthesised *in vitro* has a different glycan structure to that of plasma VWF, particularly in that *in vitro* synthesised VWF fails to present the ABO(H) sugars.[348,349] However, ABO blood group status has no effect on plasma levels of the VWF propeptide, which is released in a 1:1 ratio with VWF;[350] no effect is observed on platelet VWF, that does not present the ABO sugars[351], and finally ABO does blood group does not influence the rate of VWF secretion from the regulated pathway following DDAVP administration.[352] It therefore seems likely that the ABO effect is

mediated by proteolysis and/or secretion. The interesting observation that ABO blood group altered susceptibility to cleavage by ADAMTS13 was therefore investigated using Bombay VWF.

3.10.4 ADAMTS13 Proteolysis of Blood Group Specific VWF

Ethanol cryoprecipitation and gel filtration was used to purify blood group specific VWF from AB, O and Bombay plasma. Cryoprecipitation exploits the fact that VWF is a cold insoluble protein and thus proteins (including VWF) that precipitate out of solution during thawing from -80°C to 4°C are isolated for further purification.[353] The factors governing the cryoprecipitation of VWF are unknown, however it has been demonstrated that fibronectin needs to be present in the plasma for efficient cryoprecipitation.[354] Gel filtration or size exclusion chromatography separates proteins on the basis of size; larger proteins are unable to enter the gel filtration matrix and are eluted from the column first, smaller proteins are able to enter the matrix and thus their passage through the column is retarded and they are eluted in later fractions. A large Sepharose 2B-CL column was used to separate out the highest molecular VWF multimers and as shown the earliest eluted fractions contained the highest molecular weight VWF, which was demonstrated by silver staining to be free of contaminants.

Bowen (2003) recently reported that VWF of different ABO blood groups exhibited different susceptibility to specific cleavage by ADAMTS13 ($O \geq B > A \geq AB$).[324]

In this study, cleavage of blood group specific VWF with ADAMTS13 and subsequent analysis with CBA and VWF multimer gels, confirmed that O VWF was proteolysed by ADAMTS13 faster than AB VWF and extended this observation to include Bombay VWF, which was proteolysed faster than both O VWF and AB VWF. The exact mechanism by which glycosylation and the presence of ABO blood group sugars can influence susceptibility of VWF to cleavage by ADAMTS13 remains unknown and forms the subject of further investigation in the preceding chapters.

A previous study observed an inverse correlation between H antigen expression and VWF levels. O'Donnell *et al* (2002) demonstrated that H antigen expression was highest in group O individuals, and in group A individuals was inversely correlated with A transferase expression, such that H-antigen expression was highest in the order $A^2O^1 > A^1O^1 > A^1A^1$.[322] (Since A transferase expression is highest in A1A1 individuals.) A correlation was also observed between H antigen expression and VWF levels in group O individuals, with increased amounts of H antigen resulting in lower VWF

levels. It was suggested that the expression of the terminal fucose moiety (i.e. H antigen) was responsible for the variation in VWF levels, with higher levels of H resulting in lower plasma VWF levels, and this was possibly mediated through accelerated clearance via a fucose-mediated mechanism.[322] Indeed distinct hepatic fucose receptors have been characterised.[286,355] However, since plasma levels were lower in Bombay individuals, that do not present terminal fucose residues, it seems unlikely that terminal fucose presentation is responsible for determining plasma VWF levels. From the data I have obtained however, it is possible to draw an indirect relationship between oligosaccharide chain length and the susceptibility to cleavage by ADAMTS13. Moreover the length of the glycan chain correlates with plasma VWF levels – so that levels are highest in group AB, intermediate in groups A and B, lower in group O and lowest in Bombay. This hypothesis also fits with previous observations regarding the dosage effect of ABO genotype on the amount of ABH expressed per unit VWF ($A^1A^1 > A^1O^1 > A^2O^1 > O^1O^1$).[319,320,322]

How the length of the glycan chain may affect ADAMTS13 proteolysis is unclear. One hypothesis is that the glycan structures affect the conformation of VWF; with Bombay and O VWF, that have the shortest glycan chains, being able to adopt a conformation more permissive to ADAMTS13 cleavage. Glycosylation is known to directly affect protein folding and thus the glycans of VWF may play an important role in mediating and maintaining the tertiary structure of VWF.

To investigate this, cleavage of AB, O and Bombay VWF by ADAMTS13 was repeated using increasing urea concentrations to "open up" VWF and mimic the effect of shear stress that VWF is subjected to *in vivo*. With increasing urea concentration the overall rate at which WVF was proteolysed by ADAMTS13 was increased, suggesting that with increasing urea concentration more VWF molecules adopt a confirmation apt to ADAMTS13 cleavage. The ABO effect on cleavage was most pronounced at 1M urea, but with increasing urea concentration the difference between the groups was diminished. This provides support to the hypothesis that the terminal VWF sugars alter the permissiveness of the molecule to ADAMTS13 cleavage.

How this effect on susceptibility to ADAMTS13 proteolysis is translated into a quantitative effect on plasma VWF levels remains unclear. However it is interesting that despite the increased rate of cleavage, plasma multimer analysis in Bombay individuals appeared normal. Although the collagen binding activity of Bombay VWF was significantly lower than normal, the CBA to VWF:Ag ratio was normal (1:1), indicating

that the lower CBA was due to the lower VWF:Ag level. Furthermore, plasma multimer distribution was normal in the Bombay plasmas. This apparent paradox between an increased susceptibility to ADAMTS13, yet normal plasma multimer distribution, has previously described in association with the Tyr1584Cys polymorphism of VWF.[356] Although this polymorphism does not result in any VWD like phenotype, it was demonstrated that it conferred an increased susceptibility to ADAMTS13 cleavage but still retained normal multimer distribution.[356] Once again, this polymorphism may result in a VWF molecule that is more readily able to adopt the confirmation required for ADAMTS13 cleavage.

How these observations are integrated *in vivo* remains to be explored. Increased proteolysis alone is unlikely to be the sole mechanism for the differences observed in VWF levels between blood groups. However, the lower levels in combination with the increased rate of proteolysis does none the less suggest that there is a link between proteolysis and clearance. However the relationship between ADAMTS13 cleavage, VWF multimer size and rate of clearance has yet to be established.

In conclusion, the results presented in this chapter demonstrate that plasma levels of VWF in Bombay individuals are significantly lower than levels observed in non-O blood groups and are also lower than levels observed in blood group O. Bombay VWF is also more susceptible to cleavage by ADAMTS13 than O VWF, which is more susceptible to ADAMTS13 cleavage than AB VWF. It is hypothesised that the altered propensity to ADAMTS13 cleavage is due to the size of VWF glycan chain affecting the ability of VWF to adopt a conformation permissive for ADAMST13 cleavage. This hypothesis is pursued in Chapters 5 and 6 by making further modifications to the VWF glycans.

Chapter 4

4. ANALYSIS OF VWF GLYCAN STRUCTURE

4.1 INTRODUCTION

Based on its primary amino acid structure, the VWF monomer is predicted to contain a number of *N*-linked and O-linked glycosylation sites. Although there has been some detailed chemical analysis of the overall structure of the glycans chains; in particular the observation that the *N*-linked glycans present the ABO(H) sugars, a number of questions remain unresolved. For example, it is not known which specific sites present the blood group sugars and indeed, if all the predicted sites are occupied by glycan chains. Furthermore, Matsui *et al's* original analysis of the *N*-linked glycans does not give information about their sialylation status.

The observation that VWF glycans present the ABO(H) sugars is particularly pertinent with regard to the results presented in the previous chapter. Given the demonstrated ABO effect on ADAMTS13 cleavage and the proximity of two predicted *N*-linked sites, N1515 and N1574, to the ADAMTS13 cleavage site at Y1605M1606, it becomes critical to know whether these sites are glycosylated and if they present blood group sugars. Presence of the ABO(H) sugars at these sites may illuminate the potential role of these glycans in mediating susceptibility to ADAMTS13 cleavage.

To further analyse the glycan structure of VWF, the primary VWF protein sequence was analysed using neural network algorithms to predict the probability of potential glycosylation sites being occupied. Furthermore, parts of the human VWF protein sequence were aligned with the VWF sequence of other species and with other proteins sharing homologous domains. Proteolytic fragments of purified VWF were generated and sequenced and analysed for the presence of glycan chains and the ABO blood group sugars.

4.2 *IN SILICO* ANALYSIS OF VWF GLYCAN STRUCTURE

4.2.1 Prediction of O and *N*-linked Glycosylation Sites in VWF

The NetOGlyc and NetNGlyc algorithms use a jury of artificial trained neural networks to predict the probability of a potential O- or *N*-linked glycan site being occupied based on the amino acid sequences surrounding the potential site. The algorithms are available from:

http://www.cbs.dtu.dk/services/NetOGlyc - O-linked glycosylation prediction

http://www.cbs.dtu.dk/services/NetNGlyc - *N*-linked glycosylation prediction

In both programmes potential sites are assigned an O or *N*-linked glycosylation potential score, ranging from 0 to 1. The value of 0.5 is deemed to be the threshold value, over which, sites are likely to be occupied.

O-linked glycosylation

Based on the basic amino acid structure, known rules governing O-linked glycosylation and initial observations made by Titani *et al*,[16] VWF is predicted to contain 10 O-linked glycan chains: T1248, T1255, T1256, S1263, T1468, T1477, S1486, T1487, T1679, T2298.

The results of the NetOGlyc analysis gave positive (over the 0.5 threshold) scores for 5 sites; T1248, T1468, T1477, T1679, T2298, furthermore a 6th additional O-linked site was predicted to occur at T1859, this site was not predicted to be occupied based on the primary amino acid sequence of VWF. (Figure 4.1)

Sites T1255, T1256, S1263, S1486, T1487 are all predicted to fall below the 0.5 threshold value and as such may not be occupied by an O-linked glycan chain. (Figure 4.1)

N-linked glycosylation

Based on the basic amino acid structure, the pro-VWF monomer is predicted to contain sixteen *N*-linked glycosylation sites, four sites within the propeptide; N99, N156, N211 and N666 and twelve sites within the mature subunit; N857, N1147, N1231, N1515, N1574, N2223, N2290, N2357, N2400, N2546, N2585, N2790.

The results of the NetNGlyc analysis gave positive scores for 13 sites; N99, N156, N211, N666, N857, N1231, N1515, N1574, N2223, N2357, N2400, N2585, N2790.

Sites, N2290, N2546, N2635 were all given values lower than 0.5, indicating that these potential sites may not be utilised. (Figure 4.2)

As mentioned (Introduction, Section 1.14.1), there are exceptional cases where glycosylation can occur at the sequence N-X-C.[230] Within the primary VWF sequence there are nine potential N-X-C sites that could be glycosylated, two in the propeptide, N368 and N819, and seven in the mature subunit: N847, N1147, N2210, N2416, N2526, N2531 and N2625. To predict glycosylation at these sites, the NetNGlyc algorithm was used to predict the potential glycosylation status of all asparagine residues with in the VWF sequence.

The results of the prediction returned positive scores for; N368, N819, N847, N1147, and N2526. A borderline score of exactly 0.5 was obtained for site N2210. Therefore there is the potential for these sites to be occupied by an *N*-linked glycan chain.

Sites; N2416, N2531 and N2625 all returned below threshold scores and are highly unlikely to be glycosylated.

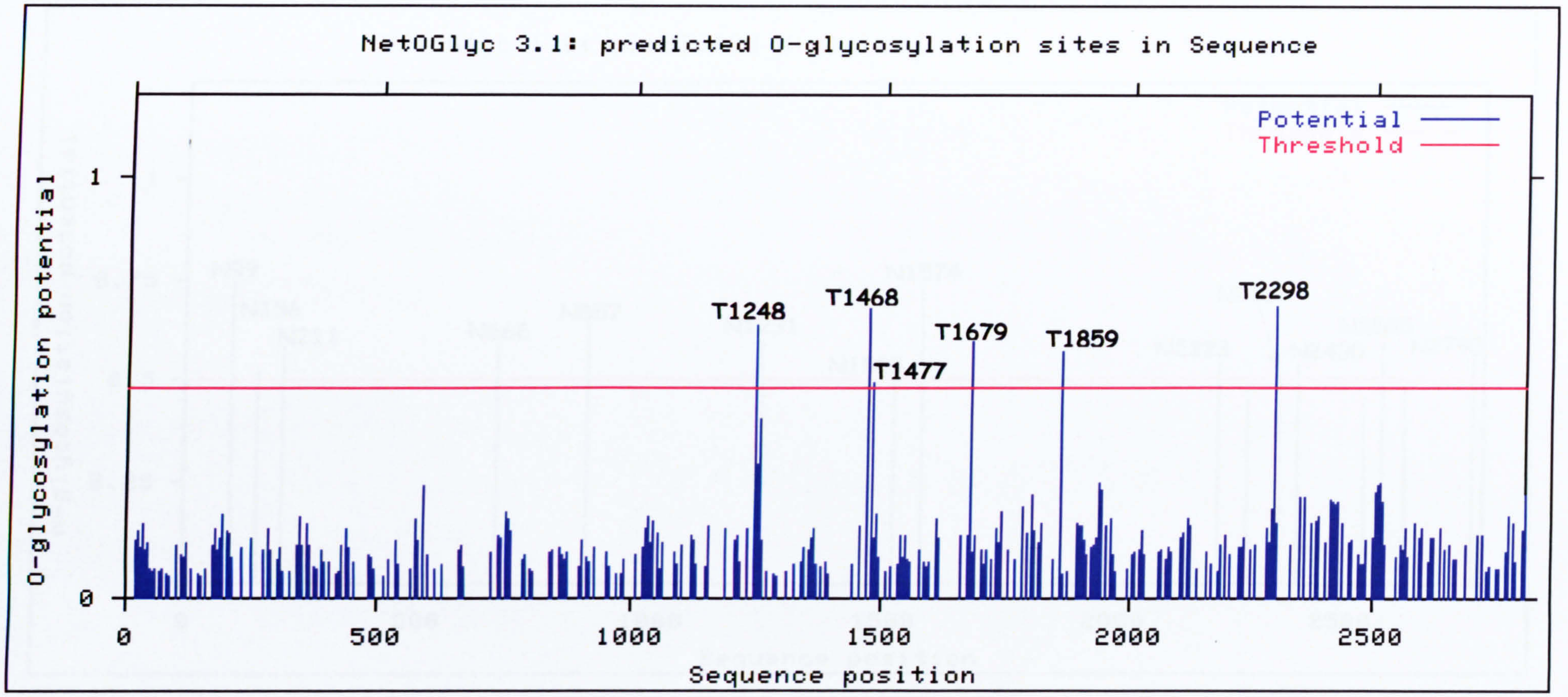


Figure 4.1. NetOGlyc prediction of O-linked glycosylation of VWF

Ten O-linked glycosylation sites are predicted to occur based on the primary amino acid structure of VWF. The NetOGlyc algorithm gives positive (above the 0.5 threshold value) scores for predicted sites T1248, T1468, T1477, T1679 and T2298 indicating that these sites are likely to be glycosylated. Furthermore, site T1859 (not originally predicted to be O-linked glycosylated) is given a positive score for potential O-linked glycosylation.

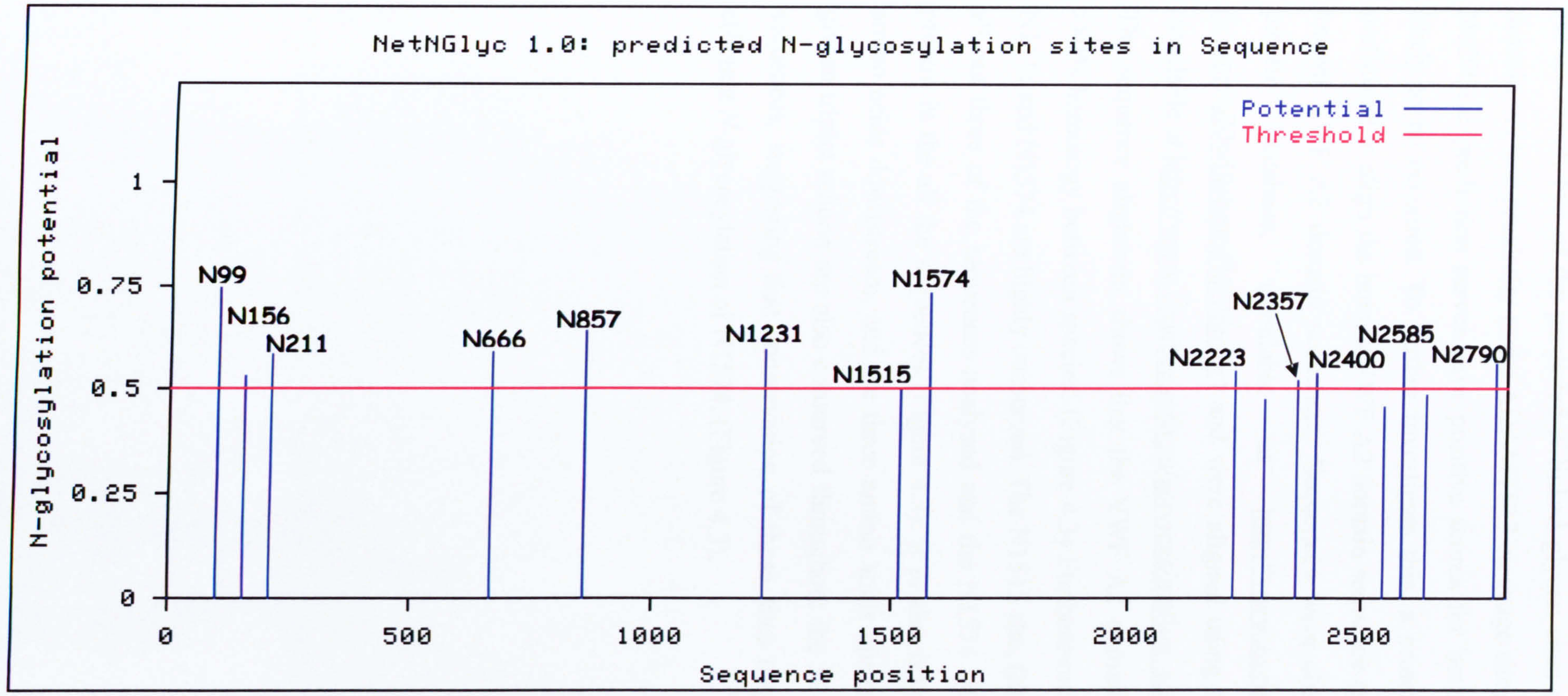


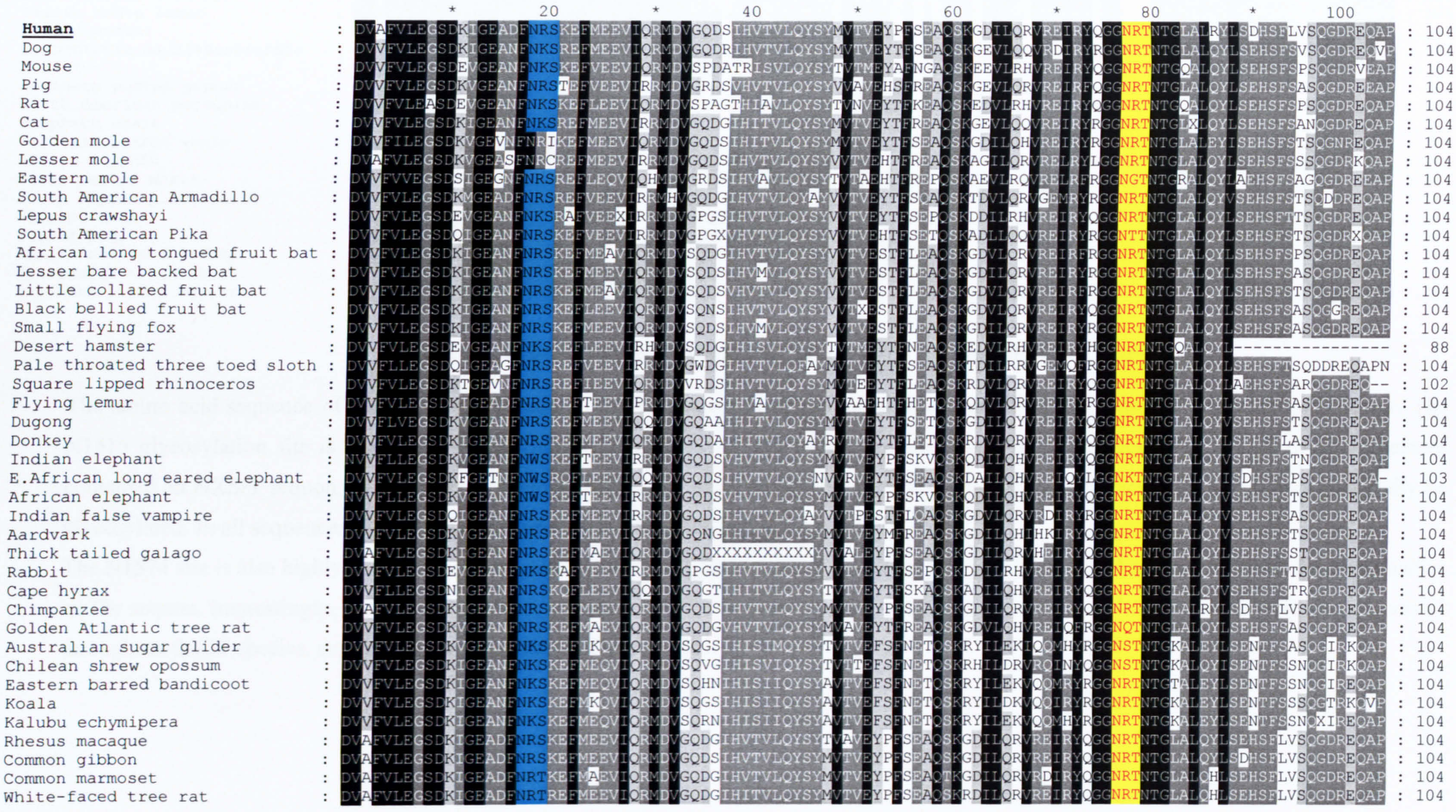
Figure 4.2. NetNGlyc prediction of *N*-linked glycosylation of VWF

Twelve *N*-linked glycosylation sites are predicted to occur based on the primary amino acid structure of VWF. The NetNGlyc algorithm gives positive (above the 0.5 threshold value) scores for predicted sites N99, N156, N211, N666, N857, N1231, N1515, N1574, N2223, N2357, N2400, N2585, N2790. Although not shown, the site N1147 in the sequence NCT, is also given a positive score and is likely to be *N*-linked glycosylated.

4.2.2 Alignment of VWF A2 Domain Sequences

As discussed, two of the predicted *N*-linked glycan sites occur with in the VWF A2 domain in close proximity to the ADAMTS13 cleavage site; N1515 and N1574 and the NetNGlyc prediction server gave positive scores for both sites. Thus both sites are likely to be occupied. To further investigate this, a protein sequence alignment was performed to align the human VWF A2 domain sequence against 58 other species with known VWF A2 domain sequences. Sequences were obtained from the Swiss-Prot protein database, (available at http://www.expasy.org/cgi-bin/sprot-search-de?von%20willebrand%20factor) and were aligned using AliBee Multiple Alignment (available at http://www.genebee.msu.su/services/malign_reduced.html)

The sequence alignment shows that the VWF A2 domain is highly conserved with >80% homology between species. (Figure 4.3) Furthermore the two glycosylation sites N1515 and N1574 are highly conserved. The N1515 site, (highlighted blue) is present in all but three of the sequences analysed and the N1574 site (highlighted yellow) was present in the all the sequences (Figure 4.3). It is also interesting to note that the two amino acids downstream, and the three amino acids upstream of the N1574 *N*-linked glycan triplet sequon are also conserved throughout the 59 analysed VWF A2 domain sequences, suggesting that conservation of these sites may be important in enabling efficient *N*-glycosylation of N1574. (Figure 4.3).


* 20 * 40 * 60 * 80 * 100
Human : DVAFVLEGSDKIGEADFNRSKEFMEEVIQRMDVGQDSIHVTVLQYSYMVTVEYPFSEAQSKGDILQRVREIRYQGGNRTNTGLALRYLSDHSFLVSQGDREQAP : 104
Dog : DVVFVLEGSDKIGEANFNKSREFMEEVIQRMDVGQDRIHVTVLQYSYMVTVEYTFSEAQSKGEVLQQVRDIRYRGGNRTNTGLALQYLSEHSFSVSQGDREQVP : 104
Mouse : DVVFVLEGSDEVGEANFNKSKEFVEEVIQRMDVSPDATRISVLQYSYTVTMEYAFNGAQSKEEVLRHVREIRYQGGNRTNTGQALQYLSEHSFSPSQGDRVEAP : 104
Pig : DVVFVLEGSDKVGEANFNRSTEFVEEVIRRMDVGRDSVHVTVLQYSYVVAVEHSFREAQSKGEVLQRVREIRFQGGNRTNTGLALQYLSEHSFSASQGDREEAP : 104
Rat : DVVFVLEASDEVGEANFNKSKEFLEEVIQRMDVSPAGTHIAVLQYSYTVNVEYTFKEAQSKEDVLRHVREIRYQGGNRTNTGQALQYLSEHSFSPSQGDREQAP : 104
Cat : DVVFVLEGSDKIGEANFNKSREFMEEVIRRMDVGQDGIHITVLQYSYMVTVEYTFREAQSKGEVLQQVREIRYRGGNRTNTGLXLQYLSEHSFSANQGDREQAP : 104
Golden mole : DVVFILEGSDKVGEVNFNRIKEFMEEVIQRMDVGQDSIHITVLQYSYMVTVEYTFSEAQSKGDILQHVREIRYRGGNRTNTGLALEYISEHSFSTSQGNREQAP : 104
Lesser mole : DVAFVLEGSDKVGEASFNRCREFMEEVIRRMDVGQDSIHVTVLQYSYVVTVEHTFREAQSKAGILQRVRELRYLGGNRTNTGLALQYLSEHSFSSSQGDRKQAP : 104
Eastern mole : DVVFVVEGSDSIGEGNFNRSREFLEQVIQHMDVGRDSIHVAVLQYSYTVTAEHTFREPQSKAEVLRQVRELRFRGGNGTNTGRALQYLAEHSFSAGQGDREEAP : 104
South American Armadillo : DVVFVLEGSDKMGEADFNRSREFVEEVIRRMHVGQDGIHVTVLQYAYVVTVEYTFSQAQSKTDVLQRVGEMRYRGGNRTNTGLALQYVSEHSFSTSQDDREQAP : 104
Lepus crawshayi : DVVFVLEGSDEVGEANFNKSRAFVEEXIRRMDVGPGSIHVTVLQYSYVVTVEYTFSEPQSKDDILRHVREIRYQGGNRTNTGLALQYLSEHSFTTSQGDREQAP : 104
South American Pika : DVVFVLEGSDQIGEANFNRSKEFVEEVIRRMDVGPGXVHVTVLQYSYVVTVEHTFSETQSKADLLQQVREIRYRGGNTTNTGLALQYLSEHSFSTSQGDRXQAP : 104
African long tongued fruit bat : DVVFVLEGSDKIGEANFNRSKEFMEAVIQRMDVSQDGIHVTVLQYSYVVTVESTFLEAQSKGDVLQRVREIRFRGGNRTNTGLALQYLSEHSFSPSQGDREQAP : 104
Lesser bare backed bat : DVVFVLEGSDKIGEANFNRSKEFMEEVIQRMDVSQDSIHVMVLQYSYVVTVESTFLEAQSKGDILQRVREIRYRGGNRTNTGLALQYLSEHSFSASQGDREQAP : 104
Little collared fruit bat : DVVFVLEGSDKIGEANFNRSKEFMEAVIQRMDVSQDSVHVTVLQYSYVVTVESTFLEAQSKGDVLQRVREIRFRGGNRTNTGLALQYLSEHSFSTSQGDREQAP : 104
Black bellied fruit bat : DVVFVLEGSDKIGEANFNRSKEFLEEVIQRMDVSQNSIHVTVLQYSYVVTXESTFLEAQSKGDVLQRVREIRYQGGNRTNTGLALQYLSEHSFSASQGGREQAP : 104
Small flying fox : DVVFVLEGSDKIGEANFNRSKEFMEEVIQRMDVSQDSIHVMVLQYSYVVTVESTFLEAQSKGDILQRVREIRYRGGNRTNTGLALQYLSEHSFSASQGDREQAP : 104
Desert hamster : DVVFVLEGSDEVGEANFNKSKEFLEEVIRHMDVSQDGIHISVLQYSYTVTMEYTFNEAQSKEDVLRHVREIRYHGGNRTNTGQALQYL---------- : 88
Pale throated three toed sloth : DVVFLLEGSDQIGEAGFNRSREFVEEVIRRMDVGWDGIHVTVLQFAYMVTVEYTFSEAQSKTDILRRVGEMQFRGGNRTNTGLALQYLSEHSFTSQDDREQAPN : 104
Square lipped rhinoceros : DVVFVLEGSDKTGEVNFNRSREFIEEVIQRMDVVRDSIHVTVLQYSYMVTEEYTFLEAQSKRDVLQRVREIRYQGGNRTNTGLALQYLAEHSFSARQGDREQ-- : 102
Flying lemur : DVVFVLEGSDKIGEADFNRSREFTEEVIPRMDVGQGSIHVAVLQYSYVVAAEHTFHETQSKQDVLQRVREIRYRGGNRTNTGLALQYLSEHSFSASQGDREQAP : 104
Dugong : DVVFLVEGSDKVGEANFNRSKEFMEEVIQQMDVGQAAIHITVLQYSYMVTVEYTFSETQSKGDILQYVREIRYQGGNRTNTGLALQYVSEHSFSTSQGDREQAP : 104
Donkey : DVVFVLEGSDKIGEANFNRSREFMEEVIQRMDVGQDAIHITVLQYAYRVTMEYTFLETQSKRDVLQRVREIRYQGGNRTNTGLALQYLSEHSFLASQGDREQAP : 104
Indian elephant : NVVFLLEGSDKVGEANFNWSKEFTEEVIRRMDVGQDSVHVTVLQYSYMVTVEYPFSKVQSKQDILQHVREIRYQGGNRTNTGLALQYVSEHSFSTNQGDREQAP : 104
E.African long eared elephant : DVVFVLEGSDKFGETNFNWSRQFLEEVIQQMDVGQDSIHVTVLQYSNVVRVEYTFSEAQSKDAILQHVREIQYLGGNKTNTGLALQYISDHSFSPSQGDREQA- : 103
African elephant : NVVFLLEGSDKVGEANFNWSKEFTEEVIRRMDVGQDSVHVTVLQYSYMVTVEYPFSKVQSKQDILQHVREIRYQGGNRTNTGLALQYVSEHSFSTSQGDREQAP : 104
Indian false vampire : DVVFVLEGSDQIGEANFNRSKEFMEEVIRRMDVGQDSIHVTVLQYAYVVTPESTFLQAQSKGDVLQRVRDIRYRGGNRTNTGLALQYVSEHSFSASQGDREQAP : 104
Aardvark : DVVFVLEGSDKVGEANFNRSREFMEEVIQRMDVGQNGIHITVLQYSYMVTVEYMFREAQSKGDILQHIHKIRYQGGNRTNTGLALQYVSEHSFSTSQGDREEAP : 104
Thick tailed galago : DVAFVLEGSDKIGEANFNRSKEFMAEVIQRMDVGQDXXXXXXXXXXYVVALEYPFSEAQSKGDILQRVHEIRYQGGNRTNTGLALQYLSEHSFSSTQGDREQAP : 104
Rabbit : DVVFVLEGSDEVGEANFNKSKAFVEEVIRRMDVGPGSIHVTVLQYSYVVTVEYTFSEPQSKDDILRHVREIRYQGGNRTNTGLALQYLSEHSFTTSQGDREQAP : 104
Cape hyrax : DVVFLLEGSDNIGEANFNRSKQFLEEVIQQMDVGQGTIHITVLQYSYTVTVEYTFSKAQSKADILQHVREIRYQGGNRTNTGLALQYVSEHSFSTRQGDREQAP : 104
Chimpanzee : DVAFVLEGSDKIGEADFNRSKEFMEEVIQRMDVGQDSIHVTVLQYSYMVTVEYPFSEAQSKGDILQRVREIRYQGGNRTNTGLALRYLSDHSFLVSQGDREQAP : 104
Golden Atlantic tree rat : DVVFVLEGSDKVGEANFNRSKEFMAEVIQRMDVGQDGVHVTVLQYSYMVAVEYTFREAQSKGDVLQHVREIQFRGGNQTNTGLALQYLSEHSFSASQGDREQAP : 104
Australian sugar glider : DVVFVLEGSDKVGEANFNKSKEFIKQVIQRMDVSQGSIHISIMQYSYTVTVEFSFNETQSKRYILEKIQQMHYRGGNSTNTGKALEYLSENTFSASQGIRKQAP : 104
Chilean shrew opossum : DVVFVLEGSDKIGEANFNKSKEFMEQVIQRMDVSQVGIHISVIQYSYTVTTEFSFNETQSKRHILDRVRQINYQGGNSTNTGKALQYISENTFSSNQGIRKQAP : 104
Eastern barred bandicoot : DVVFVLEGSDKIGEANFNKSKEFMEQVIQRMDVSQHNIHISIIQYSYAVTVEFSFNETQSKRYILEKVQQMRYRGGNRTNTGTALEYLSENTFSSNQGIREQAP : 104
Koala : DVVFVLEGSDKIGEANFNKSKEFMKQVIQRMDVSQGSIHISIIQYSYAVTVEFSFNETQSKRYILDKVQQIRYRGGNRTNTGKALEYLSENTFSSSQGTRKQVP : 104
Kalubu echymipera : DVVFVLEGSDKIGEANFNKSKEFMEQVIQRMDVSQRNIHISIIQYSYAVTVEFSFNETQSKRYILEKVQQMHYRGGNRTNTGKALEYLSENTFSSNQXIREQAP : 104
Rhesus macaque : DVAFVLEGSDKIGEADFNRSKEFMEEVIQRMDVGQDGIHVTVLQYSYTVAVEYPFSEAQSKGDILQRVREIRYQGGNRTNTGLALQYLSEHSFLVSQGDREQAP : 104
Common gibbon : DVAFVLEGSDKIGEADFNRSKEFMEEVIQRMDVGQDSIHVTVLQYSYMVTVEYPFSEAQSKGDILQRVREIRYQGGNRTNTGLALQYLSDHSFLVSQGDREQAP : 104
Common marmoset : DVAFVLEGSDKIGEADFNRTKEFMAEVIQRMDVGQDGIHVTVLQYSYMVTVEYPFSEAQTKGDILQRVRDIRYQGGNRTNTGLALQHLSEHSFLVSQGDREQAP : 104
White-faced tree rat : DVAFVLEGSDKIGEADFNRTREFMEEVIQRMDVGQDGIHITVLQYSYMVTVEYPFSEAQSKRDILQRVREIRYQGGNRTNTGLALQHLSEHSFLVSQGDREQAP : 104

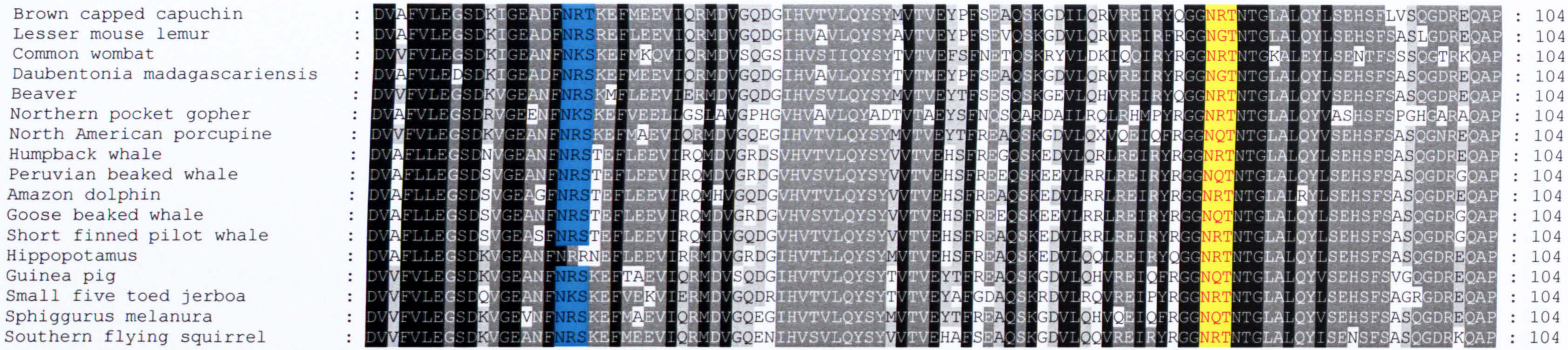


Figure 4.3. Protein sequence alignment of the VWF A2 domain from 59 species

The amino acid sequence of the VWF A2 domain from 59 different species was aligned using a protein sequence alignment programme. The N1515 glycosylation site is highly conserved (highlighted blue). All the sequences contained Asn at position 1515 and 56 of the sequences contained an NXS/T sequon, of the three sequences without the appropriate sequon, one contained the sequence NRC which may potentially be glycosylated. In all sequences the N1515 site is preceded by a phenylalanine residue.

The N1574 site is also highly conserved (highlighted yellow). All 59 sequences contained Asn at position 1574 and all contained the Asn/Xaa/Ser or Thr sequon. Interestingly, the two amino acids upstream and the three amino acids downstream of the 1574-1576 sequon were also conserved throughout the 59 species, suggesting the importance of this region.

4.3 EXPERIMENTAL ANALYSIS OF VWF GLYCAN STRUCTURE

4.3.1 Purification of VWF from Haemate P – Gel Filtration

In order to analyse the glycan content of VWF in more detail, a large quantity of highly pure VWF was required. To obtain this, VWF was purified from a commercial VWF-FVIII concentrate; Haemate P. This concentrate is reported to contain the highest content of HMW VWF multimers and has been shown to have a multimer pattern resembling normal human plasma.[357,358]

Lyophilised Haemate P was resuspended in 10mls of ddH_2O, then gel filtered through a Sephacryl 400 gel filtration column. The column was eluted at a flow rate of 1ml/min and 5ml fraction were collected. Protein began to elute from the column typically at fraction B6. (Figure 4.4) Early eluted fractions and selected later fractions were analysed by SDS-PAGE under reducing conditions in 4-12% gels and protein bands were visualised by Coomassie staining. Fractions B6-D12 demonstrated a major 250kDa band, consistent with monomeric VWF.(Figure 4.4) To remove contaminating proteins and to concentrate the VWF samples, fractions B6-D12 were pooled and further purified using Heparin-Sepharose affinity chromatography.

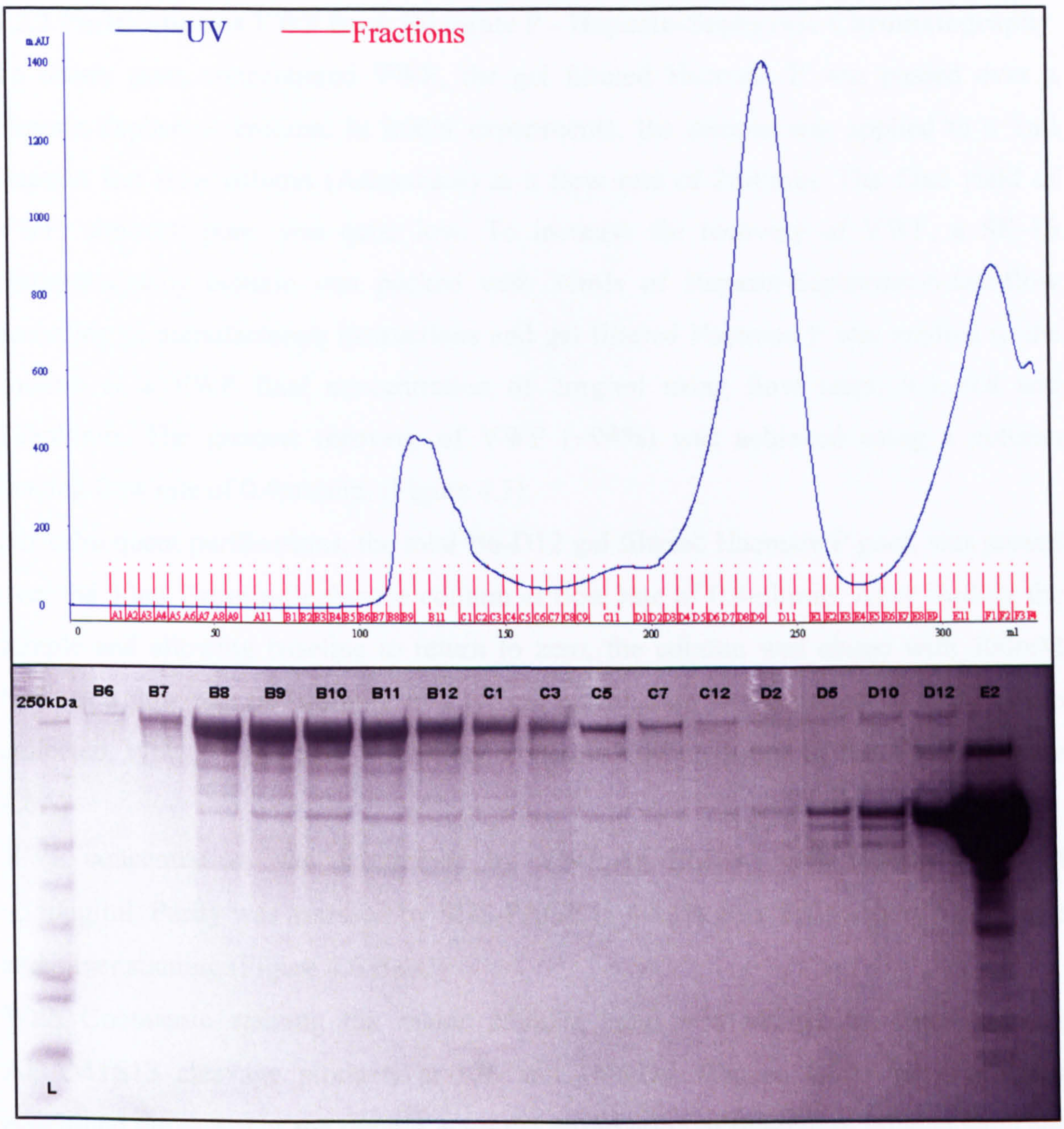


Figure 4.4 Gel filtration of Haemate P

Haemate P was gel filtered through a Sephacryl 400 gel filtration column and 5ml fractions were collected. Protein began to elute from the column typically at fraction B6 (Top frame). Early eluted fractions and selected later fractions were analysed using reducing SDS-PAGE in 4-12% gels followed by Coomassie staining (Bottom frame). Fractions B6-D12, demonstrating a major 250kDa band consistent with monomeric VWF, were pooled and VWF was further purified by Heparin-Sepharose chromatography.

4.3.2 Purification of VWF from Haemate P - Heparin-Sepharose Chromatography

To obtain pure, concentrated VWF, the gel filtered Haemate P was passed over a Heparin-Sepharose column. In initial experiments, the sample was applied to a 1ml Heparin fast flow column (Amersham) at a flow rate of 2ml/min. The final yield of VWF, although pure, was quite low. To increase the recovery of VWF, a SK-16 chromatography column was packed with 30mls of Heparin-Sepharose-6-fast-flow according to manufacturers instructions and gel filtered Haemate P was applied to the column at a VWF final concentration of 2mg/ml using flow rates; 0.4, 0.8 and 1.6ml/min. The greatest recovery of VWF (~94%) was achieved using a column loading flow rate of 0.4ml/min. (Figure 4.5)

For subsequent purifications, the total B6-D12 gel filtered Haemate P pool, was passed over the 30ml Heparin-Sepharose column at flow rate of 0.4ml/min. After loading the sample and allowing baseline to return to zero, the column was eluted with 300mM NaCl at a flow rate of 1ml/min. In a typical purification five fractions of ~10ml were collected, typically the first 3 fractions contained the majority of the VWF. (Figure 4.6A)

VWF concentration was determined by VWF:Ag ELISA; with typical yields of ~350μg/ml. Purity was assessed by SDS-PAGE in 4-12% gels, followed by Coomassie and silver staining (Figure 4.6 B&C)

With Coomassie staining the major 250kDa band was visible, as were the two ADAMTS13 cleavage products at 176 and 140kDa. (Figure 4.6B) Silver staining confirmed the purity of the sample, with the observation of the major 250kDa band and the smaller ADAMTS13 cleavage product bands. A band of ~100kDa was also seen on the silver stain, this may represent the VWF propeptide. (Figure 4.6C) Interestingly, it was also possible to clearly see that the major 250kDa band is a doublet. (Figure 4.6C) The reason for this is unknown, however the two bands may represent VWF with differing glycosylation patterns. Normally when the doublet band is observed, the band of the highest molecular weight represents the major species. The multimeric composition of the samples was analysed by VWF multimer analysis. (Figure 4.6D) The flow through fractions contained a small quantity of low molecular weight multimers, and the eluted fractions were comprised of mainly high to medium molecular weight multimers.

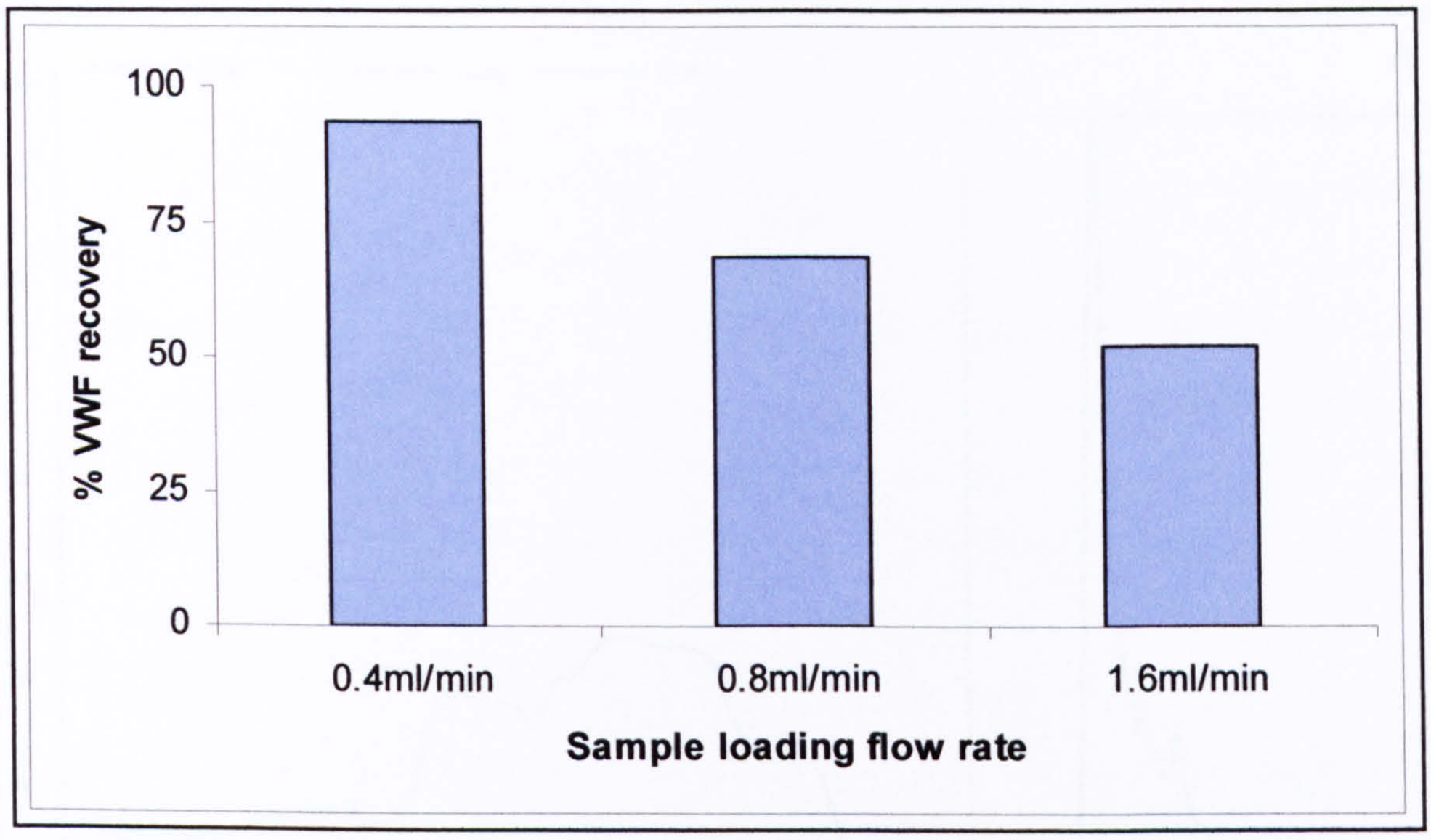


Figure 4.5 Effect of sample loading flow rate on VWF recovery from a Heparin-Sepharose column

A total of 2mg/ml of VWF was loaded on to a 30ml Heparin-Sepharose column at flow rates 0.4, 0.8 & 1.6ml/min and eluted at 1ml/min. The greatest recovery of VWF was obtained using the slowest flow rate of 0.4ml/mins.

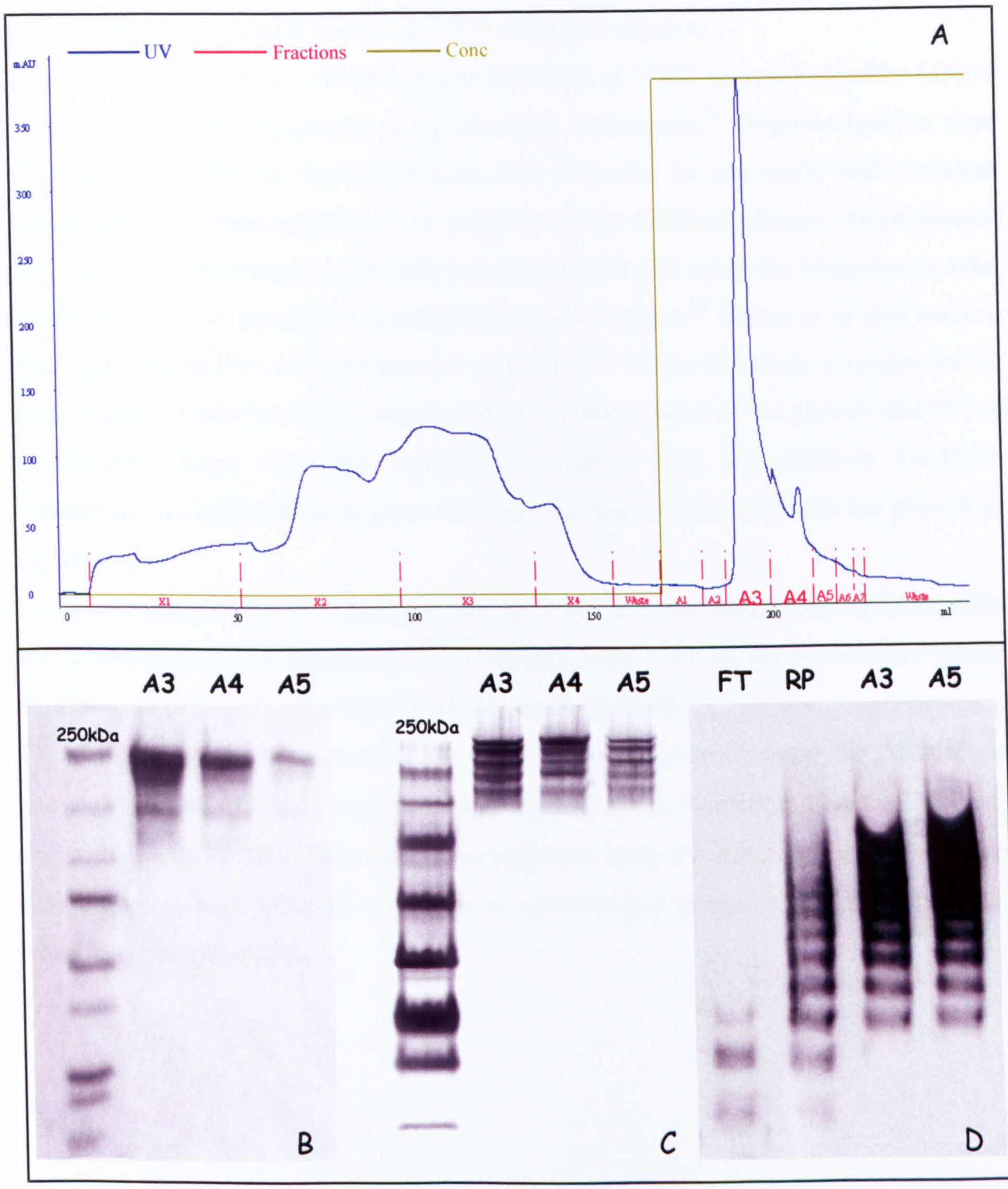


Figure 4.6 Heparin-Sepharose purification of gel filtered Haemate P

Pooled fractions B6-D12 of gel filtered Haemate P were passed over a 30ml Heparin-Sepharose column and the column eluted with 300mM NaCl. Three fractions, A3-A5 were analysed for purity by reducing SDS-PAGE followed by Coomassie staining (gel B) and silver staining (gel C). In both cases only the major 250kDa band and the 176kDa and 140kDa ADAMTS13 cleavage products are present, indicating the fractions are of high purity. A fifth band is also seen on the silver stain at ~100kDa and most likely represents the VWF propeptide. The multimeric pattern was determined using VWF multimer analysis (gel D). The flow through fractions contained a small number of low molecular weight multimers, whilst fractions A3-A5 contained the highest to medium molecular weight VWF multimers.

4.3.3 Preliminary Glycan Profile of VWF *N*-linked Glycans

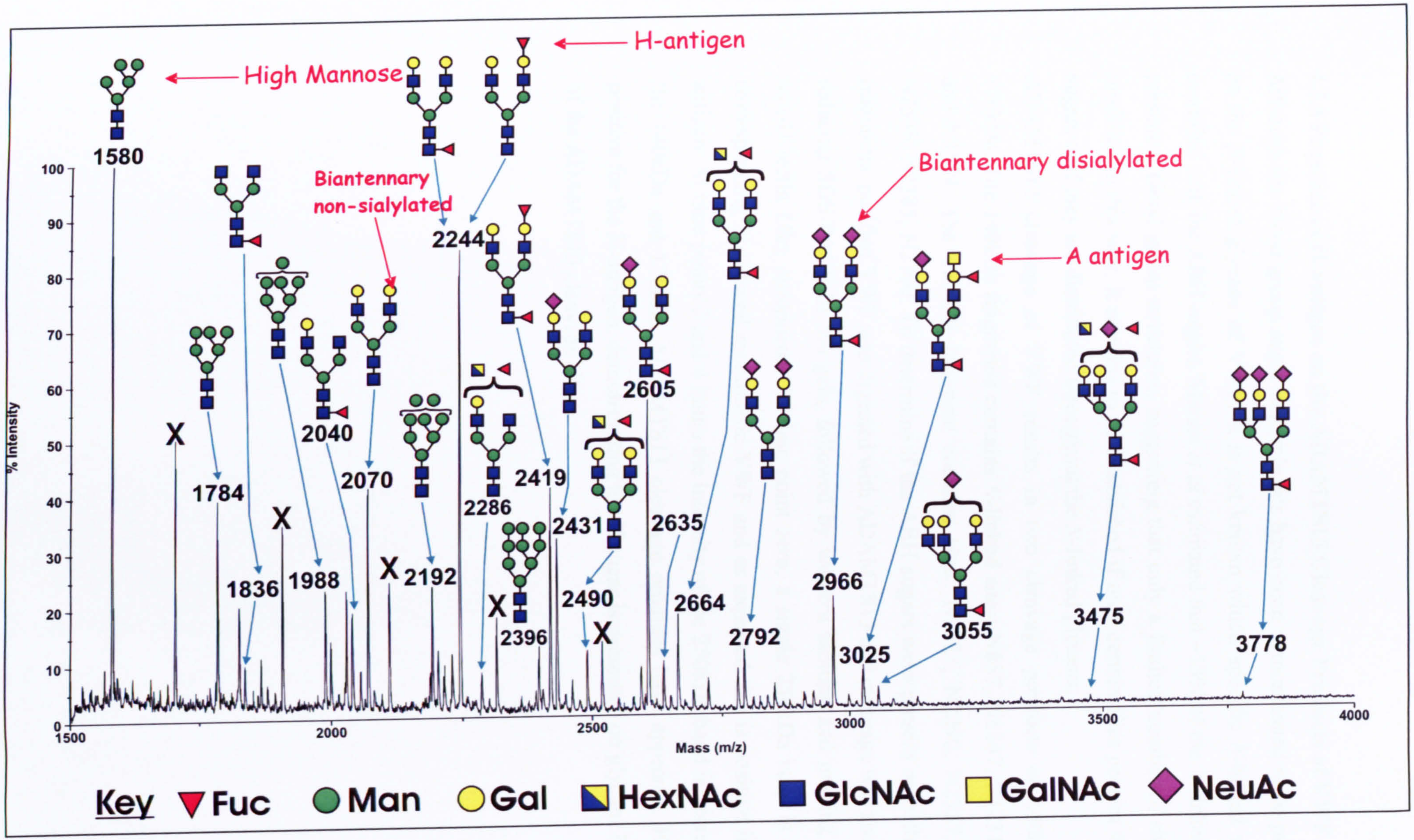
A detailed analysis of the *N*-linked glycan structures of VWF was performed by Matsui *et al* on de-sialyated fragments using chemical techniques.[23] Oligosaccharides were liberated from VWF by hydrazionolysis and subjected to enzymatic and chemical separation and microsequencing. The majority of the *N*-linked glycans, as previously described, were the complex type with the majority (78.2%) being the bi-antennary type and of these, ~13% terminated in ABO blood group sugars.[23] Matsui *et al* also noted a small minority (0.8%) of high mannose structures.[23] Whilst this study provides useful data, it does not give any information on the sialylation status of the glycans and 6% of the isolated chains were too complex to analyse with the methods available. Furthermore no information is given on what specific glycan structures are present at specific sites.

To further analyse the *N*-linked glycans of VWF a preliminary mass spectrometric profile was obtained of *N*-linked glycans released from VWF by digestion with PNGase F. (This data was kindly provided by Dr James O'Donnell)

The preliminary results confirmed that VWF *N*-linked glycans present the ABO blood group sugars and indicated that approximately half of the biantennary glycans are non-sialyated and up to 40% of the biantennary glycans carry the ABO antigens. In addition the number of high mannose structures is considerably greater than that reported by Matsui *et al* (Figure 4.7).

Next page – **Figure 4.7 Preliminary glycan profile of VWF *N*-linked glycans**

A preliminary analysis of VWF *N*-linked glycans was obtained by release of *N*-linked glycans by PNGase F digestion and purification followed by mass spectrometric profiling. Selected glycan structures are labelled – High mannose, H and A antigens, biantennary disialylated and biantennary non-sialylated.


H-antigen
High Mannose
Biantennary disialylated
Biantennary non-sialylated
A antigen
1580
2244
2605
2040
2070
2419
1784
2286
2431
2635
1836
1988
2192
2490
2664
2966
2396
2792
3025
3055
3475
3778
X
% Intensity
Mass (m/z)
Key
Fuc
Man
Gal
HexNAc
GlcNAc
GalNAc
NeuAc

4.3.4 Presence of H-antigen on the ADAMTS13 Cleavage Products of VWF

Although the blood group sugar determinants have been demonstrated to be presented on the *N*-linked glycans of VWF, it is not known which specific *N*-linked sites are modified with the ABH sugars. Matsui *et al* estimated that ~13% of the *N*-linked chains presented blood group structures, suggesting that only a limited number of sites were modified in this way. It remains to be established if only certain sites present the ABO sugars or if they are distributed throughout the *N*-linked glycans.

ADAMTS13 cleavage of VWF results in two cleavage products of 140kDa and 176kDa. The 140kDa fragments contains *N*-linked sites: N857, N1147, N1231, N1515 and N1574. The 176kDa fragment contains sites: N2223, N2290, N2357, N2400, N2546, N2585, N2790. To determine if the ABH sugars were present on both of these fragments, purified VWF was digested with ADAMTS13 and cleavage was analysed by reducing SDS-PAGE in 5% gels, followed by western blotting and probing with the anti-H lectin *Ulex europaeus*. At time point zero, a single 250kDa band is observed corresponding to reduced monomeric VWF and as expected this is positive for the H-antigen. At time points 2 and 4 hours the intensity of the 250kDa band is decreased and the 140kDa and 176kDa ADAMTS13 cleavage products have appeared. Both stain positive for the H-antigen, demonstrating the H sugar is presented on glycans both sides of the ADAMTS13 cleavage site.

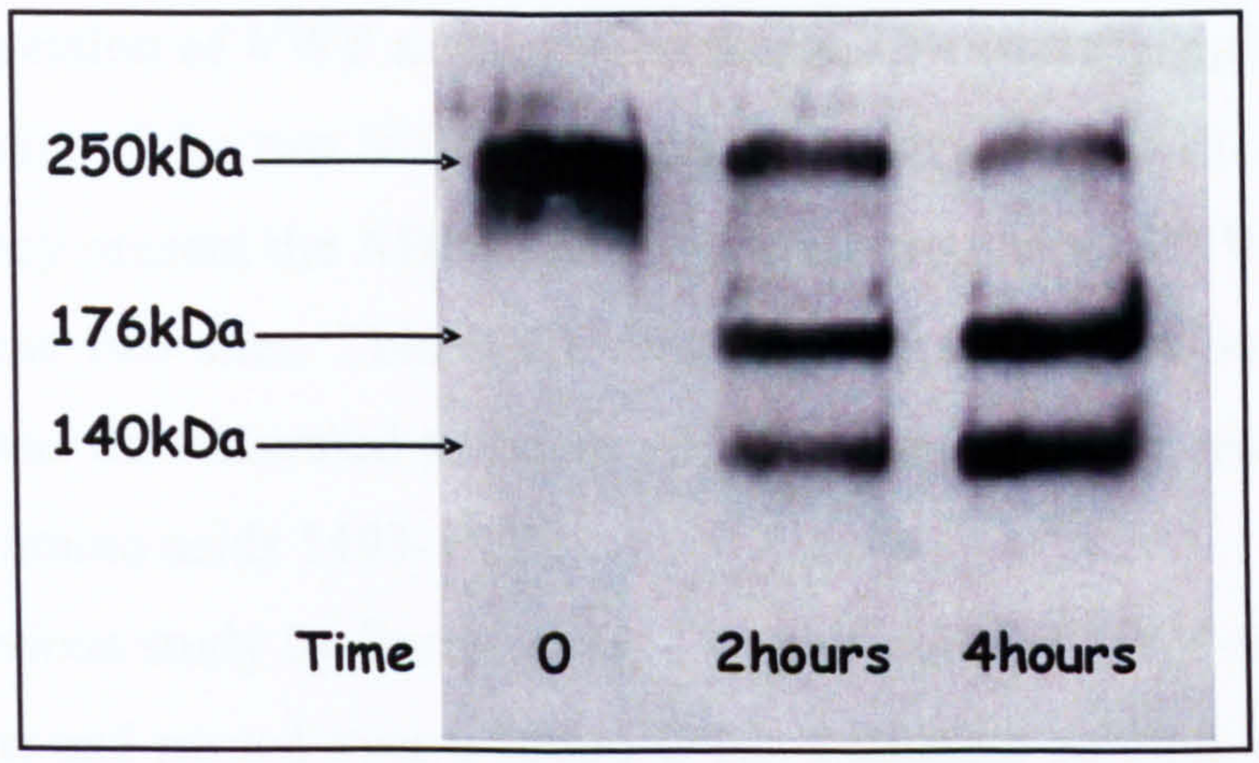


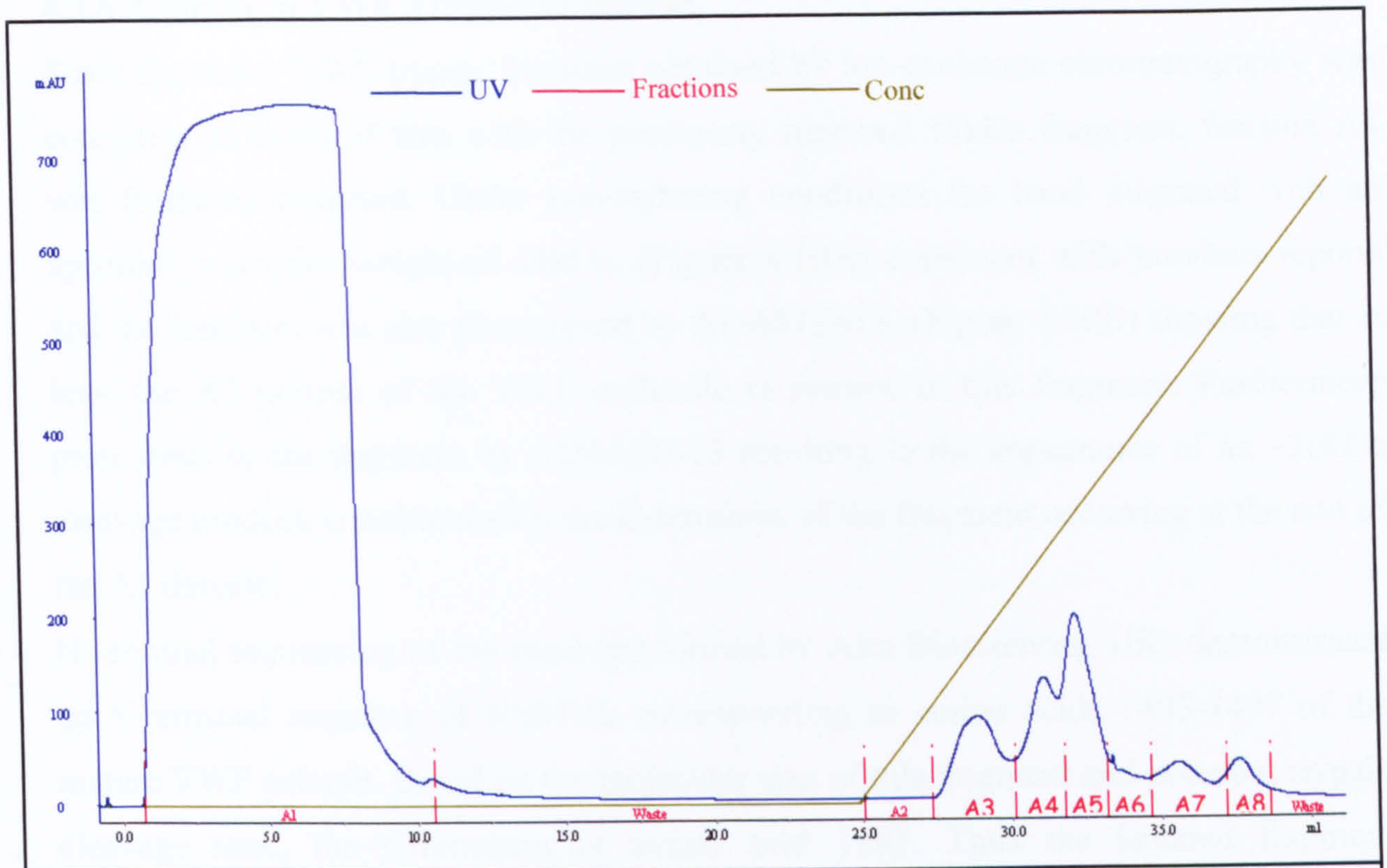
Figure 4.8 H-antigen on ADAMTS13 cleavage products

VWF was digested with ADAMTS13 and cleavage analysed by SDS-PAGE in 5% gels followed by western blotting and probing with the H-antigen specific lectin, *Ulex europaeus*. At time zero only the 250kDa band is present, after incubation with ADAMTS13 for 2 and 4 hours the 176kDa and 140kDa cleavage products appear, whilst the 250kDa reduces in intensity. Both the cleavage products stain positive for the presence of the H-antigen.

4.3.5 Trypsin Digestion of VWF and Ion-Exchange Chromatography

In order to determine if the two *N*-linked glycan sites located at N1515 and N1574 are occupied and if they present the ABH sugars, a tryptic fragment of VWF was generated encompassing these two sites. This VWF fragment has been previously described by Pareti *et al* and was demonstrated to be an ~55kDa species under reducing conditions corresponding to amino acids 1493-1887.

Based on the previous study by Pareti *et al*; ~5mg of purified VWF was digested with trypsin for 30mins and passed over a Mono Q ion-exchange column. This method was used in the Pareti *at al* study to specifically isolate the 55kDa band. The column was eluted with a 0-500mM NaCl gradient and fractions A3-A8 were collected corresponding to generated peaks. Collected fractions were analysed using SDS-PAGE in 10% gels under reducing conditions and Coomassie staining, with protein bands detected in fractions A3, A4 and A5. Fraction A4 contained a major band of ~55kDa, with two smaller and much fainter bands. The 55kDa species was also present in fraction A5, but at much less intensity. No protein bands were detected in fractions A6, A7 or A8. This may have been due to insufficient protein in the fractions for detection by Coomassie staining.



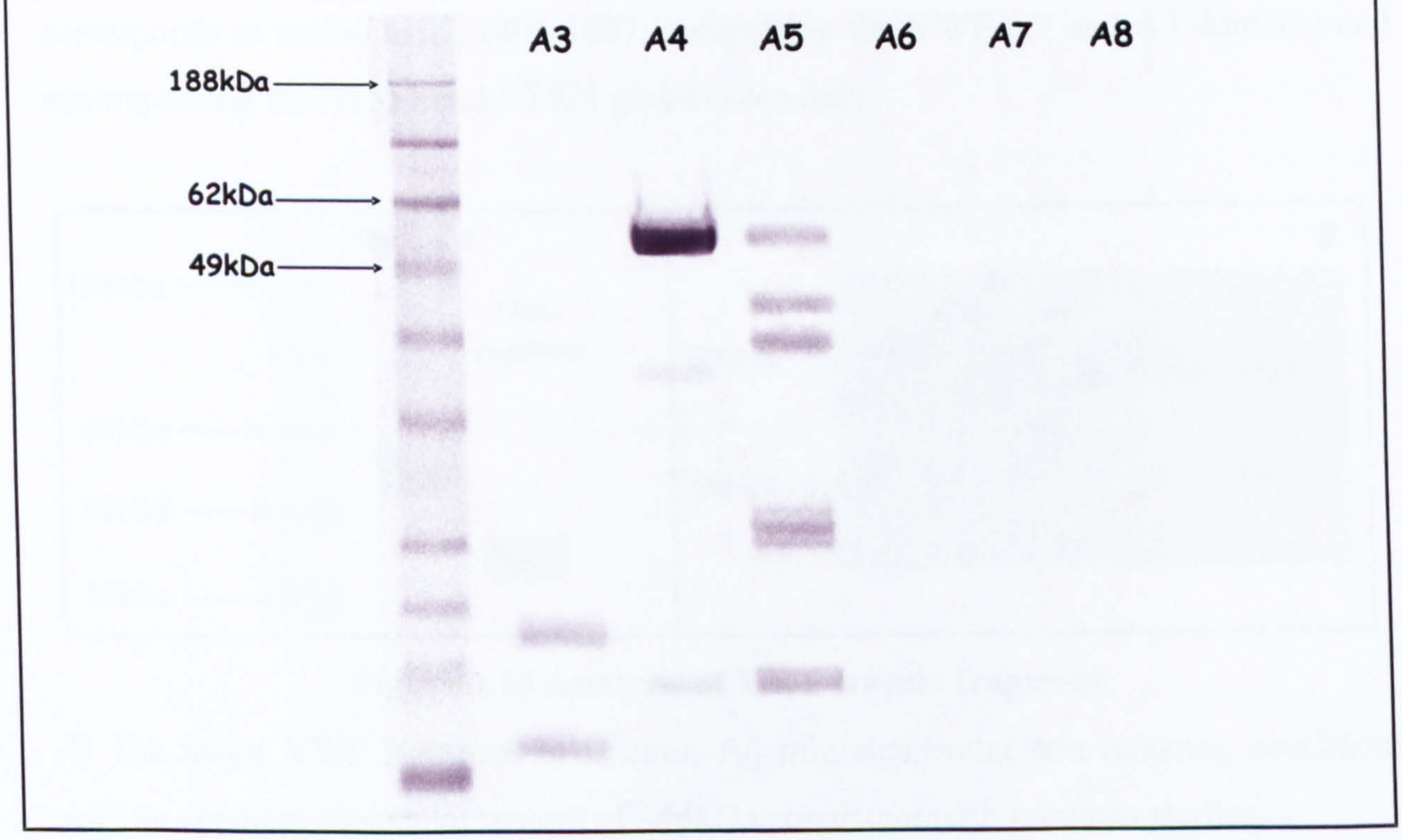


Figure 4.9 Ion-exchange chromatography of trypsin digested VWF

Trypsin digested VWF (5mg/ml) was passed over a Mono Q ion exchange column and the column eluted with a 0-500mM NaCl gradient (Top frame). Six fractions, A3-A8 were obtained and were analysed by reducing SDS-PAGE followed by Coomassie staining (Bottom frame). Fractions A3-A5 contained protein bands with the major species being an ~55kDa band present in fraction A4 and to a lesser extent in fraction A5.

4.3.6 Analysis of VWF Tryptic Fragment

Since the major VWF tryptic fragment obtained by ion-exchange chromatography was consistent in terms of size with the previously reported 55kDa fragment, fraction A4 was furthered analysed. Under non-reducing conditions the band migrated with an apparent molecular weight of 44kDa, (Figure 4.10A) consistent with previous reports and the fragment was also proteolysed by ADAMTS13, (Figure 4.10B) showing that at least the A2 portion of the VWF molecule is present in this fragment. Furthermore proteolysis of the fragment by ADAMTS13 resulting in the appearance of an ~30kDa cleavage product, consistent with the C-terminus of the fragment occurring at the end of the A3 domain.

N-terminal sequencing of the band (performed by Alta Biosciences, UK) demonstrated an N-terminal sequence of NSMVL corresponding to amino acids 1493-1497 of the mature VWF subunit. Based on the molecular size of this fragment and potential trypsin cleavage sites, the C-terminus is amino acid 1887. Thus the isolated fragment corresponds to amino acids 1493-1887, comprising the VWF A2 and A3 domains and encompassing the N1515 and N1574 glycan sites only.

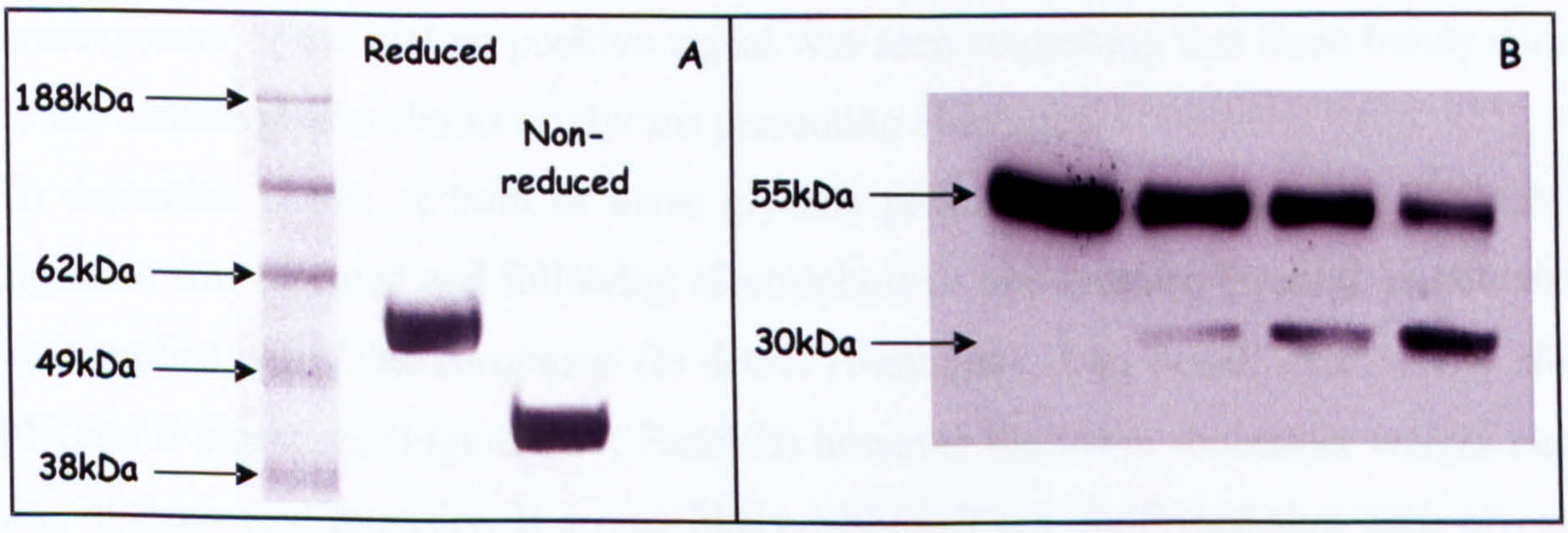


Figure 4.10 Analysis of VWF tryptic fragment

A) The major VWF fragment in fraction A4 migrates under non-reducing conditions with an apparent molecular weight of ~44kDa consistent with previous studies.

B) The fragment is also cleaved by ADAMTS13 demonstrating that at least part of the A2 domain is contained with in the fragment. With increasing time the intensity of the 55kDa band is reduced and the 30kDa cleavage product appears.

N-terminal sequencing of the 55kDa band and analysis of its molecular weight and potential trypsin cleavage sites, confirmed that it was the previously reported VWF fragment spanning amino acids 1493-1887.

4.3.7 Analysis of Glycosylation and Presence of H-antigen on VWF 55kDa Tryptic Fragment

In order to determine if the 55kDa fragment was glycosylated, the fraction was digested with PNGase F overnight at 37°C, followed by western blotting and probing with anti-VWF-HRP. Three separate bands were observed, (Figure 4.11, Panel C) demonstrating that both the N1515 and N1574 sites must be glycosylated: Band 1 corresponding to the presence of both glycans, band 2 the presence of only one of the glycans and band 3 removal of both glycans.

The fragment was also analysed for the presence of the H-antigen. Following gel electrophoresis and western blotting, lanes were probed with either anti-VWF-HRP or *Ulex europaeus.* When probed with the anti-VWF the major species is the 55kDa band, but the smaller, less intense bands observed with Coomassie staining are also present, as is a doublet band of ~17kDa not present on the Coomassie stain. (Figure 4.11, lane A) When probed with *Ulex europaeus* only the 55kDa band stains positive for the H-antigen; (Figure 4.11, lane B) demonstrating that either one or both of the *N*-linked present the blood group sugars. The lack of positive signal from the other bands may be due insufficient material in the sample to produce a positive, however even on overexposure of the blot no positive signal was seen suggesting that these bands either do not contain glycan chains or glycans presenting H-antigen.

To determine if one or both of these glycans present the H-antigen; the PNGase F digestion was repeated and following electrophoresis and western blotting, membranes were probed with *Ulex europaeus* (to detect H-antigen). Two bands were visible after PNGase F digestion, (Figure 4.11, Panel D) however the lower molecular weight band was of decreased intensity. It seems likely, although not confirmed that both glycans present the H-antigen and are thus also able to present A and B blood group antigens. The PNGase F digest was also probed with EBL to detect terminal sialic acid residues. The same pattern of two bands, with Band 2 being less intense than Band 1 was observed, indicating that both glycans also present terminal sialic acid. Furthermore, the observation that these two glycans present sialic acid and H-antigen demonstrates that these glycans are likely to be of the complex type.

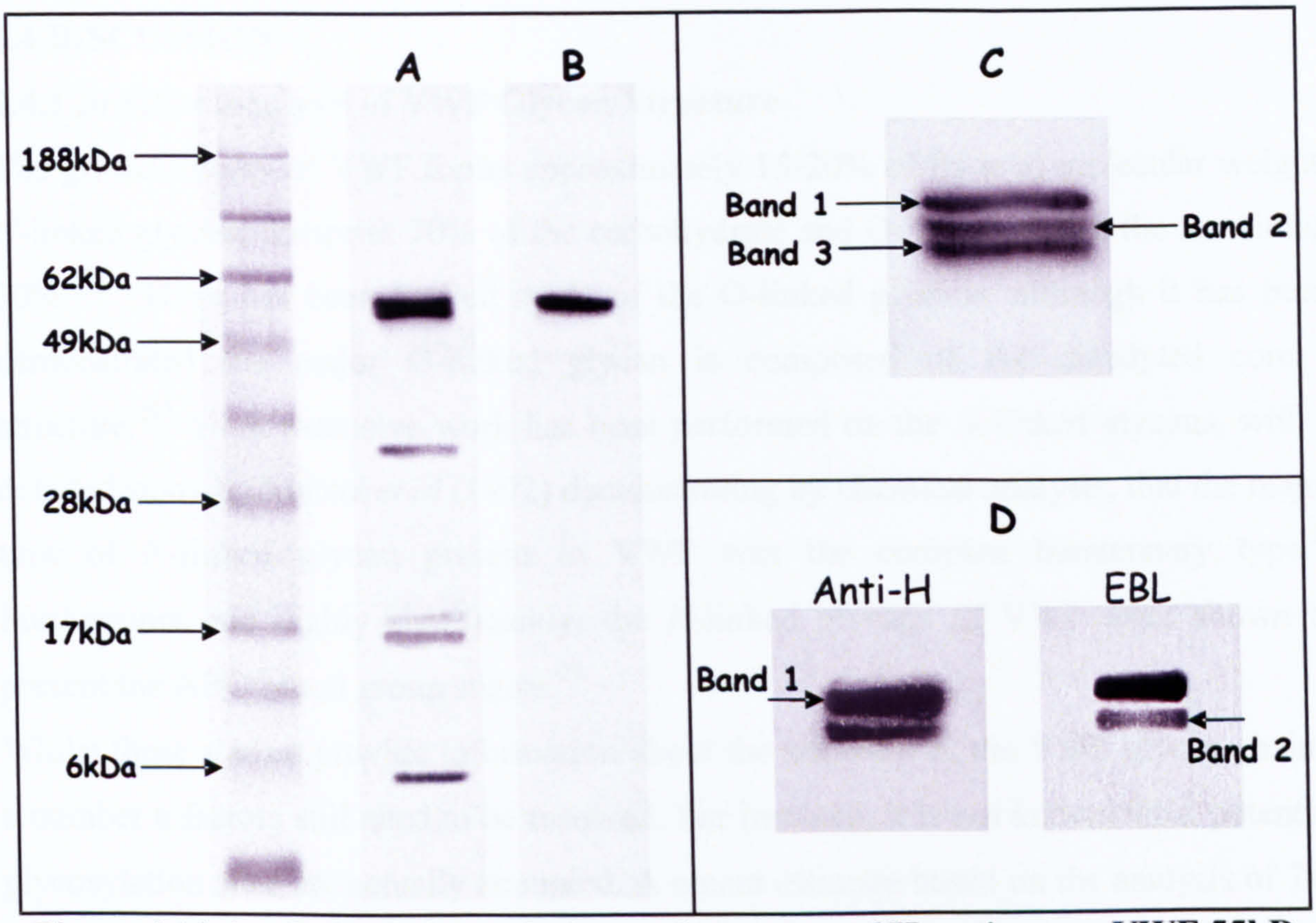


Figure 4.11 Analysis of glycosylation and presence of H-antigen on VWF 55kDa tryptic fragment

Following reducing SDS-PAGE and western blotting, the VWF 55kDa fragment was probed with anti-VWF-HRP (lane A) and Ulex europaeus (lane B). Probing with anti-VWF shows the presence of the 55kDa band and of the smaller, less intense species observed with Coomassie staining (see figure 4.7). An ~17kDa doublet band, not seen on the Coomassie stain, is also present. The 55kDa fragment stains positive with the anti-H lectin, demonstrating that one or both of the glycans on the fragment present the H-antigen. Upon digestion with PNGase F, three discrete bands can be seen (panel C), demonstrating that both the N1515 and N1574 sites are utilised. Band 1 representing both glycans intact; Band 2 – only one of the glycans removed and Band 3 – both glycans removed. The PNGase F digested fragment was also probed with the anti H lectin (panel D). Band 1 represents both glycans intact. Band 2 represents one glycan chain removed and stains positive for the H-antigen but to a lesser extent than Band 1, suggesting that both sites present the H-antigen. Probing with EBL to detect terminal sialic acid also showed the same pattern of two bands, with Band 2 being of less intensity, demonstrating that both glycans may also present terminal sialic acid.

4.4 DISCUSSION

4.4.1 *In Silico* Analysis of VWF Glycan Structure

The glycan moiety of VWF forms approximately 15-20% of its total molecular weight. *N*-linked glycans comprise 70% of the carbohydrate and O-linked chains the remaining 30%.[254] There has been limited study of the O-linked glycans, although it has been demonstrated the major O-linked glycan is composed of the disialyted core I structure.[257] More extensive work has been performed on the *N*-linked glycans, with a detailed study by Matsui *et al* (1992) demonstrating by chemical analysis, that the major type of *N*-linked glycan present in VWF was the complex biantennary type.[23] Furthermore and highly significantly, the *N*-linked glycans of VWF were shown to present the ABO blood group sugars.[23]

Whilst these studies provide information about the structure of the VWF glycan chains, a number a factors still need to be resolved. For instance, it is not known what potential glycosylation sites are actually occupied. A recent estimate based on the analysis of 749 well-characterized glycoproteins suggested that ~34% of potential *N*-linked glycosylation sites are not occupied.[359] Furthermore, whilst the *N*-linked glycans of VWF have been shown to present the ABO sugars, it is not known what specific sites are decorated with them. This is particularly pertinent with regard to the observation that ABO blood group alters susceptibility of VWF to cleavage by ADAMTS13.

To therefore further investigate this, I have analysed the glycan structure of VWF and paid particular attention to the potential *N*-linked glycan sites in close proximity to the ADAMTS13 cleavage site.

The initial observation that VWF contained 12 *N*-linked sites and 10 O-linked sites was made by Titani *et al*.[16] This was based on the primary amino acid structure of VWF, known rules regarding O-linked glycosylation and experimental evidence obtained whilst determining the amino acid sequence of VWF. However no direct study has been performed to map the glycan sites and determine if they are occupied.

I analysed the probability of the potential *N* and O-linked sites being glycosylated by using the NetNGlyc and NetOGlyc algorithms to predict glycosylation status based on the primary amino acid sequence of VWF.[360]

From the results of the O-linked prediction, five of the original predicted O-linked sites; T1248, T1468, T1477, T1679, T2298 were given positive scores, and are therefore likely to be occupied and one site *not* found in Titani's study, T1859, was also predicted to be occupied by an O-linked glycan.

Based on the original prediction it was interesting that 8 of the O-linked sites were clustered around the A1 domain at sites; T1248, T1255, T1256, S1263 and T1468, T1477, S1486, S1487. However, based on the NetOGlyc prediction only three of these sites are occupied. Experimental evidence suggests that the predicted cluster of O-linked glycans around the VWF A1 domain are important for the VWF-GPIb interaction,[280] and therefore further study is needed to confirm the occupancy of these sites, but the work presented in this thesis will focus on the *N*-linked glycans of VWF.

From the results of the NetNGlyc prediction, it was predicted that VWF contains thirteen *N*-linked sites in the NXT/S sequon, with four of these occurring in the propeptide. The two A2 domain glycans, N1515 and N1574 both scored positive and in particular N1574 scored 0.75, indicating it is highly probable that this site is occupied. Three of the originally predicted sites, N2290, N2546 and N2635 all fell below the threshold value and are therefore less likely to be occupied. These sites all occur in the C-terminal region of the molecule where the likelihood of *N*-linked glycosylation is decreased.[230]

Titani *et al* also predicted a probable glycosylation site at N1147, in the sequence N-S-C. There are also nine other potentials sites in VWF with a N-X-C sequence. Prediction of glycan occupancy on these sites returned positive scores for sites N368, N819, N847, N1147, and N2526 and a borderline score of exactly 0.5, for site N2210. Significantly, N1147 received a high score, 0.75, indicating it is highly probable that this site is occupied. Occupancy of the other sites remains to be investigated. The presence of *N*-linked glycans at the N-X-C sequon has been noted in other proteins, including human and bovine protein C.[361] Addition of a glycan chain at this sequon is rare however due to the inefficiency of the oligosaccharyltransferase to transfer the precursor glycan chain to the protein.[362] It is also interesting to note the prediction of four *N*-linked sites within the propeptide. Plasma levels of VWFpp were determined not to be significantly different between blood groups,[321] this may be highly significant in that the propeptide has been shown not to present the ABO blood group sugars.[363]

Although the NetOGlyc and NetNGlyc provide information about the potential glycosylation status of a molecule, they are only predictions and results need to be interpreted with a degree of caution and confirmation of glycosylation needs to be determined experimentally.

As previously described two potential *N*-linked sites flank the ADAMTS13 cleavage site within the A2 domain with both these sites; N1515 and N1574 predicted to be

occupied. To further analyse this, I aligned the human VWF A2 domain sequence was against known VWF A2 domain sequences from 58 other species. The protein alignment shown in Figure 4.3 demonstrates that the sequence of the A2 domain is highly conserved with >80% homology between species. Significantly, the N1515 and N1574 sites are also highly conserved suggesting they play an important role within the molecule. The N1515 site is present in all but three of the sequences; with the sequon, NXS where X is either R or K. In the three sequences that do not contain this sequence, one contains the sequon NRC that still may potentially be glycosylated. The N1574 site is conserved throughout all the 59 sequences, with the sequon being either NRT, NQT, or NGT. It was also observed that the two downstream amino acids and three upstream amino acids around N1574 were also conserved throughout, with the region GGNXTNTG being the most highly conserved portion of the aligned A2 domains. As previously discussed, the initial step in the addition of a glycan chain to a growing peptide chain occurs on the luminal side of the ER with transfer of the $Glc_3Man_9GlcNAc_2$ structure to the nascent polypeptide chain by the enzyme oligosaccharyltransferase (OST). Successful transfer of the glycan structure is thought to be dependent on the amino acids in close proximity to the asparagine residue.[364,365] It is therefore feasible that the amino acids surrounding N1574 are important in facilitating successful glycosylation of the site. The highly conserved nature of the sites also suggests that both sites are important and are required for proper VWF structure/function.

Although VWF is only found in vertebrates, the VWF A domains (VWA) are present in proteins from Eukaryota (Metazoa, fungi, plants, and protists), Eubacteria, and Archaea.[366] In the most ancient organisms VWA domains are present in intracellular proteins involved in functions such as transcription, DNA repair, ribosomal and membrane transport.[366] Within higher organisms, VWA domains are principally found in cell adhesion and matrix proteins; such as VWF, collagens, matrilins, integrins and complement proteins.[367] Based on the resolved crystal structure of homologous proteins, a molecular model of the A2 domain has been determined (Figure 4.12).[161] From this model it is apparent that the N1515 and N1574 sites are located on the outside of the domain, with the N1515 site located on an alpha-helix and the N1574 site located on a loop. How these glycans affect the conformation of the A2 domain is unclear and indeed it needs to be considered that VWF contains other domains that may interact

with the A2 domain. Furthermore, although only speculative, one or both of the glycans could affect access to the ADAMTS13 cleavage site.

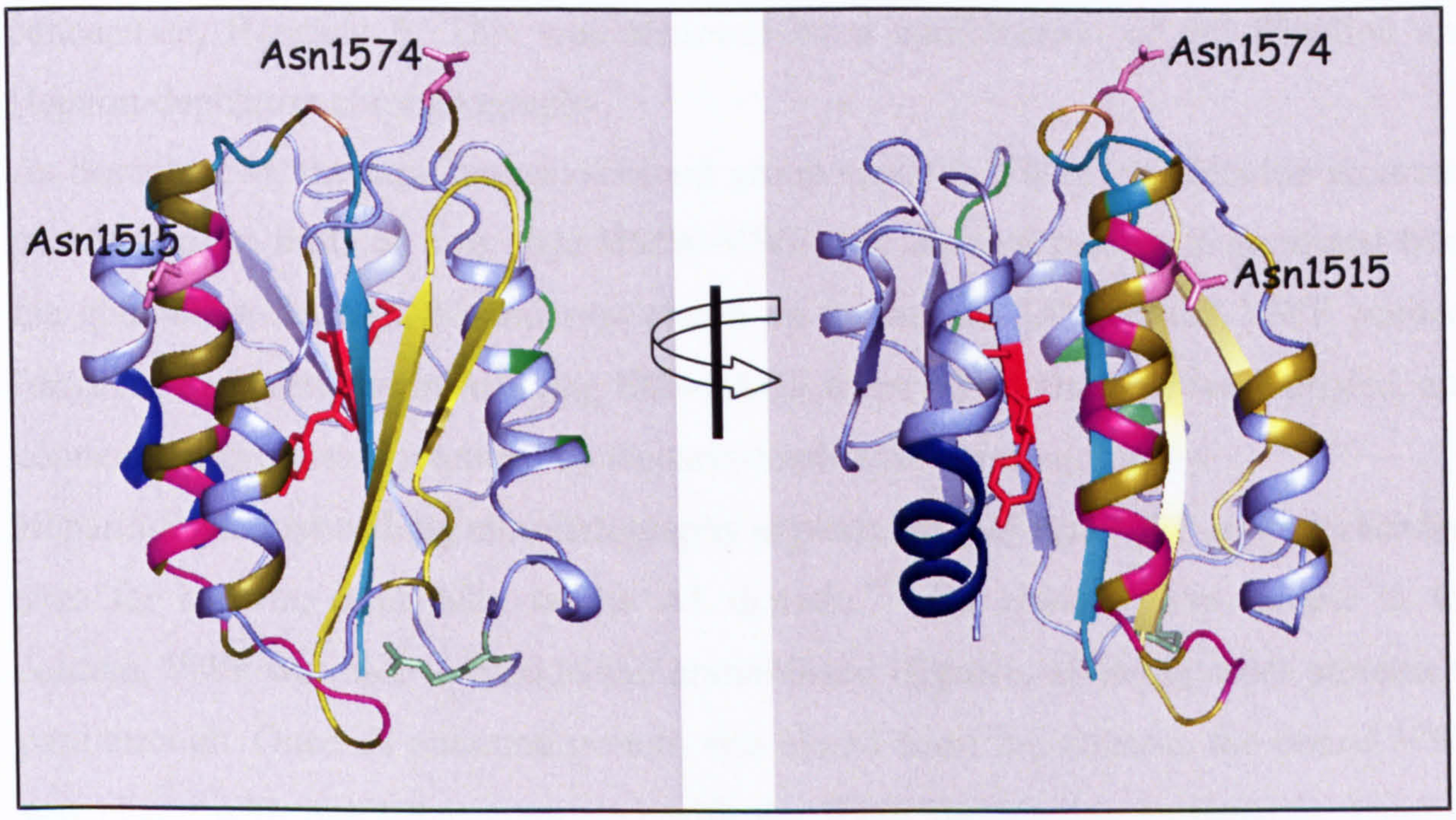


Figure 4.12 Predicted model of the VWF A2 domain

The two A2 domain glycans are predicted to occur on the outside of the domain, with N1515 located on an alpha-helix and N1574 on a loop region. The ADAMTS13 cleavage site is shown in red in the centre of the model.

4.4.2 Experimental Analysis of VWF *N*-linked Glycans

To confirm that sites N1515 and N1574 were indeed occupied by *N*-linked glycan chains and to determine if they presented the blood group sugars a previously described 55kDa tryptic fragment of VWF was isolated, that spanned residues 1493-1887.[142]

In order to achieve this VWF was first purified from a commercial VWF-FVIII concentrate, Haemate P. This was achieved by a combination of gel filtration and Heparin-Sepharose chromatography.

As described for the purification of blood group specific VWF, gel filtration separates proteins on the basis on size; thus HMW-VWF was the first protein to be eluted from the column, at fraction B6 and was eluted up to fraction D12. These VWF positive fractions, demonstrated in reducing SDS-PAGE as an ~250kDa band were pooled, and contaminating proteins removed by Heparin-Sepharose chromatography.

Heparin-Sepharose affinity chromatography exploits the fact that VWF contains binding sites for heparin, principally in the A1 domain.[124] On applying the sample to the column, VWF was able to bind to the immobilised Heparin, allowing other proteins to pass through. Once all unbound protein was eluted form the column, the bound VWF was eluted with NaCl that competed with the VWF for binding to Heparin. Optimal purification of VWF was achieved using a SK-16 column packed with 30ml of Heparin-Sepharose 6 fast flow (Amersham) with the gel filtered Haemate P sample applied over the column at a flow rate of 0.4ml/min. At higher loading flow rates the recovery of VWF was lower. The slower flow rate probably gives optimal time for the interaction to occur between VWF and Heparin. Eluted VWF fractions were pure, demonstrated by silver staining and were comprised of high to medium molecular multimers. The flow through fraction from the Heparin-Sepharose column contained the lowest molecular weight multimers, indicating that HMW-VWF has a greater affinity for Heparin.

From Matsui *et al's* study it was predicted that ~13% of the VWF *N*-linked glycan chains presented the ABO sugars, but as discussed, no evidence is given regarding the specific sites that present them. In an attempted to elucidate which sites do present the ABO sugars, VWF was digested with ADAMTS13 to produce the two ADAMTS13 cleavage products. The N-terminal fragment spanning residues 763-1605 encompassing sites N857, N1147, N1231, N1515 and N1574 and the C-terminal fragment, residues 1605-2813 encompassing sites N2223, N2290, N2357, N2400, N2546, N2585 and N2790. Analysis of the digestion in SDS-PAGE, followed by western blotting and probing with Ulex europaeus demonstrated that the H-antigen was present on both

fragments. Furthermore the intensity of the cleavage product bands suggests that a number of the *N*-linked sites on both fragments were presenting H-antigen.

To isolate the 55kDa fragment of VWF, purified VWF was subjected to trypsin digestion as and the digest passed over a Mono Q ion exchange column as described.[142] A number of fractions were eluted from the column, with fraction A4 containing an ~55kDa band under reducing conditions. Further characterisation of the fragment showed that under non-reducing conditions it migrated with an apparent molecular weight of ~44kDa and it was also cleaved by ADAMTS13, demonstrating that at least part of the A2 domain was present. Finally, N-terminal sequencing of the molecule confirmed that the fragment began at residue 1493.

The presence of three bands detected by western blotting and probing with anti-VWF-HRP, after PNGase digestion of the fragment confirmed that both sites; N1515 and N1574 were occupied. Each band represents a particular state of glycosylation; i.e. both glycans present, one glycan present, neither glycan present.

Probing with *Ulex europaeus* demonstrated that these glycans present the H-antigen and are thus able to present the A and B antigens. Analysis of the blot also suggests that both sites present the H-antigen (Figure 4.11). However, further investigation is need to confirm this observation. In the same way, analysis with EBL also showed that both glycans appear to present terminal sialic acid. The presence of these sugar residues also show that both glycans must be of the complex type.

This result significantly demonstrates that the two potential *N*-linked glycan sites within the VWF A2 domain are firstly occupied, and secondly present the H-antigen, and are thus able to present the A/B sugars. It is still unclear how the blood group sugars mediate susceptibility to ADAMTS13 cleavage, but it is certainly an interesting observation that the two glycans in closest proximity to the ADAMTS13 cleavage site present them. The functional implications of altering VWF glycan structure is examined in the next chapter.

CHAPTER 5

5. EFFECT OF VWF GLYCAN MODIFICATION ON THE INTERACTION WITH ADAMTS13

5.1 INTRODUCTION

A number of previous studies have been performed investigating the effect of VWF glycan modification on VWF function. The majority of these have focused on the effects of removing terminal sialic acid and galactose residues from plasma derived VWF, and have provided sometimes conflicting results. Although some studies have been carried out examining the effect of VWF glycan structure on susceptibility of VWF to proteolysis, as yet, no study has been performed to investigate the role VWF glycans play in mediating the interaction with ADAMTS13. This is particularly pertinent with regard to the observations presented in Chapter 3, that ABO blood group sugars presented on the *N*-linked glycans of VWF mediate susceptibility to ADAMTS13 proteolysis. Since these naturally occurring alterations in VWF glycan structure have a profound effect on VWF cleavage by ADAMTS13, it is probable that other modification of VWF glycan structure will also affect the interaction of the molecule with ADAMTS13.

To investigate this further, highly purified VWF was digested with specific endo/exoglycosidases to modify the glycan structure of the molecule and the extent of glycan removal was analysed with sugar specific lectins. The function of glycan modified VWF was analysed by CBA and VWF multimer analysis, and the interaction of glycan modified VWF with ADAMTS13 was assessed by ADAMTS13 cleavage and binding assays.

5.2 GLYCOSIDASE DIGESTION AND LECTIN ANALYSIS

In order to assess the role of specific sugar residues/structures on VWF function, the glycan structure of VWF was altered by digestion with endo and exoglycosidases.

VWF purified from Haemate P by a combination of gel filtration and Heparin-Sepharose chromatography, (described in Section 2.2) was subjected to digestion with endo and exoglycosidase enzymes as described in Section 2.9.

1) α-2(3,6,8,9) Neuraminidase to remove terminal sialic acid residues

2) β-galactosidase to remove terminal galactose residues

3) A combination of both neuraminidase and β-galactosidase to remove sialic acid and then exposed galactose residues

4) PNGase F to remove whole *N*-linked glycan chains at the linkage between protein and glycan

5) PNGase F and sialic acid to remove whole *N*-linked glycan chains and terminal sialic acid present on O-linked glycans

A panel of lectins were used to assess the alteration in glycan structure achieved (described in Section 2.10)

1) Elderberry Bark lectin (EBL) – terminal sialic acid resides

2) Ricinus Communis Agglutinin I (RCA-I) – terminal galactose residues

3) Concanavalin A (ConA) – whole *N*-linked glycan chains

In keeping with previous reports, treatment of VWF with neuraminidase (Neu-VWF) resulted in the removal of >99% of sialic acid residues as demonstrated by a total loss of EBL binding (Figure 5.1). Treatment with β-galactosidase resulted in the removal of ~20% of galactose residues (βgal-VWF), demonstrated by an ~20% decrease in RCA-I binding (Figure 5.1). Treatment of VWF with both neuraminidase and β-galactosidase (Neu/βgal-VWF) resulted in the removal of >99% sialic acid and increased removal of galactose, with a 47% reduction in RCA-I binding. Increasing the final concentration of β-galactosidase in the digestion or alteration of reaction conditions did not result in increased galactose removal.

Digestion of VWF with PNGase F (PNG-VWF) resulted in the removal of >90% of the *N*-linked glycan chains (Figure 5.2). Since the vast majority of the *N*-linked glycans were able to be removed by PNGase F, the PNG-VWF was analysed for sialic acid content. As demonstrated by EBL binding, PNG-VWF had ~35% less sialic acid than control VWF (Ctrl-VWF), demonstrating that ~65% of VWF sialic acid is presented on the O-linked glycan chains (Figure 5.2).

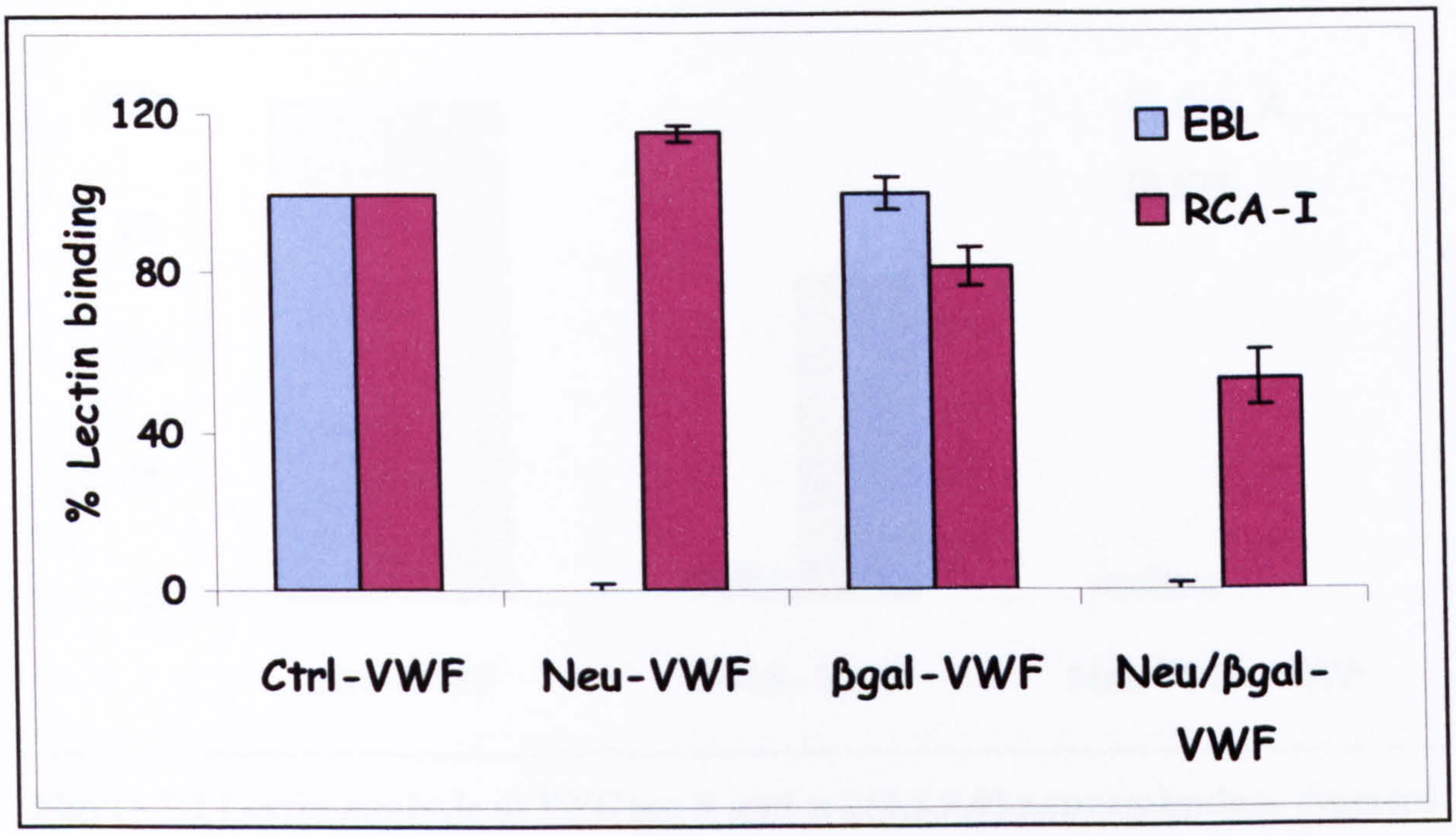


Figure 5.1 Lectin analysis of α-2(3,6,8,9) neuraminidase and β-galactosidase digested VWF

Purified VWF was subjected to glycosidase digestion with neuraminidase and β-galactosidase and removal of sugars analysed with EBL specific for sialic acid and RCA-I specific for galactose. Digestion with neuraminidase resulted in >99% removal of sialic acid residues. Digestion with β-galactosidase resulted in an ~20% reduction in RCA-I binding and digestion with both enzymes resulted in >99% sialic removal and increased galactose removal with an ~47% drop in RCA-I binding.

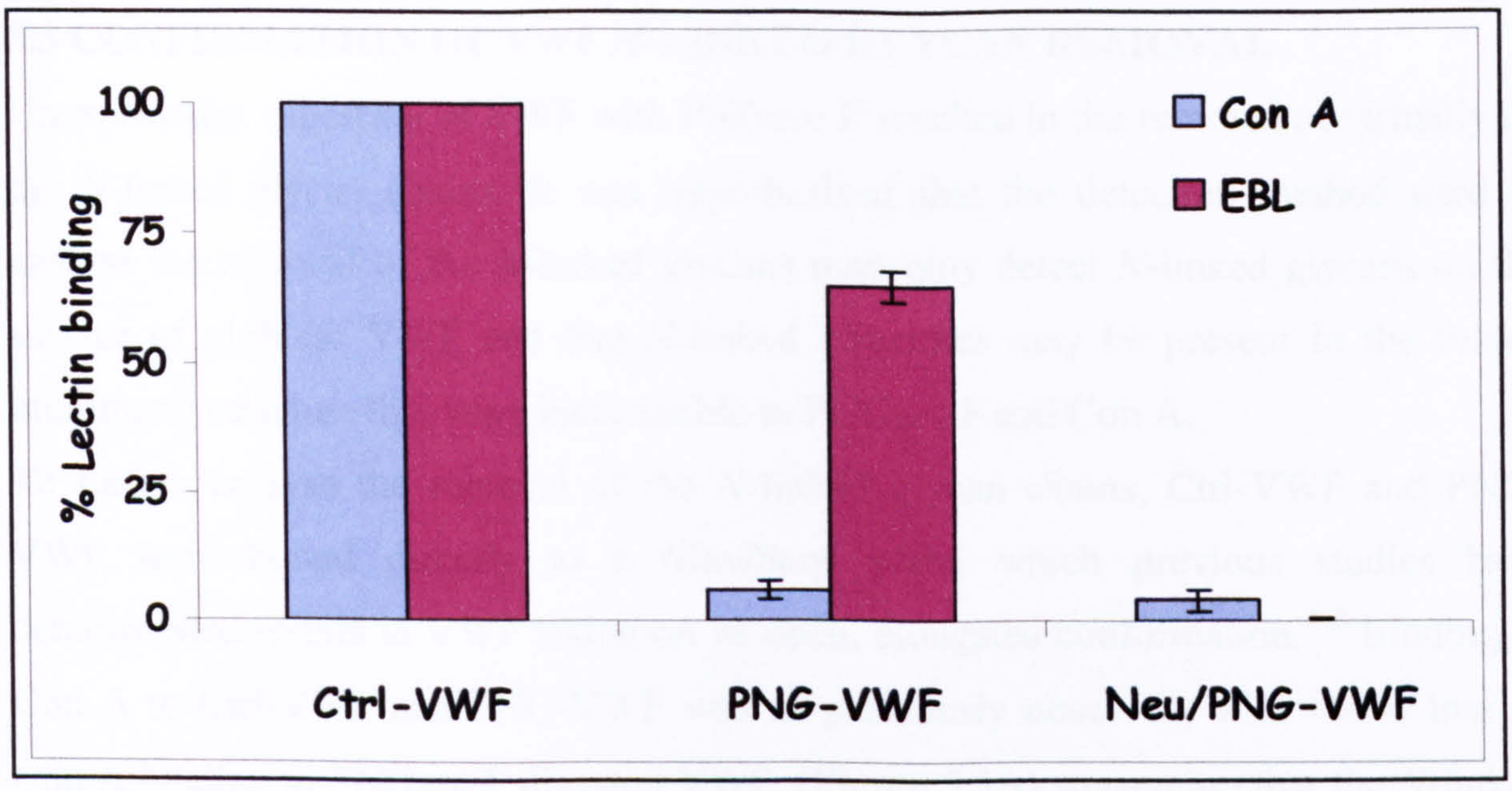


Figure 5.2 Lectin analysis of PNGase F and α-2(3,6,8,9) neuraminidase digested VWF

Purified VWF was treated with PNGase F, neuraminidase and a combination of both enzymes and removal of sugars analysed with Con A, specific for *N*-linked glycan structures and EBL, specific for terminal sialic acid residues. Treatment of VWF with PNGase F resulted in the removal of >90% of the *N*-linked glycan chains, demonstrated by only minimal binding to Con A compared to Ctrl-VWF. Detection of sialic acid residues on PNG-VWF showed that it has ~35% less sialic acid than Ctrl-VWF. Thus the remaining ~65% of VWF sialic acid is presented on the O-linked glycans. Treatment of VWF with both PNGase F and neuraminidase (Neu/PNG-VWF) resulted in only minimal binding to Con A and EBL. (Error bars represent the mean and standard deviation of six separate digestions of 3 different VWF preparations).

5.3 CONFIRMATION OF VWF *N*-LINKED GLYCAN REMOVAL

Unexpectedly, digestion of VWF with PNGase F resulted in the removal of virtually all the *N*-linked glycan chains. It was hypothesised that the detection method used to analyse the removal of the *N*-linked glycans may only detect *N*-linked glycans on the surface of globular VWF and that *N*-linked structures may be present in the folded multimeric structure that were inaccessible to PNGase F and Con A.

To further analyse the removal of the *N*-linked glycan chains, Ctrl-VWF and PNG-VWF were bound directly to a MaxiSorp plate, which previous studies have demonstrated results in VWF taking on its open, elongated conformation.[368] Binding of Con A to Ctrl-VWF and PNG-VWF was as previously observed, with >90% loss of Con A binding to PNGase F digested VWF, (Figure 5.3A) suggesting that the *N*-linked glycans of VWF are accessible to PNGase F while VWF is in a globular conformation and are not buried within the fully folded multimeric structure.

To further confirm this observation, VWF was reduced then digested with PNGase F and analysed by reducing SDS-PAGE in 3-8% gels to compare the shift in band migration compared to Ctrl-VWF and non-reduced VWF digested with PNGase F (Figure 5.3B). Compared to Ctrl-VWF, both the PNGase digested samples migrate further through the gel, demonstrating a reduction in molecular weight consistent with glycan removal. However there is no observable difference in migration between the two samples, indicating that similar amounts of *N*-linked glycans have been removed from both. Therefore digestion of VWF with PNGase F does indeed remove the vast majority of *N*-linked glycans from the molecule.

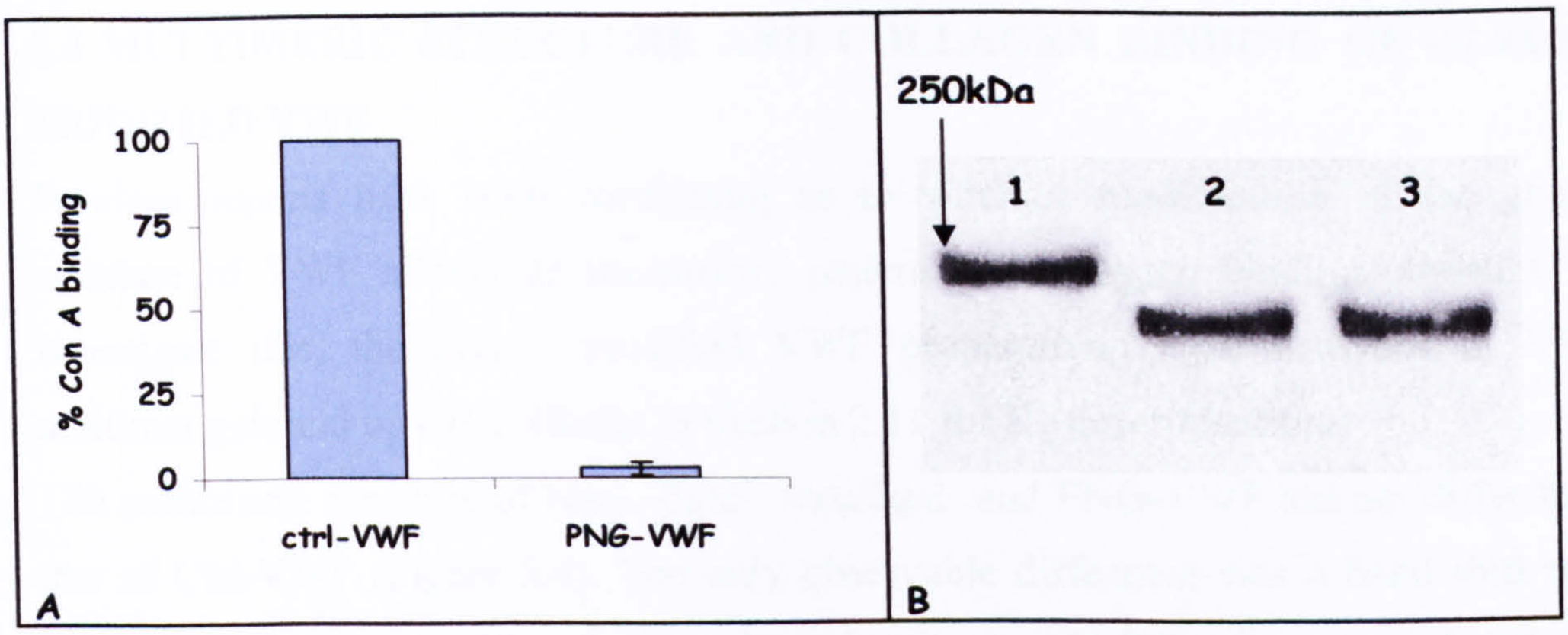


Figure 5.3 Conformation of VWF *N*-linked glycan removal

A) PNGase F digested VWF was further analysed using a modified plate binding assay where control and PNGase F digested VWF were directly bound to a MaxiSorp plate and probed with Con A. Compared to Ctrl-VWF; PNG-VWF demonstrated only minimal Con A binding (<10%) confirming that almost all the *N*-linked glycans are removed by PNGase F digestion.

B) Reduced VWF was digested with PNGase F and its mobility in 3-8% gels compared to non-reduced PNGase F digested VWF and control VWF. Ctrl-VWF migrated with an approximate molecular weight of 250kDa (lane 1). Non reduced (lane 2) and reduced (lane 3) PNGase F digested VWF both migrated further in the gel compared to wild type, but no difference in migration was seen between the two samples.

5.4 MULTIMERIC STRUCTURE AND COLLAGEN BINDING OF GLYCAN MODIFIED VWF

Previous reports have been conflicting as to whether modification of the glycan structure of VWF affects its multimeric pattern and collagen binding potential. To investigate this, the glycan modified VWF preparations were analysed in VWF multimer gels and by CBA. (Refer to Section 2.11 for K_D determination.)

The multimeric structure of Neu-, βgal-, Neu/βgal- and PNG-VWF did not differ from that of Ctrl-VWF (Figure 5.4). The only observable difference was a band shift with PNG-VWF, consistent with a decrease in molecular weight following removal of the *N*-linked glycan chains (Figure 5.4). Furthermore, alteration of the glycan structure did not affect the affinity of VWF for collagen, (Figure 5.5) with all the VWF preparations binding to collagen with similar affinity and with K_D comparable to previously published values for plasma derived VWF: K_D = Ctrl 1.3nM, Neu 1.8nM, βgal 1.5nM, Neu/βgal 1.6nM, PNG 1.6nM. (K_D based on VWF monomeric weight of 250kDa).

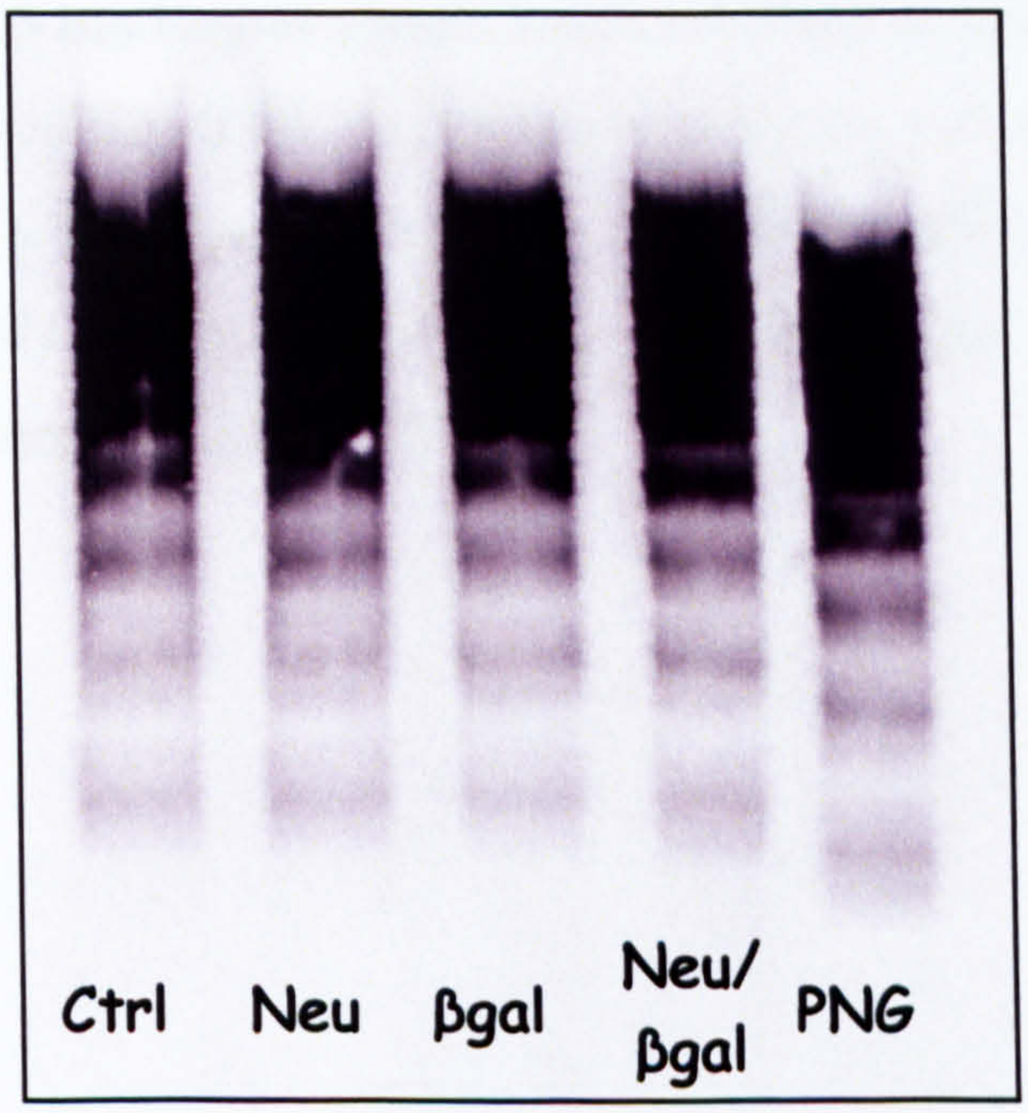


Figure 5.4 Multimer analysis of glycan modified VWF

The multimeric structure of glycan modified VWF was analysed in 1.8% agarose multimer gels. The multimeric structure of Neu-, βgal-, Neu/βgal- and PNG-VWF did not differ from that of Ctrl-VWF. The multimeric structure of PNG-VWF was also the same as Ctrl-VWF, however a band shift is observed with the PNG-VWF sample due to the decrease in molecular weight.

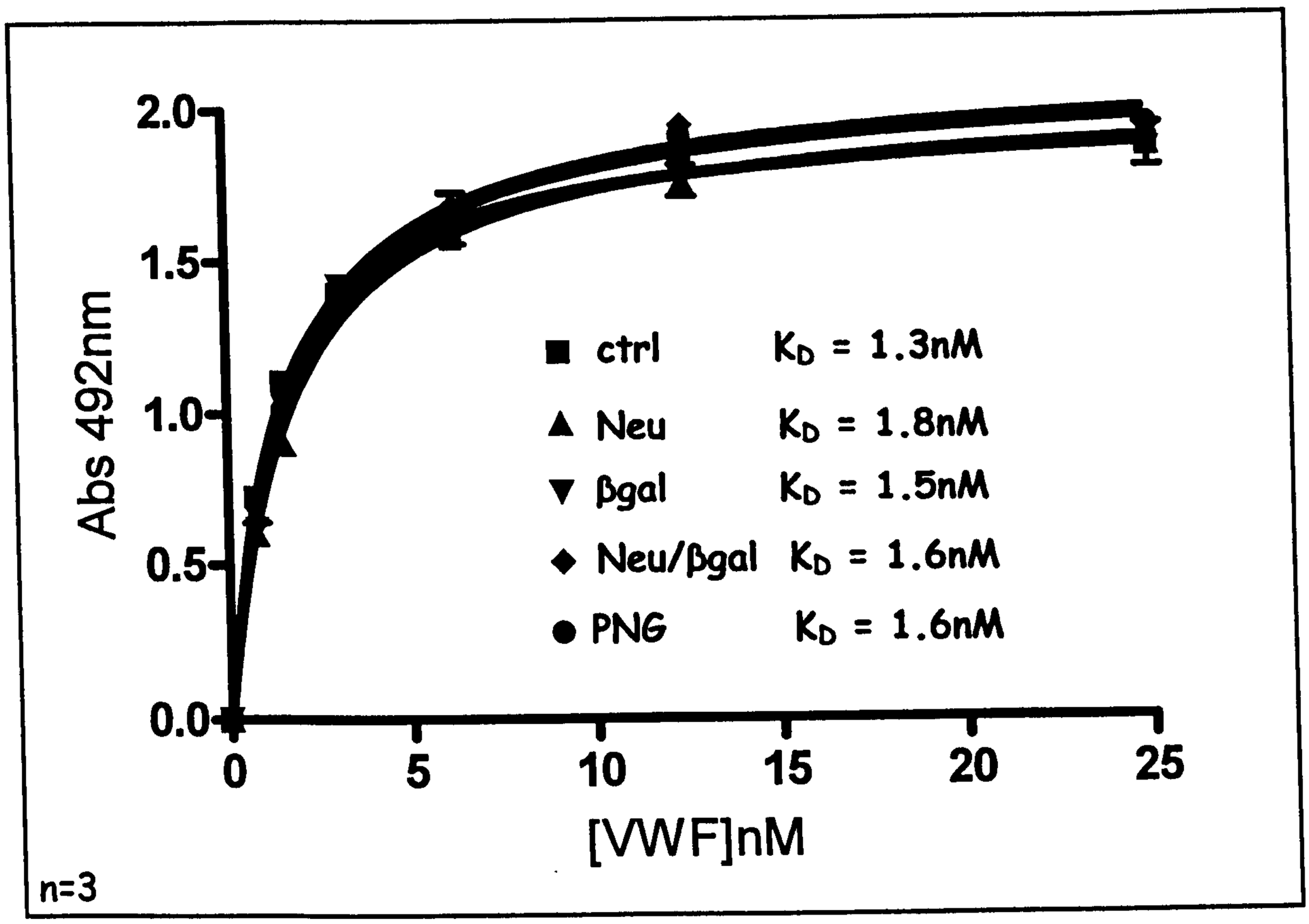


Figure 5.5 Binding of glycan modified VWF to collagen

The ability of glycan modified VWF to binding to collagen was analysed using CBA. All the preparations of VWF bound to collagen with similar affinity (K_D = 1.3-1.8nM) comparable to previously published values (K_D = 1-7nM). The K_D concentration is based on a VWF monomeric weight of 250kDa.*

* The monomeric weight of 250kDa was used to allow a K_D to be calculated, although it should be noted that due to the removal of sugars structures the monomeric weight of the glycan modified samples will be reduced. However, as is apparent from the graph, no difference in collagen binding was observed and the binding curves still remained the same if the VWF concentration was expressed in μg/ml. Furthermore, no difference was seen between the reactivity of the glycan modified samples to the anti-VWF-HRP polyclonal antibody.

5.5 EFFECT OF VWF GLYCAN MODIFICATION ON SUSCEPTIBILITY TO CLEAVAGE BY ADAMTS13

Since the ABO(H) sugars affected the susceptibility of VWF to cleavage by ADAMTS13, it was hypothesised that other sugar structures or further reduction to the length of the *N*-linked glycan chains may also affect cleavage of VWF by ADAMTS13. It was not possible to obtain sufficient quantities of βgal-VWF and Neu/βgal-VWF to obtain data on the interaction with ADAMTS13, therefore the following presented data focuses on the effect of terminal sialic removal and whole *N*-linked glycan removal on the interaction with ADAMTS13.

5.5.1 Effect of VWF Sialic Acid on Susceptibility to Cleavage by ADAMTS13

Previous studies demonstrated that Neu-VWF* was more susceptible to proteolysis by a number of proteases including, trypsin, chymotrypsin and plasmin. It is therefore possible that terminal sialic acid residues may protect against ADAMTS13 cleavage.

Wild type and Neu-VWF were incubated with ADAMTS13 and extent of cleavage analysed using CBA and VWF multimer gels. Surprisingly, Neu-VWF was proteolysed at a significantly slower rate slower rate by ADAMTS13 than Ctrl-VWF as demonstrated by CBA (Figure 5.6). At all time points (60, 120 and 240mins) Neu-VWF had significantly more collagen binding potential than Ctrl-VWF ($p = <0.0001$).

This effect was visualised by VWF multimer analysis (Figure 5.7). At time zero all the VWF preparations have a similar multimeric pattern. However is it apparent at time points 60mins and 120mins that Neu-VWF is less susceptible to cleavage by ADAMTS13, demonstrated by less reduction of HMW multimers.

---

* The term Asialo VWF (Neu-VWF) has been used in previous studies to describe neuraminidase treated VWF. Neuraminidase treated VWF in this study is referred to as Neu-VWF and the use of the term AsVWF refers to previous work.

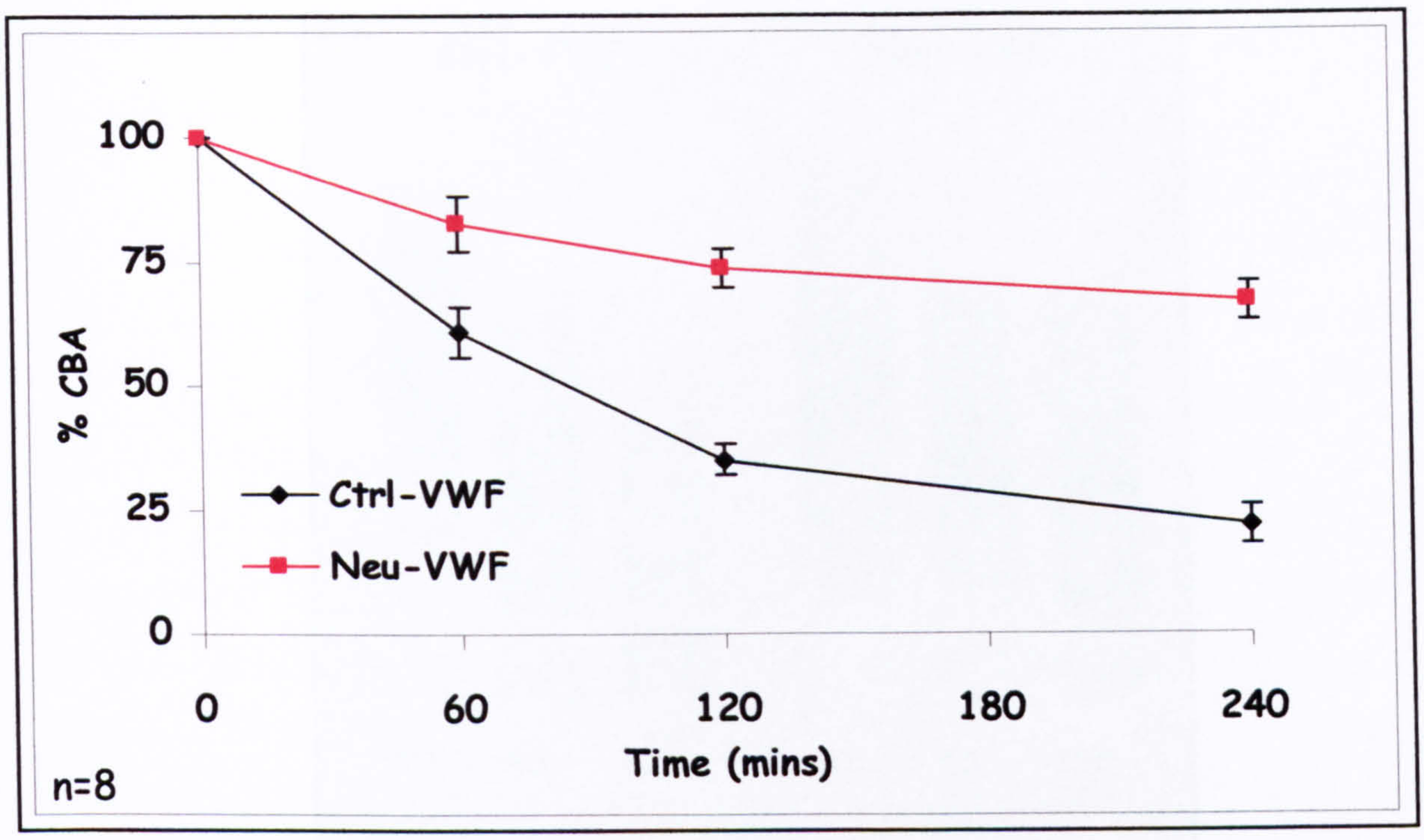


Figure 5.6 Collagen binding assay of ADAMTS13 cleavage of Ctrl and Neu-VWF

Control and Neu-VWF were subjected to proteolysis by ADAMTS13 and the extent of cleavage analysed by CBA. Over the time course Neu-VWF (red) was proteolysed slower than Ctrl-VWF (black), demonstrated by significantly higher collagen binding activity at all time points compared to Ctrl-VWF; $p = < 0.0001$. (Error bars represent the mean and standard deviation of 8 separate experiments performed using 3 different VWF preparations.

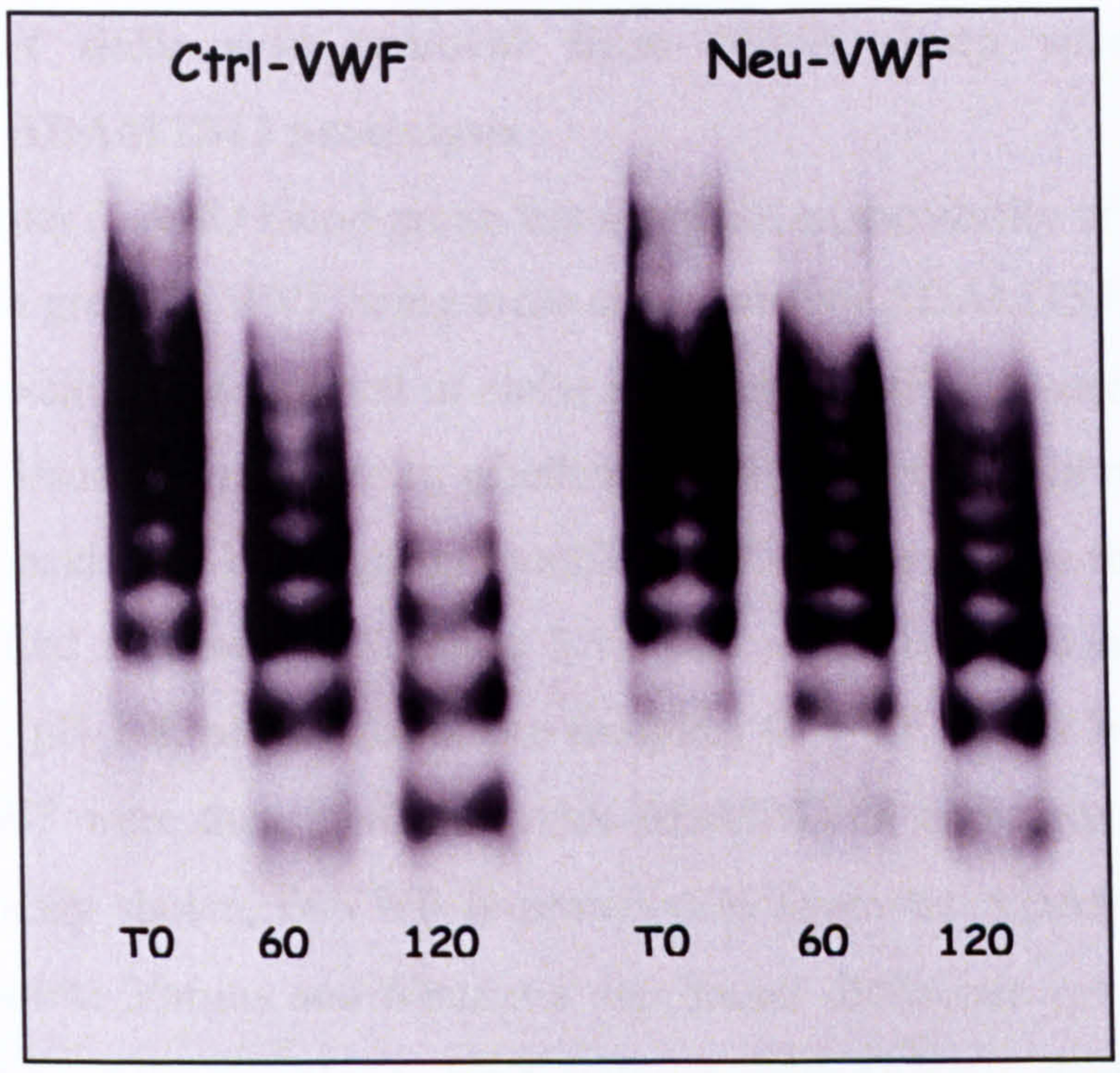


Figure 5.7 Multimer gel analysis of ADAMTS13 cleavage of Ctrl and Neu-VWF

At time point zero (T0) the multimer pattern for Ctrl and Neu-VWF is similar, however it is apparent at time points 60min and 120mins that Neu-VWF has been cleaved at a reduced rate by ADAMTS13, demonstrated by less reduction of HMW multimers and appearance of lower molecular weight bands compared to Ctrl-VWF.

5.5.1.2 Effect of sialic acid removal from blood group specific VWF on susceptibility to ADAMTS13 proteolysis

As shown in chapter 3, ABO blood group has an effect on the ability of ADAMTS13 to cleave VWF, with group O VWF being more susceptible to ADAMTS13 proteolysis. In light of the observation that removal of sialic acid from VWF *decreases* proteolysis by ADAMTS13, an issue was raised as to whether the ABO effect would remain following removal of sialic acid from blood group specific VWF. To investigate this, HMW O and AB VWF, (purified as described Section 2.1), was incubated with neuraminidase or 20mM Tris-HCl, pH 7.8, as a control. The samples; O-VWF, AB-VWF, Neu-O-VWF and Neu-AB-VWF were then incubated with ADAMTS13 and cleavage analysed by CBA. As previously shown, O-VWF is proteolysed faster by ADAMTS13 than AB-VWF; at time points 30mins and 60mins a significant difference ($p = <0.005$) is seen between the ability of the samples to bind collagen, with O-VWF demonstrating lower collagen binding activity (Figure 5.8). The CBA also shows that Neu-O-VWF and Neu-AB-VWF are cleaved significantly slower than the wild type samples, ($p=0.0001$), demonstrated by higher collagen binding activity at all time points. However, the ABO effect is no longer observed with Neu-O and Neu-AB-VWF samples; with both de-sialylated samples being cleaved at a similar rate (Figure 5.8).

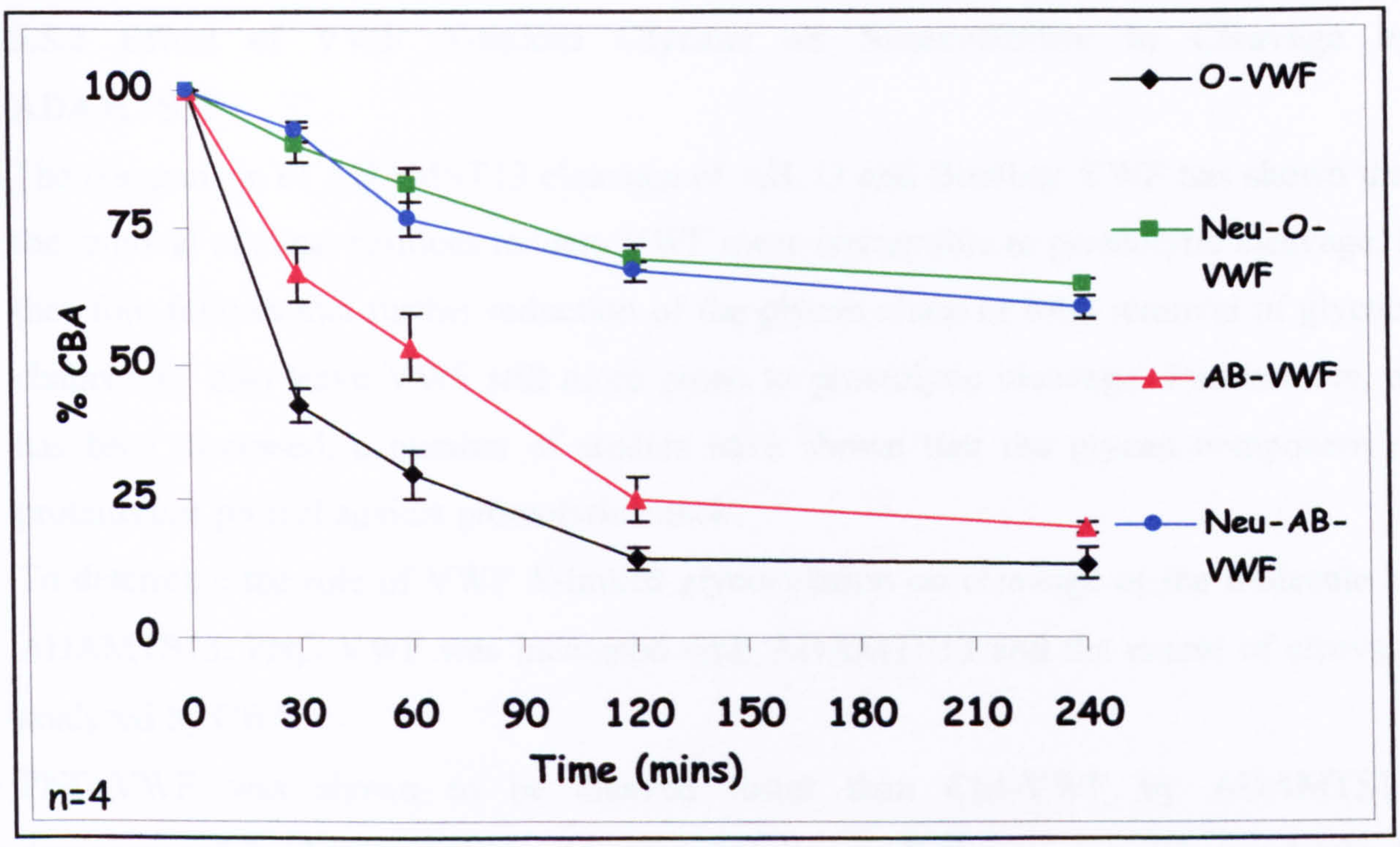


Figure 5.8 The effect of sialic acid removal from blood group specific VWF on susceptibility to cleavage by ADAMTS13

Blood group specific O and AB VWF purified as previously described was incubated in the presence or absence of neuraminidase then subjected to cleavage by ADAMTS13 and the extent of proteolysis was analysed by CBA. In keeping with the previous observations, O-VWF (black) was proteolysed significantly faster than AB-VWF (red), $p = <0.05$. Also in keeping with previous observation, the Neu-VWF samples were cleaved significantly slower by ADAMTS13, $p = <0.0001$, however the ABO effect on ADAMTS13 proteolysis was lost, with both Neu-O-VWF (green) and Neu-AB-VWF (blue) being cleaved at similar rates. (Error bars represent the mean and standard deviation of 4 separate experiments performed in duplicate.)

5.5.2 Effect of VWF *N*-linked Glycans on Susceptibility to Cleavage by ADAMTS13

The comparison of ADAMST13 cleavage of AB, O and Bombay VWF has shown that the removal of sugar residues renders VWF more susceptible to proteolytic cleavage. It therefore follows that further reduction of the glycan chain or total removal of glycans chains may also leave VWF still more prone to proteolytic cleavage. Furthermore, as has been discussed, a number of studies have shown that the glycan component of proteins can protect against proteolytic attack.

To determine the role of VWF *N*-linked glycosylation on cleavage of the molecule by ADAMTS13, PNG-VWF was incubated with ADAMTS13 and the extent of cleavage analysed by CBA.

PNG-VWF was shown to be cleaved faster than Ctrl-VWF by ADAMTS13, demonstrated by lower collagen binding activity at all time points (Figure 5.10). In particular the initial extent of proteolysis was significantly faster for PNG-VWF ($p = <0.0001$), with the greatest difference in CBA seen at time points 30mins and 60mins.

Since the PNG-VWF was cleaved faster than Ctrl-VWF, and Neu-VWF cleaved slower, an ADAMTS13 cleavage assay was performed subjecting Ctrl-, Neu-, PNG- and Neu/PNG-VWF to ADAMTS13 proteolysis in order to determine the contribution of the O-linked sialic acid residues on ADAMTS13 cleavage. As already observed, Neu-VWF was proteolysed slower than Ctrl-VWF and PNG-VWF was proteolysed faster. Neu/PNG-VWF was cleaved faster than Ctrl-VWF at a rate similar to PNG-VWF (Figure 5.11). Removal of the sialic acid from the PNG-VWF sample did offer some slight protection from cleavage, with the collagen binding activity of the Neu/PNG-VWF samples being slightly higher (~5%) at all time points, although this failed to reach significance.

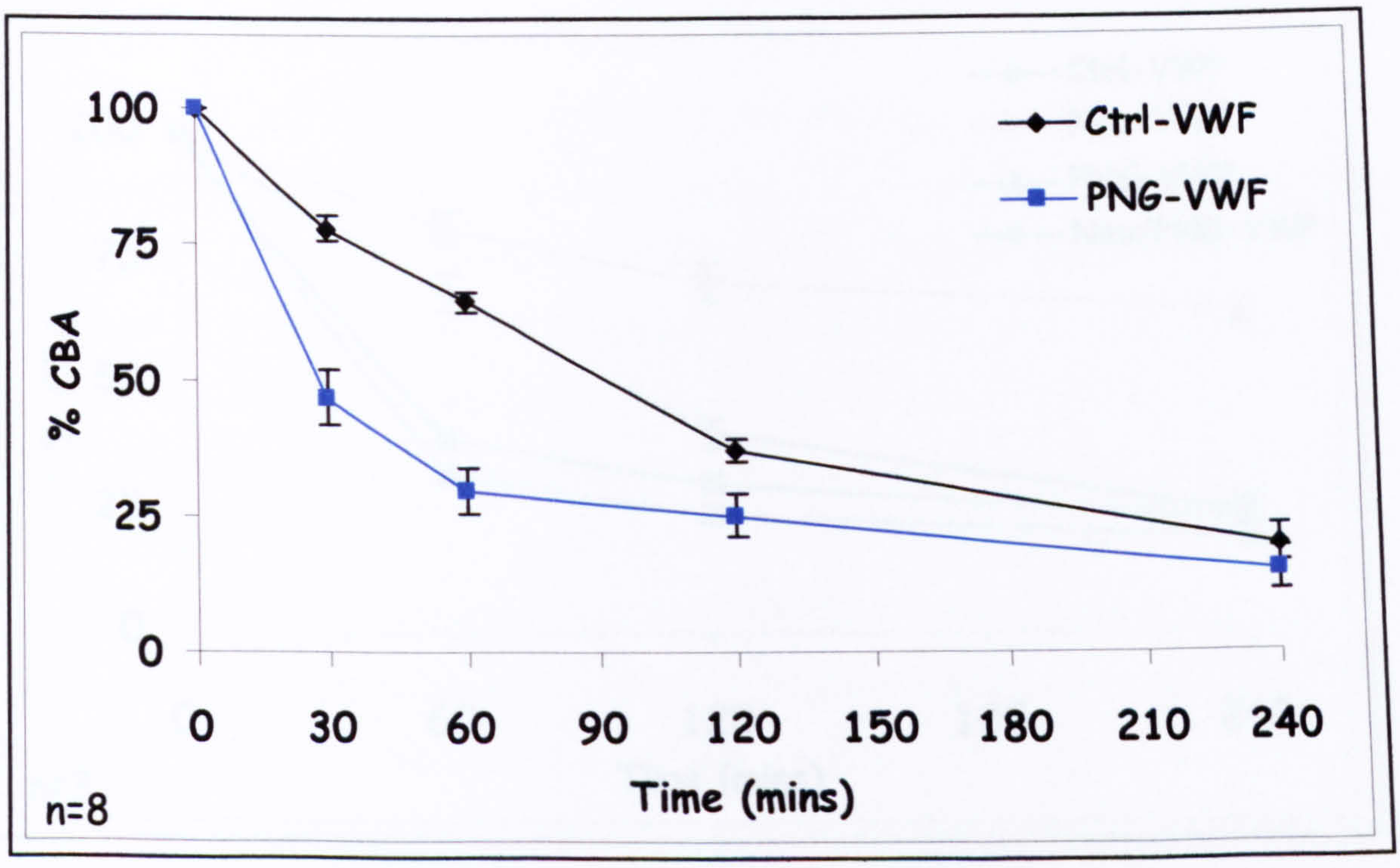


Figure 5.10 Collagen binding assay of ADAMTS13 cleavage of control and PNG-VWF

Control and PNG-VWF were subjected to proteolysis by ADAMTS13 and the extent of cleavage analysed by CBA. PNG-VWF (blue) was proteolysed faster than Ctrl-VWF (black), demonstrated by significantly reduced collagen binding activity ($p=<0.0004$ at time points 30mins and 60mins), compared to Ctrl-VWF.

(Error bars represent the mean and standard deviation of 8 separate experiments performed using 3 different VWF preparations)

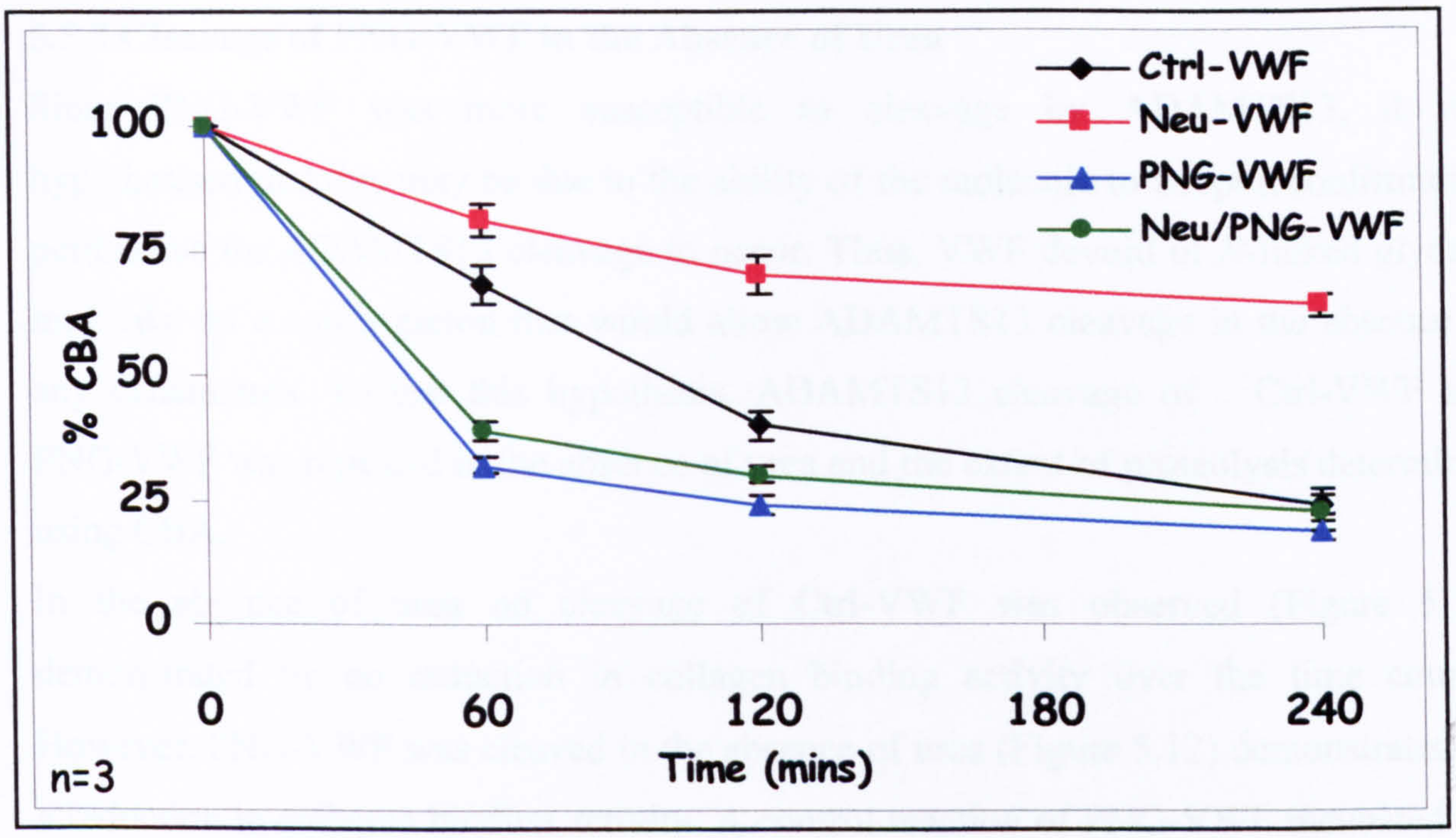


Figure 5.11 Cleavage of Neu/PNG-VWF

Neu/PNG-VWF was subjected to cleavage by ADAMTS13 and compared to Ctrl, Neu and PNG-VWF preparations. As already observed, Neu-VWF was cleaved slower than Ctrl-VWF and PNG-VWF cleaved faster. Neu/PNG-VWF was cleaved at a similar rate to PNG-VWF. However, the removal of sialic acid residues appeared to a slight protective effect, with the collagen binding activity of the Neu/PNG-VWF being slightly higher (~5%) at all time points, although this failed to reach significance.

(Error bars represent the mean and standard deviation of 3 separate experiments)

5.5.3 Cleavage of PNG-VWF in the Absence of Urea

Since PNG-VWF was more susceptible to cleavage by ADAMTS13, it was hypothesised that this may be due to the ability of the molecule to adopt a confirmation permissive for ADAMTS13 cleavage to occur. Thus, VWF devoid of *N*-linked glycans may take on a confirmation that would allow ADAMTS13 cleavage in the absence of any denaturants. To test this hypothesis, ADAMTS13 cleavage of Ctrl-VWF and PNG-VWF was repeated in the absence of urea and the extent of proteolysis determined using CBA.

In the absence of urea no cleavage of Ctrl-VWF was observed (Figure 5.12) demonstrated by no reduction in collagen binding activity over the time course. However, PNG-VWF was cleaved in the absence of urea (Figure 5.12) demonstrated by a reduction in collagen binding activity. A control reaction of PNG-VWF incubated for the duration of the time course without ADAMTS13, did not show any reduction in collagen binding, indicating that the PNG-VWF was stable and the reduction in collagen binding observed was solely due to cleavage by ADAMTS13 (Figure 5.12). Also shown on the figure is PNG-VWF cleaved in the presence of urea for comparison. Although PNG-VWF is cleaved faster in the presence of urea, it is still highly significant that cleavage can still occur in its absence.

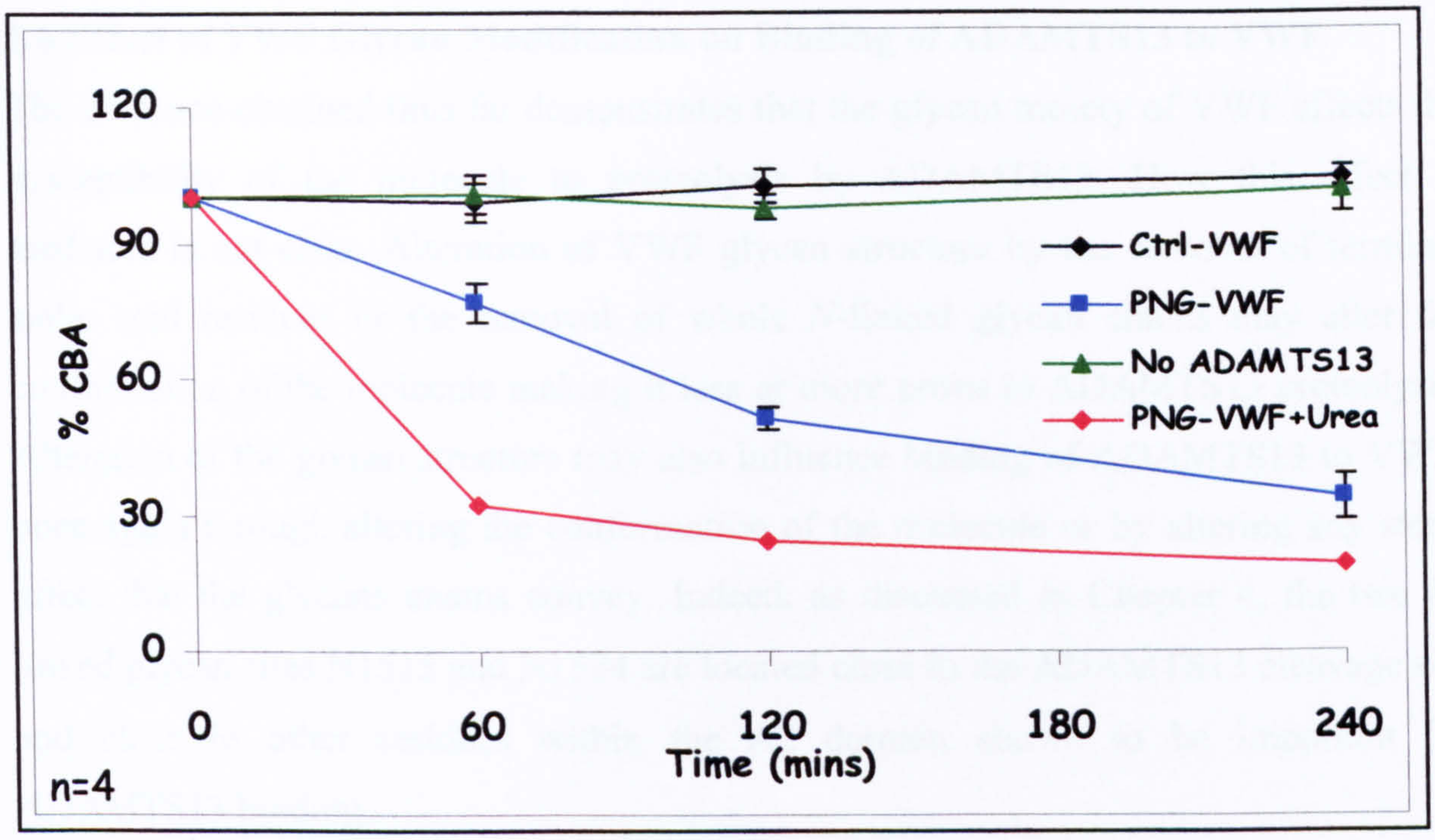


Figure 5.12 Cleavage of PNG-VWF in the absence of urea

ADAMTS13 cleavage of control and PNG-VWF was performed in the absence of urea and analysed by CBA. No proteolysis of Ctrl-VWF was observed (black), demonstrated by no reduction in collagen binding over the time course. PNG-VWF was cleaved in the absence of urea (blue) shown by the reduction in collagen binding. A control reaction, where PNG-VWF was incubated without ADAMTS13 for the duration of reaction, was also analysed (green). No reduction in collagen binding was observed, indicating that PNG-VWF is stable and the observed cleavage of PNG- VWF is solely due to ADAMTS13. Also shown on the graph for comparison, is cleavage of PNG-VWF in the presence of 1.5M urea (red). (Error bars represent the mean and standard deviation of 4 separate experiments performed in duplicate).

5.6 Effect of VWF Glycan Modification on Binding of ADAMTS13 to VWF

The evidence obtained thus far demonstrates that the glycan moiety of VWF affects the susceptibility of the molecule to proteolysis by ADAMTS13. How this effect is mediated is not clear. Alteration of VWF glycan structure by the removal of terminal sialic acid residues or the removal of whole *N*-linked glycan chains may alter the conformation of the molecule making it less or more prone to ADAMTS13 proteolysis. Alteration of the glycan structure may also influence binding of ADAMTS13 to VWF, once again through altering the conformation of the molecule or by altering any steric effect that the glycans chains convey. Indeed, as discussed in Chapter 4, the two *N*-linked glycan sites N1515 and N1574 are located close to the ADAMTS13 cleavage site and close to other residues within the A2 domain shown to be important for ADAMTS13 binding.

In a previous study by Majerus *et al* a plate binding assay was developed to examine the binding of ADAMTS13 to VWF.[222] The assay operated on the basis that when bound to surfaces, VWF takes on its "unwound" confirmation and enables the binding of ADAMTS13. The authors of the study showed that soluble, globular VWF bound ADAMTS13 with low affinity, where as plate bound VWF bound ADAMTS13 with high affinity; K_D = 14nM.[222]

To further investigate the effect of VWF glycan modification on the interaction with ADAMTS13, a plate binding assay was optimised based on the study of Majerus *et al* and used to examine the binding of ADAMTS13 to Neu- and PNG-VWF.

5.6.1 Optimisation of VWF:ADAMTS13 Plate Binding Assay

To determine the optimal plate coating concentration of VWF, purified VWF was diluted to final concentrations of 0-15μg/ml in PBS and used to coat MaxiSorp plates overnight at 4°C. After removal of unbound protein and blocking with 2%BSA-PBS-Tween, bound VWF was detected with anti-VWF-HRP as described in materials and methods. At a VWF concentration of ~7.5μg/ml the wells were saturated (Figure 5.13) and thus for all subsequent experiments a VWF coating concentration of 7.5μg/ml was used. In all binding assays performed, duplicate wells of each VWF preparation were analysed with anti-VWF-HRP to ensure that equal amounts of protein were bound to the wells.

In initial experiments, VWF coated plates were incubated with 0-125nM ADAMTS13 in the presence and absence of 10mM EDTA and the obtained data fitted to the equation:

$$B = \frac{Bmax \times [X]}{K_D + [X]}$$

(where B is the binding expressed in absorbance unit, B_{max} is the maximal binding when saturation is reached, [X] is the ligand (ADAMTS13) concentration and K_D is the equilibrium dissociation constant)

Binding of ADAMTS13 to VWF in the presence of EDTA was determined to be K_D = 4nM and in the absence of EDTA, K_D = 14nM (Figure 5.14).

The reduced binding in the absence of EDTA suggested that, although the ADAMTS13 had not been activated with divalent ions, some residual enzymatic activity was present and the VWF substrate could be proteolysed. This was further supported by the use of an ADAMTS13 mutant that had its catalytic site mutated and thus was unable to cleave VWF.* The ADAMTS13 active site mutant bound to immobilised VWF with K_D = 5.2nM, similar to wild type ADAMTS13 in the presence of EDTA (Figure 5.15) implying that EDTA does not have a conformational effect on ADAMTS13. All subsequent binding experiments were performed using wild type ADAMTS13 in the presence of 10mM EDTA.

* The ADAMTS13 active site mutant was kindly provided by Mr Jonathon Lam

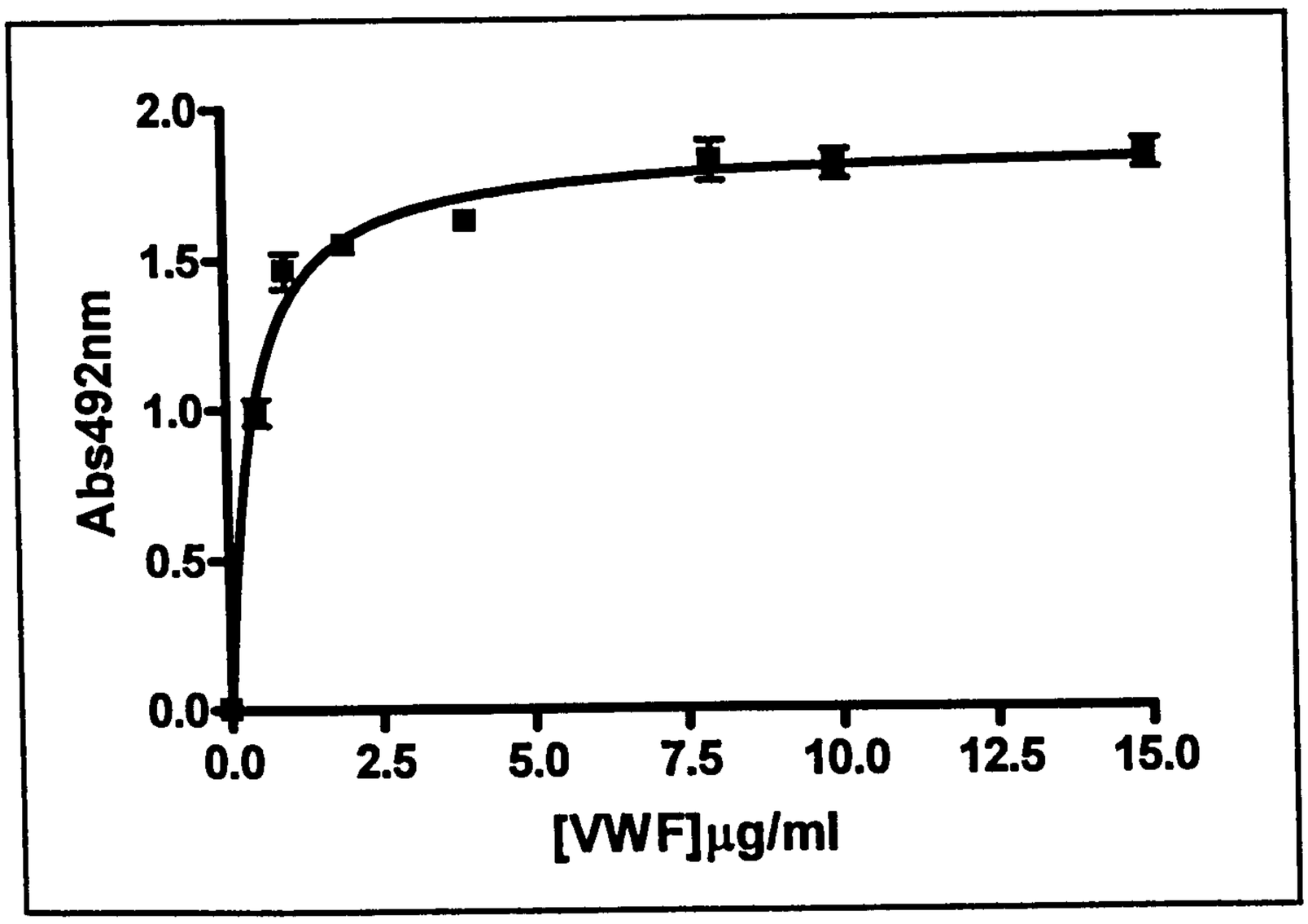


Figure 5.13 Optimal VWF plate coating concentration

The wells of MaxiSorp plates were incubated with 0-15µg/ml VWF diluted in PBS and binding of VWF detected with anti-VWF-HRP. Wells were saturated with VWF at a concentration of ~7.5µg/ml. This concentration of VWF was used to coat plates in all further VWF:ADAMTS13 binding assays.

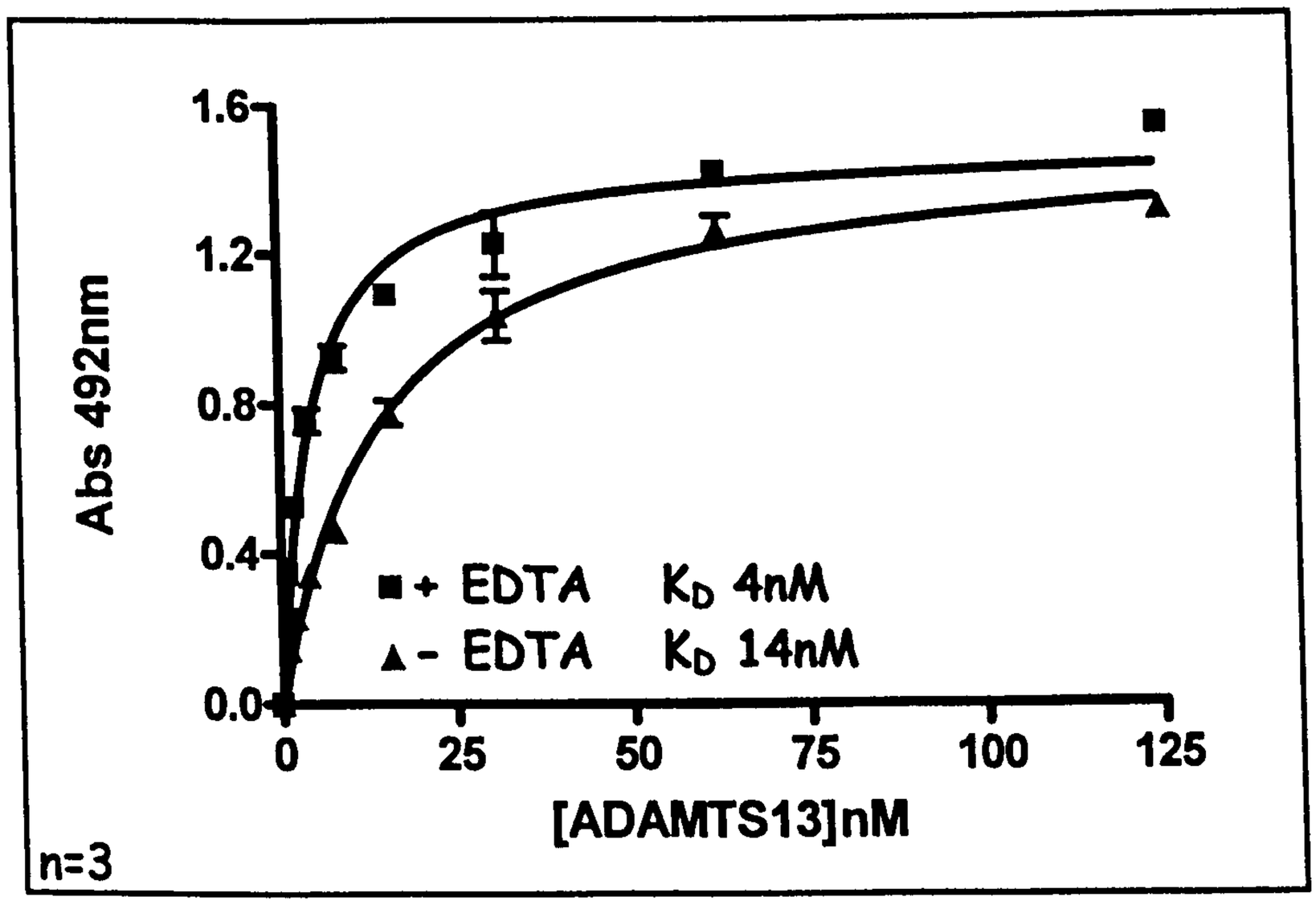


Figure 5.14 Binding of ADAMTS13 to VWF +/- EDTA

In the presence of EDTA, ADAMTS13 binds to VWF with K_D 4nM. In the absence of EDTA binding is decreased, K_D 14nM, suggesting that in the absence of EDTA some residual ADAMTS13 enzymatic activity occurs. (Error bars represent the mean and standard deviation of 3 separate experiments)

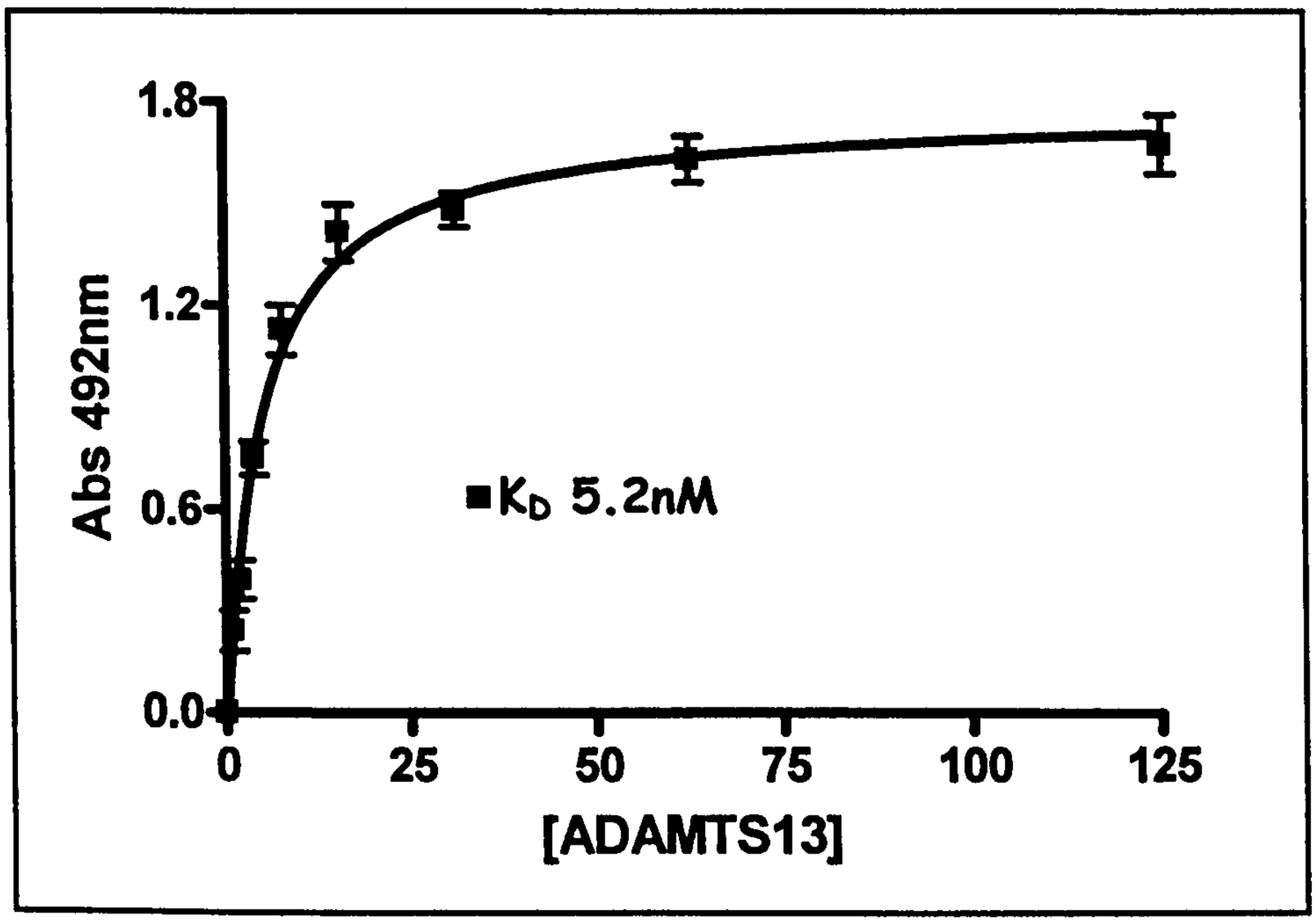


Figure 5.15 Binding of ADAMTS13 active site mutant to VWF

An ADAMTS13 active site mutant that was unable to cleave VWF was bound to immobilised VWF as described. The active site mutant bound to VWF with similar affinity to wild type ADAMTS13 +10mM EDTA, K_D = 5.2nM. (Error bars represent the mean and standard deviation of 3 separate experiments)

5.6.2 Binding of ADAMTS13 to Neu and PNG-VWF

To investigate the binding of ADAMTS13 to Neu- and PNG-VWF, MaxiSorp plates were coated with 7.5μg/ml of control, Neu- or PNG-WF and the binding of ADAMTS13 in the presence of EDTA established as described. In all binding assays, wells were probed with anti-VWF-HRP to ensure that an equal amount each VWF preparation was bound to the plate. Neu-VWF bound ADAMTS13 with similar affinity to Ctrl-VWF; K_D 4.2nM±0.5 for Ctrl-VWF and K_D 4.6nM±0.6 for Neu-VWF.

PNG-VWF bound ADAMTS13 with significantly greater affinity (~4 fold), p= <0.001, with a of K_D 1nM±0.1 (Figure 5.16).

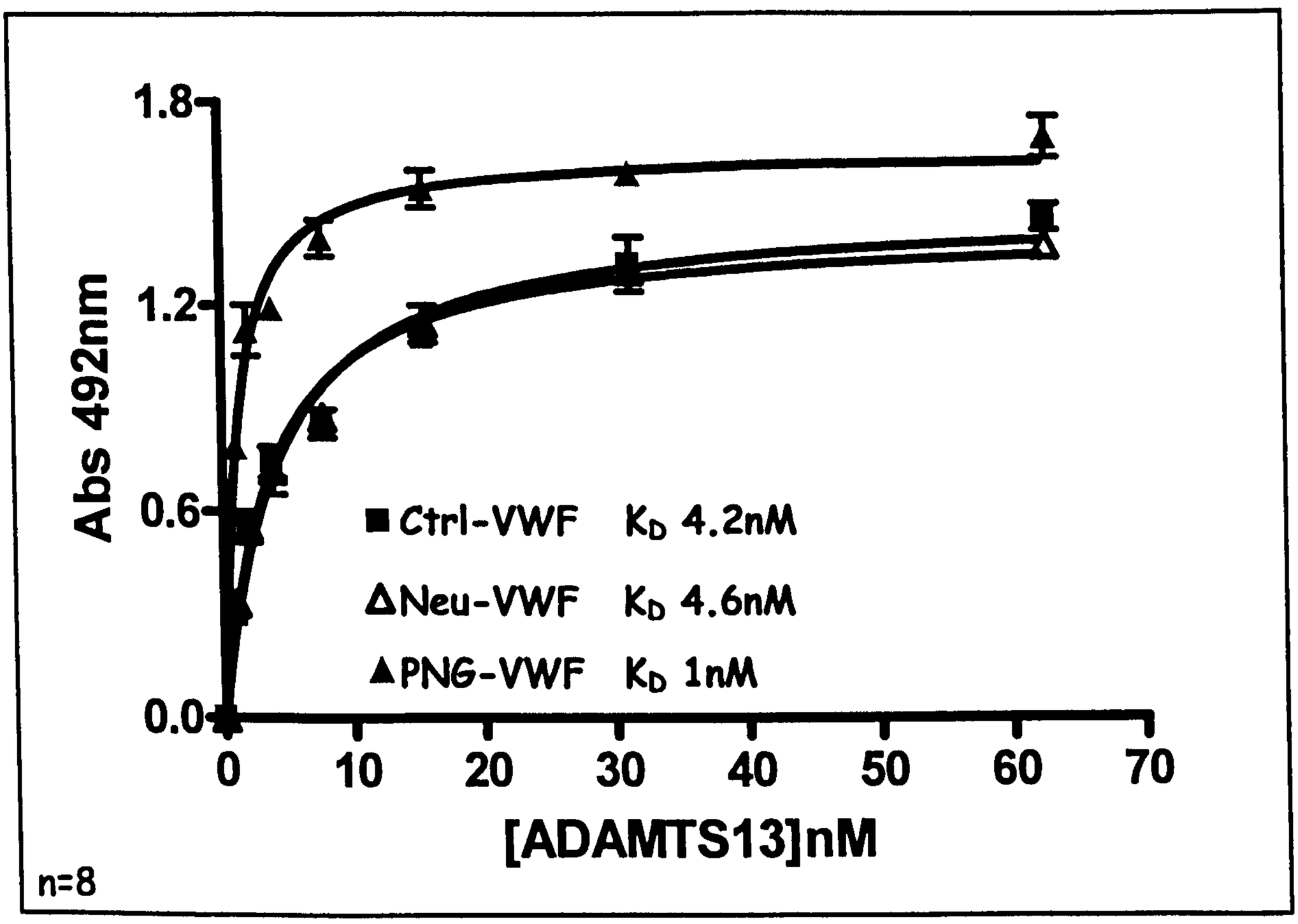


Figure 5.16 Binding of ADAMTS13 to immobilised VWF

Immobilised Ctrl-VWF and Neu-VWF bound ADAMTS13 with similar affinity, K_D 4.2nM and 4.6nM respectively. PNG-VWF bound ADAMTS13 with significantly higher affinity, (p=<0.001), K_D 1nM. (Error bars represent the mean and standard deviation of 8 separate experiments)

5.6.3 Binding of ADAMTS13 to Globular VWF

As observed, ADAMTS13 is able to cleave PNG-VWF in the absence of urea, suggesting it is able to interact with PNG-VWF whilst in a globular form. To further investigate this, the VWF:ADAMTS13 binding assay was modified to examine the interaction of ADAMTS13 with globular VWF.

Firstly, MaxiSorp plates were coated with an anti-VWF monoclonal antibody directed against the C-terminus of the molecule and this was used to capture globular VWF, which could then be incubated with increasing concentrations of ADAMTS13. Secondly, collagen plates were used to capture VWF, so that the binding of ADAMTS13 to collagen-bound VWF could be determined. Previous studies have shown that collagen bound VWF remains in a globular conformation,[368] however little is known about the interaction of ADAMTS13 with collagen-bound VWF.

When captured with the monoclonal anti-VWF antibody, Ctrl-VWF bound ADAMTS13 with low affinity, K_D 92nM±11, as did Neu-VWF, K_D 90nM±6.2. However, PNG-VWF still bound ADAMTS13 with high affinity, K_D 3.8nM±0.6 (Figure 5.17). Interestingly, collagen captured VWF bound ADAMTS13 with high affinity. As before no difference was observed between Ctrl-VWF and Neu-VWF; K_D 12nM±1.1 and 10nM±0.6 respectively, but once again PNG-VWF bound ADAMTS13 with higher affinity, K_D 3nM±0.2 (Figure 5.18)

To ensure that collagen did not bind ADAMTS13, collagen coated plates were incubated with 0-1μM ADAMTS13. No binding of ADAMTS13 to collagen was observed.

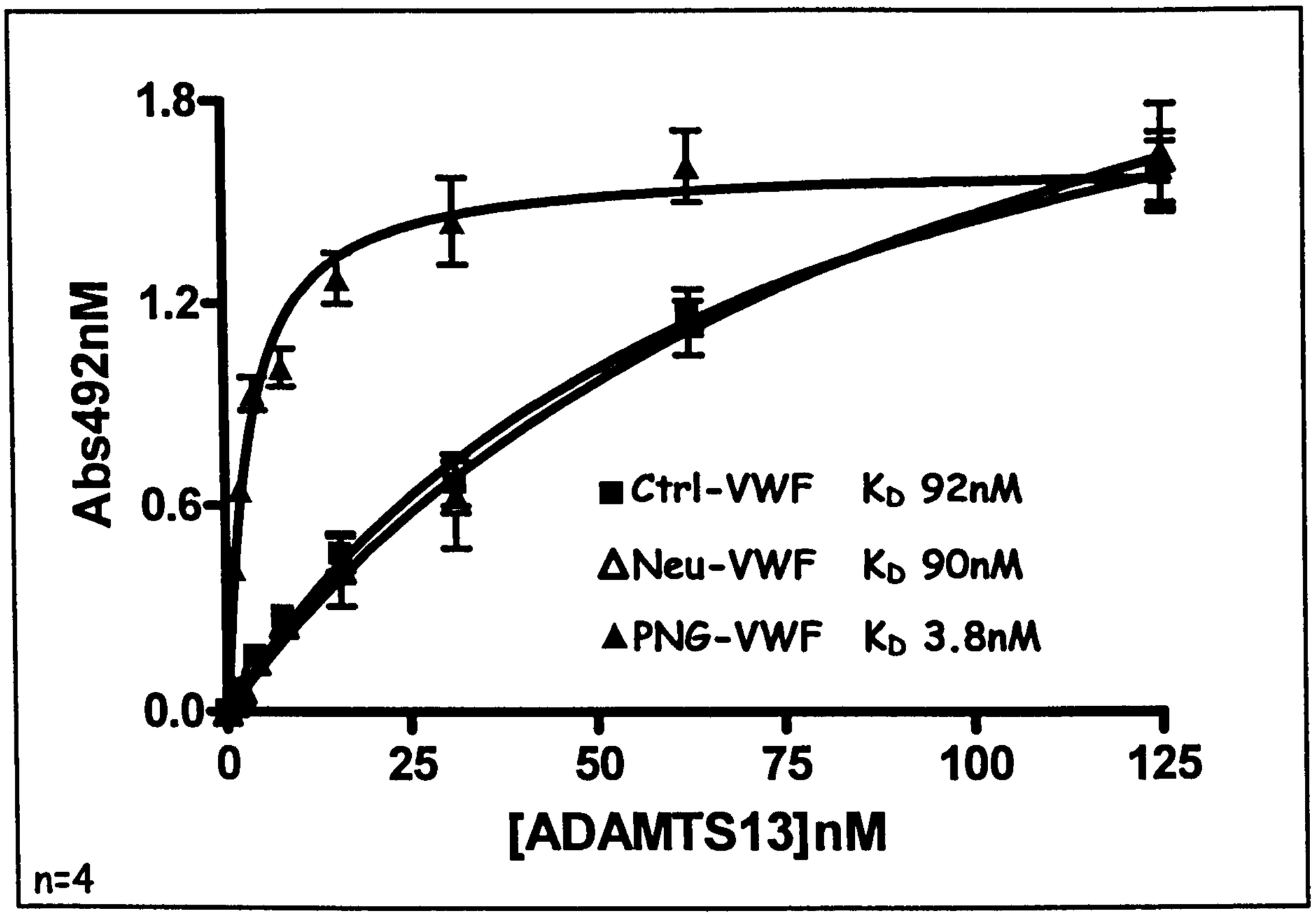


Figure 5.17 Binding of ADAMTS13 to globular VWF

VWF was captured by a monoclonal antibody directed against the C-terminus of the molecule to investigate binding of ADAMTS13 to globular VWF. Both Ctrl- and Neu-VWF bound ADAMTS13 with low affinity, K_D 92nM and 90nM respectively, indicating that the VWF was in a globular conformation not apt for ADAMTS13 binding. PNG-VWF was able to bind ADAMTS13 with high affinity, K_D 3.8nM suggesting that its confirmation was permissive for ADAMTS13 binding or the removal of the *N*-linked glycans prevented steric hindrance between ADAMTS13 and VWF. (Error bars represent the mean and standard deviation of 4 separate experiments)

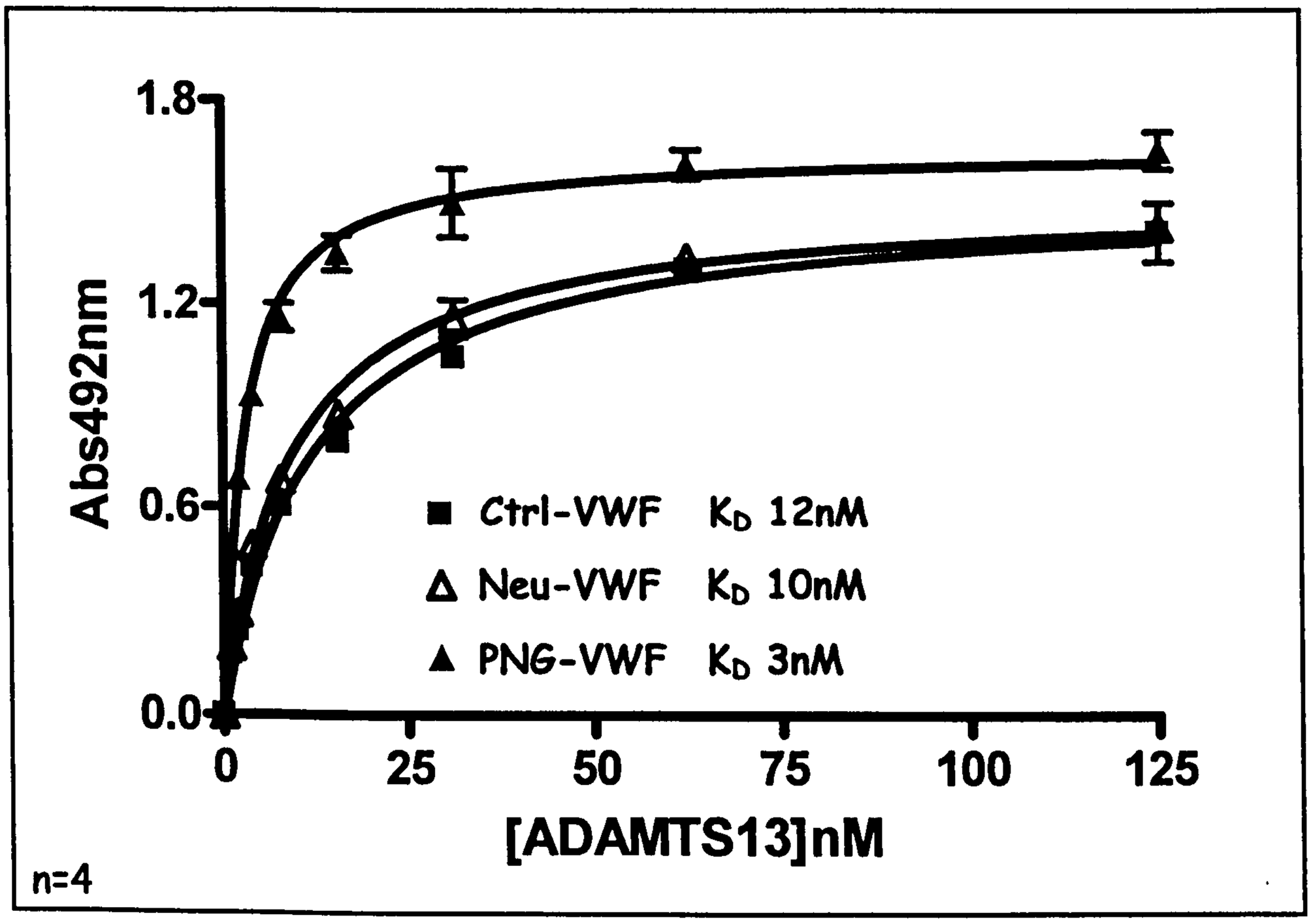


Figure 5.18 Binding of ADAMTS13 to collagen bound VWF

Collagen coated plates were used to capture VWF and binding of ADAMTS13 to collagen bound VWF analysed. Both Ctrl- and Neu-VWF bound ADAMTS13 with high affinity, K_D 12nM and 10nM respectively, indicating that collagen bound VWF was permissive to ADAMTS13 binding. As in the previous binding assays, PNG-VWF bound ADAMTS13 with higher affinity than control VWF, (K_D 3nM Vs 12nM). No binding of ADAMTS13 to collagen was observed. (Error bars represent the mean and standard deviation of 4 separate experiments)

5.7 DISCUSSION

Various studies have the reported the functional effects of VWF glycan modification, sometimes with conflicting results. However the naturally occurring effect of ABO blood group on VWF levels and susceptibility to ADAMTS13 cleavage gives a strong indication of their importance. The results presented in this chapter provide the first *in vitro* analysis of the effect of VWF glycan modification on the interaction of VWF with ADAMTS13.

5.7.1 Modification of VWF Glycan Structure

Modification of VWF glycan structure was performed by digestion of VWF with exo/endo-glycosidases to remove specific sugar residues or structures. In keeping with previous reports, >95% of VWF terminal sialic acid could be removed by digestion with α-2(3,6,8,9) neuraminidase as demonstrated by abolition of EBL binding to VWF.[261,262,264,270] EBL is a lectin specific for terminal sialic residues, preferentially binding sialic acid in an α2-6 linkage, but also recognising sialic acid in α2-(3,8,9) linkages.[369] The majority of human VWF sialic acid is either α2-3 or α2-6 linked.

In keeping with previous studies, digestion of VWF with β-galactosidase resulted in the removal of only ~20% of galactose residues,[264] as demonstrated by a drop in RCA-I binding. RCA-I is a lectin specific for terminal galactose resides.[370] Digestion of Neu-VWF with β-galactosidase resulted in the removal of ~47% of VWF galactose, once again in-keeping with previous studies.[261,264] It is not known why complete removal of VWF galactose cannot be achieved. A possible explanation is that some of the galactose resides are inaccessible to the β-galactosidase enzyme, although this seems unlikely in view of the observation that >90% of the *N*-linked glycans chains can be removed by PNGase F.

To remove whole *N*-linked glycan chains, VWF was treated with Peptide-*N*-glycosidase F (PNGase F) that cleaves high mannose, hybrid and complex *N*-linked glycan structures deaminating the asparagine residue to aspartic acid.[371,372] Removal of *N*-linked glycans was detected by analysis with Concanavalin A (Con A) lectin that recognises α-linked mannose residues in high mannose, hybrid and complex *N*-linked glycans.[373] Significantly, digestion of VWF with PNGase F resulted in the removal of >90% of the *N*-linked glycan chains. There have been conflicting reports concerning the effect of removal of VWF *N*-linked glycans from VWF. Federici *et al* (1984) demonstrated that treatment of VWF with endo-β-*N*-acetyl-glucosaminidase (endo F)

removed ~69% of the total carbohydrate content of VWF.[262] Endo F cleaves after the second GlcNAc residue in the basic $GlcMan_3GlcNAc_2$ core of high mannose, hybrid and complex *N*-linked glycans, thus leaving a single GlcNAc residue attached to the asparagine residue.[374] Since ~70% of the total VWF carbohydrate is *N*-linked glycan, 69% reduction in total sugar would reflect almost total removal of the *N*-linked glycan moiety. Surprisingly, a study by Fischer *et al* (1997) using recombinant VWF suggested that quantitative removal of glycans from rVWF could only be achieved after denaturation of the molecule.[375] Although not consistent with Federici *et al's* observation this might have indicated that some of the *N*-linked glycans are buried within the three-dimensional VWF protein structure and are not accessible to PNGase F digestion.

To further investigate this the method used to analyse *N*-linked glycan chain removal was modified to examine VWF in its "uncoiled" conformation. In the lectin ELISA method, VWF is captured by anti-VWF antibodies and can be assumed to remain in a globular state. Thus Con A may only bind to those glycans accessible on the protein surface, and the reduction in Con A binding observed with PNGase F treated VWF may represent the removal of only the accessible glycans. Other non-accessible *N*-linked chains may still be present within the folded VWF molecule but are unable to bind Con A. To detect any potential non-accessible N-linked glycans, VWF was bound directly to a MaxiSorp plate. As will be discussed later, this causes the molecule to uncoil into its elongated conformation and therefore should expose any buried glycan sites. However, the binding of Con A to PNGase F digested VWF using this system was still <10%, as observed with the lectin ELISA, demonstrating that VWF *N*-linked glycans are accessible to PNGase F while the molecule is in a globular conformation. Furthermore, VWF was denatured and subjected to PNGase F digestion and the extent of *N*-linked glycan removal compared to a no PNGase F control sample and non-denatured VWF digested with PNGase F as before. Under reducing SDS-PAGE in 3-8% gels the PNGase F digested samples migrate further than Ctrl-VWF, consistent with a reduction in molecular weight, however both the non-denatured and denatured VWF samples migrate at the same rate. Thus prior denaturation is not required for removal of VWF *N*-linked glycans. Therefore, in conclusion, PNGase F is capable of removing almost all the *N*-linked glycan chains from VWF.

Since it was possible to produce VWF almost devoid of *N*-linked glycans (PNG-VWF), the sialic acid content of PNG-VWF was analysed. PNG-VWF demonstrated 65%

binding to EBL compared to Ctrl-VWF, indicating that 35% of VWF sialic acid is presented on the *N*-linked glycan chains. This is consistent with the preliminary mass spectrometry analysis suggesting that 50% of VWF *N*-linked glycans present sialic acid.

5.7.2 Functional Analysis of Glycan Modified VWF

Conflicting evidence has been previously presented regarding the effect of VWF glycan modification on multimeric structure and collagen binding. Some studies have reported that removal of galactose or sialic acid and galactose affects multimer structure.[263-265] However, Federici *et al* reported no effect on VWF multimer structure following sialic acid and galactose removal, and furthermore removal of 83% of total VWF carbohydrate with neuraminidase, β-galactosidase and endo F did not alter multimeric structure.[262] Multimer analysis of glycan modified VWF in this study demonstrated that removal of VWF sugars had no effect on multimer structure. The only difference observed was a distinct band shift with PNG-VWF; however this is due to the decrease in molecular weight of the PNGase F digested molecule.

Analysis of collagen binding demonstrated that all the glycan modified VWF preparations had a similar affinity for collagen, K_D 1.3-1.8nM. The value for the K_D was calculated based on a VWF monomeric weight of 250kDa, and was in keeping with previously published values.[156]

5.7.3 Effect of Sialic Acid Removal on the Interaction with ADAMTS13

The sialic acid moiety of VWF has previously been shown to protect the molecule from proteolytic degradation, with AsVWF being more prone to digestion by plasmin, trypsin and chymotrypsin.[261,262] Furthermore the sialic component of other proteins has been shown to protect against proteolytic attack.[376,377] It was therefore hypothesised that Neu-VWF would be more susceptible to ADAMTS13 proteolysis compared to Ctrl-VWF. Furthermore in view of my previous observation with blood group specific VWF, that reduction in *N*-linked glycan length increased the rate of ADAMTS13 cleavage, it was expected that reducing the glycan chain by removal of sialic acid would also increase susceptibility to ADAMTS13 proteolysis. However, as was shown by CBA and multimer analysis, Neu-VWF is cleaved slower by ADAMTS13 than Ctrl-VWF. To further this observation, blood group specific VWF was digested with neuraminidase and then O-VWF, AB-VWF, Neu-O-VWF and Neu-AB-VWF were subjected to ADAMTS13 cleavage. The CBA showed that O-VWF VWF was cleaved faster than

AB-VWF VWF (as previously observed), both Neu-O-VWF and Neu-AB-VWF VWF were cleaved slower than the wild types, but the ABO effect on cleavage was lost, with both asialo preparations cleaved at the same rate. The loss of the ABO effect implies that either:

1) The sialic acid effect is dominant over the ABO effect, or

2) The ABO effect is mediated by its effect on the number of sialic acid residues presented on VWF glycans.

The blood group transferases and sialyltransferase enzymes are located in the post-Golgi[22,378] and may compete with each other for the glycan substrate. AB VWF may present more A and B structures and hence less sialic acid. However this seems highly unlikely; firstly the rate limiting step in the formation of A or B antigens is the formation of the H antigen. Thus any competition would be between the H transferase and the sialyltransferases and there is no evidence for increased H transferase expression in blood group A or B individuals. Potentially the formation of A or B structures may make it more difficult to sialylate the other branch(es) of an *N*-linked glycan chain. However the preliminary mass spectrometry analysis of VWF *N*-linked glycans did present a biantennary glycan with one branch terminated by the A antigen and the other branch terminated by sialic acid (see Chapter 4, figure 4.7). Finally, a study by de Romeuf *et al* demonstrated that ABO blood group had no effect on levels of VWF sialic acid or β1-4 linked galactose.[379]

Sialic acid imparts a negative charge to glycoproteins due its carboxyl group dissociating a proton at physiological pH.[380] The removal of VWF sialic acid may decrease the overall charge on the protein and this may affect the ability of ADAMTS13 to interact with VWF. However, analysis of ADAMTS13 binding to VWF (to be discussed in detail shortly) showed that Neu-VWF bound ADAMTS13 with similar affinity to wild type. The mechanism by which sialic acid removal from VWF affects susceptibility to ADAMTS13 proteolysis requires further investigation.

VWF sialic acid has been shown to be decreased in patients with primary pulmonary hypertension (PPH).[381,382] In a study by Collados *et al* patients with PPH presented *increased* VWF levels and *decreased* VWF sialic acid levels. Based on the patients' response to a vasodilator, the patients were grouped as either responders or non-responders. Interestingly, the "responders" group presented ~50% less sialic acid compared to control patients and lacked the highest molecular weight VWF multimers. The non-responders group presented ~70% less sialic acid than the control group, but

multimer analysis showed the presence of ultra large VWF mulitimers.[381] The authors concluded that the presence of the lower molecular weight multimers in the responders group may have represented increased consumption of VWF due to increased platelet binding and/or increased cleavage of VWF, (based on the previous observation that AsVWF is more prone to proteolytic degradation[261]), similar to a VWD type 2B phenotype. The presence of UL-VWF multimers was largely unexplained, although this is consistent with the observation made in this study that Neu-VWF is less susceptible to ADAMTS13 cleavage. The lower level of sialic acid in the non-responders group may represent a critical level of VWF sialic acid content, below which ADAMTS13 proteolysis is inhibited, however this is only a speculative suggestion.

5.7.4 Effect of *N*-linked Glycan Removal on the Interaction with ADAMTS13

In contrast to Neu-VWF, CBA analysis of ADAMTS13 cleavage assays showed that PNG-VWF was proteolysed significantly faster than Ctrl-VWF. This was expected since the N-linked glycans of other glycoproteins have been shown to protect against proteolytic cleavage. For example, non-glycosylated fibronectin is more susceptible to proteolysis than the glycosylated form and glycosylation of single-chain tissue-type plasminogen activator (tPA) at a specific site modulates proteolysis of the molecule by plasmin.[281,383]

The observation that PNG-VWF was cleaved faster by ADAMTS13 was extended by subjecting the modified molecule to ADAMTS13 cleavage in the absence of urea. Previous work has shown that VWF is not proteolysed *in vitro* by ADAMTS13 in the absence of denaturants[159,161]

CBA analysis showed that Ctrl-VWF was not proteolysed and also PNG-VWF incubated in the absence of urea and ADAMTS13 did not lose any collagen binding activity, demonstrating that PNG-VWF was stable for the duration of the reaction. Significantly, PNG-VWF was cleaved by ADAMTS13 in the absence of urea, indicating that removal of the *N*-linked glycans affects either the conformation of the VWF molecule or the accessibility of the ADAMTS13 cleavage site.

The binding of ADAMTS13 to VWF was investigated using a plate based assay taking advantage of the fact that VWF takes on its elongated conformation when bound to the plate surface.[384] Using this assay the K_D for ADAMTS13 binding to Ctrl-VWF was determined to be 4.2nM. This is close to a previous estimate by Majerus *et al* of 14nM using a similar assay.[222] The difference in the K_D is most likely explained by the

antibody used to detect bound ADAMTS13; Majerus *et al* detected ADAMTS13 with the anti-V5 epitope antibody where as I used a polyclonal anti-ADAMTS13 antibody which is likely to be more sensitive. Significantly, PNG-VWF bound ADAMTS13 with increased affinity, K_D 1nM.

Since PNG-VWF was cleaved in the absence of urea, the binding of ADAMTS13 to globular VWF was investigated. The binding assay was modified to capture VWF on to the plate via a monoclonal antibody directed against the C-terminal portion of the molecule. This antibody was shown not to inhibit ADAMTS13 cleavage of VWF or binding (data not shown). In this assay ADAMTS13 bound Ctrl-VWF with low affinity, K_D 90nM, reflecting the globular nature of VWF. Significantly, PNG-VWF bound ADAMTS13 with high affinity, K_D 3.8nM, thus consistent with the observation that PNG-VWF could be cleaved by ADAMTS13 in the absence of a denaturant.

Finally, the binding of ADAMTS13 to collagen bound VWF was investigated. Analysis of the morphology of collagen-bound VWF by atomic force microscopy demonstrated that it remained in a globular state with no apparent elongation.[368] ADAMTS13 bound to collagen-bound control and PNG-VWF with high affinity, but once again the affinity was greater for PNG-VWF, (K_D 10nM and 3nM respectively). The observation that ADAMTS13 can bind with high affinity to collagen bound VWF is significant itself, suggesting that the binding of VWF to collagen causes a conformational change that enables binding of ADAMTS13.

The exact mechanism by which the *N*-linked glycans of VWF mediate/facilitate the VWF:ADAMTS13 interaction is not yet resolved. The effect may be due to steric hindrance by the glycans affecting the interaction between the molecules. If the glycan-protein linkage is flexible the glycan may be able to cover a portion of the protein surface and protect it from proteolytic attack.[383] In the case of VWF, the most likely candidate glycans would be N1515 or N1574. Potentially one or both of these glycans may define access to the ADAMTS13 cleavage site. Equally, ADAMTS13 binding sites or sites of access to the cleavage site could theoretically be masked by the presence of an *N*-linked glycan chain. This might explain why ADAMTS13 can bind with increased affinity to PNG-VWF, particularly when VWF is in a globular conformation. Steric hindrance may also provide a suitable explanation for the observation that PNG-VWF is cleaved by ADAMTS13 in the absence of urea, with the cleavage site protected by *N*-linked glycosylation and removal of glycans allowing ADAMTS13 to access the cleavage site. However, although PNG-VWF is cleaved without urea, the rate of

proteolysis is increased in its presence, implying that the molecule still needs to undergo a conformational change to allow efficient ADAMTS13 cleavage. Therefore removal of VWF *N*-linked glycans may affect the conformation of the molecule, making it more permissive to ADAMTS13 binding and cleavage.

In conclusion this Chapter represents the first analysis of VWF glycan modification on susceptibility to ADAMTS13 cleavage, demonstrating that removal of terminal sialic acid residues reducing the rate of cleavage, while the removal of whole *N*-linked glycan chains enhances ADAMTS13 cleavage and binding. These results however, do not indicate whether this is a global effect of glycan modification, or if modification of specific VWF glycan sites results in the altered cleavage patterns observed. Although it is not possible to prevent sialylation at specific sites, *N*-linked glycosylation at specific sites can be prevented and this forms the basis for the next chapter.

CHAPTER 6

6. EXPRESSION AND CHARACTERISATION OF VWF A2 DOMAIN GLYCOSYLATION MUTANTS

6.1 INTRODUCTION

From the results obtained in the previous chapter it is apparent that the *N*-linked glycans of VWF affect the VWF-ADAMTS13 interaction. Removal of the *N*-linked glycans from VWF increases the rate at which the molecule is cleaved by ADAMTS13 and increases the affinity with which ADAMTS13 can bind to VWF. The removal of the *N*-linked glycans with PNGase F is non-specific however, and it maybe the case that only certain *N*-linked sites affect the interaction of ADAMTS13 with VWF. The most likely candidates are hypothesised to be the two A2 domain *N*-linked glycans, located at sites N1515 and N1574, that occur in the vicinity of the ADAMTS13 cleavage site at Y1605M1606. As demonstrated in Chapter 4, both these potential glycosylation sites are occupied and therefore may play an important role in mediating the effect of *N*-linked glycosylation on the interaction of VWF with ADAMTS13.

To further investigate this, the full length VWF (FL-VWF) cDNA was prepared in a mammalian expression vector and the N1515 and N1574 glycan sites were mutated individually and as a pair. Recombinant VWF (rVWF) was then expressed in HEK293T cells and its functional activity and glycan content analysed. Finally mutated VWF was cleaved by ADAMTS13 and the extent of cleavage compared to that of wild type rVWF.

6.2 Construction of a Full Length VWF Expression Vector and Mutagenesis of N1515 and N1574

The mammalian expression vector pSVhVWF, containing the full length VWF cDNA, was a kind gift from Dr Said Enyayt, (Birmingham's Children's Hospital). Sequencing of the VWF clone provided showed the sequence to be 8676bp long, with the first 234bp comprising part of the 5'UTR. The sequence has been numbered relative to the ATG start codon, thus bases -234 to 0 represent the 5'UTR. An EcoRI site was located at bases -234 to -229.

To facilitate efficient mutagenesis of the VWF gene, a smaller fragment of the cDNA sequence was generate by restriction digest and cloned into the pGEM cloning vector. Full length VWF cDNA was then cloned into the pBS cloning vector (that had been mutated to remove the KpnI restriction site), using a number of steps and then cloned into the mammalian expression vector pcDNA3.1 for expression in HEK293T cells. Figure 6.1 shows a diagrammatic representation of the VWF cDNA with selected restriction sites and the restrictions fragments used to prepare the VWF construct.

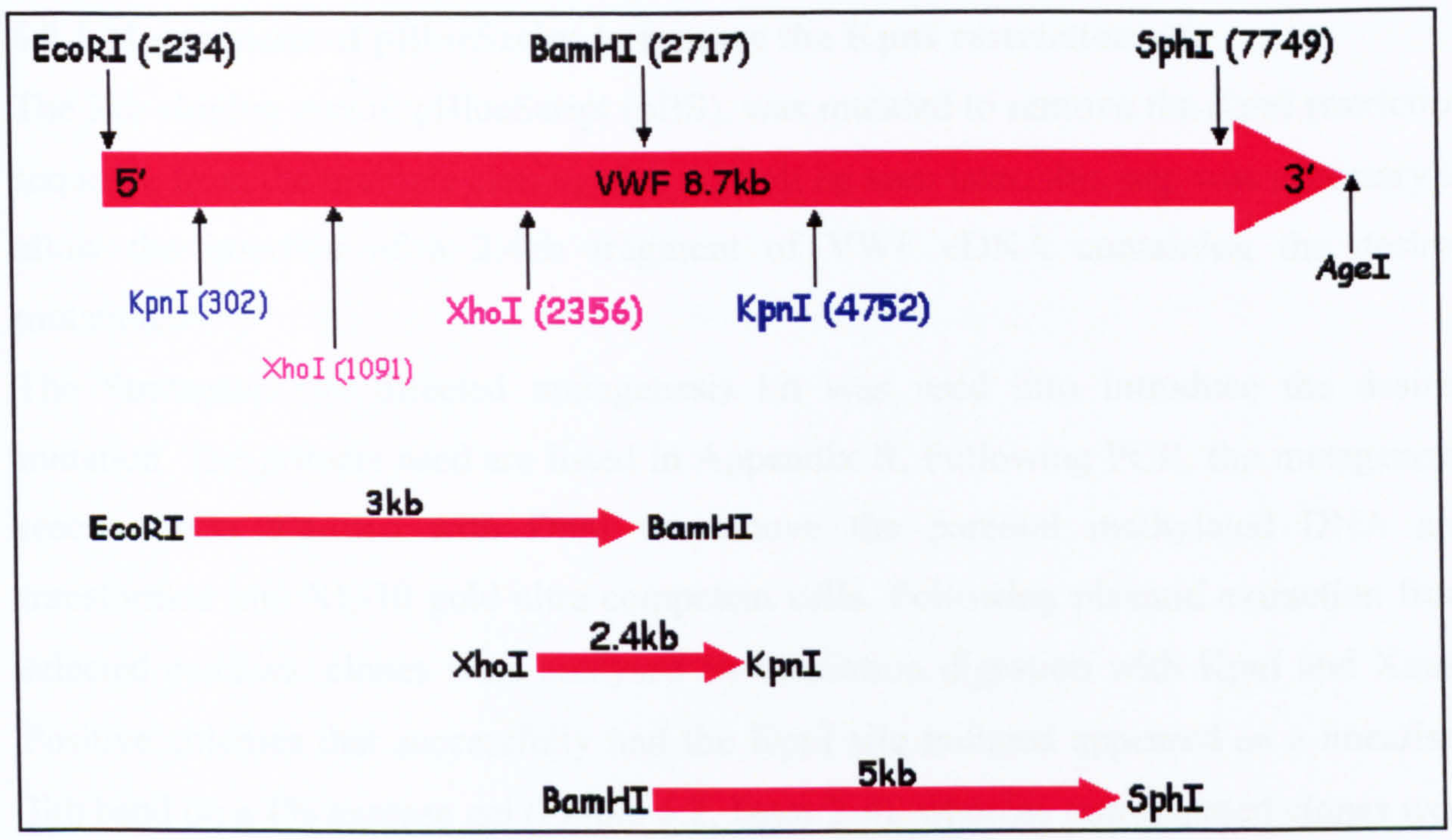


Figure 6.1 VWF restriction sites and digestion fragments

The VWF cDNA contained in pSVhVWF is ~8.7kb with the first 234bp comprising part of the 5'UTR. Base number 1 is taken from the start codon. Shown on the figure are the restriction fragments used to prepare the final VWF construct. The 3' AgeI site was introduced by PCR of the 3' end of the sequence described in section 6.1.2.

6.2.1 Mutagenesis of pBlueScript to remove the KpnI restriction site

The 3kb cloning vector, pBlueScript (pBS), was mutated to remove the KpnI restriction sequence from the multiple cloning site. As will be seen later, this step was necessary to allow the insertion of a 2.4kb fragment of VWF cDNA containing the desired mutations.

The Stratagene site directed mutagenesis kit was used into introduce the desired mutation. The primers used are listed in Appendix II. Following PCR, the mutagenesis reaction was digested with DpnI to remove the parental methylated DNA and transformed into XL-10 gold ultra competent cells. Following plasmid extraction from selected colonies, clones were analysed by restriction digestion with KpnI and XmnI. Positive colonies that successfully had the KpnI site mutated appeared as a linearised 3kb band on a 1% agarose gel (Figure 6.2, lanes 2-4), whereas non-mutated clones were cut by both enzymes and appeared as two bands of ~1 and 2kb (Figure 6.2, lane 1). Clones were further verified by DNA sequencing and positive clones were labelled pBS^{-Kpn1}.

6.2.2 PCR of VWF 3' end

Sequencing of the pSVhVWF vector demonstrated that a number of useful restriction sites were located after the VWF cDNA sequence, and as such it would be impossible to remove an appropriate size fragment of VWF cDNA for mutagenesis and then replace it again. Therefore, PCR was used to generate a fragment of VWF cDNA comprising the final 955bp pairs, beginning at base 7487 of the sequence, encompassing the SphI site (see figure 6.1) and including the stop codon. As described in materials and methods, the PCR primers were designed to introduce at the 3' end an unique AgeI restriction site immediately after the stop codon, a SacI site immediately after the AgeI site, and 7 other bases pair to aid efficient restriction digest of the PCR product. At the 5' end of the PCR product the primers were designed to introduce an XbaI site flanked by 7 bases to aid restriction digestion. Following PCR, the reaction was digested with XbaI and SacI, then visualised on a 1.2% agarose gel. The resulting band of ~900bp, was consistent with the size of fragment expected (Figure 6.3A). Following purification from the gel, the fragment was cloned into the pBS^{-Kpn1} cloning vector, that had been digested with XbaI and SacI and treated with calf intestinal alkaline phosphatase (CIAP). Following transformation into DH5α cells and culture of obtained colonies,

clones were analysed by restriction digestion with XmnI – present in the vector only, and SphI – present in the insert only. Non-positive clones appeared as a linearised 3kb band on agarose gel electrophoresis (Figure 6.3B lane 1); positive clones were digested to two fragments of 2.6kb and 1.3kb (Figure 6.3B, lane 2). The presence of the insert was confirmed by DNA sequencing and the construct designated pBS^{-KpnI}VWF3'

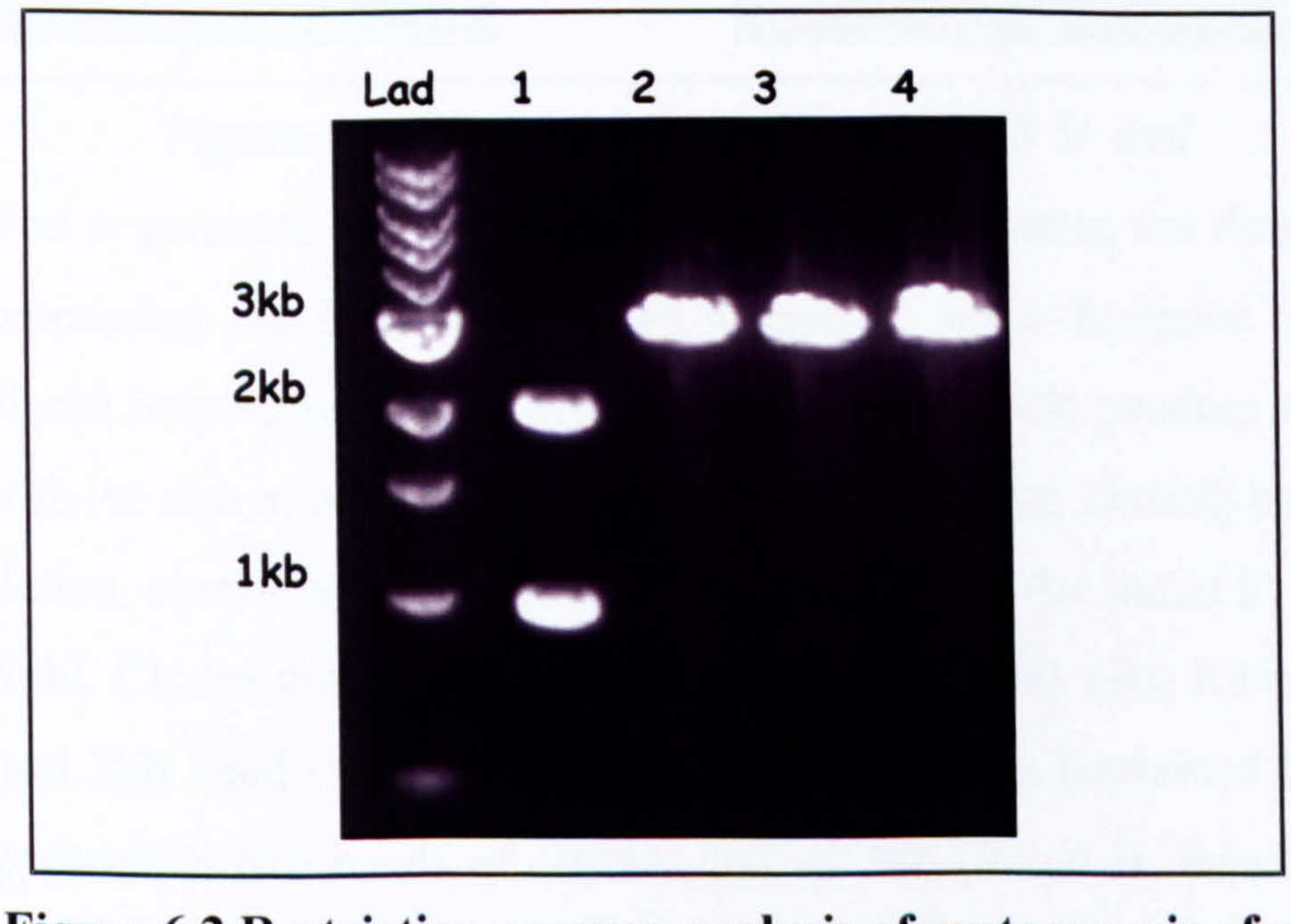


Figure 6.2 Restriction enzyme analysis of mutagenesis of pBS

Site directed mutagenesis was used to mutate the KpnI restriction site in the pBS cloning vector. Following digestion with XmnI and KpnI, clones containing the mutated site were only digested with XmnI and appeared as a linearised ~3kb band (lanes 2-4). Negative clones could be digested with both enzymes and appeared as two bands of ~1kb and 2kb (lane 1).

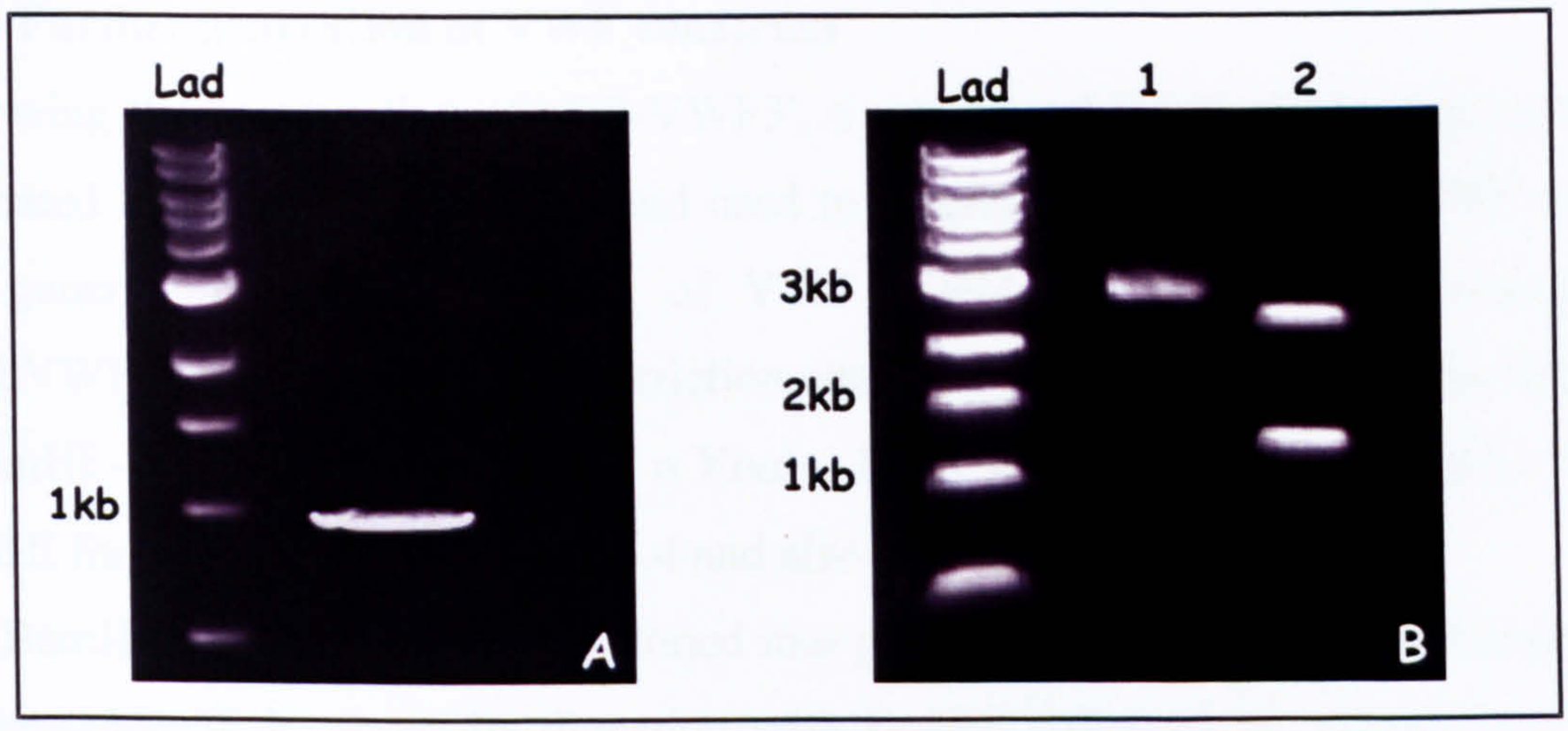


Figure 6.3 PCR and generation of VWF 3' end

PCR was used to generate a 3' end fragment of VWF spanning the final 955bp of the cDNA encompassing the SphI site. The PCR primers were designed to introduce an unique AgeI site immediately after the stop codon. The PCR product of ~900bp was consistent with the size of band expected (Panel A). Following cloning into pBS^{-KpnI} and plasmid isolation, clones were analysed for the presence of the insert by digestion with XmnI and SphI. Clones without the insert were only digested with XmnI and appeared as a linearised 3kb band (Panel B, lane 1). Positive clones contained both restriction sites and appeared as two bands of ~2.6kb and ~1.3kb (Panel B, lane 2). All positive clones were further confirmed by DNA sequencing and the construct named $pBS^{-KpnI}VWF3'$.

6.2.3 Further generation of VWF construct

Following the construction of pBS-VWF3', a number of VWF cDNA fragments were generated by restriction digestion and used to assemble the full length VWF construct and generate a smaller fragment of VWF cDNA for mutagenesis. Digestion of pSVhVWF with the appropriate restriction enzymes generated the following fragments: a BamHI - SphI fragment of ~5kb, a XhoI – KpnI fragment of ~2.4kb, and a EcoRI – BamHI fragment of ~ 3kb (Figure 6.4 and also see figure 6.1).

The BamHI – SphI fragment was cloned into pBS-VWF3' and clones were analysed for the presence of the insert by digestion with EcoRI, followed by visualisation on 1% agarose gels. Negative clones appeared as a ~4kb linearised bands and positive clones as ~8.6kb bands. Positive clones were sequenced to confirm the presence of the insert and to ensure that no random mutations were introduced. This construct was designated $pBS^{-KpnI}VWF(BamHI\text{-}AgeI)$.

The XhoI – KpnI fragment was cloned into pGEM and the presence of the insert confirmed by DNA sequencing and named pGEM-VWF(XhoI-KpnI).

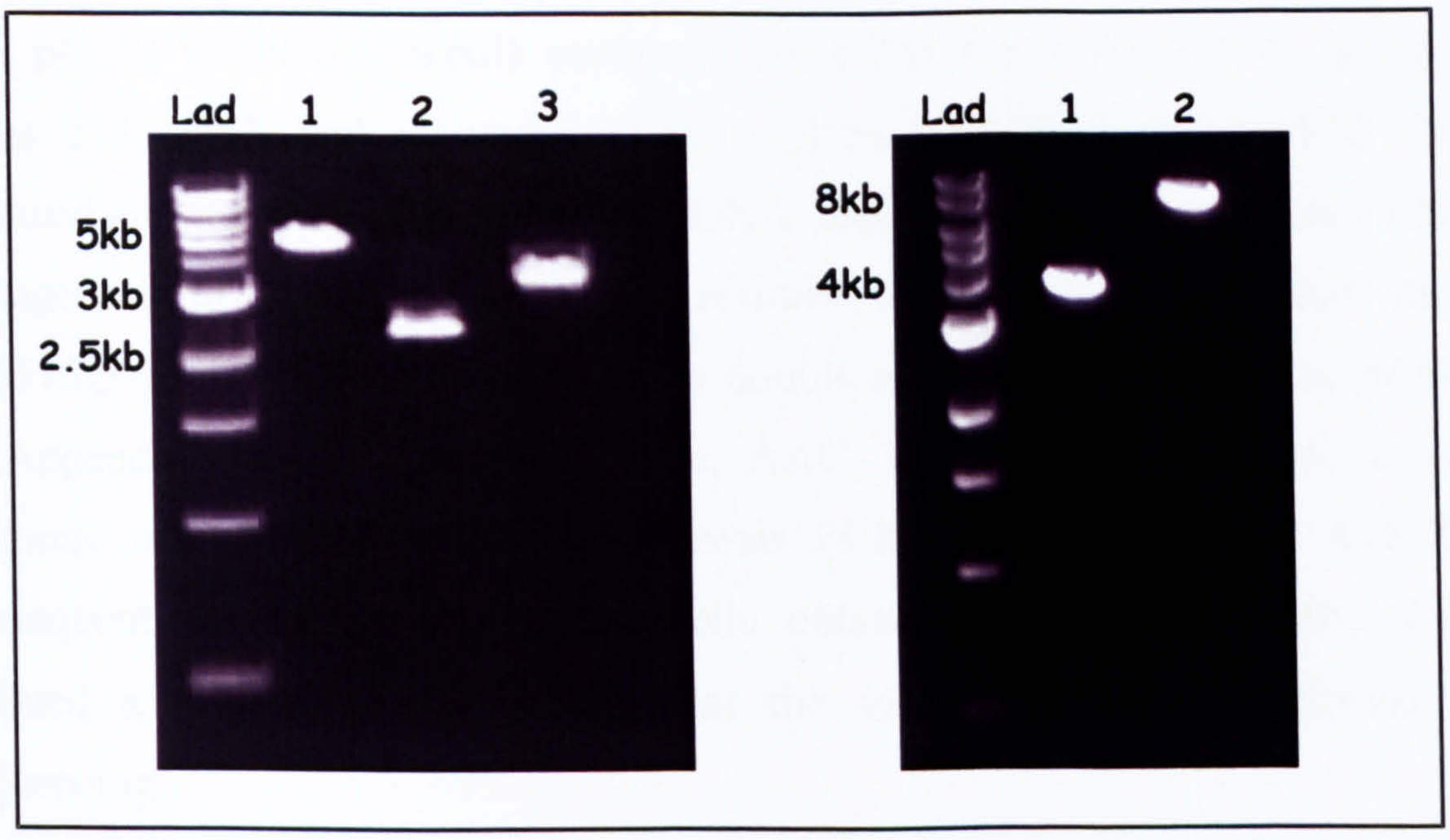


Figure 6.4 VWF restriction fragments and analysis of pBS^{-KpnI}VWF(BamHI-AgeI)

To further clone VWF three restriction fragments were generated by digestion of pSVhVWF: a ~5kb BamHI-SphI fragment (Panel A, lane 1), an ~2.4kb XhoI-KpnI fragment (Panel A, lane 2), and an ~3kb EcoRI-BamHI fragment (Panel A, lane 3). (Also refer to Figure 6.1). The BamHI-SphI fragment was cloned into pBS^{-KpnI}VWF3' and the presence of the insert confirmed by restriction digestion with EcoRI. Clones without the insert appeared as a linearised band of ~4kb consistent with the size of pBS^{-KpnI}VWF3'. Positive clones appeared as a linearised band of ~8.6kb demonstrating the presence of the 5kb insert. Positive clones were further verified by DNA sequencing and named pBS^{-KpnI}VWF(BamHI-AgeI).

6.2.4 Generation of VWF glycan mutants

The pGEM-VWF(XhoI-KpnI) construct contained the VWF cDNA sequence from bases 2356-4752, and encompassed the codons for N1515 and N1574. To prevent glycosylation at these sites the VWF cDNA sequence was mutated using site-directed mutagenesis to change the asparagine residues to glutamic acid residues individually (N1515Q or N1574Q) and together as a double mutant (DM). Using the primers listed in Appendix II, the asparagine codon, AAC, was mutated to CAA, encoding for glutamic acid. Following the mutagenesis PCR reaction, digestion with DpnI and subsequent cloning into XL-10 gold cells, obtained colonies were cultured and DNA isolated as described. The presence of the mutation(s) were confirmed by DNA sequencing.

Clones that contained the desired mutation(s) were digested from pGEM-VWF(XhoI-KpnI) with BamHI and KpnI and cloned into pBS^{-KpnI}VWF(BamHI-AgeI) and then re-sequenced to confirm the presence of the newly inserted fragment and the mutation.

6.2.5 Completion of FL-VWF construct and cloning into pcDNA3.1

To complete the FL-VWF construct, the ~3kb EcoRI-BamHI fragment described in section 6.1.3, comprising the 5' end of VWF (also see Figure 6.1), was cloned into pBS^{-KpnI}VWF(BamHI-AgeI) containing wtVWF or mutated VWF. Clones were analysed by restriction analysis with EcoRI; where positive clones migrated as an ~11.6kb band (Figure 6.5, lane 1) and negative clones migrated as an ~8.6kb band (Figure 6.5, lane 2). Furthermore, digestion of positive clones with KpnI demonstrated two bands of ~4.4kb and ~7.2kb, consistent with the presence of a second KpnI site within the EcoRI-BamHI fragment (Figure 6.5, lane3). This construct was named pBS^{-KpnI}FL-VWF

Finally, to complete the construct, the FL-VWF cDNA was digested from pBS^{-KpnI}FL-VWF with EcoRI and AgeI and cloned into pcDNA3.1 and named pcDNA3.1-wtVWF or pcDNA3.1-N1515Q/N1574Q/DM-VWF depending on the mutation present. Clones were then sequenced to confirm that no random mutations had been introduced.



Figure 6.5 Analysis of pBS^{-KpnI}FL-VWF

The 3kb EcoRI-BamHI fragment comprising the 5' end of VWF was cloned into pBS^{-} ^{KpnI}VWF(BamHI-AgeI) and analysed by restriction digest with EcoRI. Positive clones appeared as an ~11.6kb band consistent with the expected size for the full length VWF cDNA and pBS vector (Lane 1). Clones without the insert appeared as an ~8.6kb band (lane 2). Positive clones were also digested with KpnI and appeared as two bands of ~4.4kb and ~7.2kb consistent with the presence of two KpnI sites in the full length VWF cDNA (Lane 3). The FL-VWF was digested from pBS with EcoRI and AgeI then cloned into pcDNA3.1 and re-sequenced to confirm that no random mutations had been introduced.

6.3 EXPRESSION OF RECOMBINANT VWF

Expression of rVWF was performed as described (materials and methods section 2.14) by transfecting HEK293T cells with 33μg DNA per 10cm^2 dish using 10mM polyethylenimine (PEI) as the transfection reagent. Following 2 days incubation, conditioned media was collected and concentrated 10-fold as described and VWF concentration determined by VWF:Ag ELISA. No difference was seen in the level of expression between wtVWF, N1515Q, N1574Q and the DM, with ~20μg/ml of each concentrated sample being obtained (Figure 6.6). Four separate transfections were performed, each with a similar level of VWF expression (~20μg/ml concentrated), indicating the reproducibility of this transfection method and demonstrating that all the mutants could be synthesised and secreted as efficiently as wild type. In all transfection experiments control cells were transfected with empty pcDNA3.1 plasmid, and no VWF expression was observed (Figure 6.6)

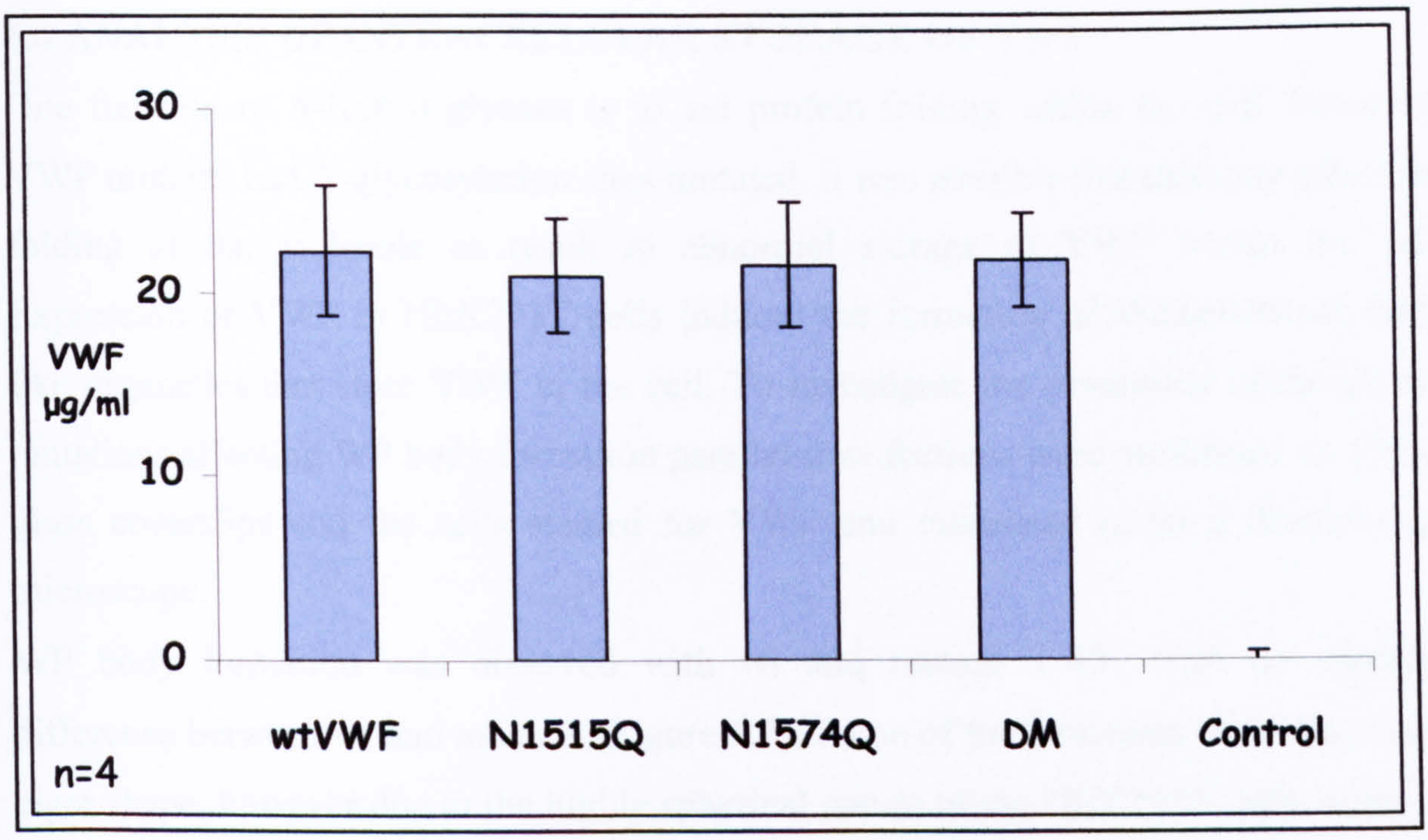


Figure 6.6 Expression of rVWF in HEK293T cells

Recombinant VWF was expressed in HEK293T cells using 10mM PEI as transfection reagent. Conditioned media was concentrated 10 fold and analysed for VWF content. No difference was observed in the amount of VWF expressed between wt, N1515Q, N1574Q and the DM. No VWF expression was observed when cells were transfected with empty pcDNA3.1 vector (control).

(Error bars are the mean and standard deviation of the VWF concentration obtained from 4 separate transfections)

6.4 ANALYSIS OF INTRACELLULAR STORAGE OF VWF

One function of *N*-linked glycans is to aid protein folding within the cell. Since the VWF mutants had *N*-glycosylation sites mutated, it was possible that this may affect the folding of the molecule or result in abnormal storage of VWF within the cell. Expression of VWF in HEK293T cells induces the formation of Weibel-Palade body like organelles that store VWF in the cell. To investigate the possibility of the glycan mutations affecting WP body formation parallel transfections were preformed on 13mm glass coverslips and the cells stained for VWF and visualised under a fluorescence microscope.

WP body formation was observed with wt and mutant VWF, with no apparent difference between wt and mutants (Figure 6.7). Some of the structures have the classic cigar shape, however due to the highly spherical nature of the HEK293T cells, many of the WP bodies have a more rounded appearance. No WP bodies were observed in control cells transfected with empty pcDNA3.1 vector

This, in conjunction with the similar expression levels between wt and mutant VWF, indicates that the *N*-linked glycans at sites N1515 and N1574, do not influence secretion or storage of VWF.

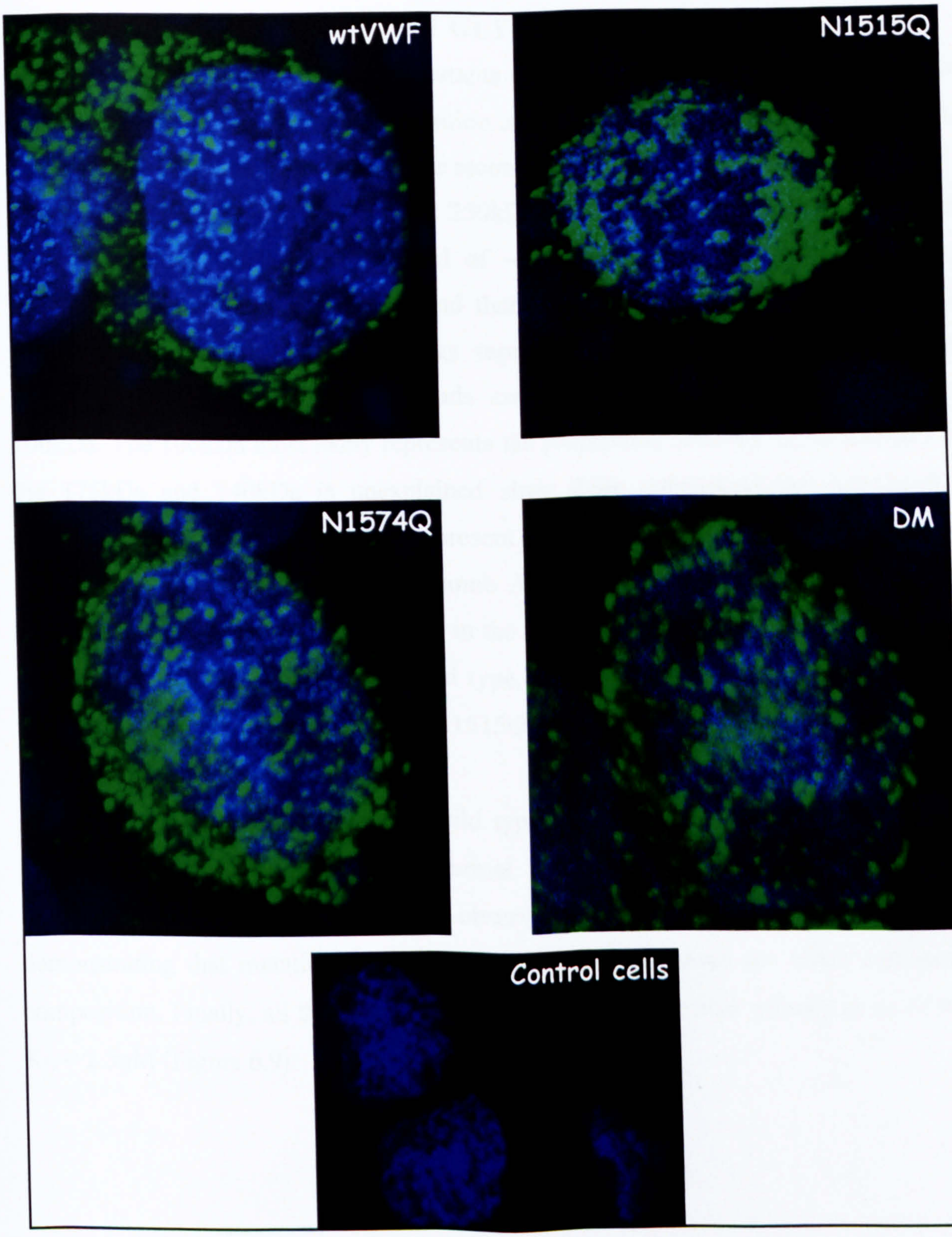


Figure 6.7 Analysis of intracellular storage of VWF

Transfected and non-transfected control cells were stained with anti-VWF antibodies and visualised under a fluorescence microscope. WP body formation was seen with wtVWF and mutant VWF, with no observable differences. No WP body formation was seen in the control cells.

6.5 CHARACTERISATION OF VWF GLYCAN MUTANTS

Wild type VWF and the VWF glycan mutants were analysed by reducing SDS-PAGE in 3-8% gels to determine subunit composition and by CBA and multimer gel analysis to determine the multimeric structure of the recombinant VWF (Figure 6.8A)

Under reducing SDS-PAGE a major 250kDa band was observed consistent with monomeric VWF. A faint larger band of ~350kDa was also present, representing unprocessed proVWF. The doublet band that runs below the 250kDa band was also present. As discussed before this may represent an altered glycosylation pattern. Furthermore a number of smaller bands are also present at 176kDa, 140kDa and 100kDa. The 100kDa most likely represents the propeptide, however the appearance of the 176kDa and 140kDa is unexplained since these correspond the ADAMTS13 cleavage product bands. Either they represent naturally occurring by-products of VWF synthesis or HEK293T cells possess some ADAMTS13 expression and activity. As expected there is also a slight difference in the rate of migration between the bands, with N1515Q and N1574Q further than wild type, due to the absence of one glycan chain and the DM migrating further than N1515Q and N1574Q, due the absence of two glycan chains.

Multimer analysis demonstrated that wild type rVWF presented a full range of VWF multimers and was comparable to normal plasma (Figure 6.8B) Furthermore, no difference in multimeric structure was observed between wt VWF and mutant VWF, demonstrating that mutation of VWF A2 domain glycans does not affect multimeric composition. Finally, all the mutants bound collagen with similar affinity to wt rVWF, $K_D = 2.5nM$ (Figure 6.9).

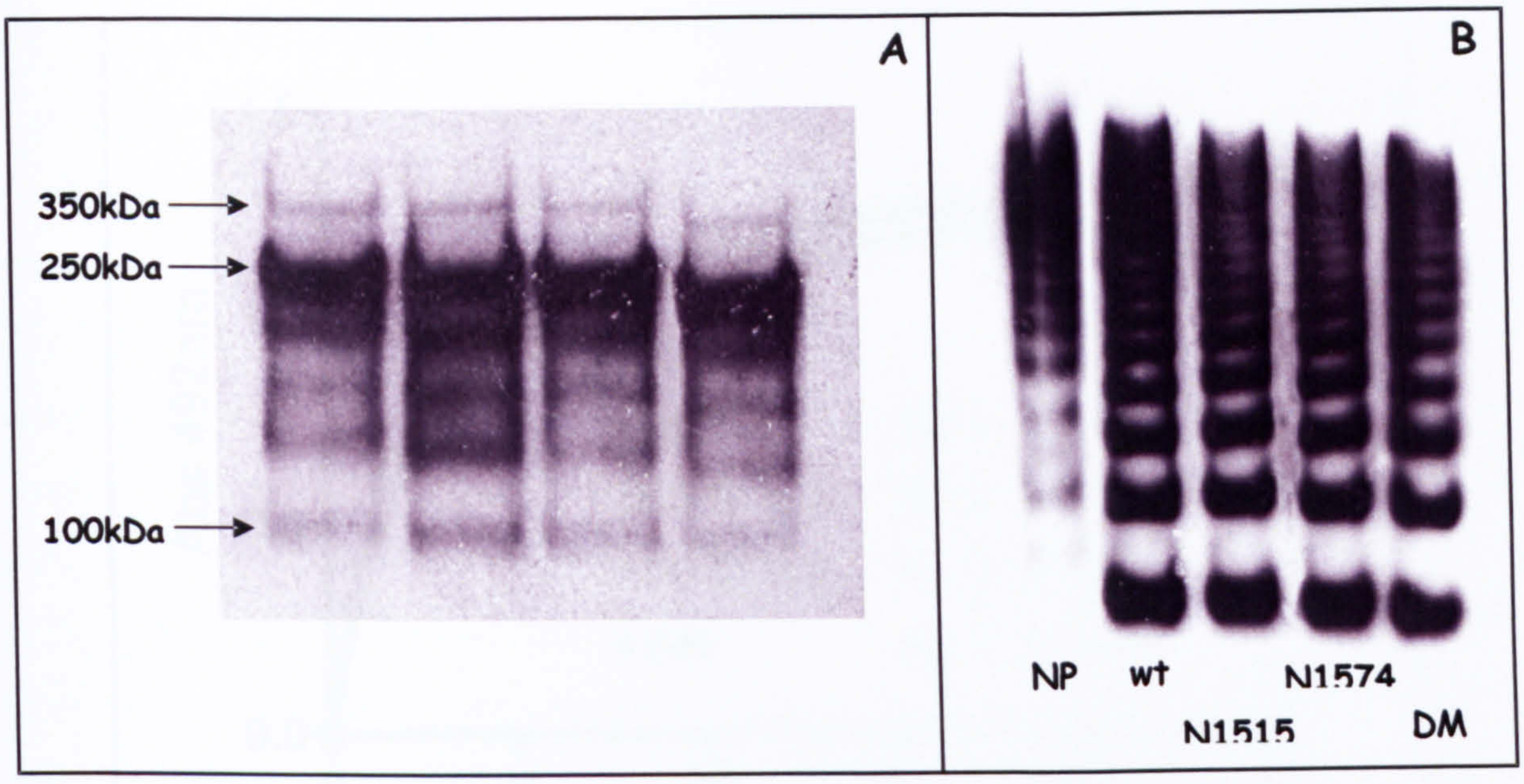


Figure 6.8 Characterisation of VWF glycan mutants

A) Analysis of rVWF by SDS-PAGE in 3-8% gels demonstrated the presence of a major 250kDa band consistent with monomeric VWF. As expected there is also a slight difference in the rate of migration between the bands, with N1515Q and N1574Q further than wild type, due to the absence of one glycan chain and the DM migrating further than N1515Q and N1574Q, due the absence of two glycan chains. A 350kDa band was also present, representing un-cleaved pro-VWF. A number of lower molecular weight bands are also present. The 100kDa band most likely represents the propeptide, however the origin of the other bands is not known. Interestingly they roughly correspond to the ADAMTS13 cleavage fragments of 176kDa and 140kDa.

B) Multimeric analysis of rVWF demonstrated that wt rVWF presented a multimer pattern comparable to normal plasma (NP). Furthermore no difference could be observed between the multimeric structure of the glycan mutants compared to wtVWF. It is possible to see that N1515Q and N1574Q have migrated slighter further than wtVWF and the DM has migrated slight further than N1515Q and N1574Q, consistent with the removal of specific glycan sites.*

* The difference in migration between wtVWF and the glycan mutants is more apparent on the multimer gel presented in Figure 6.12

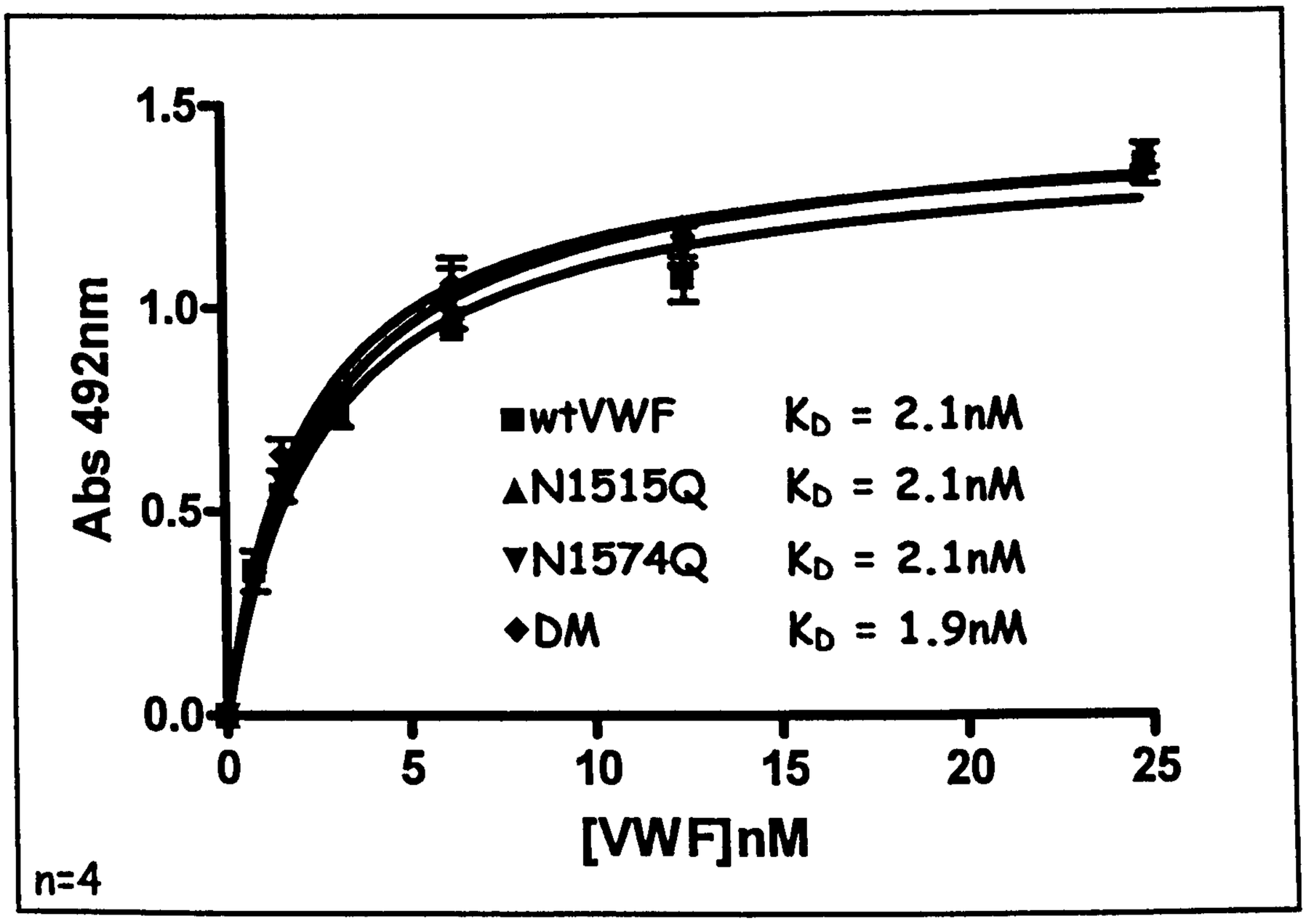


Figure 6.9 Collagen binding analysis of rVWF

The affinity of recombinant VWF for collagen was assessed using CBA. The VWF glycan mutants all bound collagen with similar affinity to wtVWF and plasma derived VWF. Confirming the observation with multimer gel analysis that mutation of *N*-linked sites N1515 and N1574 does not affect the multimeric structure of VWF.

6.6 ANALYSIS OF rVWF GLYCAN STRUCTURE

The glycan structure of HEK293T cell expressed rVWF was assessed using lectin ELISA. Plasma derived control VWF and rVWF samples were standardised for VWF antigen and captured on to a MaxiSorp plate by polyclonal anti-VWF antibodies.

EBL was used to detect terminal sialic acid residues, RCA-1 was used to detected galactose residues and Ulex europaeus was used to detect H antigen expression.

Analysis with EBL demonstrated that rVWF presents up to 50% less terminal sialic acid than plasma derived VWF (Figure 6.9) and analysis with RCA-1 demonstrated that rVWF presented ~20% more terminal galactose than plasma derived VWF. This is most likely due to the decreased amount of sialic acid leaving more galactose residues exposed. The presence of terminal sialic and galactose residues also shows that HEK293T are able to form complex *N*-linked glycan structures. Finally, as expected, no H-antigen could be detected on the rVWF samples.

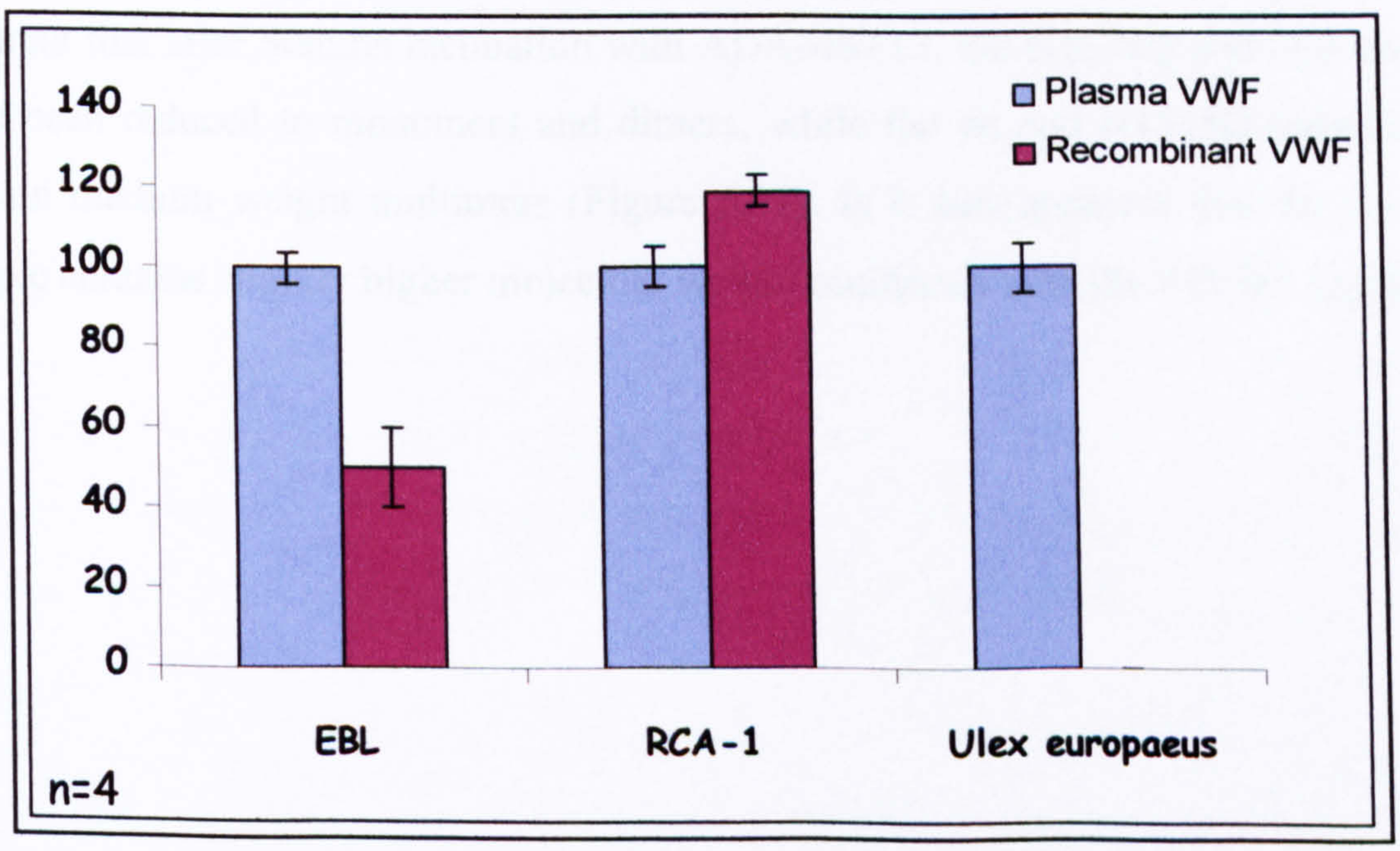


Figure 6.10 Lectin analysis of rVWF glycan structure

Compared to plasma derived VWF, rVWF presented up to 50% less sialic acid and ~20% more terminal galactose residues as demonstrated by binding to EBL and RCA-I lectins respectively. As expected, no H-antigen was detected on rVWF.

(Error bars are the mean and standard deviation of 4 recombinant VWF preparations compared to pooled normal plasma)

6.7 CLEAVAGE OF VWF GLYCAN MUTANTS BY ADAMTS13

The effect of mutating the A2 domain glycans on susceptibility to ADAMTS13 proteolysis was investigated by incubating mutant and wild type rVWF with ADAMTS13 in the presence of 1.5M urea and analysing the extent of proteolysis by CBA and multimer analysis.

The CBA demonstrated that at time points 60mins and 120mins N1574Q and the DM had been cleaved significantly ($p<0.0001$) faster then wtVWF or N1515Q (Figure 6.10), with both N1574Q and the DM mutant demonstrating only minimal collagen binding activity after 60mins incubation with ADAMTS13. A slight difference is also observed in the rate of cleavage between wtVWF and N1515Q, with wtVWF being proteolysed slightly faster as demonstrated by a greater reduction in CBA at time points 60mins and 120mins. Although this did not reach significance ($p=0.1$) (Figure 6.10).

This observation was also confirmed by low resolution multimer gel analysis. At time point zero the four VWF preparations have a similar multimer pattern; however it is apparent that after 60mins incubation with ADAMST13, the N1574Q and DM samples have been reduced to monomers and dimers, while the wt and N1515Q samples still contain medium weight multimers (Figure 6.11). Is it also apparent that the N1515Q sample contains slightly higher molecular weight multimers then the wtVWF sample.

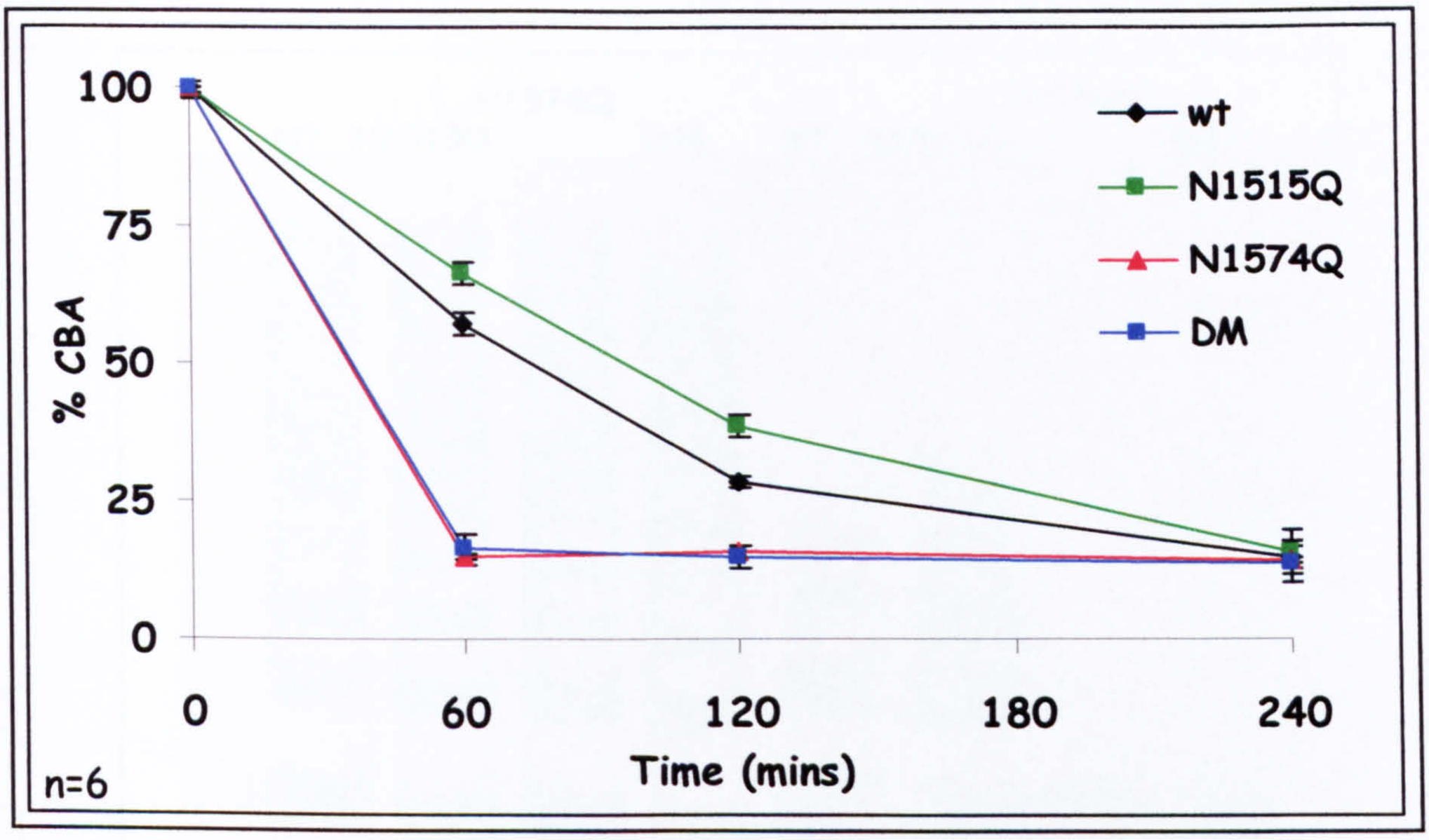


Figure 6.11 Collagen binding assay of ADAMST13 cleavage of VWF glycan mutants

Wild type and mutated rVWF was incubated with ADAMTS13 in the presence of urea and the extent of proteolysis analysed by CBA. N1574Q and the DM are more susceptible to ADAMTS13 proteolysis than wt or N1515Q as demonstrated by a significantly greater reduction in collagen binding activity after time 60mins and 120mins. The N1515Q mutant is cleaved slight slower by ADAMTS13 than wtVWF, demonstrated by slightly higher collagen binding activity at time 60mins and 120mins compared to wtVWF. (Error bars are the mean and standard deviation of 3 separate assay performed in duplicate, with rVWF from three separate transfections).

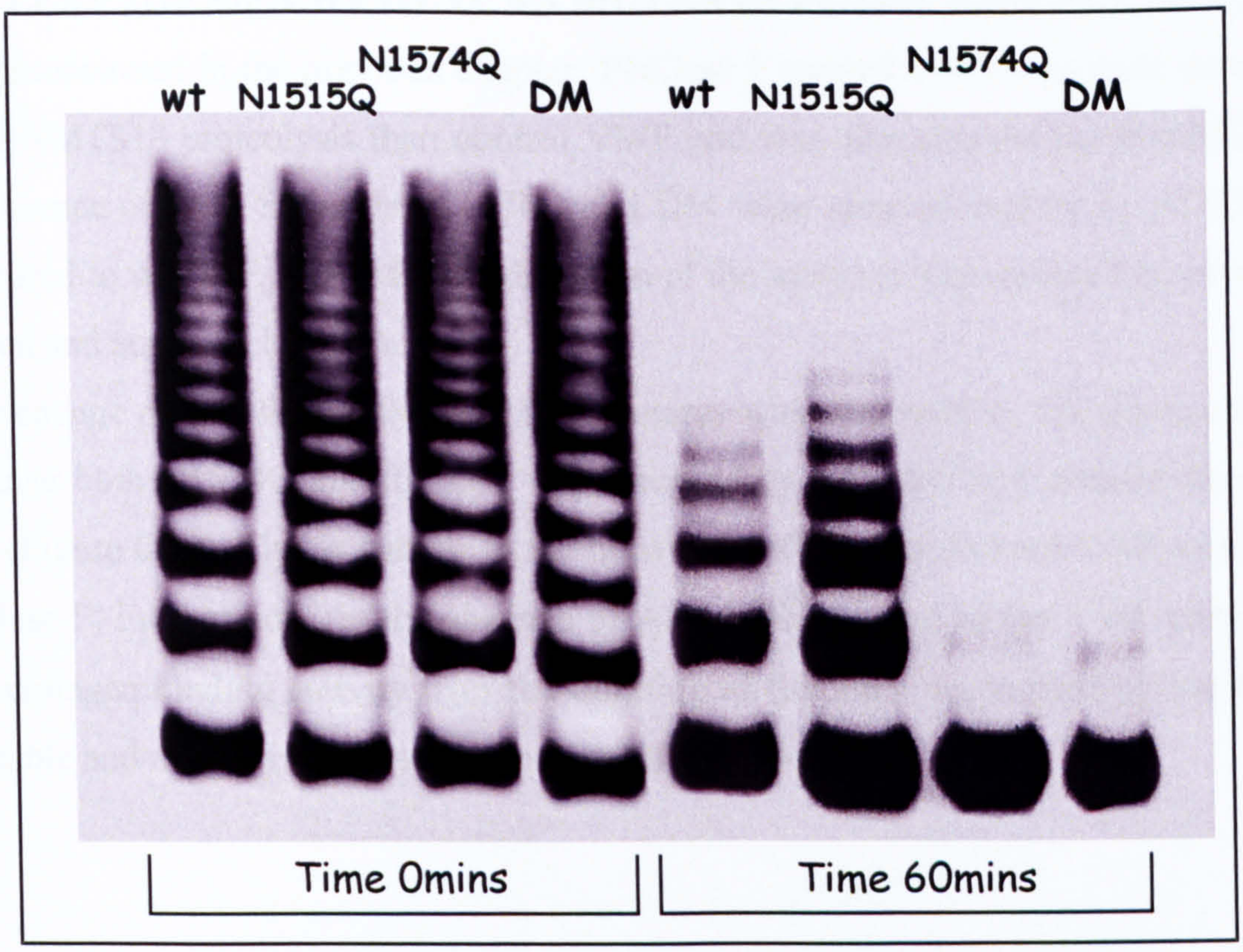


Figure 6.12 Multimer gel analysis of ADAMST13 cleavage of VWF glycan mutants

At time 0mins the multimer profile of wt and mutant VWF is similar. After 60mins incubation it is apparent that both the N1574Q mutant and the DM have been proteolysed faster by ADAMTS13 than the wt or N1515Q mutant, with only the presence of monomeric and dimeric VWF. It is also observable that the N1515Q mutant has been proteolysed slightly slower than wtVWF. Thus the multimer gel analysis confirms the results obtained with the CBA.

6.8 CLEAVAGE OF VWF GLYCAN MUTANTS IN THE ABSENCE OF UREA

As demonstrated in the previous chapter, PNGase F treated VWF was more susceptible to ADAMTS13 proteolysis than control VWF and was also cleaved by ADAMTS13 in the absence of urea. Since the N1574Q and DM were cleaved rapidly by ADAMTS13 compared to wtVWF, ADAMTS13 digestion of the mutants was repeated in the absence of urea and analysed by CBA.

No cleavage of wtVWF or the N1515Q mutants was observed in the absence of urea, however both N1574Q and the DM were cleaved by ADAMTS13 without the need of urea (Figure 6.12). This is similar to the behaviour of plasma derived VWF treated with PNGase F. Furthermore, in the absence of ADAMTS13 none of the VWF preparations lose collagen binding activity over the duration of the reaction, indicating that they are all stable and no other proteases are present (Figure 6.12).

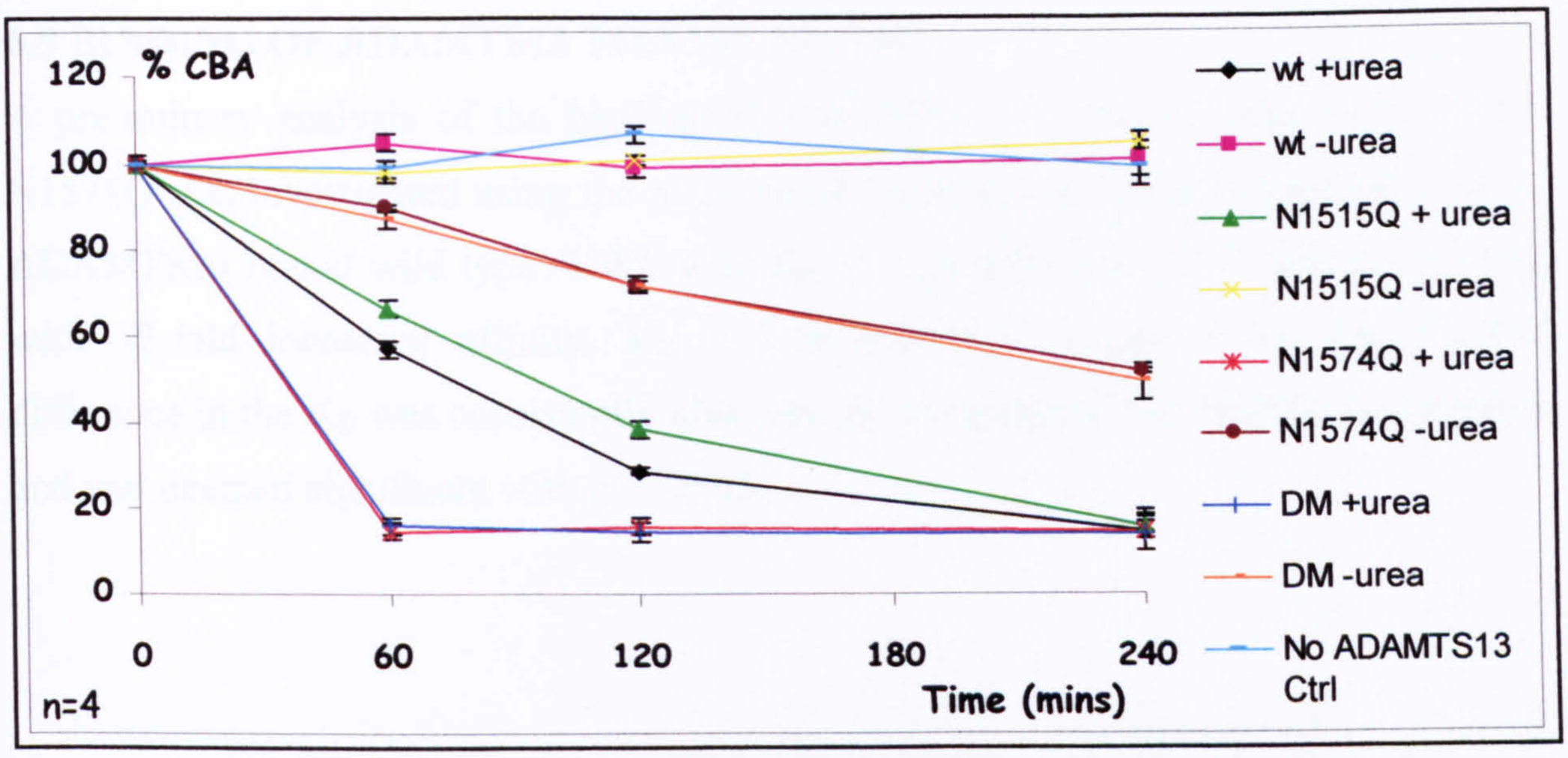


Figure 6.13 Collagen binding assay of ADAMTS13 cleavage of VWF glycan mutants in the absence of urea

VWF glycan mutants were subjected to ADAMTS13 cleavage in the absence of urea and extent of proteolysis analysed by CBA. In the absence of 1.5M urea wtVWF and N1515Q were not cleaved by ADAMTS13 and furthermore none of the samples lost collagen binding activity when incubated in 1.5M urea in the absence of ADAMTS13. For clarity this is shown as a single line on the graph (light blue). Both N1574Q and DM were proteolysed by ADAMTS13 in the absence of urea although the extent of proteolysis is greater in the presence of urea.

6.9 BINDING OF ADAMTS13 TO VWF N1574Q

A preliminary analysis of the binding of ADAMTS13 to recombinant wtVWF and N1574Q was investigated using the plate based binding assay as described previously. ADAMTS13 bound wild type rVWF with K_D = 7.5nM±0.5nM and bound to N1574Q with ~2-fold increased affinity, K_D = 3.5nM±0.6nM (Figure 6.14). The ~2-fold difference in the K_D was consistently observed in all repeats of the binding experiments and was deemed significant with p = <0.05.

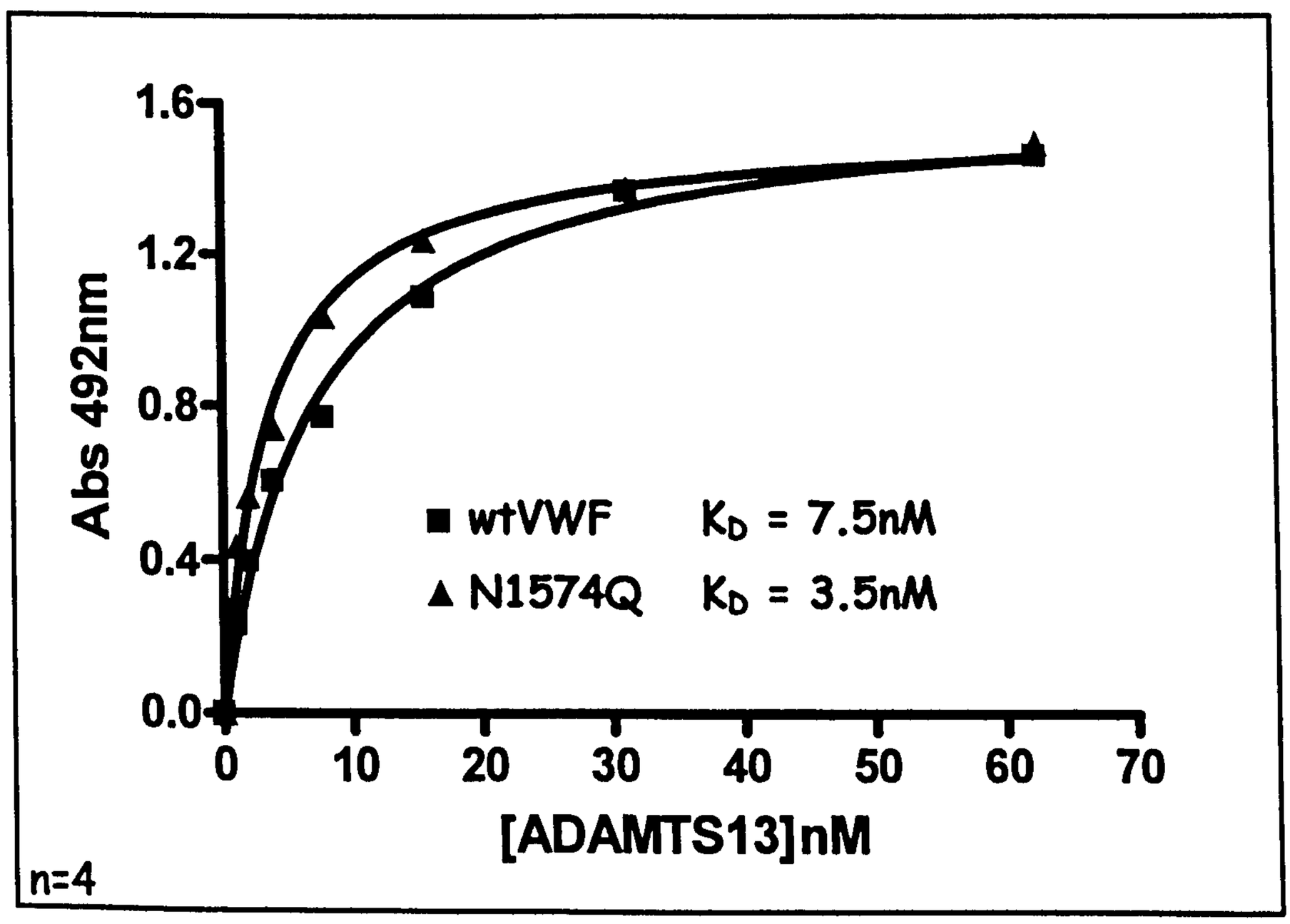


Figure 6.14 Binding of ADAMTS13 to recombinant VWF

ADAMTS13 bound to immobilised wild type rVWF with K_D = 7.5nM. ADAMTS13 bound to N1574Q with ~2-fold increased affinity, K_D = 3.5nM. In all experiments an ~2-fold difference was observed between the affinity of ADAMTS13 for wtVWF and N1574Q. (p = <0.05)

6.10 DISCUSSION

6.10.1 Expression of Recombinant VWF

The results presented in the previous chapter clearly demonstrate that the removal of VWF *N*-linked glycans increases the susceptibility of the molecule to ADAMTS13 cleavage, and allows ADAMTS13 to bind to VWF with increased affinity. However, since digestion of VWF with PNGase F results in the removal of virtually all the *N*-linked glycan chains, it is not known if the effect on the interaction with ADAMTS13 is due to the general removal of all the glycan structures or if only specific glycan sites are involved. If the effect of VWF *N*-linked glycosylation is mediate by specific sites, the most likely glycans to be implicated are the two A2 domains glycans, N1515 and N1574. As established in chapter 4, both these sites are occupied and both sites potentially present the blood group antigens and sialic acid. To specifically investigate the role of *N*-linked sites N1515 and N1574 in mediating the susceptibility of VWF to ADAMTS13 cleavage, FL-rVWF was produced in HEK293T cells with both sites mutated individually and as a pair, to prevent glycosylation.

The FL-VWF cDNA (a kind gift from Dr Said Enyayt) was provided in the mammalian expression vector pSV7d.[385] Since little information could be obtained about the pSV7d vector and its properties, the VWF cDNA was cloned into a high level mammalian expression vector, pcDNA3.1. This was achieved through a series of cloning steps, including the introduction of an unique AgeI restriction site at the 3' end of the sequence and the generation of 2.4kb fragment that encompassed the coding region for sites N1515 and N1574. Site directed mutagenesis was used to mutate the codons for the asparagine residues to glutamic acid, thus preventing the addition of an *N*-linked glycan at those sites.

The resulting VWF constructs, wt, N1515Q, N1574Q and the DM were transfected into HEK293T cells using polyethylenimine (PEI), which has been to shown to be a highly effective transfection reagent and is also extremely cost effective.[386]

A crucial role of *N*-linked glycosylation is mediating protein folding, often via the calnexin-calreticulin cycle.[387,388] For example; HIV type I glycoprotein 120, does not fold into its active state* in the absence of glycosylation.[389] Glycosylation at specific sites has also been shown to be important in mediating protein folding. Addition of a *N*-glycan chain at Asn 30 of human chorionic gonadotropin β-subunit is crucial for

---

* In its active state, HIV type I glycoprotein 120 binds to CD4 expressed on T helper cells, regulatory T cells, monocytes, macrophages, and dendritic cells.

efficient folding, whereas glycosylation at Asn 18 is not so important.[390] In light of this is was possible that the VWF glycan mutants would not be secreted or would be secreted, but at a reduced level. Moreover, *N*-linked glycosylation has been shown to essential for dimerisation of VWF monomers.[18] The observation that all the mutants were expressed at levels similar to wild type indicated that *N*-linked glycosylation at sites N1515 and N1574 is not required for dimerisation and furthermore does not appear to play an important role in the folding process of the molecule. It has also been previously observed that expression of VWF in HEK293T cells induces the formation of pseudo Weibel-Palade body type structures.[56] To investigate this, transfected HEK293T cells were stained with anti-VWF antibodies and visualised under a fluorescence microscope. Pseudo WP bodies were observed in all transfected cells, with no apparent differences in the size and number of WP bodies between wt and mutants. No WP bodies were seen in control cells that had been transfected with empty pcDNA3.1 vector, demonstrating that HEK293T cells do not express any endogenous VWF and the induction of the WP bodies is solely due to transfection of the cells with VWF cDNA. Due to the highly spherical nature of the HEK293T cells, many of the WP bodies appear as more spherical structures compared to the more classical "cigar shape." Thus N1515 and N1574 are not critical for WP body formation.

Analysis of wild type and mutant VWF demonstrated a normal multimer pattern, with the recombinant material exhibiting a full range of multimers, similar to normal plasma. In addition the collagen binding activity of the wild type and mutant VWF was similar to that of plasma derived VWF. Therefore, mutation of N1515, N1574 and both sites does not affect VWF multimeric structure or collagen binding. Analysis of the recombinant VWF samples in 3-8% gels under reducing conditions showed a major band of ~250kDa, and smaller less intense bands at ~176kDa, ~140kDa and 100kDa. The 100kDa band possibly represents the propeptide, however the nature of the 176kDa and 140kDa bands are unknown. Interestingly they appear to correspond to the ADAMTS13 cleavage products seen in normal plasma. This would suggest that HEK293T express a small quantity of ADAMTS13 that is able to process VWF. However multimer analysis of rVWF did not show the characteristic satellite bands indicative of ADAMTS13 proteolysis. Since the bands are too small to represent altered glycoforms they may be naturally occurring by-products of rVWF synthesis. A larger band of ~350kDa was also present, consistent with pro-VWF. Since the major species

present is the 250kDa band, HEK293T cells must possess furin activity to process VWF.

6.10.2 Analysis of Recombinant VWF Glycan Structure

A basic view of the glycan structure of rVWF was determined by lectin analysis with EBL and RCA-I. Since wtVWF migrated with the same apparent molecule weight as plasma derived VWF (pdVWF) it was assumed that all the *N*-linked glycan sites were occupied. This was interesting itself, since transient transfections often overwhelm the cells' processing capacity resulting in heterogeneously glycosylated products,[386] although it has been shown that all the potential *N*-linked sites of a protein can be glycosylated when transiently expressed. For example Rat CD39 contains seven potential *N*-linked sites, which have been shown to all be glycosylated when expressed in COS7 cells.[391] Mammalian cells lines have been shown to synthesize complex glycans[392] and this was confirmed by the ability of rVWF to bind EBL and RCA-I, highlighting the presence of sialic acid and terminal galactose residues that are indicative of complex glycan formation. As demonstrated by analysis with EBL, rVWF presented up to 50% less sialic acid than pdVWF. A possible explanation for this is the absence of α2-6 linked sialic acid residues. Analysis of rVWF expressed in Chinese Hamster Ovary (CHO) cells showed a total absence of α2-6 linked sialic acid.[375] This has also been demonstrated for recombinant EPO expressed in CHO cells.[393] Furthermore, analysis of the glycan structures produced by Baby Hamster Kidney cells demonstrated a lack of α2-6 sialic acid.[394] The galactose content of rVWF was shown by RCA-I binding to be ~20% higher than pdVWF, this is probably due to increased exposure of terminal galactose residues resulting from the decreased sialic acid content, rather than an increased total galactose content.

Although the presence of sialic acid and galactose indicate the synthesis of complex *N*-linked glycans, it is not known to what extent these complex structures are branched. From Matsui *et al's* study the majority of VWF *N*-linked glycans (70%) are of the bi-antennary type.[23] However tri-antennary and tetra-antennary glycans comprise 12.3% and 2.3% respectively of the total *N*-linked chains. It is not known if HEK293T cells are capable of forming tri- and tetra-antennary *N*-linked glycans, although EPO expressed in CHO cells has been shown to present tri- and tetra-antennary structures, so based on this it may be possible.[393] Finally, as expected, no H-antigen presentation was detected on rVWF.

6.10.3 ADAMTS13 Cleavage of VWF Glycan Mutants

In view of the observation made in the last chapter that PNG-VWF was proteolysed significantly faster than Ctrl-VWF, it was hypothesised that mutation of one or both of the A2 domain *N*-linked glycan sites would affect the susceptibility of VWF to proteolysis by ADAMTS13. Cleavage of wt and mutant rVWF in the presence of urea, followed by collagen binding and multimer analysis demonstrated that wtVWF and N1515Q were cleaved at a similar rate, although the N1515Q mutation did offer some slight protection against ADAMTS13 cleavage. Significantly N1574Q and the DM were proteolysed significantly faster than wtVWF. After 60mins incubation with ADAMTS13, N1574Q and the DM exhibited only minimal collagen binding activity. This was confirmed by multimer analysis that showed only the presence of monomers and dimers after 60mins incubation. The observation that N1515Q was cleaved at a comparable rate to wtVWF, implies that the critical glycan site is N1574. To further examine this ADAMTS13 cleavage assays were repeated in the absence of urea.

In the absence of urea no cleavage of wtVWF or N1515Q was observed, additionally all four samples (wt, N1515, N1574 and DM) all retained 100% collagen binding when incubated without ADAMTS13, indicating that the four preparations were stable over the duration of the reaction and that no other contaminating proteases were present. Significantly, N1574Q and the DM were proteolysed by ADAMTS13 in the absence of urea, similar to the observation made with PNG-VWF.

How the *N*-linked glycan at site N1574 affects cleavage is unknown. Once again it could be due to steric hindrance or a conformation effect. Specific *N*-linked sites have previously been shown to affect proteolysis. The addition of an *N*-linked glycan chain at Asn184 on tissue plasminogen activator reduces the rate at which the molecule is cleaved by plasmin.[383] The exact mechanism for this is undetermined, although evidence suggests it is due to the glycan covering a region of the protein surface preventing efficient proteolysis.[383] Also, the *N*-linked glycan at Asn281 in bovine lactoferrin, has been shown to protect the molecule against trypsin cleavage at the adjacent amino acid, Lys282, almost certainly via a direct steric hindrance effect.[395]

From the predicted model of the VWF A2 domain the N1574 site is predicted to occur on a loop region. Interestingly, the N1574 site occurs in fairly close proximity to some residues shown to be important for ADAMTS13 binding: D1587, D1614, E1615, K1617 and E1638. These residues are predicted to occur on the surface of the A2 domain and form a potential docking site for ADAMTS13.[216] Although only

speculative, the glycan at N1574 could limit access of ADAMTS13 to this region by masking the protein surface. The N1515 site is predicted to occur on the opposite side to this region and this may account for the mutation having no effect on susceptibility to ADAMTS13 cleavage.

Although the effect may be mediated by steric hindrance, the favoured hypothesis is altered conformation of the VWF molecule. Like PNG-VWF, N1574Q is cleaved in the absence of the urea but the rate of cleavage is increased in its presence. As with PNG-VWF, this suggests that the molecule is permissive to ADAMTS13 cleavage, but still needs to undergo a further conformational change to allow more efficient proteolysis. Analysis of the binding of ADAMTS13 to immobilised wtVWF and N1574Q demonstrated that ADAMTS13 could bind with ~2-fold increased affinity to N1574Q, whereas ADAMTS13 could bind to PNG-VWF with ~4-fold increased affinity. This suggests that another glycan(s) site is involved in modulating binding of ADAMTS13 to VWF. The nearest other *N*-linked sites, N1231 and N2223 are probably located too far from the site of ADAMTS13 interaction to exert a steric effect. It is not clear if the N1574 glycan exerts a conformation effect on the A2 domain alone or has a more long range effect on the stability of the molecule. An increasing body of experimental evidence suggests that *N*-linked glycosylation has a long range effect on the backbone flexibility of folded proteins,[396,397] therefore removal on the glycan at site N1574 may increase the flexibility of the VWF molecule, de-stabilising the multimeric structure.

CHAPTER 7

7. DISCUSSION, CONCLUSIONS & FUTURE DIRECTIONS

7.1 DISCUSSION AND CONCLUSIONS

VWF is a large multimeric plasma glycoprotein that plays an essential role in haemostasis by mediating the adhesion of platelets to thrombogenic surfaces under conditions of high shear stress.[2] Its multimeric structure is critical for its adhesive function of adhering to collagen and capturing platelets. Within the circulation it is the largest VWF multimers that the most efficient in this function.[77] The adhesive properties of VWF are regulated by ADAMTS13, which cleaves VWF within its A2 domain (Y1605-M1606) reducing its multimeric size and its ability to recruit platelets at sites of vessel injury.[159] ADAMTS13 cleavage of VWF may also affect the removal of VWF from plasma, although this relationship remains poorly understood.

A significant portion (~20%) of the VWF molecule is comprised of carbohydrate in the form of *N*- and O-linked glycan chains.[16] From the primary amino acid sequence and an initial study by Titani *et al*, VWF was predicted to contain 12 *N*-linked sites and 10 O-linked sites.[16] Interestingly the *N*-linked glycans of VWF have been shown to present the ABO blood group sugars[23] and an indication of the importance of VWF glycosylation came from the observation that a major determinant of plasma VWF levels is ABO blood group, with individuals of blood group O having ~30% less circulating VWF compared to non-O blood groups.[309,312,316-321] The mechanism by which ABO blood group has an effect on VWF levels is not understood, but linkage analysis suggests that the effect is due to a direct functional effect of the ABO locus rather than a linkage disequilibrium.[320] Current data suggest that the effect is not due to an influence on the rate of synthesis and/or secretion, thus the effect may be mediated by altered rates of clearance which in turn may be dependent on proteolysis.[350-352]

A recent study by Bowen (2003) demonstrated that ABO blood group mediates susceptibility of VWF to ADAMTS13 proteolysis.[324] This study showed that blood group O VWF was cleaved faster by ADAMTS13 than blood group A or AB VWF. (Interestingly, blood group B VWF was proteolysed at a similar rate to O VWF despite the difference in plasma levels).[324] This was the first demonstration of a functional alteration of VWF resulting from a natural variation in glycan structure. Initially, the

aim of this thesis was to further investigate this observation using Bombay VWF. As described previously, the Bombay blood group is a rare blood group that results from failure to express the H-transferase, thus no H-antigen is formed and no A or B antigens can be formed.[339] The result of this natural model is that a further sugar residue is missing from some of the *N*-linked glycan chains. Thus Bombay VWF presents one less sugar than O VWF and two less sugars than A or B VWF. Analysis of plasma VWF levels demonstrated that Bombay individuals have significantly less VWF than non-O blood groups. I also observed that Bombay VWF levels were lower than group O VWF, however this result failed to reach a significant p value. I then proceeded to confirm Bowen's observation that O VWF was cleaved faster than AB VWF by ADAMTS13, and extended this to demonstrate that Bombay VWF is cleaved faster than O VWF.

These observations clearly indicate that the terminal blood group sugars uniquely presented on VWF significantly affect ADAMTS13 proteolysis. How this relates to VWF levels is not yet resolved, however an indirect relationship does appear to exist between *N*-linked glycan chain length, susceptibility to ADAMTS13 proteolysis and plasma VWF levels. With decreasing glycan chain length, the susceptibility to ADAMTS13 cleavage is increased and VWF levels are decreased. It seems unlikely that proteolysis alone accounts for the variation in VWF levels observed between ABO blood groups and implies that there is relationship between VWF proteolysis and clearance.

The interconnection between VWF proteolysis and clearance has not yet been established. Animal models used to investigate the clearance of VWF have returned conflicting results. Although it has been established that VWF is cleared in a biphasic pattern,[269,282,283] the evidence regarding the effect of VWF multimer size on rate of clearance is not conclusive. In a murine model, using the VWF knock-out mouse, multimer size has no effect on clearance,[283] whereas HMW-multimers were cleared faster than LMW multimers in Sprague Dawley Rats and Kookier dog models.[282,284] Although useful, these studies do not take into account proteolysis of VWF. The human plasma derived VWF or human recombinant VWF used in these studies was not proteolysed by murine, canine or rat ADAMTS13, therefore any effects of ADAMTS13 proteolysis would not have been observed.

Two recent studies have estimated the half-life of VWF within the circulation using the plasma VWF propeptide to VWF:Ag ratio (VWFpp-VWF:Ag).[321,363] VWF is secreted in equimolar amounts with its propeptide, which has a shorter half-life and has been

shown not to present ABO sugars and whose levels do not vary with ABO blood group VWF propeptide can therefore be used as a measure of VWF secretion and the VWF:VWFpp ratio allows estimation of VWF half-life. Both these studies concluded that the half-life for O VWF was significantly shorter than the half-life for non-O blood groups (10 hours vs. 12 hours respectively).[321,363] Although these studies do not address ADAMTS13 cleavage of VWF, they do provide evidence that O VWF is cleared from the circulation faster than non-O VWF. However it seems a plausible conjecture that the haemostatic system would function to retain the lager, more biologically active VWF multimers and remove the less functional LMW species. At the same time, the multimeric size of VWF is controlled by ADAMTS13 preventing excess accumulation of HMW-VWF. Thus a balance is created between VWF synthesis and secretion, proteolysis and clearance. The rate of synthesis and secretion is not altered between blood groups; but it is hypothesised that as the rate of proteolysis increases, the rate of clearance increases, explaining the differences in VWF levels between blood groups.

In normal individuals the multimer distribution reflects the relationship between proteolysis and clearance. This explains my observation that although Bombay VWF was proteolysed significantly faster than O or AB VWF, a normal multimer pattern was presented comparable to normal plasma.

In individuals with some type 2A VWD mutations, the rate of cleavage increases relative to clearance so only LMW-multimers are present in the circulation. In a type of VWD called VWD Vicenza, patients have decreased VWF:Ag but multimer analysis demonstrates the presence of UL-VWF multimers. A proposed model for this observation is that the rate of clearance increases relative to proteolysis and the distribution of VWF multimers is forced the opposite way to a type 2A phenotype with the accumulation of HMW-multimers.[398]

The key unknown factor in this area is the relationship between VWF proteolysis and clearance which requires further investigation. Whether proteolysis influences clearance or *vice versa* is not clear. If it assumed that the proposed model for VWF Vicenza is correct, increased clearance in group O would lead to accumulation of HMW-multimers. However, if the increased clearance is the result of increased cleavage the two effects would cancel each other out, and the multimer distribution would remain normal. The observation that ABO sugars can affect susceptibility to ADAMTS13 proteolysis and that cleavage may determine clearance, offers a possible explanation for the effect of ABO/Bombay blood group on plasma VWF levels. Much further

investigation is need to determine if VWF proteolysis and clearance are related and the argument is only likely to be resolved by using an *in vivo* model system where multimer size and proteolysis can be manipulated independently. Establishing such a system forms part of the future work resulting from this thesis.

How the ABO sugars modulate susceptibility to ADAMTS13 proteolysis is also not fully determined, however the results presented in this thesis allow hypotheses to be proposed that may account for the differences observed. The ABO and Bombay data imply a simple relationship, in which the rate of cleavage correlates with glycan chain length. How this might affect the VWF molecule was investigated further by subjecting blood group specific VWF to ADAMTS13 proteolysis with varying urea concentrations. With increasing urea concentration the overall rate of cleavage was increased, but the differences seen between blood groups was decreased. This implies that the ABO sugars have an effect on the conformation of the VWF molecule, with reduction in glycan length increasing the permissiveness of the molecule to ADAMTS13 proteolysis, but as the rate of unfolding of the molecule increases with increasing urea concentration, the ABO effect is lost.

In this "conformational" hypothesis a contribution from both local and distant *N*-linked glycosylation sites might be expected. However local effects on the A2 domain itself are likely to predominate. A second hypothesis for my observations might be termed the "steric" hypothesis. In this model, *N*-linked glycosylation affects ADAMTS13 cleavage by physically blocking access to the ADAMTS13 cleavage site or to the ADAMTS13 binding site. This effect would be restricted to local glycosylation within the A2 domain. Both models are likely to affect ADAMTS13 cleavage and binding to VWF.

VWF has a large number of glycan chains and it is not known what structures are present at specific sites. From the effects of ABO/Bombay blood group and increasing urea concentrations it is not clear whether these effects are mediated by all the *N*-linked glycans of VWF and thus represent an overall structural effect; or by a single chain, presumably in the A2 domain, affecting local structure or forming an obstruction to the ADAMTS13 binding and cleavage sites. It may therefore be interesting, that two *N*-linked sites, N1515 and N1574 are predicted to occur in close proximity to the ADAMST13 cleavage site at Y1605M1606.

As I have shown, sites N1515 and N1574 were both predicted to be occupied by the NetNglyc prediction algorithm and are both highly conserved through out the A2 domain sequences of the 59 species analysed. To experimentally determine if these sites

were occupied by *N*-linked glycan chains, I isolated a tryptic fragment of VWF spanning the A2 and A3 domains, encompassing N1515 and N1574. As I demonstrated, both sites are occupied by complex *N*-linked glycan chains, and significantly, at least one of the sites is decorated with the H-antigen.

The observation that both sites are highly conserved, implies that they may have an important function. Consultation of the VWF mutation database (available from http://www.ragtimedesign.com/vwf/mutation/) shows that there are no known mutations of either the specific N1515 and N1574 sites, or any mutations that would affect glycosylation at these sites. This may in part be explained by the observation that loss of glycosylation mutations are relatively rare.[399] Certainly this, and the highly conserved nature of the two sites, and the observation that at least one of them presents ABO antigens suggests that they have a crucial role for the VWF molecule.

To further explore the role of VWF glycosylation more general and specific manipulations of VWF glycans were required. Therefore, as well as the effect of the ABO sugars on susceptibility to ADAMTS13 cleavage, I also investigated the effect of modifying other VWF glycan structures. The observation that Neu-VWF was cleaved at a slower rate by ADAMTS13 was slightly unexpected. Previous studies had shown that AsVWF is more prone to proteolytic degradation[261,262] and the results obtained with blood group specific VWF suggested that with reduction in *N*-linked glycan length, the rate of ADAMTS13 cleavage increased. I also showed that removal of terminal sialic acid from blood group specific VWF not only reduced the rate of cleavage, but also prevented the ABO effect, with both neuraminidase treated O and AB-VWF being proteolysed at the same rate. As previously discussed, this implies that the sialic acid effect is dominant over the ABO effect, or the ABO effect is mediated by modifying the number of sialic acid residues present on VWF glycans. The latter may be unlikely since sialic acid levels do not appear to vary between blood groups, however, this may require further investigation.[379] My findings also do not take into account that sialic acid is present on both *N*- and O-linked glycans. Therefore it may be that sialic acid residues on either specifically the *N* or O-linked glycan chains mediate the effect. However, specifically removing sialic acid residues from only *N* or O-linked chains is not yet possible. A recent study has suggested that variations in O-linked glycosylation of VWF affects plasma levels.[400] Using Peanut Agglutinin (PNA) to detected de-sialylated O-linked glycans, van Schooten *et al* demonstrated an inverse relationship between PNA binding and VWF levels. The majority of O-linked glycans present on VWF are

the disialyated core 1 type[257*] and therefore reduction in PNA binding may represent a reduction in O-linked glycosylation, which in turn would result in reduced sialic acid presentation. (Although this seems at odds with previous findings that VWF sialic acid levels do not vary over the population, hence further investigation is required.) From van Schooten *et al's* study it is not clear how altered O-linked glycosylation would affect VWF levels. Although I only propose this as a tentative suggestion, a possible mechanism could be related to the rate of proteolysis. Decreased O-linked glycosylation resulting in decreased VWF sialic acid content may result in decreased ADAMTS13 proteolysis. If ADAMTS13 proteolysis of VWF is related to VWF clearance the reduction in proteolysis would result in increased levels. This is however highly speculative, and does not account for the variation seen between ABO blood groups. Interestingly, I have recently obtained data to suggest that VWF devoid of O-linked glycans is proteolysed slower than wtVWF, implying that the O-linked glycans do play a role in mediating susceptibility of VWF to ADAMTS13 proteolysis and will form part of future investigation.

In contrast to the removal of sialic acid, removal of the *N*-linked glycans of VWF significantly increased the susceptibility of the molecule to ADAMTS13 proteolysis, even allowing cleavage by ADAMTS13 in the absence of urea. To investigate the mechanisms involved, binding studies were performed to determine the effect of glycan modification on the affinity of the VWF-ADAMTS13 interaction. The binding of ADAMTS13 to PNG-VWF was altered, with PNG-VWF binding ADAMTS13 with increased affinity compared to Ctrl-VWF. Interestingly, collagen bound VWF was capable of binding ADAMTS13 with high affinity, (K_D 12nM). Implying that binding of VWF to collagen causes a conformation change in the molecule, exposing the ADAMTS13 binding site. Collagen bound VWF has been shown by AFM to remain in a globular conformation,[368] so the conformational change required to expose the ADAMTS13 binding site may be relatively small. Binding of VWF to type III collagen has been proposed to induce a conformational change to expose the collagen binding site within the A1 domain.[153] This may also alter the conformation of the A2 domain, allowing ADAMTS13 access to its binding site.

Since the treatment of VWF with PNGase F resulted in the non-specific removal of *N*-linked glycan chains, it was not possible to determine if the effect on the interaction

---

* Also known as the T-antigen

with ADAMTS13 was due to general removal of the glycans or the removal of specific sites. To further investigate this, I mutated the two *N*-linked sites, N1515 and N1574 within the A2 domain. The results from the cleavage analysis showed that the N1574Q site represents a critical *N*-linked chain, since removal of this glycan results in a greatly increased rate of ADAMTS13 proteolysis. Interestingly, mutation of N1515 did not have any significant effect on ADAMTS13 proteolysis, suggesting that glycosylation at this site is not important in modulating the interaction with ADAMTS13. From the results presented in Chapter 4 it is evident that the site is occupied, but from the results I have obtained it does not appear that the site has any functional relevance. N1574Q also bound ADAMTS13 with increased affinity, but only ~2-fold, compared to the ~4-fold difference seen with PNG-VWF. This suggests other glycan site(s) may be involved in mediating the VWF-ADAMTS13 interaction.

It does however appear that the N1574Q mutation accounts for the majority of the effect on ADAMTS13 cleavage observed with PNG-VWF. The mechanism by which removal of VWF *N*-linked glycans or mutation of N1574 renders VWF more susceptible to ADAMTS13 proteolysis and binding is not fully clear, however the effect is likely to be either due to steric hindrance or a conformational effect, or possibly both.

As mentioned earlier, the glycan moiety of other glycoproteins can protect the molecule from proteolytic attack by covering a portion of the protein surface.[383] This is dependent on the protein-glycan linkage being flexible rather than fixed. From the predicted model N1574 occurs in close proximity to several residues on the surface of the A2 domain that have been shown to form part of the ADAMTS13 docking site within the domain: Arg1583, Asp1587, Asp1614, Glu1615 and Lys1617.[216] From the predicted model, these residues are in close enough proximity to be shielded by the *N*-linked chain at N1574 (Figure 7.1). The average length of a complex biantennary glycan chain is predicted to be 3-4nm.[401] The furthest residue from N1574 is Asp1587, predicted to occur ~24Å (2.4nm) away from N1574, is therefore close enough to be potentially shielded by the N1574 glycan chain. The presence of a glycan at N1574 may therefore define ADAMTS13 access to its docking site suggesting a local effect of removing N1574. A large majority of the effect observed with PNG-VWF may therefore represent the removal of the N1574 site. Although, since N1574Q bound ADAMTS13 with decreased affinity compared to PNG-VWF, other glycan sites appear to be involved in modulating binding of ADAMTS13 to VWF.

Previously it has been shown that recombinant A2 domain expressed in both *E.coli* (non-glycosylated) and Sf9 insect cells (glycosylated) required the presence of urea for ADAMTS13 cleavage to occur.[216,218,402] Although it is very difficult to draw a comparison between the non-glycosylated and glycosylated A2 domain, since they have been used in separate studies with different ADAMTS13 preparations and are expressed in different systems, the observation that both require urea for cleavage does suggest that they behave in similar ways. Interestingly, recent data obtained in our laboratory demonstrates that a recombinant VWF A2 domain expressed in *E.coli* is able to inhibit the binding of ADAMTS13 to immobilised VWF. It will be important to see if glycosylated A2 domain also inhibits binding of ADAMTS13 to immobilised VWF. If glycosylated A2 domain cannot inhibit ADAMTS13 binding, or is less efficient at inhibiting binding, this will provide evidence that the *N*-linked glycan at N1574 does indeed shield the ADAMTS13 docking site within the A2 domain. Expression of a glycosylated A2 domain is currently in progress and forms part of the future work relating to this thesis.

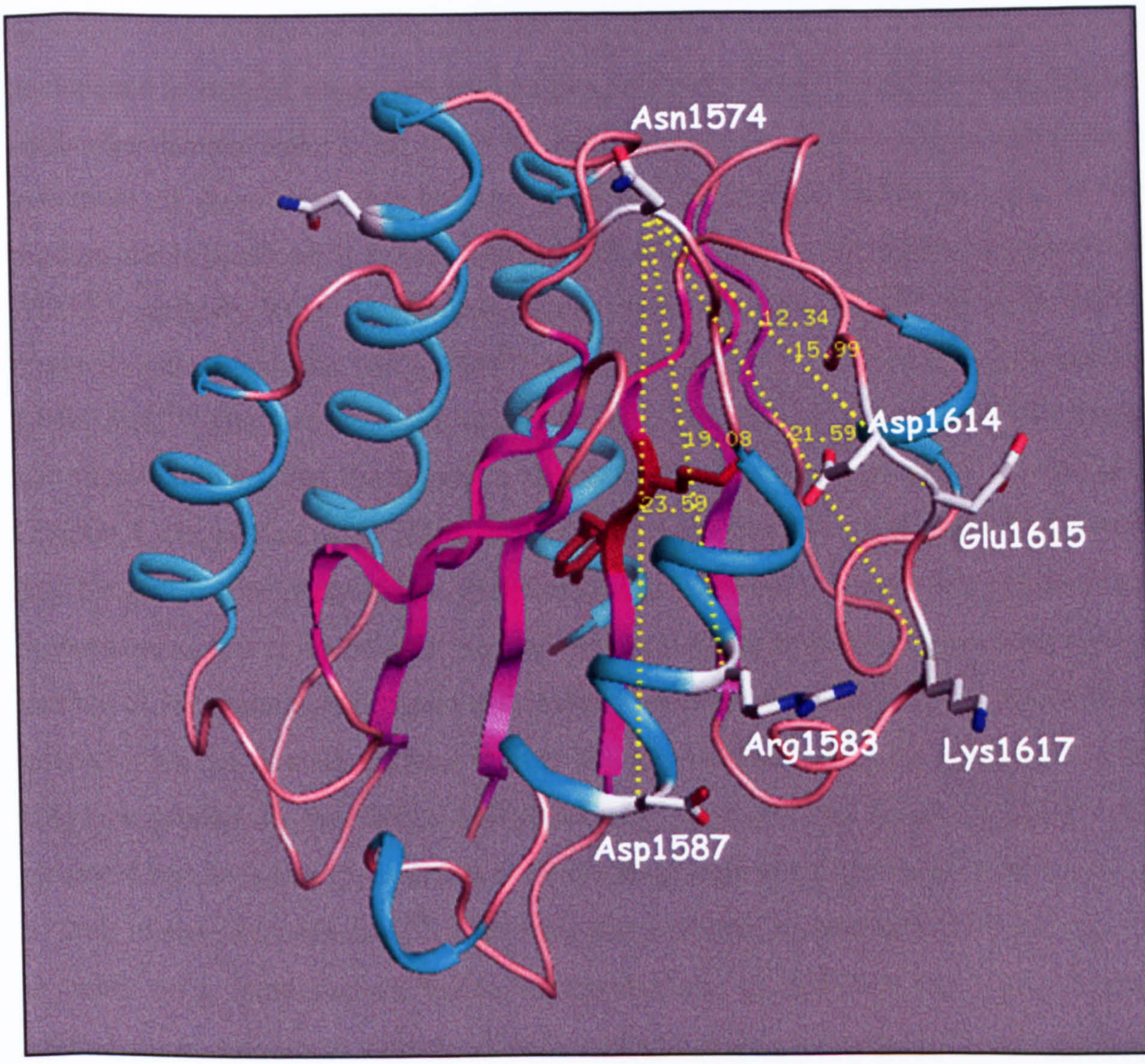


Figure 7.1 Distances between N1574 and A2 domain surface residues important for ADAMTS13 binding

The distances between Asn1574 and the residues shown to form the ADAMTS13 docking site in the A2 domain are shown in Å (0.1nm). The furthest residue from N1574 is Asp1587, predicted to occur ~24Å (2.4nm) away from the Asn1574 sites. Since the average length of a complex glycan chain is 3-4nm, the glycan at N1574 could potentially shield the ADAMTS13 docking site.

Although steric hindrance is an attractive hypothesis to explain my observations, there is evidence to suggest it may not be the most dominant factor. A number of monoclonal antibodies directed against the VWF A2 domain have been produced and significantly, a number of these recognise the region of the A2 domain where the ADAMTS13 binding site is predicted to occur. Antibody RAb7745 is directed against residues 1606-1620;[403] antibody RG69 is directed against residues 1493-1606;[261] antibody M19 is directed against residues 1607-1710;[261] and antibody VP-1 is directed against residues 1591-1605.[404] The fact that these antibodies can interact with the ADAMTS13 binding site region implies that the region is not concealed by a glycan chain. As shown in Chapter 4, the glycan at N1574 is likely to be of the complex type. This demonstrates that the glycan site is accessible to the enzymes required to convert the glycan from a high mannose to a complex structure and may imply that rather than interacting with the surface of the domain, the glycan may extend away from it. If the glycan at N1574 did interact with the domain surface, it may be shielded from complex glycan processing enzymes present in the Golgi and post-Golgi. Furthermore, it has been previously observed that *N*-linked glycans that occur on loop regions are extensively processed due to their relative accessibility.[401] Also from the predicted model the N1574 sites appears to occur on a more convex region of the domain, in this case the glycan chain is unlikely to make contact with the domain and will project away from the A2 domain.[365] However further investigation is required to predict the nature of linkage between the glycan chain and N1574 to conform this. Extension of the glycan chain away from the domain would favour a conformational effect rather than a steric one.

A major function of *N*-linked glycans is to aid protein folding and to maintain protein conformation.[405] Often *N*-linked glycans act as molecular chaperones, aiding the folding of the protein within the cell but whose removal once the protein is fully folded does not affect its biological activity.[406,407] In other cases, *N*-linked glycans may act to stabilise the conformation of the molecule, often through interaction of the glycan with specific regions of the molecule. For example: Immunoglobulin G (IgG) contains a conserved *N*-linked glycosylation site at residue N297.[408] Evidence suggest that interactions between the glycan at site N297 and surrounding amino acids stabilize the conformational integrity of the protein.[409] Glycosylation of RNase B has been shown to increase the overall dynamic stability of the protein by reducing solvent access to many regions of the peptide backbone both close to and remote from the glycosylation site suggesting that it reduces fluctuations of the backbone,[410] and the *N*-linked glycans of

Quercetin 2,3-dioxygenase have been shown to play an active role in maintaining the dimeric structure of the protein.[411] A general phenomenon observed with proteins is that the glycosylated version is more stable than the non-glycosylated form, with the stabilisation being due to largely entropic effects, rather than enthalpic effects.[412] The human chorionic gonadotropin hormone (hCG) is stabilised by *N*-linked glycosylation at Asn78.[413] Evidence suggests that this glycan chains shields a hydrophobic core on the molecule via interaction of the glycan with the protein.[413] Moreover, the *N*-linked glycans of Human Erythropoietin (EPO) have been shown to stabilise the protein conformation by interacting with hydrophobic areas of the protein surface.[414] SPR analysis demonstrated that *E.coli* produced EPO (therefore without glycans) could bind to purified bi, tri and tetra-antennary *N*-linked glycans and this binding was enhanced in the presence of high-salt conditions, indicative of a hydrophobic interaction.[415] Glycans are able to generate areas of hydrophobicity, the extent of which depends on the CH-dense surface area, degrees of polymerization and branching, and molecular planarity.[416] It was therefore concluded that complex *N*-linked glycans exhibit extensively stretched hydrophobic planes and stabilize the protein conformation through hydrophobic interactions with the hydrophobic protein surface.[415] The size of the hydrophobic surface produced by the glycan is increased with the degree of branching of the glycan chain, thus complex glycans produce more extensive hydrophobic regions than high mannose glycans.[417] Molecular modelling of *N*-acetyllactosamine units, present in complex *N*-linked glycans but not high mannose structures, showed that they have an amphiphilic structure and greatly contribute to the formation of extensive hydrophobic surfaces.[417] Therefore, the *N*-linked glycans of VWF may interact with hydrophobic regions of the molecule, adding stability to the multimeric structure. Specifically this effect could be mediated by N1574 either stabilising the A2 domain itself or by interactions with other domains of the VWF molecule, particularly the A1 and A3 domains.

Furthermore, as well as hydrophobic interactions between glycan and protein, the removal of VWF *N*-linked glycans or specifically N1574 may also confer long range effects on the VWF molecule. *N*-linked glycans have been shown to impart a long-range decrease in the backbone flexibility of folded proteins and impart long range stabilising effects on tertiary and quaternary structures remote from specific sites of glycosylation.[397,412] *N*-linked glycosylation also has short range effects on proteins by adding rigidity to the surrounding region.[397,412] Thus the N1574 site in VWF may be

critical for stabilising the A2 domain itself and the general structure of the fully folded monomer and multimer structures.

In summary, removal of the VWF *N*-linked chains or mutation of N1574 does not alter the conformation of the molecule *per se*, but may "relax" firstly, the conformation of each monomer and secondly, the conformation of the multimer. Thus, in the absence of urea, the PNG-VWF or N1574Q molecule is in a conformation already permissive enough for ADAMTS13 cleavage to occur. Upon the addition of urea, PNG-VWF or N1574Q can therefore more readily adopt a conformation fully apt for ADAMTS13 cleavage.

The observation that ADAMTS13 can bind to PNG-VWF with increased affinity may also reflect the conformation of the molecule. When PNG-VWF is bound to the plate, its more "relaxed" structure can readily adopt an elongated structure akin to normal VWF under shear stress conditions. Likewise, when captured via the monoclonal anti-VWF antibody, PNG-VWF may present a less tightly packed globular structure than normal VWF, allowing binding of ADAMTS13. As previously mentioned, the observation that ADAMTS13 can bind with high affinity to collagen-bound VWF indicates that binding of VWF to collagen induces a conformational change to allow ADAMTS13 to bind to VWF. This change in conformation is thus likely to be potentiated with PNG-VWF, allowing increased binding of ADAMTS13.

From the preliminary binding assays performed with N1574Q it was observed that N1574Q could bind ADAMTS13 with ~2-fold increased affinity rather the ~4-fold increased affinity seen with PNG-VWF. This probably reflects the involvement of another, remote, glycan site in maintaining VWF conformation.

The hypothesis that VWF *N*-linked glycans affect the conformation of the molecule through hydrophobic interactions with the protein also provides an explanation of the ABO effect on VWF cleavage by ADAMTS13. The addition of a galactose or GalNAc residue (A or B antigen respectively) to the complex glycan may increase the hydrophobic surface of the glycan and strengthen the hydrophobic interactions between glycan and protein. Moreover, this hypothesis may present a reason for the observation that Neu-VWF is proteolysed at a significantly reduced rate by ADAMTS13. Sialic acid carries a negative charge and is likely to be hydrophilic, removal of the negative charge may serve to increase the hydrophobic nature of the *N*-linked glycan and in turn increase the hydrophobic interaction of the glycan with the protein making the protein

more stable. The complex glycan at site N1574 may therefore specifically function to maintain the globular structure of VWF and protect against ADAMTS13 cleavage.

In conclusion, the glycan structure of VWF plays an important role in mediating the interaction of the molecule with ADAMTS13. Subtle, natural alterations in glycan structure, observed with VWF from different blood groups, alter the susceptibility of the molecule to proteolysis by ADAMTS13. More dramatic changes induced by enzymatic and mutational modifications also alter the interaction of VWF with ADAMTS13. Removal of terminal sialic acids residues do not alter the affinity of ADAMTS13 for VWF, but do decrease the rate of ADAMTS13 proteolysis. In contrast, removal of the *N*-linked glycans of VWF increases the affinity of ADAMTS13 for VWF and also increases the susceptibility of VWF to ADAMTS13 proteolysis; to the extent that multimeric VWF lacking *N*-linked glycans can be cleaved in the absence of urea. Specifically, site N1574, which is occupied and presents the blood group antigens, is a critical *N*-linked glycan site in VWF, with mutation of this site increasing susceptibility to ADAMTS13 cleavage. Analysis of the sugar structures of VWF therefore gives valuable insight into the structure function relationship of the molecule.

7.2 FUTURE DIRECTIONS

The data presented in this thesis has clearly demonstrated that naturally occurring and *in vitro* alterations to the glycan structures of VWF have an effect on the interaction of the molecule with ADAMTS13. It has also raised a number of questions that require further investigation. Some of the future directions that this work could take are discussed below.

7.2.1 Role of VWF *N*-linked glycosylation in Determining VWF Structure and Function

As shown, the *N*-linked glycan structure of VWF has an effect on the interaction of VWF with ADAMTS13, with the N1574 site being a crucial glycan in the interaction. However the results also indicate that other glycan sites may also affect the susceptibility of VWF to ADAMTS13 proteolysis. Moreover, the VWF glycan structure may also have an effect on other functional aspects of the VWF molecule. To further investigate this, a series of VWF *N*-linked glycan mutants will be produced and analysed for their effects on various functional aspects of the VWF molecule, including; storage and release, multimeric structure, susceptibility to ADAMTS13 cleavage and

binding, FVIII binding, GPIIbIIIa binding, GPIbα binding, collagen binding and VWF dimerisation/multimerisation and intracellular transport.

Currently the *N*-linked glycan sites predicted to occur at N857, N1147 and N1231 have been prepared are will be expressed, as described, in HEK293T cells. It is anticipated that since these mutations occur in the D'D3 region of the molecule they may effect the multimerisation of the VWF molecule. If these molecules are fully multimerised I plan to investigate the affect these glycan mutations have on the interaction of VWF with FVIII and P-Selectin.

To determine the role of the VWF the glycans I have also prepared mutations of the *N*-linked sites predicted to occur in the propeptide: N99, N157, N211, N666. Further to this, I have obtained a monoclonal antibody directed against the VWF propeptide (a kind gift from Dr Jan Voorberg) and this will be used to capture the propeptide from plasma followed by lectin analysis to give a preliminary analysis of the glycan structures presented on the propeptide.

A mutation has also been made of the *N*-linked site predicted to occur at N2790 with the CK domain. Recent studies have suggested that *N*-linked glycans present in the cysteine knot domains of dimeric proteins are required for efficient dimerisation. It is therefore likely that this site will be critical for the formation of VWF dimers.

7.2.2 Producing a Comprehensive Glycan Map of VWF

As discussed, little experimental evidence exists confirming which predicted *N* and O-linked glycosylation sites are occupied by glycans structures and indeed what specific structures occur at specific sites. It is now known from the data I have presented, that the two predicted A2 domain glycosylation sites are occupied by complex glycan chains, and certainly one, if not both chains present ABO(H) antigens. To further this, the glycan structures present on the 55kDa VWF fragment will be sequenced in detail using a mass spectroscopy approach. Using a similar strategy of generating VWF fragments encompassing specific glycan sites, followed by detailed sequencing of the glycans by mass spectroscopy, it will be possible to build a comprehensive glycan map of VWF. This will provide detail of the glycosylation status of specific sites and provide sequence analysis of the glycan structures present. From this it will be possible to determine what sites present the ABO(H) antigens and to investigate if certain glycan structures are unique to specific sites. This body of work has been accepted for a British Heart Foundation PhD studentship grant.

7.2.3 Role of VWF O-linked Glycosylation

Previous studies have demonstrated that VWF expressed lacking O-linked glycans forms normal multimers and exhibits normal collagen binding, but causes increased ristocetin mediated platelet aggregation. To investigate this further, rVWF lacking O-linked glycosylation will be expressed and analysed for its affinity to bind platelet GPIbα using a previously described GPIbα plate based binding assay that is reported to be more sensitive than the ristocetin cofactor assay. I have recently established a clone of the N-terminal of GPIbα and will express the protein in HEK293T cells. Moreover, from preliminary results that I have obtained, O-less VWF is proteolysed slower than wtVWF. To investigate this, individual and multiple mutations will be made of the predicted O-linked glycosylation sites to determine what O-linked sites mediate this effect.

7.2.4 Relationship between VWF Proteolysis and Clearance

As discussed, the relationship between VWF proteolysis and clearance has not yet been determined. This will be investigated using the VWF knock out mouse model in collaboration with Dr Cecile Denis. In these experiments we plan to inject mice with purified blood group specific VWF with and without purified human recombinant ADAMTS13 to determine the effect of, firstly, ABO blood group on VWF clearance and secondly, the effect of ADAMTS13 proteolysis on VWF clearance.

1. Nogami K, Shima M, Nishiya K, et al. A novel mechanism of factor VIII protection by von Willebrand factor from activated protein C-catalyzed inactivation. Blood. 2002;99:3993-3998.
2. Sadler JE. Biochemistry and genetics of von Willebrand factor. Annu Rev Biochem. 1998;67:395-424.
3. Wagner DD. Cell biology of von Willebrand factor. Annu Rev Cell Biol. 1990;6:217-246.
4. Cramer EM, Vainchenker W, Vinci G, Guichard J, Breton-Gorius J. Gray platelet syndrome: immunoelectron microscopic localization of fibrinogen and von Willebrand factor in platelets and megakaryocytes. Blood. 1985;66:1309-1316.
5. Nichols TC, Samama CM, Bellinger DA, et al. Function of von Willebrand factor after crossed bone marrow transplantation between normal and von Willebrand disease pigs: effect on arterial thrombosis in chimeras. Proc Natl Acad Sci U S A. 1995;92:2455-2459.
6. Rand JH, Badimon L, Gordon RE, Uson RR, Fuster V. Distribution of von Willebrand factor in porcine intima varies with blood vessel type and location. Arteriosclerosis. 1987;7:287-291.
7. Yamamoto K, de Waard V, Fearns C, Loskutoff DJ. Tissue distribution and regulation of murine von Willebrand factor gene expression in vivo. Blood. 1998;92:2791-2801.
8. Mancuso DJ, Tuley EA, Westfield LA, et al. Structure of the gene for human von Willebrand factor. J Biol Chem. 1989;264:19514-19527.
9. Bonthron D, Orkin SH. The human von Willebrand factor gene. Structure of the 5' region. Eur J Biochem. 1988;171:51-57.
10. Mancuso DJ, Tuley EA, Westfield LA, et al. Human von Willebrand factor gene and pseudogene: structural analysis and differentiation by polymerase chain reaction. Biochemistry. 1991;30:253-269.
11. Patracchini P, Calzolari E, Aiello V, et al. Sublocalization of von Willebrand factor pseudogene to 22q11.22-q11.23 by in situ hybridization in a 46,X,t(X;22)(pter;q11.21) translocation. Hum Genet. 1989;83:264-266.
12. Jahroudi N, Lynch DC. Endothelial-cell-specific regulation of von Willebrand factor gene expression. Mol Cell Biol. 1994;14:999-1008.
13. Schwachtgen JL, Janel N, Barek L, et al. Ets transcription factors bind and transactivate the core promoter of the von Willebrand factor gene. Oncogene. 1997;15:3091-3102.
14. Jahroudi N, Ardekani AM, Greenberger JS. An NF1-like protein functions as a repressor of the von Willebrand factor promoter. J Biol Chem. 1996;271:21413-21421.
15. Kaufman RJ. Post-translational modifications required for coagulation factor secretion and function. Thromb Haemost. 1998;79:1068-1079.
16. Titani K, Kumar S, Takio K, et al. Amino acid sequence of human von Willebrand factor. Biochemistry. 1986;25:3171-3184.
17. Niemann H, Klenk HD. Coronavirus glycoprotein E1, a new type of viral glycoprotein. J Mol Biol. 1981;153:993-1010.
18. Wagner DD, Mayadas T, Marder VJ. Initial glycosylation and acidic pH in the Golgi apparatus are required for multimerization of von Willebrand factor. J Cell Biol. 1986;102:1320-1324.
19. Katsumi A, Tuley EA, Bodo I, Sadler JE. Localization of disulfide bonds in the cystine knot domain of human von Willebrand factor. J Biol Chem. 2000;275:25585-25594.

20. Marti T, Rosselet SJ, Titani K, Walsh KA. Identification of disulfide-bridged substructures within human von Willebrand factor. Biochemistry. 1987;26:8099-8109.
21. Wise RJ, Pittman DD, Handin RI, Kaufman RJ, Orkin SH. The propeptide of von Willebrand factor independently mediates the assembly of von Willebrand multimers. Cell. 1988;52:229-236.
22. Kornfeld R, Kornfeld S. Assembly of asparagine-linked oligosaccharides. Annu Rev Biochem. 1985;54:631-664.
23. Matsui T, Titani K, Mizuochi T. Structures of the asparagine-linked oligosaccharide chains of human von Willebrand factor. Occurrence of blood group A, B, and H(O) structures. J Biol Chem. 1992;267:8723-8731.
24. Carew JA, Browning PJ, Lynch DC. Sulfation of von Willebrand factor. Blood. 1990;76:2530-2539.
25. Voorberg J, Fontijn R, van Mourik JA, Pannekoek H. Domains involved in multimer assembly of von willebrand factor (vWF): multimerization is independent of dimerization. Embo J. 1990;9:797-803.
26. Mayadas TN, Wagner DD. In vitro multimerization of von Willebrand factor is triggered by low pH. Importance of the propolypeptide and free sulfhydryls. J Biol Chem. 1989;264:13497-13503.
27. Verweij CL, Hart M, Pannekoek H. Expression of variant von Willebrand factor (vWF) cDNA in heterologous cells: requirement of the pro-polypeptide in vWF multimer formation. Embo J. 1987;6:2885-2890.
28. Mayadas TN, Wagner DD. Vicinal cysteines in the prosequence play a role in von Willebrand factor multimer assembly. Proc Natl Acad Sci U S A. 1992;89:3531-3535.
29. Vischer UM, Wagner DD. von Willebrand factor proteolytic processing and multimerization precede the formation of Weibel-Palade bodies. Blood. 1994;83:3536-3544.
30. Rehemtulla A, Kaufman RJ. Preferred sequence requirements for cleavage of pro-von Willebrand factor by propeptide-processing enzymes. Blood. 1992;79:2349-2355.
31. Borchiellini A, Fijnvandraat K, ten Cate JW, et al. Quantitative analysis of von Willebrand factor propeptide release in vivo: effect of experimental endotoxemia and administration of 1-deamino-8-D-arginine vasopressin in humans. Blood. 1996;88:2951-2958.
32. Kohler M, Hellstern P, Miyashita C, von Blohn G, Wenzel E. Comparative study of intranasal, subcutaneous and intravenous administration of desamino-D-arginine vasopressin (DDAVP). Thromb Haemost. 1986;55:108-111.
33. Vischer UM, Ingerslev J, Wollheim CB, et al. Acute von Willebrand factor secretion from the endothelium in vivo: assessment through plasma propeptide (vWf:AgII) Levels. Thromb Haemost. 1997;77:387-393.
34. Harrison P, Cramer EM. Platelet alpha-granules. Blood Rev. 1993;7:52-62.
35. Sporn LA, Marder VJ, Wagner DD. Inducible secretion of large, biologically potent von Willebrand factor multimers. Cell. 1986;46:185-190.
36. Sporn LA, Marder VJ, Wagner DD. von Willebrand factor released from Weibel-Palade bodies binds more avidly to extracellular matrix than that secreted constitutively. Blood. 1987;69:1531-1534.
37. Meriane F, Zerhouni L, Djeha N, Goudemand M, Mazurier C. Biological effects of a S/D-treated, very high purity, von Willebrand factor concentrate in five patients with severe von Willebrand disease. Blood Coagul Fibrinolysis. 1993;4:1023-1029.

38. Weibel ER, Palade GE. New Cytoplasmic Components in Arterial Endothelia. J Cell Biol. 1964;23:101-112.
39. van Mourik JA, Romani de Wit T, Voorberg J. Biogenesis and exocytosis of Weibel-Palade bodies. Histochem Cell Biol. 2002;117:113-122.
40. Sengel A, Stoebner P. Golgi origin of tubular inclusions in endothelial cells. J Cell Biol. 1970;44:223-226.
41. Voorberg J, Fontijn R, Calafat J, Janssen H, van Mourik JA, Pannekoek H. Biogenesis of von Willebrand factor-containing organelles in heterologous transfected CV-1 cells. Embo J. 1993;12:749-758.
42. Rosenberg JB, Foster PA, Kaufman RJ, et al. Intracellular trafficking of factor VIII to von Willebrand factor storage granules. J Clin Invest. 1998;101:613-624.
43. Bonfanti R, Furie BC, Furie B, Wagner DD. PADGEM (GMP140) is a component of Weibel-Palade bodies of human endothelial cells. Blood. 1989;73:1109-1112.
44. Fiedler U, Scharpfenecker M, Koidl S, et al. The Tie-2 ligand angiopoietin-2 is stored in and rapidly released upon stimulation from endothelial cell Weibel-Palade bodies. Blood. 2004;103:4150-4156.
45. Hattori R, Hamilton KK, Fugate RD, McEver RP, Sims PJ. Stimulated secretion of endothelial von Willebrand factor is accompanied by rapid redistribution to the cell surface of the intracellular granule membrane protein GMP-140. J Biol Chem. 1989;264:7768-7771.
46. McEver RP, Beckstead JH, Moore KL, Marshall-Carlson L, Bainton DF. GMP-140, a platelet alpha-granule membrane protein, is also synthesized by vascular endothelial cells and is localized in Weibel-Palade bodies. J Clin Invest. 1989;84:92-99.
47. Rosnoblet C, Vischer UM, Gerard RD, Irminger JC, Halban PA, Kruithof EK. Storage of tissue-type plasminogen activator in Weibel-Palade bodies of human endothelial cells. Arterioscler Thromb Vasc Biol. 1999;19:1796-1803.
48. Russell FD, Skepper JN, Davenport AP. Evidence using immunoelectron microscopy for regulated and constitutive pathways in the transport and release of endothelin. J Cardiovasc Pharmacol. 1998;31:424-430.
49. Schnyder-Candrian S, Borsig L, Moser R, Berger EG. Localization of alpha 1,3-fucosyltransferase VI in Weibel-Palade bodies of human endothelial cells. Proc Natl Acad Sci U S A. 2000;97:8369-8374.
50. Utgaard JO, Jahnsen FL, Bakka A, Brandtzaeg P, Haraldsen G. Rapid secretion of prestored interleukin 8 from Weibel-Palade bodies of microvascular endothelial cells. J Exp Med. 1998;188:1751-1756.
51. Vischer UM, Wagner DD. CD63 is a component of Weibel-Palade bodies of human endothelial cells. Blood. 1993;82:1184-1191.
52. Wolff B, Burns AR, Middleton J, Rot A. Endothelial cell "memory" of inflammatory stimulation: human venular endothelial cells store interleukin 8 in Weibel-Palade bodies. J Exp Med. 1998;188:1757-1762.
53. Denis CV, Andre P, Saffaripour S, Wagner DD. Defect in regulated secretion of P-selectin affects leukocyte recruitment in von Willebrand factor-deficient mice. Proc Natl Acad Sci U S A. 2001;98:4072-4077.
54. Gebrane-Younes J, Drouet L, Caen JP, Orcel L. Heterogeneous distribution of Weibel-Palade bodies and von Willebrand factor along the porcine vascular tree. Am J Pathol. 1991;139:1471-1484.
55. Hop C, Guilliatt A, Daly M, et al. Assembly of multimeric von Willebrand factor directs sorting of P-selectin. Arterioscler Thromb Vasc Biol. 2000;20:1763-1768.

56. Michaux G, Hewlett LJ, Messenger SL, et al. Analysis of intracellular storage and regulated secretion of 3 von Willebrand disease-causing variants of von Willebrand factor. Blood. 2003;102:2452-2458.
57. Wagner DD, Saffaripour S, Bonfanti R, et al. Induction of specific storage organelles by von Willebrand factor propolypeptide. Cell. 1991;64:403-413.
58. Hop C, Fontijn R, van Mourik JA, Pannekoek H. Polarity of constitutive and regulated von Willebrand factor secretion by transfected MDCK-II cells. Exp Cell Res. 1997;230:352-361.
59. Journet AM, Saffaripour S, Cramer EM, Tenza D, Wagner DD. von Willebrand factor storage requires intact prosequence cleavage site. Eur J Cell Biol. 1993;60:31-41.
60. Kroner PA, Foster PA, Fahs SA, Montgomery RR. The defective interaction between von Willebrand factor and factor VIII in a patient with type 1 von Willebrand disease is caused by substitution of Arg19 and His54 in mature von Willebrand factor. Blood. 1996;87:1013-1021.
61. Haberichter SL, Fahs SA, Montgomery RR. von Willebrand factor storage and multimerization: 2 independent intracellular processes. Blood. 2000;96:1808-1815.
62. Haberichter SL, Jozwiak MA, Rosenberg JB, Christopherson PA, Montgomery RR. The von Willebrand factor propeptide (VWFpp) traffics an unrelated protein to storage. Arterioscler Thromb Vasc Biol. 2002;22:921-926.
63. Birch KA, Pober JS, Zavoico GB, Means AR, *Ewenstein BM.* Calcium/calmodulin transduces thrombin-stimulated secretion: studies in intact and minimally permeabilized human umbilical vein endothelial cells. J Cell Biol. 1992;118:1501-1510.
64. Datta YH, Romano M, Jacobson BC, Golan DE, Serhan CN, Ewenstein BM. Peptido-leukotrienes are potent agonists of von Willebrand factor secretion and P-selectin surface expression in human umbilical vein endothelial cells. Circulation. 1995;92:3304-3311.
65. Foreman KE, Vaporciyan AA, Bonish BK, et al. C5a-induced expression of P-selectin in endothelial cells. J Clin Invest. 1994;94:1147-1155.
66. Hamilton KK, Sims PJ. Changes in cytosolic Ca2+ associated with von Willebrand factor release in human endothelial cells exposed to histamine. Study of microcarrier cell monolayers using the fluorescent probe indo-1. J Clin Invest. 1987;79:600-608.
67. Hattori R, Hamilton KK, McEver RP, Sims PJ. Complement proteins C5b-9 induce secretion of high molecular weight multimers of endothelial von Willebrand factor and translocation of granule membrane protein GMP-140 to the cell surface. J Biol Chem. 1989;264:9053-9060.
68. Ribes JA, Francis CW, Wagner DD. Fibrin induces release of von Willebrand factor from endothelial cells. J Clin Invest. 1987;79:117-123.
69. Vischer UM, Jornot L, Wollheim CB, Theler JM. Reactive oxygen intermediates induce regulated secretion of von Willebrand factor from cultured human vascular endothelial cells. Blood. 1995;85:3164-3172.
70. Vischer UM, Wollheim CB. Purine nucleotides induce regulated secretion of von Willebrand factor: involvement of cytosolic Ca2+ and cyclic adenosine monophosphate-dependent signaling in endothelial exocytosis. Blood. 1998;91:118-127.
71. Eyster ME, Ballard JO, Prager D. Comparison of factor VIII levels after adrenalin in classic hemophilia and von Willebrand's disease (vWd). Thromb Haemost. 1978;39:657-662.

72. Mannucci PM. Desmopressin (DDAVP) in the treatment of bleeding disorders: the first 20 years. Blood. 1997;90:2515-2521.
73. Rickles FR, Hoyer LW, Rick ME, Ahr DJ. The effects of epinephrine infusion in patients with von Willebrand's disease. J Clin Invest. 1976;57:1618-1625.
74. Cohen RJ, Epstein SE, Cohen LS, Dennis LH. Alterations of fibrinolysis and blood coagulation induced by exercise, and the role of beta-adrenergic-receptor stimulation. Lancet. 1968;2:1264-1266.
75. Galbusera M, Zoja C, Donadelli R, et al. Fluid shear stress modulates von Willebrand factor release from human vascular endothelium. Blood. 1997;90:1558-1564.
76. Pinsky DJ, Naka Y, Liao H, et al. Hypoxia-induced exocytosis of endothelial cell Weibel-Palade bodies. A mechanism for rapid neutrophil recruitment after cardiac preservation. J Clin Invest. 1996;97:493-500.
77. de Romeuf C, Mazurier C. Heparin binding assay of von Willebrand factor (vWF) in plasma milieu--evidence of the importance of the multimerization degree of vWF. Thromb Haemost. 1993;69:436-440.
78. Enayat MS, Hill FG. Analysis of the complexity of the multimeric structure of factor VIII related antigen/von Willebrand protein using a modified electrophoretic technique. J Clin Pathol. 1983;36:915-919.
79. Fowler WE, Fretto LJ, Hamilton KK, Erickson HP, McKee PA. Substructure of human von Willebrand factor. J Clin Invest. 1985;76:1491-1500.
80. Siedlecki CA, Lestini BJ, Kottke-Marchant KK, Eppell SJ, Wilson DL, Marchant RE. Shear-dependent changes in the three-dimensional structure of human von Willebrand factor. Blood. 1996;88:2939-2950.
81. Tangelder GJ, Slaaf DW, Arts T, Reneman RS. Wall shear rate in arterioles in vivo: least estimates from platelet velocity profiles. Am J Physiol. 1988;254:H1059-1064.
82. Verweij CL, Diergaarde PJ, Hart M, Pannekoek H. Full-length von Willebrand factor (vWF) cDNA encodes a highly repetitive protein considerably larger than the mature vWF subunit. Embo J. 1986;5:1839-1847.
83. Inouye M. Intramolecular chaperone: the role of the pro-peptide in protein folding. Enzyme. 1991;45:314-321.
84. Shinde U, Inouye M. Intramolecular chaperones: polypeptide extensions that modulate protein folding. Semin Cell Dev Biol. 2000;11:35-44.
85. Sevarino KA, Stork P, Ventimiglia R, Mandel G, Goodman RH. Amino-terminal sequences of prosomatostatin direct intracellular targeting but not processing specificity. Cell. 1989;57:11-19.
86. Stoller TJ, Shields D. The propeptide of preprosomatostatin mediates intracellular transport and secretion of alpha-globin from mammalian cells. J Cell Biol. 1989;108:1647-1655.
87. Shinde U, Li Y, Chatterjee S, Inouye M. Folding pathway mediated by an intramolecular chaperone. Proc Natl Acad Sci U S A. 1993;90:6924-6928.
88. Naim HY, Jacob R, Naim H, Sambrook JF, Gething MJ. The pro region of human intestinal lactase-phlorizin hydrolase. J Biol Chem. 1994;269:26933-26943.
89. Hidaka Y, Shimono C, Ohno M, et al. Dual function of the propeptide of prouroguanylin in the folding of the mature peptide: disulfide-coupled folding and dimerization. J Biol Chem. 2000;275:25155-25162.
90. Rosenberg JB, Haberichter SL, Jozwiak MA, et al. The role of the D1 domain of the von Willebrand factor propeptide in multimerization of VWF. Blood. 2002;100:1699-1706.

91. Journet AM, Saffaripour S, Wagner DD. Requirement for both D domains of the propolypeptide in von Willebrand factor multimerization and storage. Thromb Haemost. 1993;70:1053-1057.
92. Allen S, Abuzenadah AM, Hinks J, et al. A novel von Willebrand disease-causing mutation (Arg273Trp) in the von Willebrand factor propeptide that results in defective multimerization and secretion. Blood. 2000;96:560-568.
93. Gaucher C, Uno H, Yamazaki T, Mashiba H, Mazurier C. A new candidate mutation (N528S) within the von Willebrand factor propeptide identified in a Japanese patient with phenotype IIC of von Willebrand disease. Eur J Haematol. 1998;61:145-148.
94. Schneppenheim R, Thomas KB, Krey S, et al. Identification of a candidate missense mutation in a family with von Willebrand disease type IIC. Hum Genet. 1995;95:681-686.
95. Gaucher C, Dieval J, Mazurier C. Characterization of von Willebrand factor gene defects in two unrelated patients with type IIC von Willebrand disease. Blood. 1994;84:1024-1030.
96. Fujimura Y, Titani K, Holland LZ, et al. von Willebrand factor. A reduced and alkylated 52/48-kDa fragment beginning at amino acid residue 449 contains the domain interacting with platelet glycoprotein Ib. J Biol Chem. 1986;261:381-385.
97. Azuma H, Hayashi T, Dent JA, Ruggeri ZM, Ware J. Disulfide bond requirements for assembly of the platelet glycoprotein Ib-binding domain of von Willebrand factor. J Biol Chem. 1993;268:2821-2827.
98. Dong Z, Thoma RS, Crimmins DL, McCourt DW, Tuley EA, Sadler JE. Disulfide bonds required to assemble functional von Willebrand factor multimers. J Biol Chem. 1994;269:6753-6758.
99. Tjernberg P, Vos HL, Castaman G, Bertina RM, Eikenboom JC. Dimerization and multimerization defects of von Willebrand factor due to mutated cysteine residues. J Thromb Haemost. 2004;2:257-265.
100. Hommais A, Stepanian A, Fressinaud E, et al. Mutations C1157F and C1234W of von Willebrand factor cause intracellular retention with defective multimerization and secretion. J Thromb Haemost. 2006;4:148-157.
101. Allen S, Abuzenadah AM, Blagg JL, et al. Two novel type 2N von Willebrand disease-causing mutations that result in defective factor VIII binding, multimerization, and secretion of von Willebrand factor. Blood. 2000;95:2000-2007.
102. Hilbert L, Jorieux S, Fontenay-Roupie M, et al. Expression of two type 2N von Willebrand disease mutations identified in exon 18 of von Willebrand factor gene. Br J Haematol. 2004;127:184-189.
103. Tuddenham EG, Lane RS, Rotblat F, et al. Response to infusions of polyelectrolyte fractionated human factor VIII concentrate in human haemophilia A and von Willebrand's disease. Br J Haematol. 1982;52:259-267.
104. Koedam JA, Meijers JC, Sixma JJ, Bouma BN. Inactivation of human factor VIII by activated protein C. Cofactor activity of protein S and protective effect of von Willebrand factor. J Clin Invest. 1988;82:1236-1243.
105. Rick ME, Esmon NL, Krizek DM. Factor IXa and von Willebrand factor modify the inactivation of factor VIII by activated protein C. J Lab Clin Med. 1990;115:415-421.
106. Koedam JA, Hamer RJ, Beeser-Visser NH, Bouma BN, Sixma JJ. The effect of von Willebrand factor on activation of factor VIII by factor Xa. Eur J Biochem. 1990;189:229-234.

107. Koppelman SJ, Koedam JA, van Wijnen M, et al. von Willebrand factor as a regulator of intrinsic factor X activation. J Lab Clin Med. 1994;123:585-593.
108. Hill-Eubanks DC, Lollar P. von Willebrand factor is a cofactor for thrombin-catalyzed cleavage of the factor VIII light chain. J Biol Chem. 1990;265:17854-17858.
109. Vlot AJ, Koppelman SJ, van den Berg MH, Bouma BN, Sixma JJ. The affinity and stoichiometry of binding of human factor VIII to von Willebrand factor. Blood. 1995;85:3150-3157.
110. Bendetowicz AV, Wise RJ, Gilbert GE. Collagen-bound von Willebrand factor has reduced affinity for factor VIII. J Biol Chem. 1999;274:12300-12307.
111. Vlot AJ, Koppelman SJ, Meijers JC, et al. Kinetics of factor VIII-von Willebrand factor association. Blood. 1996;87:1809-1816.
112. Vlot AJ, Koppelman SJ, Bouma BN, Sixma JJ. Factor VIII and von Willebrand factor. Thromb Haemost. 1998;79:456-465.
113. Foster PA, Fulcher CA, Marti T, Titani K, Zimmerman TS. A major factor VIII binding domain resides within the amino-terminal 272 amino acid residues of von Willebrand factor. J Biol Chem. 1987;262:8443-8446.
114. Takahashi Y, Kalafatis M, Girma JP, Sewerin K, Andersson LO, Meyer D. Localization of a factor VIII binding domain on a 34 kilodalton fragment of the N-terminal portion of von Willebrand factor. Blood. 1987;70:1679-1682.
115. Pietu G, Ribba AS, Meulien P, Meyer D. Localization within the 106 N-terminal amino acids of von Willebrand factor (vWF) of the epitope corresponding to a monoclonal antibody which inhibits vWF binding to factor VIII. Biochem Biophys Res Commun. 1989;163:618-626.
116. Bahou WF, Ginsburg D, Sikkink R, Litwiller R, Fass DN. A monoclonal antibody to von Willebrand factor (vWF) inhibits factor VIII binding. Localization of its antigenic determinant to a nonadecapeptide at the amino terminus of the mature vWF polypeptide. J Clin Invest. 1989;84:56-61.
117. Ginsburg D, Bockenstedt PL, Allen EA, et al. Fine mapping of monoclonal antibody epitopes on human von Willebrand factor using a recombinant peptide library. Thromb Haemost. 1992;67:166-171.
118. Padilla A, Moake JL, Bernardo A, et al. P-selectin anchors newly released ultralarge von Willebrand factor multimers to the endothelial cell surface. Blood. 2004;103:2150-2156.
119. Michaux G, Pullen TJ, Haberichter SL, Cutler DF. P-selectin binds to the D'-D3 domains of von Willebrand factor in Weibel-Palade bodies. Blood. 2006;107:3922-3924.
120. Sadler JE, Shelton-Inloes BB, Sorace JM, Harlan JM, Titani K, Davie EW. Cloning and characterization of two cDNAs coding for human von Willebrand factor. Proc Natl Acad Sci U S A. 1985;82:6394-6398.
121. Emsley J, Cruz M, Handin R, Liddington R. Crystal structure of the von Willebrand Factor A1 domain and implications for the binding of platelet glycoprotein Ib. J Biol Chem. 1998;273:10396-10401.
122. Huizinga EG, Martijn van der Plas R, Kroon J, Sixma JJ, Gros P. Crystal structure of the A3 domain of human von Willebrand factor: implications for collagen binding. Structure. 1997;5:1147-1156.
123. Colombatti A, Bonaldo P. The superfamily of proteins with von Willebrand factor type A-like domains: one theme common to components of extracellular matrix, hemostasis, cellular adhesion, and defense mechanisms. Blood. 1991;77:2305-2315.

124. Fujimura Y, Titani K, Holland LZ, et al. A heparin-binding domain of human von Willebrand factor. Characterization and localization to a tryptic fragment extending from amino acid residue Val-449 to Lys-728. J Biol Chem. 1987;262:1734-1739.
125. Christophe O, Obert B, Meyer D, Girma JP. The binding domain of von Willebrand factor to sulfatides is distinct from those interacting with glycoprotein Ib, heparin, and collagen and resides between amino acid residues Leu 512 and Lys 673. Blood. 1991;78:2310-2317.
126. Data RE, Williams SB, Roberts DD, Gralnick HR. Platelets adhere to sulfatides by von Willebrand factor dependent and independent mechanisms. Thromb Haemost. 1991;65:581-587.
127. Koivunen E, Ranta TM, Annila A, et al. Inhibition of beta(2) integrin-mediated leukocyte cell adhesion by leucine-leucine-glycine motif-containing peptides. J Cell Biol. 2001;153:905-916.
128. Ware J. Molecular analyses of the platelet glycoprotein Ib-IX-V receptor. Thromb Haemost. 1998;79:466-478.
129. Sugimoto M, Ricca G, Hrinda ME, et al. Functional modulation of the isolated glycoprotein Ib binding domain of von Willebrand factor expressed in Escherichia coli. Biochemistry. 1991;30:5202-5209.
130. Sixma JJ, Schiphorst ME, Verweij CL, Pannekoek H. Effect of deletion of the A1 domain of von Willebrand factor on its binding to heparin, collagen and platelets in the presence of ristocetin. Eur J Biochem. 1991;196:369-375.
131. Sugimoto M, Dent J, McClintock R, Ware J, Ruggeri ZM. Analysis of structure-function relationships in the platelet membrane glycoprotein Ib-binding domain of von Willebrand's factor by expression of deletion mutants. J Biol Chem. 1993;268:12185-12192.
132. Berndt MC, Ward CM, Booth WJ, Castaldi PA, Mazurov AV, Andrews RK. Identification of aspartic acid 514 through glutamic acid 542 as a glycoprotein Ib-IX complex receptor recognition sequence in von Willebrand factor. Mechanism of modulation of von Willebrand factor by ristocetin and botrocetin. Biochemistry. 1992;31:11144-11151.
133. Cruz MA, Diacovo TG, Emsley J, Liddington R, Handin RI. Mapping the glycoprotein Ib-binding site in the von willebrand factor A1 domain. J Biol Chem. 2000;275:19098-19105.
134. Matsushita T, Sadler JE. Identification of amino acid residues essential for von Willebrand factor binding to platelet glycoprotein Ib. Charged-to-alanine scanning mutagenesis of the A1 domain of human von Willebrand factor. J Biol Chem. 1995;270:13406-13414.
135. Miura S, Li CQ, Cao Z, Wang H, Wardell MR, Sadler JE. Interaction of von Willebrand factor domain A1 with platelet glycoprotein Ibalpha-(1-289). Slow intrinsic binding kinetics mediate rapid platelet adhesion. J Biol Chem. 2000;275:7539-7546.
136. Huizinga EG, Tsuji S, Romijn RA, et al. Structures of glycoprotein Ibalpha and its complex with von Willebrand factor A1 domain. Science. 2002;297:1176-1179.
137. Ulrichts H, Udvardy M, Lenting PJ, et al. Shielding of the A1 domain by the D'D3 domains of von Willebrand factor modulates its interaction with platelet glycoprotein Ib-IX-V. J Biol Chem. 2006;281:4699-4707.
138. Maita N, Nishio K, Nishimoto E, et al. Crystal structure of von Willebrand factor A1 domain complexed with snake venom, bitiscetin: insight into glycoprotein Ibalpha binding mechanism induced by snake venom proteins. J Biol Chem. 2003;278:37777-37781.

139. Mohri H, Yoshioka A, Zimmerman TS, Ruggeri ZM. Isolation of the von Willebrand factor domain interacting with platelet glycoprotein Ib, heparin, and collagen and characterization of its three distinct functional sites. J Biol Chem. 1989;264:17361-17367.
140. Adachi T, Matsushita T, Dong Z, et al. Identification of amino acid residues essential for heparin binding by the A1 domain of human von Willebrand factor. Biochem Biophys Res Commun. 2006;339:1178-1183.
141. Pareti FI, Fujimura Y, Dent JA, Holland LZ, Zimmerman TS, Ruggeri ZM. Isolation and characterization of a collagen binding domain in human von Willebrand factor. J Biol Chem. 1986;261:15310-15315.
142. Pareti FI, Niiya K, McPherson JM, Ruggeri ZM. Isolation and characterization of two domains of human von Willebrand factor that interact with fibrillar collagen types I and III. J Biol Chem. 1987;262:13835-13841.
143. Kalafatis M, Takahashi Y, Girma JP, Meyer D. Localization of a collagen-interactive domain of human von Willebrand factor between amino acid residues Gly 911 and Glu 1,365. Blood. 1987;70:1577-1583.
144. Takagi J, Sekiya F, Kasahara K, Inada Y, Saito Y. Inhibition of platelet-collagen interaction by propolypeptide of von Willebrand factor. J Biol Chem. 1989;264:6017-6020.
145. Azuma H, Dent JA, Sugimoto M, Ruggeri ZM, Ware J. Independent assembly and secretion of a dimeric adhesive domain of von Willebrand factor containing the glycoprotein Ib-binding site. J Biol Chem. 1991;266:12342-12347.
146. Cruz MA, Handin RI, Wise RJ. The interaction of the von Willebrand factor-A1 domain with platelet glycoprotein Ib/IX. The role of glycosylation and disulfide bonding in a monomeric recombinant A1 domain protein. J Biol Chem. 1993;268:21238-21245.
147. Cruz MA, Yuan H, Lee JR, Wise RJ, Handin RI. Interaction of the von Willebrand factor (vWF) with collagen. Localization of the primary collagen-binding site by analysis of recombinant vWF a domain polypeptides. J Biol Chem. 1995;270:10822-10827.
148. Lankhof H, van Hoeij M, Schiphorst ME, et al. A3 domain is essential for interaction of von Willebrand factor with collagen type III. Thromb Haemost. 1996;75:950-958.
149. Romijn RA, Bouma B, Wuyster W, et al. Identification of the collagen-binding site of the von Willebrand factor A3-domain. J Biol Chem. 2001;276:9985-9991.
150. Romijn RA, Westein E, Bouma B, et al. Mapping the collagen-binding site in the von Willebrand factor-A3 domain. J Biol Chem. 2003;278:15035-15039.
151. Nishida N, Sumikawa H, Sakakura M, et al. Collagen-binding mode of vWF-A3 domain determined by a transferred cross-saturation experiment. Nat Struct Biol. 2003;10:53-58.
152. Lisman T, Raynal N, Groeneveld D, et al. A single high-affinity binding site for von Willebrand Factor in collagen III, identified using synthetic triple-helical peptides. Blood. 2006.
153. Morales LD, Martin C, Cruz MA. The interaction of von Willebrand factor-A1 domain with collagen: mutation G1324S (type 2M von Willebrand disease) impairs the conformational change in A1 domain induced by collagen. J Thromb Haemost. 2006;4:417-425.
154. Baronciani L, Federici AB, Beretta M, Cozzi G, Canciani MT, Mannucci PM. Expression studies on a novel type 2B variant of the von Willebrand factor gene

(R1308L) characterized by defective collagen binding. J Thromb Haemost. 2005;3:2689-2694.
155. Fischer BE, Kramer G, Mitterer A, et al. Effect of multimerization of human and recombinant von Willebrand factor on platelet aggregation, binding to collagen and binding of coagulation factor VIII. Thromb Res. 1996;84:55-66.
156. van der Plas RM, Gomes L, Marquart JA, et al. Binding of von Willebrand factor to collagen type III: role of specific amino acids in the collagen binding domain of vWF and effects of neighboring domains. Thromb Haemost. 2000;84:1005-1011.
157. Hoylaerts MF, Yamamoto H, Nuyts K, Vreys I, Deckmyn H, Vermylen J. von Willebrand factor binds to native collagen VI primarily via its A1 domain. Biochem J. 1997;324 (Pt 1):185-191.
158. Mazzucato M, Spessotto P, Masotti A, et al. Identification of domains responsible for von Willebrand factor type VI collagen interaction mediating platelet adhesion under high flow. J Biol Chem. 1999;274:3033-3041.
159. Furlan M, Robles R, Lamie B. Partial purification and characterization of a protease from human plasma cleaving von Willebrand factor to fragments produced by in vivo proteolysis. Blood. 1996;87:4223-4234.
160. Lankhof H, Damas C, Schiphorst ME, et al. von Willebrand factor without the A2 domain is resistant to proteolysis. Thromb Haemost. 1997;77:1008-1013.
161. Sutherland JJ, O'Brien LA, Lillicrap D, Weaver DF. Molecular modeling of the von Willebrand factor A2 Domain and the effects of associated type 2A von Willebrand disease mutations. J Mol Model (Online). 2004;10:259-270.
162. Tsai HM, Sussman, II, Nagel RL. Shear stress enhances the proteolysis of von Willebrand factor in normal plasma. Blood. 1994;83:2171-2179.
163. Hunt LT, Barker WC. von Willebrand factor shares a distinctive cysteine-rich domain with thrombospondin and procollagen. Biochem Biophys Res Commun. 1987;144:876-882.
164. Beacham DA, Wise RJ, Turci SM, *Handin RI. Selective* inactivation of the Arg-Gly-Asp-Ser (RGDS) binding site in von Willebrand factor by site-directed mutagenesis. J Biol Chem. 1992;267:3409-3415.
165. Chen ZY, Hendriks RW, Jobling MA, et al. Isolation and characterization of a candidate gene for Norrie disease. Nat Genet. 1992;1:204-208.
166. Eckhardt AE, Timpte CS, DeLuca AW, Hill RL. The complete cDNA sequence and structural polymorphism of the polypeptide chain of porcine submaxillary mucin. J Biol Chem. 1997;272:33204-33210.
167. Lesuffleur T, Roche F, Hill AS, et al. Characterization of a mucin cDNA clone isolated from HT-29 mucus-secreting cells. The 3' end of MUC5AC? J Biol Chem. 1995;270:13665-13673.
168. Meitinger T, Meindl A, Bork P, et al. Molecular modelling of the Norrie disease protein predicts a cystine knot growth factor tertiary structure. Nat Genet. 1993;5:376-380.
169. Enayat MS, Guilliatt AM, Surdhar GK, et al. Aberrant dimerization of von Willebrand factor as the result of mutations in the carboxy-terminal region: identification of 3 mutations in members of 3 different families with type 2A (phenotype IID) von Willebrand disease. Blood. 2001;98:674-680.
170. Ruggeri ZM. Structure of von Willebrand factor and its function in platelet adhesion and thrombus formation. Best Pract Res Clin Haematol. 2001;14:257-279.
171. Goldsmith HL, Turitto VT. Rheological aspects of thrombosis and haemostasis: basic principles and applications. ICTH-Report--Subcommittee on Rheology of the

International Committee on Thrombosis and Haemostasis. Thromb Haemost. 1986;55:415-435.
172. Sakariassen KS, Bolhuis PA, Sixma JJ. Human blood platelet adhesion to artery subendothelium is mediated by factor VIII-Von Willebrand factor bound to the subendothelium. Nature. 1979;279:636-638.
173. Savage B, Saldivar E, Ruggeri ZM. Initiation of platelet adhesion by arrest onto fibrinogen or translocation on von Willebrand factor. Cell. 1996;84:289-297.
174. Sporn LA, Marder VJ, Wagner DD. Differing polarity of the constitutive and regulated secretory pathways for von Willebrand factor in endothelial cells. J Cell Biol. 1989;108:1283-1289.
175. Baruch D, Denis C, Marteaux C, Schoevaert D, Coulombel L, Meyer D. Role of von Willebrand factor associated to extracellular matrices in platelet adhesion. Blood. 1991;77:519-527.
176. Houdijk WP, de Groot PG, Nievelstein PF, Sakariassen KS, Sixma JJ. Subendothelial proteins and platelet adhesion. von Willebrand factor and fibronectin, not thrombospondin, are involved in platelet adhesion to extracellular matrix of human vascular endothelial cells. Arteriosclerosis. 1986;6:24-33.
177. Bernardo A, Bergeron AL, Sun CW, et al. Von Willebrand factor present in fibrillar collagen enhances platelet adhesion to collagen and collagen-induced platelet aggregation. J Thromb Haemost. 2004;2:660-669.
178. Badimon L, Badimon JJ, Turitto VT, Rand J, Fuster V. Functional behavior of vessels from pigs with von Willebrand disease. Values of platelet deposition are identical to those obtained on normal vessels. Arteriosclerosis. 1989;9:184-188.
179. Kroll MH, Harris TS, Moake JL, Handin RI, Schafer AI. von Willebrand factor binding to platelet GpIb initiates signals for platelet activation. J Clin Invest. 1991;88:1568-1573.
180. Ruggeri ZM. von Willebrand factor. J Clin Invest. 1997;99:559-564.
181. Savage B, Shattil SJ, Ruggeri ZM. Modulation of platelet function through adhesion receptors. A dual role for glycoprotein IIb-IIIa (integrin alpha IIb beta 3) mediated by fibrinogen and glycoprotein Ib-von Willebrand factor. J Biol Chem. 1992;267:11300-11306.
182. Miura Y, Ohnuma M, Jung SM, Moroi M. Cloning and expression of the platelet-specific collagen receptor glycoprotein VI. Thromb Res. 2000;98:301-309.
183. Miura Y, Takahashi T, Jung SM, Moroi M. Analysis of the interaction of platelet collagen receptor glycoprotein VI (GPVI) with collagen. A dimeric form of GPVI, but not the monomeric form, shows affinity to fibrous collagen. J Biol Chem. 2002;277:46197-46204.
184. Nieswandt B, Bergmeier W, Eckly A, et al. Evidence for cross-talk between glycoprotein VI and Gi-coupled receptors during collagen-induced platelet aggregation. Blood. 2001;97:3829-3835.
185. Sixma JJ, van Zanten GH, Saelman EU, et al. Platelet adhesion to collagen. Thromb Haemost. 1995;74:454-459.
186. Moog S, Mangin P, Lenain N, et al. Platelet glycoprotein V binds to collagen and participates in platelet adhesion and aggregation. Blood. 2001;98:1038-1046.
187. Romo GM, Dong JF, Schade AJ, et al. The glycoprotein Ib-IX-V complex is a platelet counterreceptor for P-selectin. J Exp Med. 1999;190:803-814.
188. Lefkovits J, Plow EF, Topol EJ. Platelet glycoprotein IIb/IIIa receptors in cardiovascular medicine. N Engl J Med. 1995;332:1553-1559.

189. Hantgan RR, Nichols WL, Ruggeri ZM. von Willebrand factor competes with fibrin for occupancy of GPIIb:IIIa on thrombin-stimulated platelets. Blood. 1990;75:889-894.
190. Goto S, Ikeda Y, Saldivar E, Ruggeri ZM. Distinct mechanisms of platelet aggregation as a consequence of different shearing flow conditions. J Clin Invest. 1998;101:479-486.
191. Moake JL, Turner NA, Stathopoulos NA, Nolasco LH, Hellums JD. Involvement of large plasma von Willebrand factor (vWF) multimers and unusually large vWF forms derived from endothelial cells in shear stress-induced platelet aggregation. J Clin Invest. 1986;78:1456-1461.
192. Moake JL, Turner NA, Stathopoulos NA, Nolasco L, Hellums JD. Shear-induced platelet aggregation can be mediated by vWF released from platelets, as well as by exogenous large or unusually large vWF multimers, requires adenosine diphosphate, and is resistant to aspirin. Blood. 1988;71:1366-1374.
193. Savage B, Sixma JJ, Ruggeri ZM. Functional self-association of von Willebrand factor during platelet adhesion under flow. Proc Natl Acad Sci U S A. 2002;99:425-430.
194. Shankaran H, Alexandridis P, Neelamegham S. Aspects of hydrodynamic shear regulating shear-induced platelet activation and self-association of von Willebrand factor in suspension. Blood. 2003;101:2637-2645.
195. Ulrichts H, Vanhoorelbeke K, Girma JP, Lenting PJ, Vauterin S, Deckmyn H. The von Willebrand factor self-association is modulated by a multiple domain interaction. J Thromb Haemost. 2005;3:552-561.
196. Furlan M. Von Willebrand factor: molecular size and functional activity. Ann Hematol. 1996;72:341-348.
197. Shindo T, Kurihara H, Kuno K, et al. ADAMTS-1: a metalloproteinase-disintegrin essential for normal growth, fertility, and organ morphology and function. J Clin Invest. 2000;105:1345-1352.
198. Colige A, Sieron AL, Li SW, et al. Human Ehlers-Danlos syndrome type VII C and bovine dermatosparaxis are caused by mutations in the procollagen I N-proteinase gene. Am J Hum Genet. 1999;65:308-317.
199. Fernandes RJ, Hirohata S, Engle JM, et al. Procollagen II amino propeptide processing by ADAMTS-3. Insights on dermatosparaxis. J Biol Chem. 2001;276:31502-31509.
200. Nakamura H, Fujii Y, Inoki I, et al. Brevican is degraded by matrix metalloproteinases and aggrecanase-1 (ADAMTS4) at different sites. J Biol Chem. 2000;275:38885-38890.
201. Abbaszade I, Liu RQ, Yang F, et al. Cloning and characterization of ADAMTS11, an aggrecanase from the ADAMTS family. J Biol Chem. 1999;274:23443-23450.
202. Levy GG, Nichols WC, Lian EC, et al. Mutations in a member of the ADAMTS gene family cause thrombotic thrombocytopenic purpura. Nature. 2001;413:488-494.
203. Zheng X, Chung D, Takayama TK, Majerus EM, Sadler JE, Fujikawa K. Structure of von Willebrand factor-cleaving protease (ADAMTS13), a metalloprotease involved in thrombotic thrombocytopenic purpura. J Biol Chem. 2001;276:41059-41063.
204. Plaimauer B, Zimmermann K, Volkel D, et al. Cloning, expression, and functional characterization of the von Willebrand factor-cleaving protease (ADAMTS13). Blood. 2002;100:3626-3632.

205. Soejima K, Mimura N, Hirashima M, et al. A novel human metalloprotease synthesized in the liver and secreted into the blood: possibly, the von Willebrand factor-cleaving protease? J Biochem (Tokyo). 2001;130:475-480.
206. Uemura M, Tatsumi K, Matsumoto M, et al. Localization of ADAMTS13 to the stellate cells of human liver. Blood. 2005;106:922-924.
207. Zhou W, Inada M, Lee TP, et al. ADAMTS13 is expressed in hepatic stellate cells. Lab Invest. 2005;85:780-788.
208. Turner N, Nolasco L, Tao Z, Dong JF, Moake J. Human endothelial cells synthesize and release ADAMTS-13. J Thromb Haemost. 2006;4:1396-1404.
209. Furlan M, Robles R, Morselli B, Sandoz P, Lammle B. Recovery and half-life of von Willebrand factor-cleaving protease after plasma therapy in patients with thrombotic thrombocytopenic purpura. Thromb Haemost. 1999;81:8-13.
210. Gerritsen HE, Robles R, Lammle B, Furlan M. Partial amino acid sequence of purified von Willebrand factor-cleaving protease. Blood. 2001;98:1654-1661.
211. Andreini C, Banci L, Bertini I, Elmi S, Rosato A. Comparative analysis of the ADAM and ADAMTS families. J Proteome Res. 2005;4:881-888.
212. Dent JA, Galbusera M, Ruggeri ZM. Heterogeneity of plasma von Willebrand factor multimers resulting from proteolysis of the constituent subunit. J Clin Invest. 1991;88:774-782.
213. Jenkins PV, Pasi KJ, Perkins SJ. Molecular modeling of ligand and mutation sites of the type A domains of human von Willebrand factor and their relevance to von Willebrand's disease. Blood. 1998;91:2032-2044.
214. Dong JF, Moake JL, Nolasco L, et al. ADAMTS-13 rapidly cleaves newly secreted ultralarge von Willebrand factor multimers on the endothelial surface under flowing conditions. Blood. 2002;100:4033-4039.
215. Kokame K, Matsumoto M, Fujimura Y, Miyata T. VWF73, a region from D1596 to R1668 of von Willebrand factor, provides a minimal substrate for ADAMTS-13. Blood. 2004;103:607-612.
216. Zanardelli S, Crawley JT, Chion CK, Lam JK, Preston RJ, Lane DA. ADAMTS13 substrate recognition of von Willebrand factor A2 domain. J Biol Chem. 2006;281:1555-1563.
217. Dong JF, Moake JL, Bernardo A, et al. ADAMTS-13 metalloprotease interacts with the endothelial cell-derived ultra-large von Willebrand factor. J Biol Chem. 2003;278:29633-29639.
218. Nishio K, Anderson PJ, Zheng XL, Sadler JE. Binding of platelet glycoprotein Ibalpha to von Willebrand factor domain A1 stimulates the cleavage of the adjacent domain A2 by ADAMTS13. Proc Natl Acad Sci U S A. 2004;101:10578-10583.
219. De Cristofaro R, Peyvandi F, Palla R, et al. Role of chloride ions in modulation of the interaction between von Willebrand factor and ADAMTS-13. J Biol Chem. 2005;280:23295-23302.
220. Soejima K, Matsumoto M, Kokame K, et al. ADAMTS-13 cysteine-rich/spacer domains are functionally essential for von Willebrand factor cleavage. Blood. 2003;102:3232-3237.
221. Zheng X, Nishio K, Majerus EM, Sadler JE. Cleavage of von Willebrand factor requires the spacer domain of the metalloprotease ADAMTS13. J Biol Chem. 2003;278:30136-30141.
222. Majerus EM, Anderson PJ, Sadler JE. Binding of ADAMTS13 to von Willebrand factor. J Biol Chem. 2005;280:21773-21778.

223. Ai J, Smith P, Wang S, Zhang P, Zheng XL. The proximal carboxyl-terminal domains of ADAMTS13 determine substrate specificity and are all required for cleavage of von Willebrand factor. J Biol Chem. 2005;280:29428-29434.
224. Bork P, Beckmann G. The CUB domain. A widespread module in developmentally regulated proteins. J Mol Biol. 1993;231:539-545.
225. Xie L, Chesterman CN, Hogg PJ. Control of von Willebrand factor multimer size by thrombospondin-1. J Exp Med. 2001;193:1341-1349.
226. Pimanda JE, Ganderton T, Maekawa A, et al. Role of thrombospondin-1 in control of von Willebrand factor multimer size in mice. J Biol Chem. 2004;279:21439-21448.
227. Hounsell EF, Davies MJ, Renouf DV. O-linked protein glycosylation structure and function. Glycoconj J. 1996;13:19-26.
228. Stanley P. Glycosylation engineering. Glycobiology. 1992;2:99-107.
229. Varki A. Biological roles of oligosaccharides: all of the theories are correct. Glycobiology. 1993;3:97-130.
230. Gavel Y, von Heijne G. Sequence differences between glycosylated and non-glycosylated Asn-X-Thr/Ser acceptor sites: implications for protein engineering. Protein Eng. 1990;3:433-442.
231. Kasturi L, Eshleman JR, Wunner WH, Shakin-Eshleman SH. The hydroxy amino acid in an Asn-X-Ser/Thr sequon can influence N-linked core glycosylation efficiency and the level of expression of a cell surface glycoprotein. J Biol Chem. 1995;270:14756-14761.
232. Miletich JP, Broze GJ, Jr. Beta protein C is not glycosylated at asparagine 329. The rate of translation may influence the frequency of usage at asparagine-X-cysteine sites. J Biol Chem. 1990;265:11397-11404.
233. Burda P, Aebi M. The dolichol pathway of N-linked glycosylation. Biochim Biophys Acta. 1999;1426:239-257.
234. Gahmberg CG, Tolvanen M. Why mammalian cell surface proteins are glycoproteins. Trends Biochem Sci. 1996;21:308-311.
235. Knauer R, Lehle L. The oligosaccharyltransferase complex from Saccharomyces cerevisiae. Isolation of the OST6 gene, its synthetic interaction with OST3, and analysis of the native complex. J Biol Chem. 1999;274:17249-17256.
236. Knauer R, Lehle L. The oligosaccharyltransferase complex from yeast. Biochim Biophys Acta. 1999;1426:259-273.
237. Moremen KW, Trimble RB, Herscovics A. Glycosidases of the asparagine-linked oligosaccharide processing pathway. Glycobiology. 1994;4:113-125.
238. Hammond C, Braakman I, Helenius A. Role of N-linked oligosaccharide recognition, glucose trimming, and calnexin in glycoprotein folding and quality control. Proc Natl Acad Sci U S A. 1994;91:913-917.
239. Ou WJ, Cameron PH, Thomas DY, Bergeron JJ. Association of folding intermediates of glycoproteins with calnexin during protein maturation. Nature. 1993;364:771-776.
240. Spiro RG, Zhu Q, Bhoyroo V, Soling HD. Definition of the lectin-like properties of the molecular chaperone, calreticulin, and demonstration of its copurification with endomannosidase from rat liver Golgi. J Biol Chem. 1996;271:11588-11594.
241. Ware FE, Vassilakos A, Peterson PA, Jackson MR, Lehrman MA, Williams DB. The molecular chaperone calnexin binds Glc1Man9GlcNAc2 oligosaccharide as an initial step in recognizing unfolded glycoproteins. J Biol Chem. 1995;270:4697-4704.
242. Oliver JD, van der Wal FJ, Bulleid NJ, High S. Interaction of the thiol-dependent reductase ERp57 with nascent glycoproteins. Science. 1997;275:86-88.

243. Huppa JB, Ploegh HL. The eS-Sence of -SH in the ER. Cell. 1998;92:145-148.
244. Hauri H, Appenzeller C, Kuhn F, Nufer O. Lectins and traffic in the secretory pathway. FEBS Lett. 2000;476:32-37.
245. Elhammer AP, Poorman RA, Brown E, Maggiora LL, Hoogerheide JG, Kezdy FJ. The specificity of UDP-GalNAc:polypeptide N-acetylgalactosaminyltransferase as inferred from a database of in vivo substrates and from the in vitro glycosylation of proteins and peptides. J Biol Chem. 1993;268:10029-10038.
246. Hansen JE, Lund O, Engelbrecht J, Bohr H, Nielsen JO, Hansen JE. Prediction of O-glycosylation of mammalian proteins: specificity patterns of UDP-GalNAc:polypeptide N-acetylgalactosaminyltransferase. Biochem J. 1995;308 (Pt 3):801-813.
247. Schachter H, Brockhausen I. The biosynthesis of branched O-glycans. Symp Soc Exp Biol. 1989;43:1-26.
248. Clausen H, Bennett EP. A family of UDP-GalNAc: polypeptide N-acetylgalactosaminyl-transferases control the initiation of mucin-type O-linked glycosylation. Glycobiology. 1996;6:635-646.
249. Ten Hagen KG, Bedi GS, Tetaert D, et al. Cloning and characterization of a ninth member of the UDP-GalNAc:polypeptide N-acetylgalactosaminyltransferase family, ppGaNTase-T9. J Biol Chem. 2001;276:17395-17404.
250. Van den Steen P, Rudd PM, Dwek RA, Opdenakker G. Concepts and principles of O-linked glycosylation. Crit Rev Biochem Mol Biol. 1998;33:151-208.
251. Sangadala S, Sivakami S, Mendicino J. UDP-GlcNAc: Gal beta 3GalNAc-mucin: (GlcNAc----GalNAc) beta 6-N-acetylglucosaminyltransferase and UDP-GlcNAc: Gal beta 3(GlcNAc beta 6) GalNAc-mucin (GlcNAc----Gal)beta 3-N-acetylglucosaminyltransferase from swine trachea epithelium. Mol Cell Biochem. 1991;101:125-143.
252. Montreuil J. Primary structure of glycoprotein glycans: basis for the molecular biology of glycoproteins. Adv Carbohydr Chem Biochem. 1980;37:157-223.
253. Sodetz JM, Paulson JC, McKee PA. Carbohydrate composition and identification of blood group A, B, and H oligosaccharide structures on human Factor VIII/von Willebrand factor. J Biol Chem. 1979;254:10754-10760.
254. Samor B, Mazurier C, Goudemand M, Debeire P, Fournet B, Montreuil J. Preliminary results on the carbohydrate moiety of factor VIII/von Willebrand factor (FVIII/vWf). Thromb Res. 1982;25:81-89.
255. Biller M, Mardberg K, Hassan H, et al. Early steps in O-linked glycosylation and clustered O-linked glycans of herpes simplex virus type 1 glycoprotein C: effects on glycoprotein properties. Glycobiology. 2000;10:1259-1269.
256. Jentoft N. Why are proteins O-glycosylated? Trends Biochem Sci. 1990;15:291-294.
257. Samor B, Michalski JC, Mazurier C, et al. Primary structure of the major O-glycosidically linked carbohydrate unit of human von Willebrand factor. Glycoconj J. 1989;6:263-270.
258. Debeire P, Montreuil J, Samor B, et al. Structure determination of the major asparagine-linked sugar chain of human factor VIII--von Willebrand factor. FEBS Lett. 1983;151:22-26.
259. Samor B, Michalski JC, Debray H, et al. Primary structure of a new tetraantennary glycan of the N-acetyllactosaminic type isolated from human factor VIII/von Willebrand factor. Eur J Biochem. 1986;158:295-298.
260. Matsui T, Fujimura Y, Nishida S, Titani K. Human plasma alpha 2-macroglobulin and von Willebrand factor possess covalently linked ABO(H) blood

group antigens in subjects with corresponding ABO phenotype. Blood. 1993;82:663-668.
261. Berkowitz SD, Federici AB. Sialic acid prevents loss of large von Willebrand factor multimers by protecting against amino-terminal proteolytic cleavage. Blood. 1988;72:1790-1796.
262. Federici AB, Elder JH, De Marco L, Ruggeri ZM, Zimmerman TS. Carbohydrate moiety of von Willebrand factor is not necessary for maintaining multimeric structure and ristocetin cofactor activity but protects from proteolytic degradation. J Clin Invest. 1984;74:2049-2055.
263. Goudemand J, Mazurier C, Samor B, Bouquelet S, Montreuil J, Goudemand M. Effect of carbohydrate modifications of factor VIII/von Willebrand factor on binding to platelets. Thromb Haemost. 1985;53:390-395.
264. Gralnick HR, Williams SB, Rick ME. Role of carbohydrate in multimeric structure of factor VIII/von Willebrand factor protein. Proc Natl Acad Sci U S A. 1983;80:2771-2774.
265. Kessler CM, Floyd CM, Frantz SC, Orthner C. Critical role of the carbohydrate moiety in human von Willebrand factor protein for interactions with type I collagen. Thromb Res. 1990;57:59-76.
266. De Marco L, Shapiro SS. Properties of human asialo-factor VIII. A ristocetin-independent platelet-aggregating agent. J Clin Invest. 1981;68:321-328.
267. Vermylen J, De Gaetano G, Donati MB, Verstraete M. Platelet-aggregating activity in neuraminidase-treated human cryoprecipitates: its correlation with factor-VIII-related antigen. Br J Haematol. 1974;26:645-650.
268. Vermylen J, Donati MB, De Gaetano G, Verstraete M. Aggregation of human platelets by bovine or human factor VIII: role of carbohydrate side chains. Nature. 1973;244:167-168.
269. Sodetz JM, Pizzo SV, McKee PA. Relationship of sialic acid to function and in vivo survival of human factor VIII/von Willebrand factor protein. J Biol Chem. 1977;252:5538-5546.
270. Sodetz JM, Paulson JC, Pizzo SV, McKee PA. Carbohydrate on human factor VIII/von Willebrand factor. Impairment of function by removal of specific galactose residues. J Biol Chem. 1978;253:7202-7206.
271. Levy-Toledano S, Caen JP, Halmos T, Mester L. Dissociation between human platelet agglomerating activity and factor VIII procoagulant activity of bovine plasma preparations by chemical treatment. I. Effect of neuraminidase. Pathol Biol (Paris). 1973;21:Suppl:60-62.
272. Fukui H, Mikami S, Okuda T, Murashima N, Takase T. Studies of von Willebrand factor: effects of different kinds of carbohydrate oxidases, SH-inhibitors and some other chemical reagents. Br J Haematol. 1977;36:259-270.
273. Gralnick HR. Factor VIII/von Willebrand factor protein. Galactose a cryptic determinant of von Willebrand factor activity. J Clin Invest. 1978;62:496-499.
274. Morisato DK, Gralnick HR. Selective binding of the factor VIII/von Willebrand factor protein to human platelets. Blood. *1980;55:9-15.*
275. Rosenfeld L, Kirby EP. The effects of neuraminidase treatment on the biological activities of factor VIII. Thromb Res. 1979;15:255-261.
276. Lawrence JB, Gralnick HR. Asialo-von Willebrand factor inhibits platelet adherence to human arterial subendothelium: discrepancy between ristocetin cofactor activity and primary hemostatic function. Blood. 1987;70:1084-1089.

277. Bastida E, Monteagudo J, Ordinas A, De Marco L, Castillo R. Asialo von Willebrand factor enhances platelet adhesion to vessel subendothelium. Thromb Haemost. 1988;60:30-34.
278. Carew JA, Quinn SM, Stoddart JH, Lynch DC. O-linked carbohydrate of recombinant von Willebrand factor influences ristocetin-induced binding to platelet glycoprotein 1b. J Clin Invest. 1992;90:2258-2267.
279. Kuan SF, Byrd JC, Basbaum C, Kim YS. Inhibition of mucin glycosylation by aryl-N-acetyl-alpha-galactosaminides in human colon cancer cells. J Biol Chem. 1989;264:19271-19277.
280. Schulte am Esch J, 2nd, Robson SC, Knoefel WT, Eisenberger CF, Peiper M, Rogiers X. Impact of O-linked glycosylation of the VWF-A1-domain flanking regions on platelet interaction. Br J Haematol. 2005;128:82-90.
281. Bernard BA, Yamada KM, Olden K. Carbohydrates selectively protect a specific domain of fibronectin against proteases. J Biol Chem. 1982;257:8549-8554.
282. Stoddart JH, Jr., Andersen J, Lynch DC. Clearance of normal and type 2A von Willebrand factor in the rat. Blood. 1996;88:1692-1699.
283. Lenting PJ, Westein E, Terraube V, et al. An experimental model to study the in vivo survival of von Willebrand factor. Basic aspects and application to the R1205H mutation. J Biol Chem. 2004;279:12102-12109.
284. Turecek PL, Gritsch H, Pichler L, et al. In vivo characterization of recombinant von Willebrand factor in dogs with von Willebrand disease. Blood. 1997;90:3555-3567.
285. Schooten CJ, Tjernberg P, Westein E, et al. Cysteine-mutations in von Willebrand factor associated with increased clearance. J Thromb Haemost. 2005;3:2228-2237.
286. Ashwell G, Harford J. Carbohydrate-specific receptors of the liver. Annu Rev Biochem. 1982;51:531-554.
287. Ain KB, Mori Y, Refetoff S. Reduced clearance rate of thyroxine-binding globulin (TBG) with increased sialylation: a mechanism for estrogen-induced elevation of serum TBG concentration. J Clin Endocrinol Metab. 1987;65:689-696.
288. Durocher JR, Payne RC, Conrad ME. Role of sialic acid in erythrocyte survival. Blood. 1975;45:11-20.
289. Morell AG, Gregoriadis G, Scheinberg IH, Hickman J, Ashwell G. The role of sialic acid in determining the survival of glycoproteins in the circulation. J Biol Chem. 1971;246:1461-1467.
290. Nelsestuen GL, Suttie JW. Properties of asialo and aglycoprothrombin. Biochem Biophys Res Commun. 1971;45:198-203.
291. Stockert RJ, Morell AG, Scheinberg IH. The existence of a second route for the transfer of certain glycoproteins from the circulation into the liver. Biochem Biophys Res Commun. 1976;68:988-993.
292. Baynes JW, Wold F. Effect of glycosylation on the in vivo circulating half-life of ribonuclease. J Biol Chem. 1976;251:6016-6024.
293. Kolatkar AR, Leung AK, Isecke R, Brossmer R, Drickamer K, Weis WI. Mechanism of N-acetylgalactosamine binding to a C-type animal lectin carbohydrate-recognition domain. J Biol Chem. 1998;273:19502-19508.
294. Ellies LG, Ditto D, Levy GG, et al. Sialyltransferase ST3Gal-IV operates as a dominant modifier of hemostasis by concealing asialoglycoprotein receptor ligands. Proc Natl Acad Sci U S A. 2002;99:10042-10047.
295. Sweeney JD, Novak EK, Reddington M, Takeuchi KH, Swank RT. The RIIIS/J inbred mouse strain as a model for von Willebrand disease. Blood. 1990;76:2258-2265.

296. Mohlke KL, Purkayastha AA, Westrick RJ, Ginsburg D. Comparative mapping of distal murine chromosome 11 and human 17q21.3 in a region containing a modifying locus for murine plasma von Willebrand factor level. Genomics. 1998;54:19-30.
297. Nichols WC, Cooney KA, Mohlke KL, et al. von Willebrand disease in the RIIIS/J mouse is caused by a defect outside of the von Willebrand factor gene. Blood. 1995;86:2461.
298. Mohlke KL, Purkayastha AA, Westrick RJ, et al. Mvwf, a dominant modifier of murine von Willebrand factor, results from altered lineage-specific expression of a glycosyltransferase. Cell. 1999;96:111-120.
299. Preston AE, Barr A. The Plasma Concentration of Factor Viii in the Normal Population. Ii. the Effects of Age, Sex and Blood Group. Br J Haematol. 1964;10:238-245.
300. Conlan MG, Folsom AR, Finch A, et al. Associations of factor VIII and von Willebrand factor with age, race, sex, and risk factors for atherosclerosis. The Atherosclerosis Risk in Communities (ARIC) Study. Thromb Haemost. 1993;70:380-385.
301. Koster T, Blann AD, Briet E, Vandenbroucke JP, Rosendaal FR. Role of clotting factor VIII in effect of von Willebrand factor on occurrence of deep-vein thrombosis. Lancet. 1995;345:152-155.
302. Bellinger DA, Nichols TC, Read MS, et al. Prevention of occlusive coronary artery thrombosis by a murine monoclonal antibody to porcine von Willebrand factor. Proc Natl Acad Sci U S A. 1987;84:8100-8104.
303. Rumley A, Lowe GD, Sweetnam PM, Yarnell JW, Ford RP. Factor VIII, von Willebrand factor and the risk of major ischaemic heart disease in the Caerphilly Heart Study. Br J Haematol. 1999;105:110-116.
304. Smith FB, Lee AJ, Fowkes FG, Price JF, Rumley A, Lowe GD. Hemostatic factors as predictors of ischemic heart disease and stroke in the Edinburgh Artery Study. Arterioscler Thromb Vasc Biol. 1997;17:3321-3325.
305. Bongers TN, de Maat MP, van Goor ML, et al. High von Willebrand Factor Levels Increase the Risk of First Ischemic Stroke. Influence of ADAMTS13, Inflammation, and Genetic Variability. Stroke. 2006.
306. Keightley AM, Lam YM, Brady JN, Cameron CL, Lillicrap D. Variation at the von Willebrand factor (vWF) gene locus is associated with plasma vWF:Ag levels: identification of three novel single nucleotide polymorphisms in the vWF gene promoter. Blood. 1999;93:4277-4283.
307. Mannucci PM. von Willebrand factor: a marker of endothelial damage? Arterioscler Thromb Vasc Biol. 1998;18:1359-1362.
308. Green D, Ruth KJ, Folsom AR, Liu K. Hemostatic factors in the Coronary Artery Risk Development in Young Adults (CARDIA) Study. Arterioscler Thromb. 1994;14:686-693.
309. Miller CH, Haff E, Platt SJ, et al. Measurement of von Willebrand factor activity: relative effects of ABO blood type and race. J Thromb Haemost. 2003;1:2191-2197.
310. Sukhu K, Poovalingam V, Mahomed R, Giangrande PL. Ethnic variation in von Willebrand factor levels can influence the diagnosis of von Willebrand disease. Clin Lab Haematol. 2003;25:247-249.
311. Schneppenheim R, Krey S, Bergmann F, et al. Genetic heterogeneity of severe von Willebrand disease type III in the German population. Hum Genet. 1994;94:640-652.

312. Orstavik KH, Magnus P, Reisner H, Berg K, Graham JB, Nance W. Factor VIII and factor IX in a twin population. Evidence for a major effect of ABO locus on factor VIII level. Am J Hum Genet. 1985;37:89-101.
313. Yamamoto F, Clausen H, White T, Marken J, Hakomori S. Molecular genetic basis of the histo-blood group ABO system. Nature. 1990;345:229-233.
314. Lowe JB. The blood group-specific human glycosyltransferases. Baillieres Clin Haematol. 1993;6:465-492.
315. Yamamoto F, McNeill PD, Hakomori S. Human histo-blood group A2 transferase coded by A2 allele, one of the A subtypes, is characterized by a single base deletion in the coding sequence, which results in an additional domain at the carboxyl terminal. Biochem Biophys Res Commun. 1992;187:366-374.
316. Gill JC, Endres-Brooks J, Bauer PJ, Marks WJ, Jr., Montgomery RR. The effect of ABO blood group on the diagnosis of von Willebrand disease. Blood. 1987;69:1691-1695.
317. McCallum CJ, Peake IR, Newcombe RG, Bloom AL. Factor VIII levels and blood group antigens. Thromb Haemost. 1983;50:757.
318. Mohanty D, Ghosh K, Marwaha N, Kaur S, Chauhan AP, Das KC. Major blood group antigens--a determinant of factor VIII levels in blood? Thromb Haemost. 1984;51:414.
319. Shima M, Fujimura Y, Nishiyama T, et al. ABO blood group genotype and plasma von Willebrand factor in normal individuals. Vox Sang. 1995;68:236-240.
320. Souto JC, Almasy L, Muniz-Diaz E, et al. Functional effects of the ABO locus polymorphism on plasma levels of von Willebrand factor, factor VIII, and activated partial thromboplastin time. Arterioscler Thromb Vasc Biol. 2000;20:2024-2028.
321. Haberichter SL, Balistreri M, Christopherson P, et al. Assay of the von Willebrand factor (VWF) propeptide to identify type 1 von Willebrand disease patients with decreased VWF survival. Blood. 2006.
322. O'Donnell J, Boulton FE, Manning RA, Laffan MA. Amount of H antigen expressed on circulating von Willebrand factor is modified by ABO blood group genotype and is a major determinant of plasma von Willebrand factor antigen levels. Arterioscler Thromb Vasc Biol. 2002;22:335-341.
323. Brown SA, Collins PW, Bowen DJ. Heterogeneous detection of A-antigen on von Willebrand factor derived from platelets, endothelial cells and plasma. Thromb Haemost. 2002;87:990-996.
324. Bowen DJ. An influence of ABO blood group on the rate of proteolysis of von Willebrand factor by ADAMTS13. J Thromb Haemost. 2003;1:33-40.
325. Fischer BE, Thomas KB, Dorner F. von Willebrand factor: measuring its antigen or function? Correlation between the level of antigen, activity, and multimer size using various detection systems. Thromb Res. 1998;91:39-43.
326. Paczuski R. Determination of von Willebrand factor activity with collagen-binding assay and diagnosis of von Willebrand disease: effect of collagen source and coating conditions. J Lab Clin Med. 2002;140:250-254.
327. Siekmann J, Turecek PL, Schwarz HP. The determination of von Willebrand factor activity by collagen binding assay. Haemophilia. 1998;4 Suppl 3:15-24.
328. Favaloro EJ. Collagen binding assay for von Willebrand factor (VWF:CBA): detection of von Willebrands Disease (VWD), and discrimination of VWD subtypes, depends on collagen source. Thromb Haemost. 2000;83:127-135.
329. Ruggeri ZM, Zimmerman TS. The complex multimeric composition of factor VIII/von Willebrand factor. Blood. 1981;57:1140-1143.

330. Aihara M, Sawada Y, Ueno K, et al. Visualization of von Willebrand factor multimers by immunoenzymatic stain using avidin-biotin peroxidase complex. Thromb Haemost. 1986;55:263-267.
331. Bukh A, Ingerslev J, Stenbjerg S, Moller NP. The multimeric structure of plasma F VIII:RAg studied by electroelution and immunoperoxidase detection. Thromb Res. 1986;43:579-584.
332. Lombardi R, Gelfi C, Righetti PG, Lattuada A, Mannucci PM. Electroblot and immunoperoxidase staining for rapid screening of the abnormalities of the multimeric structure of von Willebrand factor in von Willebrand's disease. Thromb Haemost. 1986;55:246-249.
333. Krizek DR, Rick ME. A rapid method to visualize von willebrand factor multimers by using agarose gel electrophoresis, immunolocalization and luminographic detection. Thromb Res. 2000;97:457-462.
334. Budde U, Schneppenheim R, Plendl H, Dent J, Ruggeri ZM, Zimmerman TS. Luminographic detection of von Willebrand factor multimers in agarose gels and on nitrocellulose membranes. Thromb Haemost. 1990;63:312-315.
335. Schneppenheim R, Plendl H, Budde U. Luminography--an alternative assay for detection of von Willebrand factor multimers. Thromb Haemost. 1988;60:133-136.
336. Baillod P, Affolter B, Kurt GH, Pflugshaupt R. Multimeric analysis of von Willebrand factor by vertical sodium dodecyl sulphate agarose gel electrophoresis, vacuum blotting technology and sensitive visualization by alkaline phosphatase anti-alkaline phosphatase complex. Thromb Res. 1992;66:745-755.
337. Smejkal GB, Shainoff JR, Kottke-Marchant KM. Rapid high-resolution electrophoresis of multimeric von Willebrand Factor using a thermopiloted gel apparatus. Electrophoresis. 2003;24:582-587.
338. Smejkal GB, Hoff HF. Cholesterol-specific probe for lipoproteins immobilized on nitrocellulose membranes. Biotechniques. 1994;16:68-70.
339. Bhende YM, Deshpande CK, Bhatia HM, et al. A "new" blood group character related to the ABO system. Lancet. 1951;1:903-904.
340. Kelly RJ, Ernst LK, Larsen RD, Bryant JG, Robinson JS, Lowe JB. Molecular basis for H blood group deficiency in Bombay (Oh) and para-Bombay individuals. Proc Natl Acad Sci U S A. 1994;91:5843-5847.
341. Rajan VP, Larsen RD, Ajmera S, Ernst LK, Lowe JB. A cloned human DNA restriction fragment determines expression of a GDP-L-fucose: beta-D-galactoside 2-alpha-L-fucosyltransferase in transfected cells. Evidence for isolation and transfer of the human H blood group locus. J Biol Chem. 1989;264:11158-11167.
342. Larsen RD, Ernst LK, Nair RP, Lowe JB. Molecular cloning, sequence, and expression of a human GDP-L-fucose:beta-D-galactoside 2-alpha-L-fucosyltransferase cDNA that can form the H blood group antigen. Proc Natl Acad Sci U S A. 1990;87:6674-6678.
343. Watkins WM. Biochemistry and Genetics of the ABO, Lewis, and P blood group systems. Adv Hum Genet. 1980;10:1-136, 379-185.
344. Oriol R, Danilovs J, Hawkins BR. A new genetic model proposing that the Se gene is a structural gene closely linked to the H gene. Am J Hum Genet. 1981;33:421-431.
345. Wagner FF, Kasulke D, Kerowgan M, Flegel WA. Frequencies of the blood groups ABO, Rhesus, D category VI, Kell, and of clinically relevant high-frequency antigens in south-western Germany. Infusionsther Transfusionsmed. 1995;22:285-290.

346. Kaneko M, Nishihara S, Shinya N, et al. Wide variety of point mutations in the H gene of Bombay and para-Bombay individuals that inactivate H enzyme. Blood. 1997;90:839-849.
347. Yu LC, Yang YH, Broadberry RE, Chen YH, Lin M. Heterogeneity of the human H blood group alpha(1,2)fucosyltransferase gene among para-Bombay individuals. Vox Sang. 1997;72:36-40.
348. O'Donnell J, Laffan MA. Dissociation of ABH antigen expression from von Willebrand factor synthesis in endothelial cell lines. Br J Haematol. 2003;121:928-931.
349. O'Donnell J, Mille-Baker B, Laffan M. Human umbilical vein endothelial cells differ from other endothelial cells in failing to express ABO blood group antigens. J Vasc Res. 2000;37:540-547.
350. O'Donnell J, Laffan MA. The relationship between ABO histo-blood group, factor VIII and von Willebrand factor. Transfus Med. 2001;11:343-351.
351. Sweeney JD, Hoernig LA. Intraplatelet von Willebrand factor and ABO blood group. Thromb Res. 1992;68:393-398.
352. Brown SA, Eldridge A, Collins PW, Bowen DJ. Increased clearance of von Willebrand factor antigen post-DDAVP in Type 1 von Willebrand disease: is it a potential pathogenic process? J Thromb Haemost. 2003;1:1714-1717.
353. Kaersgaard P, Barington KA. Isolation of the factor VIII-von Willebrand factor complex directly from plasma by gel filtration. J Chromatogr B Biomed Sci Appl. 1998;715:357-367.
354. Mazurier C, Samor B, Deromeuf C, Goudemand M. The role of fibronectin in factor VIII/von Willebrand factor cryoprecipitation. Thromb Res. 1985;37:651-658.
355. Biessen EA, Bakkeren HF, Beuting DM, Kuiper J, Van Berkel TJ. Ligand size is a major determinant of high-affinity binding of fucose- and galactose-exposing (lipo)proteins by the hepatic fucose receptor. Biochem J. 1994;299 (Pt 1):291-296.
356. Bowen DJ, Collins PW. An amino acid polymorphism in von Willebrand factor correlates with increased susceptibility to proteolysis by ADAMTS13. Blood. 2004;103:941-947.
357. Budde U, Metzner HJ, Muller HG. Comparative analysis and classification of von Willebrand factor/factor VIII concentrates: impact on treatment of patients with von Willebrand disease. Semin Thromb Hemost. 2006;32:626-635.
358. Lethagen S, Carlson M, Hillarp A. A comparative in vitro evaluation of six von Willebrand factor concentrates. Haemophilia. 2004;10:243-249.
359. Apweiler R, Hermjakob H, Sharon N. On the frequency of protein glycosylation, as deduced from analysis of the SWISS-PROT database. Biochim Biophys Acta. 1999;1473:4-8.
360. Julenius K, Molgaard A, Gupta R, Brunak S. Prediction, conservation analysis, and structural characterization of mammalian mucin-type O-glycosylation sites. Glycobiology. 2005;15:153-164.
361. Nakai K, Kanehisa M. Prediction of in-vivo modification sites of proteins from their primary structures. J Biochem (Tokyo). 1988;104:693-699.
362. Bause E, Legler G. The role of the hydroxy amino acid in the triplet sequence Asn-Xaa-Thr(Ser) for the N-glycosylation step during glycoprotein biosynthesis. Biochem J. 1981;195:639-644.
363. Nossent AY, van Marion V, van Tilburg NH, et al. Von Willebrand factor and its propeptide: the influence of secretion and clearance on protein levels and the risk of venous thrombosis. J Thromb Haemost. 2006.

364. Christlet TH, Biswas M, Veluraja K. A database analysis of potential glycosylating Asn-X-Ser/Thr consensus sequences. Acta Crystallogr D Biol Crystallogr. 1999;55:1414-1420.
365. Petrescu AJ, Milac AL, Petrescu SM, Dwek RA, Wormald MR. Statistical analysis of the protein environment of N-glycosylation sites: implications for occupancy, structure, and folding. Glycobiology. 2004;14:103-114.
366. Whittaker CA, Hynes RO. Distribution and evolution of von Willebrand/integrin A domains: widely dispersed domains with roles in cell adhesion and elsewhere. Mol Biol Cell. 2002;13:3369-3387.
367. Tuckwell D. Evolution of von Willebrand factor A (VWA) domains. Biochem Soc Trans. 1999;27:835-840.
368. Novak L, Deckmyn H, Damjanovich S, Harsfalvi J. Shear-dependent morphology of von Willebrand factor bound to immobilized collagen. Blood. 2002;99:2070-2076.
369. Shibuya N, Goldstein IJ, Broekaert WF, Nsimba-Lubaki M, Peeters B, Peumans WJ. The elderberry (Sambucus nigra L.) bark lectin recognizes the Neu5Ac(alpha 2-6)Gal/GalNAc sequence. J Biol Chem. 1987;262:1596-1601.
370. Nicolson GL, Blaustein J, Etzler ME. Characterization of two plant lectins from Ricinus communis and their quantitative interaction with a murine lymphoma. Biochemistry. 1974;13:196-204.
371. Maley F, Trimble RB, Tarentino AL, Plummer TH, Jr. Characterization of glycoproteins and their associated oligosaccharides through the use of endoglycosidases. Anal Biochem. 1989;180:195-204.
372. Plummer TH, Jr., Tarentino AL. Purification of the oligosaccharide-cleaving enzymes of Flavobacterium meningosepticum. Glycobiology. 1991;1:257-263.
373. Baenziger JU, Fiete D. Structural determinants of concanavalin A specificity for oligosaccharides. J Biol Chem. 1979;254:2400-2407.
374. Elder JH, Alexander S. endo-beta-N-acetylglucosaminidase F: endoglycosidase from Flavobacterium meningosepticum that cleaves both high-mannose and complex glycoproteins. Proc Natl Acad Sci U S A. 1982;79:4540-4544.
375. Fischer BE, Schlokat U, Reiter M, Mundt W, Dorner F. Biochemical and functional characterization of recombinant von Willebrand factor produced on a large scale. Cell Mol Life Sci. 1997;53:943-950.
376. Gronbaek Frandsen EV. Bacterial degradation of immunoglobulin A1 in relation to periodontal diseases. APMIS Suppl. 1999;87:1-54.
377. Rutledge EA, Enns CA. Cleavage of the transferrin receptor is influenced by the composition of the O-linked carbohydrate at position 104. J Cell Physiol. 1996;168:284-293.
378. Ma J, Qian R, Rausa FM, 3rd, Colley KJ. Two naturally occurring alpha2,6-sialyltransferase forms with a single amino acid change in the catalytic domain differ in their catalytic activity and proteolytic processing. J Biol Chem. 1997;272:672-679.
379. de Romeuf C, Samor B, Mazurier C. Estimation of the carbohydrate moiety of von Willebrand factor in the plasma of patients with subtypes 2a and 2b of von Willebrand disease. Thromb Haemost. 1995;74:1180-1184.
380. Reglero A, Rodriguez-Aparicio LB, Luengo JM. Polysialic acids. Int J Biochem. 1993;25:1517-1527.
381. Collados MT, Sandoval J, Lopez S, et al. Characterization of von Willebrand factor in primary pulmonary hypertension. Heart Vessels. 1999;14:246-252.

382. Lopes AA, Ferraz de Souza B, Maeda NY. Decreased sialic acid content of plasma von Willebrand factor in precapillary pulmonary hypertension. Thromb Haemost. 2000;83:683-687.
383. Wittwer AJ, Howard SC. Glycosylation at Asn-184 inhibits the conversion of single-chain to two-chain tissue-type plasminogen activator by plasmin. Biochemistry. 1990;29:4175-4180.
384. Raghavachari M, Kottke-Marchant K, Marchant RE. Determining intramolecular binding sites on surface-bound von Willebrand factor under aqueous conditions. Thromb Res. 2000;98:351-358.
385. Burke RL, Pachl C, Quiroga M, et al. The functional domains of coagulation factor VIII:C. J Biol Chem. 1986;261:12574-12578.
386. Aricescu AR, Lu W, Jones EY. A time- and cost-efficient system for high-level protein production in mammalian cells. Acta Crystallogr D Biol Crystallogr. 2006;62:1243-1250.
387. Ellgaard L, Molinari M, Helenius A. Setting the standards: quality control in the secretory pathway. Science. 1999;286:1882-1888.
388. Trombetta ES, Parodi AJ. N-glycan processing and glycoprotein folding. Adv Protein Chem. 2001;59:303-344.
389. Li Y, Luo L, Rasool N, Kang CY. Glycosylation is necessary for the correct folding of human immunodeficiency virus gp120 in CD4 binding. J Virol. 1993;67:584-588.
390. Feng W, Huth JR, Norton SE, Ruddon RW. Asparagine-linked oligosaccharides facilitate human chorionic gonadotropin beta-subunit folding but not assembly of prefolded beta with alpha. Endocrinology. 1995;136:52-61.
391. Wu JJ, Choi LE, Guidotti G. N-linked oligosaccharides affect the enzymatic activity of CD39: diverse interactions between seven N-linked glycosylation sites. Mol Biol Cell. 2005;16:1661-1672.
392. Davis SJ, Puklavec MJ, Ashford DA, et al. Expression of soluble recombinant glycoproteins with predefined glycosylation: application to the crystallization of the T-cell glycoprotein CD2. Protein Eng. 1993;6:229-232.
393. Takeuchi M, Takasaki S, Miyazaki H, et al. Comparative study of the asparagine-linked sugar chains of human erythropoietins purified from urine and the culture medium of recombinant Chinese hamster ovary cells. J Biol Chem. 1988;263:3657-3663.
394. Legrand D, Salmon V, Coddeville B, Benaissa M, Plancke Y, Spik G. Structural determination of two N-linked glycans isolated from recombinant human lactoferrin expressed in BHK cells. FEBS Lett. 1995;365:57-60.
395. van Veen HA, Geerts ME, van Berkel PH, Nuijens JH. The role of N-linked glycosylation in the protection of human and bovine lactoferrin against tryptic proteolysis. Eur J Biochem. 2004;271:678-684.
396. Imperiali B, Rickert KW. Conformational implications of asparagine-linked glycosylation. Proc Natl Acad Sci U S A. 1995;92:97-101.
397. Wormald MR, Dwek RA. Glycoproteins: glycan presentation and protein-fold stability. Structure. 1999;7:R155-160.
398. Sadler JE. von Willebrand factor: two sides of a coin. J Thromb Haemost. 2005;3:1702-1709.
399. Vogt G, Chapgier A, Yang K, et al. Gains of glycosylation comprise an unexpectedly large group of pathogenic mutations. Nat Genet. 2005;37:692-700.

400. van Schooten CJ, Denis CV, Lisman T, et al. Variations in glycosylation of von Willebrand factor with O-linked sialylated T-antigen are associated with its plasma levels. Blood. 2006.
401. Rudd PM, Wormald MR, Harvey DJ, et al. Oligosaccharide analysis and molecular modeling of soluble forms of glycoproteins belonging to the Ly-6, scavenger receptor, and immunoglobulin superfamilies expressed in Chinese hamster ovary cells. Glycobiology. 1999;9:443-458.
402. Cruz MA, Whitelock J, Dong JF. Evaluation of ADAMTS-13 activity in plasma using recombinant von Willebrand Factor A2 domain polypeptide as substrate. Thromb Haemost. 2003;90:1204-1209.
403. Casonato A, Pontara E, Doria A, et al. Lack of multimer organization of von Willebrand factor in an acquired von Willebrand syndrome. Br J Haematol. 2002;116:899-904.
404. Tsai HM, Sussman, II, Ginsburg D, Lankhof H, Sixma JJ, Nagel RL. Proteolytic cleavage of recombinant type 2A von Willebrand factor mutants R834W and R834Q: inhibition by doxycycline and by monoclonal antibody VP-1. Blood. 1997;89:1954-1962.
405. Wang C, Eufemi M, Turano C, Giartosio A. Influence of the carbohydrate moiety on the stability of glycoproteins. Biochemistry. 1996;35:7299-7307.
406. Helenius A. How N-linked oligosaccharides affect glycoprotein folding in the endoplasmic reticulum. Mol Biol Cell. 1994;5:253-265.
407. Mitra N, Sharon N, Surolia A. Role of N-linked glycan in the unfolding pathway of Erythrina corallodendron lectin. Biochemistry. 2003;42:12208-12216.
408. Dwek RA, Lellouch AC, Wormald MR. Glycobiology: 'the function of sugar in the IgG molecule'. J Anat. 1995;187 (Pt 2):279-292.
409. Stuike-Prill R, Meyer B. A new force-field program for the calculation of glycopeptides and its application to a heptacosapeptide-decasaccharide of immunoglobulin G1. Importance of 1-6-glycosidic linkages in carbohydrate.peptide interactions. Eur J Biochem. 1990;194:903-919.
410. Joao HC, Dwek RA. Effects of glycosylation on protein structure and dynamics in ribonuclease B and some of its individual glycoforms. Eur J Biochem. 1993;218:239-244.
411. Fusetti F, Schroter KH, Steiner RA, et al. Crystal structure of the copper-containing quercetin 2,3-dioxygenase from Aspergillus japonicus. Structure. 2002;10:259-268.
412. Imperiali B, O'Connor SE. Effect of N-linked glycosylation on glycopeptide and glycoprotein structure. Curr Opin Chem Biol. 1999;3:643-649.
413. De Beer T, Van Zuylen CW, Leeflang BR, et al. NMR studies of the free alpha subunit of human chorionic gonadotropin. Structural influences of N-glycosylation and the beta subunit on the conformation of the alpha subunit. Eur J Biochem. 1996;241:229-242.
414. Toyoda T, Itai T, Arakawa T, Aoki KH, Yamaguchi H. Stabilization of human recombinant erythropoietin through interactions with the highly branched N-glycans. J Biochem (Tokyo). 2000;128:731-737.
415. Toyoda T, Arakawa T, Yamaguchi H. N-glycans stabilize human erythropoietin through hydrophobic interactions with the hydrophobic protein surface: studies by surface plasmon resonance analysis. J Biochem (Tokyo). 2002;131:511-515.
416. Yano y, Tanaka K, Doi y, Jando m. The Polystyrene Affinity of Methylglycosides, Deoxysugars and Glucooligosaccharides. J Solution Chem. 1988;17:347-358.

417. Jitsuhara Y, Toyoda T, Itai T, Yamaguchi H. Chaperone-like functions of high-mannose type and complex-type N-glycans and their molecular basis. J Biochem (Tokyo). 2002;132:803-811.

Appendices

Appendix I - Restriction enzymes and buffers

Digest	NEB Buffer	BSA 100µg/ml
XmnI & KpnI	1	yes
XbaI & SacI	4	yes
XmnI & SphI	1	no
BamHI & SphI	BamHI Buffer	yes
XhoI & KpnI	1	yes
EcoRI & BamHI	4	yes
EcoRI	EcoRI Buffer	no
KpnI	1	yes
BamHI & AgeI	4	yes

NEB Buffer 1

10 mM Bis-Tris-Propane-HCl
10 mM $MgCl_2$
1 mM Dithiothreitol
pH 7.0 @ 25°C

NEB Buffer 4

20mM Tris-acetate
50mM Potassium acetate
10mM Magnesium acetate
1 mM Dithiothreitol
pH 7.9 @ 25°C

NEB Buffer BamHI

10mM Tris-HCl
150mM NaCl
10mM $MgCl_2$
1mM Dithiothreitol
pH 7.9 @ 25°C

NEB Buffer EcoRI

100mM Tris-HCl
50mM NaCl
10mM $MgCl_2$
0.025% TritonX-100
pH 7.5 @25°C

Appendix II – Oligonucleotide primers

Primer	Sequence (5' → 3')
VWF3' fwd	ACGTTAGAGCTCGAATTCTCACTTGCTGCACTTCCTG
VWF3' rev	ACGTTATGAGCTCACCGGTTCACTTGCTGCACTTCCTG
pBS KpnI fwd	GCGAATTGGGTA**TT**GGGCCCCCCCTCG
pBS KpnI rev	CGAGGGGGGGCCC**AA**TACCCAATTCGC
N1515Q fwd	GGTGAAGCCGACTTC**CAA**AGGAGCAAGGAGTTC
N1515Q rev	GAACTCCTTGCTCCT**TTG**GAAGTCGGCTTCAC
N1574Q fwd	CCGCTACCAGGGCGGC**CAA**AGGACCAACACTGGGC
N1574Q rev	GCCCAGTGTTGGTCCT**TTG**GCCGCCCTGGTAGCGG

Appendix III – Buffers and solutions

10 X DNA loading buffer

0.125% (w/v) xilene cyanol, 0.125% (w/v) bromophenol blue, 0.625% SDS (w/v), 20% (v/v) glycerol

10 X TBE buffer

0.89 M Tris-borate (pH 8.3), 20 mM EDTA. Prior to use, this was diluted to 1 x TBE buffer with purified water.

TE buffer

10 mM Tris (pH 8.0), 1 mM EDTA

SDS-PAGE Electrophoresis buffer

25 mM Tris-HCl (pH 8.3) 192 mM glycine and 0.1% (w/v) SDS

2 x Protein Loading buffer

150 mM Tris-HCl (pH 6.8), 20% (v/v) glycerol, 4% (w/v) SDS, 0.125% (w/v) bromophenol blue

Transfer buffer

25 mM Tris-HCl (pH 8.3), 192 mM glycine, 20% (v/v) methanol

PBS buffer

Dissolve 5 PBS tablets (Sigma) to 1 litre of distilled H_2O

LB (Luria-Bertani) broth

1% (w/v) bacto-tryptone, 0.5% (w/v) bacto-yeast extract, 1% (w/v) NaCl

LB agar

1% (w/v) bacto-tryptone, 0.5% (w/v) bacto-yeast extract, 1% (w/v) NaCl, 1.5% bacto-agar

(The components of each medium are dissolved in ultra-pure water and autoclaved)

PUBLICATIONS ARISING FROM THIS WORK

PAPERS PUBLISHED

Bombay phenotype is associated with reduced plasma VWF levels and an increased susceptibility to ADAMTS13 proteolysis.

O'Donnell J, **McKinnon TAJ**, Crawley JTB, Lane DA and Laffan MA. Blood (2005), 106, 1988-1991

ABSTRACTS LEADING TO ORAL PRESENTATION

1. ***Reduced VWF:Ag levels in Bombay phenotype are explained by a conformation-related increased susceptibility to ADAMTS13 proteolysis.***

McKinnon TAJ, Laffan MA and O'Donnell JS

British Society of Haematology annual meeting, Manchester, UK April 2005

2. ***Loss of terminal fucose expression in Bombay phenotype produces reduced plasma VWF levels through a conformation-related increased susceptibility to ADAMTS13.***

McKinnon TAJ, Laffan MA, O'Donnell, JS

International Society of Thrombosis and Haemostasis meeting , Sydney, Australia August 2005

ABSTRACTS LEADING TO POSTER PRESENTATION

1. ***Reduced plasma VWF antigen levels in Bombay phenotype are due to an increased susceptibility to proteolysis by ADAMTS13.***

McKinnon TAJ, Laffan MA, Riddell AF, O'Donnell JS

British Society of Haematology annual meeting, Manchester, UK April 2005

2. ***The effect of Von Willebrand Factor glycans on the interaction with ADAMTS13.***

McKinnon TAJ, Chion ACK, Laffan MA

American Society of Haematology, Florida, USA, December 2006